7 nicotinic acetylcholine receptors: regulation of plasticity and network activity in the prelimbic cortex

Udakis, Matthew

Award date:
2016

Awarding institution:
University of Bath

α7 nicotinic acetylcholine receptors: regulation of plasticity and network activity in the prelimbic cortex

Matthew Robert Udakis

A thesis submitted for the degree of Doctor of Philosophy

University of Bath

Department of Pharmacy and Pharmacology

Department of Biology and Biochemistry

June 2016

Table of contents

List of figures

Chapter 1: Introduction

Chapter 2: Methods

Chapter 3: α7 nicotinic acetylcholine receptor regulation of synaptic plasticity within the mouse prelimbic cortex

Chapter 4: α7 nAChR modulation of the excitatory and inhibitory network activity of the prelimbic cortex

Chapter 5: Localisation of presynaptic α7 nAChRs in the mPFC

Chapter 6: Discussion

List of tables

Acknowledgements

This work was performed under the supervision of Dr Chris Bailey and Prof Sue Wonnacott, with financial support from the MRC. All data presented in this thesis was generated by myself with the exception of some field recording experiments in chapter 1 that were conducted jointly with project students Noorje Marbelis and Mohamed Rupawala. Thanks go to Prof Huib Mansvelder for allowing me to conduct a three month research visit to his laboratory at Vrjie University in Amsterdam, and thanks go to the members of his laboratory for helping me learn the optogenetic procedures.

I would especially like to thank my supervisors Chris and Sue for their brilliant guidance during my PhD I couldn't have asked for better supervisors. Thanks go to Nora and Moe for their help with field potential experiments in this thesis. I would like to thank all of the staff in the 4 south annex for all of their help and brilliant care for all of the animals used for this thesis.

Special thanks go to all of my fellow PhD students past and present, especially all of the members in the 5West PhD office. Annelisa for being such a great friend and reminding me that if not today, tomorrow will be a good day! Vicki for all the great chat, help and friendship during my PhD. Special thanks to Robin and Emma for all the laughs, knowing exactly when to go to the pub and for being fellow Pultney dunkers.

Special thanks go to my fantastic parents, Elaine and Pete for being just brilliant, and for all the support during my studies, and my brother and sister James and Laura for all their support. And finally to Fran, my rock and best friend, thanks for all of your love and support throughout this PhD - you've had to go through a lot and I am eternally grateful.

Abstract

Abnormalities in the connectivity and activity of the prefrontal cortex (PFC) is the cause of many of the symptoms of neuropsychiatric disorders such as schizophrenia and Alzheimer's disease. The PFC relies on a complex regulation of network activity and synaptic plasticity for healthy PFC function. These fundamental processes can be modulated by the neuromodulator acetylcholine, acting at α7 nicotinic acetylcholine receptors (α7 nAChRs), a system also compromised in neuropsychiatric disorders. Despite the evidence that α7 nAChRs are essential for healthy PFC function relatively little is known about how activity at this receptor can modulate the fundamental network activity and synaptic plasticity within the PFC. This thesis aims to address some of these issues by using brain slice electrophysiology to measure network activity and synaptic plasticity in response to α7 nAChR activity within the prelimbic cortex (PrL) of C57BL/6J mice. Extracellular field recordings revealed that the selective α7 nAChR antagonist MLA, can reduce and enhance the levels of stimulus-induce long-term potentiation (LTP) and depression (LTD) respectively. In contrast global activation of α7 nAChRs with the selective α7 nAChRs agonist PNU-282987 and positive allosteric modulator PNU-120596 also reduced the levels of LTP. To provide a mechanism for these observations, whole-cell patch clamp recordings were carried out. These experiments revealed that α7 nAChRs reside presynaptically on glutamate inputs and somatodendritically on non-fast-spiking inhibitory interneurons enabling them to enhance both excitation and inhibition in a dynamic way. Further work demonstrated that tonic endogenous ACh acting at α7 nAChRs preferentially enhances excitation rather than inhibition. To further investigate if presynaptic α7 nAChRs were expressed selectively on a subset of the many afferent fibres connecting to the PrL, optogenetic methodologies were used to selectively evoke glutamate release from discrete afferent inputs, these experiments revealed α7 nAChRs may potentially reside on thalamic inputs to the PrL.

List of Abbreviations

5-HT	5-Hydroxytryptamine
AAV	Adeno-associated virus
AC	Adenylyl cyclase
ACh	Acetylcholine
ACSF	Artificial cerebrospinal fluid
AMPA	2-amino-3-(3-hydroxy-5-methyl-isoxazol-4-yl)propanoic acid
ANOVA	Analysis of variance
ATP	Adenosine triphosphate
BLA	Basolateral amygdala
CA1-3	Cornu ammonis regions 1-3
CAG	Cytomegalovirus (CMV) enhancer fused to the chicken beta-actin and rabbit beta-globin
CaM	Calmodulin
CaMK II	Ca2+/calmodulin-dependent protein kinase II - IV
cAMP	Cyclic adenosine monophosphate
ChR2	Channelrhodopsin
CNQX	6-cyano-7-nitroquinoxaline-2,3-dione
CREB	cAMP response element-binding protein
DA	Dopamine
DAMGO	[D-Ala2, N-MePhe4, Gly-ol]-enkephalin
DAP5	D-(-)-2-Amino-5-phosphonopentanoic acid
DNQX	6,7-dinitroquinoxaline-2,3-dione
E-LTP	Early long-term potentiation
eEPCS	Evoked excitatory post synaptic current
EGTA	Ethylene glycol tetraacetic acid
EPSC	Excitatory postsynaptic current
ERK	Extracellular signal–regulated kinases
eYFP	Enhanced yellow fluorescent protein
fEPSP	Field exitatory postsynaptic potential
fMRI	Functional magnetic resonance imaging
FS	Fast spiking (interneuron)
G-protein	Guanosine nucleotide-binding protein

GABA	Gamma-aminobutyric acid
GAD	Glutamate decarboxylase
GFP	Green fluorescent protein
GPCR	G-protein coupled receptor
GTP	Guanosine triphosphate
HEPES	Hydroxyethyl piperazineethanesulfonic acid
i.p	Intraperitoneal
I1	Inhibitor 1
IP_3	Inositol 1,4,5-trisphosphate 3
IP3R	Inositol 1,4,5-trisphosphate 3 receptor
IPSC	Inhibitory postsynaptic current
K-S test	Kolmogorov–Smirnov test
KYA	Kynurenic acid
L-LTP	Late long-term potentiation
LED	Light emitting diode
LFS	Low frequency stimulation
LTD	Long-term depression
LTP	Long-term potentiation
LTS	Low threshold spiking (interneuron)
mAChR	Muscarinic acetylcholine receptor
MAPK	Mitogen-activated protein kinase
MEK	Mitogen-activated protein kinase kinase
mEPSC	Miniature excitatory postsynaptic current
mGluR	Metabotropic glutamate receptor
mIPSC	Miniature inhibitory postsynaptic current
MK-801	Dizocilpine
MLA	Methyllycaconitine
mPFC	Medial prefrontal cortex
mRNA	Messenger ribonucleic acid
NA	Noradrenaline
NAc	Nucleus accumbens
nAChR	Nicotinic acetylcholine receptor
NFS	Non-fast spiking (interneuron)
NMDAR	N-methyl-D-aspartate receptor
PAM	Positive allosteric modulator

PBS	Phosphate buffered saline
PFA	Paraformaldehyde
PFC	Prefrontal cortex
PKA	cAMP dependent protein kinase
PKC	Protein kinase C
PNU-120596	N-(5-Chloro-2,4-dimethoxyphenyl)-N'-(5-methyl-3-isoxazolyl)-urea
PNU-282987	N-(3R)-1-Azabicyclo[2.2.2]oct-3-yl-4-chlorobenzamide
PP1	Protein phosphatase 1
PP2B	Protein phosphatase 2 B (calcineurin)
PPR	Paired pulse ratio
PrL	Prelimbic cortex
PV	Pavalbumin
QX314	N-(2,6-Dimethylphenylcarbamoylmethyl) triethylammonium
RSNP	Regular spiking non-pyramidal (interneuron)
RyR	Ryanodine receptor
s.c	Subcutaneous
S.E.M.	Standard error of the mean
sEPSC	Spontaneous excitatory post synaptic current
SOM	Somatostatin
Syn	Synapsin
TBS	Theta burst stimulation
Thal	Thalamus
TTX	Tetrodotoxin
VGCC	Voltage gated calcium channel
vHip	Ventral hippocampus
VIP	Vasoactive intestinal polypeptide
VTA	Ventral tegmental area
WT	Wild type

Chapter 1:

Introduction

Chapter 1: Introduction

This thesis concerns investigations into the cellular mechanism of network activity and synaptic plasticity and is focussed particularly on the prefrontal cortex and its regulation by α7 nAChRs. As a mediator of many cognitive functions the prefrontal cortex is vital and impairments in its function are implicated in multiple disease states. This introduction will focus first on the prefrontal cortex before considering its regulation by the neurotransmitter acetylcholine acting at the α7 nAChR.

1.1 The prefrontal cortex

1.1.1 A historical perspective on the prefrontal cortex

The most famous incident involving the frontal cortex is likely the case of Phineas Gage. Mr Gage, an industrial worker on the railroads in 1848, was using an iron rod to lodge explosives into rocks to clear a passage for a railroad track, when an explosive accidently discharged, launching the iron rod through the front of his skull. Surprisingly Phineas seemed perfectly fine, he quickly regained consciousness, drove a stage coach back to town and waited patiently for a doctor. However time would tell and Phineas started to behave in an abnormal way, the previously intelligent and well mannered man became a man described as un-inhibited, rude and obnoxious, or as people who knew him would say, “Gage, was no longer Gage” (Macmillan, 2002). This was the first realisation that the frontal cortex serves to control our behaviours and makes us who we are.

Indeed in the early mid 20th century the frontal cortex was touted as a region of the brain responsible for mental disorders. With limited treatment at the time, medicine took drastic measures in a bid to treat these illnesses. A procedure was introduced, based on the early work of Antonio Egas Moniz for which he won the Nobel prize in physiology and medicine, termed frontal leucotomy. Frontal leucotomy, which was adapted and made infamous by Walter Freeman, involved using an ice pick-like tool inserted through the eye socket into the

frontal cortex and crudely lodged from side to side to sever the connections between the prefrontal cortex (PFC) and the thalamus (Freeman, 1948). This procedure was used to treat patients with such conditions as schizophrenia, bipolar disorder and other mental illnesses. In the UK this procedure became increasingly popular with approximately 1000 surgeries conducted a year. The procedure had mixed success with roughly a third benefiting, a third having no effect and a third having severe negative effects (Soares et al., 2013). This procedure was met with stern criticism and was largely eradicated in the 1950s, with the advent of antipsychotic drugs most likely the major reason for its diminishing use (Mashour et al., 2005). Although a controversial procedure, the frontal leucotomy highlighted the importance of the PFC in neuropsychiatry. However the treatments for frontal cortex disease states still remain relativity unsuccessful and this stems down to our lack of understanding of the PFC, and the intricacies of its neuronal signalling.

1.1.2 Structure and function of the human PFC

The human PFC part of the frontal lobe of the cerebral cortex consists of several defined Brodmann areas, including areas 8 - 13 and 44 – 47 (Fig. 1.1). The human PFC is often characterised into two main regions the dorsolateral and ventromedial PFC. The dorsolateral PFC consists of Brodmann areas 8, 9 and 46, whilst the ventromedial PFC consists of area 13, area 44 (the inferior frontal gyrus) and areas 10, 11 and 47 (the orbitofrontal cortex) (Teffer & Semendeferi, 2012). The dorsolateral PFC regulates motor control, higher order sensory processing and performance monitoring via its reciprocal connections with other regions such as the motor cortices, cingulate cortex, basal ganglia and parietal cortex. The ventromedial PFC regulates emotional processes, memory and sensory processing through its connections with the amygdala, hippocampus and visual cortices (Wood & Grafman, 2003).

It is the extensive reciprocal connections between the PFC and other cortical and subcortical regions, that enables information integration from multiple sensory and emotional inputs. This interconnectivity allows the PFC to perform

'executive functions', that are vital for advanced behaviours (Jurardo & Rosselli, 2007).

Executive function is the ability to conduct complex cognitive processes in order to optimise performance in a certain situation. The types of cognitive processes include planning, decision making, overcoming habitual behaviours, dealing with novelty and sustained attention, amongst others (Jurado & Rosselli, 2007). These processes enable us to deal with demanding cognitive situations, adapt to our environment and perform advanced cognitive tasks.

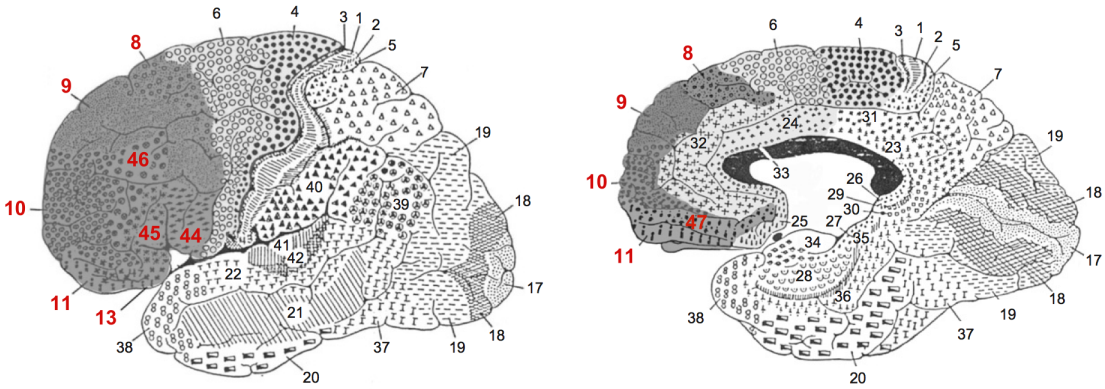

Figure 1.1 The human prefrontal cortex

Lateral and medial view of the human brain from the early work of Brodmann, (1909) The human prefrontal cortex, highlighted in dark grey is often divided into the ventromedial and dorsolateral regions (see text). Each region is split into separate subregions indicated by Brodmann areas shown here in red. Image adapted from Teffer & Semendeferi (2012).

Two well-known processes mediated by the PFC are working-memory and attention. Working-memory is the ability to store and manipulate information for a short period of time to perform a task. Studies conducted in non-human primates show that this information is held in the PFC via persistent neuronal firing through a delay period even after removal of the source of information (Goldman-Rakic, 1995). Humans with lesions to the PFC show impairments in working-memory and suffer cognitive deficits (Müller et al., 2002). Attention is the neurological process that enables us to direct our focus to a particular stimulus. Attention is thought to be mediated via the PFC's ability to selectively process only behaviourally relevant information and discarding other less important sensory information. This process is critical in guiding our behaviour

in novel and important situations, demonstrated by studies in humans with lesions to the PFC (Knight, 1984).

With the numerous cognitive process mediated by the PFC, it is no surprise this region is implicated in multiple neurological disorders. Such disorders include schizophrenia, ADHD, Alzheimer's disease and addiction, all that involve impairments to normal neuronal network function within the PFC. Consequently the majority of theses disease show impairments in working-memory, attention and other executive functions mediated by the PFC. A brief summary of how the PFC is implicated in these diseases is shown in table 1.1.

1.1.3 Studying the prefrontal cortex in the rodent

The PFC in humans is critical for normal neurological function and is impaired in many neurological disorders. Major strides have been made with human functional imaging to understand on a global level how the activity of the PFC relates to its cognitive functions. However to better understand how the PFC might regulate these processes requires a more detailed understanding of the complex cellular network interactions within the PFC, a process that is difficult to study in humans. Research in non-human primates has helped us better understand the functioning of the PFC in working memory, namely work by Patricia Goldman-Rakic on the cellular networks in working-memory (Goldman-Rakic, 1995). However studies in non-human primates are not often possible, and so research has focused on understanding PFC network function using rodents as animal models.

	Symptoms	Cause	Implications with the PFC
Schizophrenia	– **Positive symptoms:** auditory hallucinations, delusions, thought and movement disorders – **Negative systems:** decreases in executive function, working memory, inhibitory control, pleasure, emotion and attention[1]	– Aberrant network development due to a series of environmental and genetic risk factors.	– Decreased White matter volume[2] – Decrease connectivity to PFC[3] – Decreased dorsolateral PFC activity[4] – Impaired PFC GABA and glutamate signalling – Decreased PFC FS inhibitory interneurons[5] – NMDA receptor hypofunction in PFC[6]
ADHD	Mainly found in children: – Inability to withhold attention – Increased hyperactivity – Increased impulsivity. – Impaired executive function[7]	– Aberrant neuronal development through series of environmental and genetic risk factors	– Decreased PFC volume[8] – Decrease white matter connecting to PFC[8] – Deregulation of PFC network[9] – Imbalances in DA and NA neuromodulation in PFC[10,]
Alzheimer's disease	– Decrease in memory recall and forming new memories – Decreased cognition – Decreased motor functions[11]	– Environmental and genetic risk factors – Increase in neurofibrillary tangles and amyloid beta plaques	– Neuron loss within PFC – Decreased PFC synaptic connections[12] – Loss neuronal function within PFC[13] – Decrease in ACh neuromodulation of PFC[14]
Drug Addiction	– Uncontrolled consumption of drug – Impaired of inhibitory control – Decreased stimulation from natural rewards – High relapse rates after abstinence[15]	– Genetic predispositions – Environmental risks – Consumption of illicit addictive compounds[15]	– Overall decrease in PFC activity[15] – Increased PFC activity during drug craving[15] – PFC thought to be key region in relapse to addiction[16]

Table 1.1 Prefrontal cortex involvement in multiple neurological disorders and diseases

Articles referenced in table: ***(1)*** *(NHS UK, 2014),* ***(2)*** (Kuperberg et al., 2003)*,* ***(3)*** (van den Heuvel & Fornito, 2014)*,* ***(4)*** (Molina et al., 2005)*,* ***(5)*** (Hashimoto et al., 2003)*,* ***(6)*** (Moghaddam, 2003)*,* ***(7)*** (Rubia et al., 2014)*,* ***(8)*** (Makris et al., 2008)*,* ***(9)*** (Rubia et al., 1999)*,* ***(10)*** (Pliszka, 2005)*,* ***(11)*** (Kumar et al., 2015)*,* ***(12)*** (DeKosky & Scheff, 1990)*,* ***(13)*** (Battaglia et al., 2007)*,* ***(14)*** (Croxson et al., 2011)*,* ***(15)*** (Goldstein & Volkow, 2002)*,* ***(17)*** (Van den Oever et al., 2010).

Due to the obvious cognitive abilities and size differences between rodents and primates, the existence of an equivalent PFC has been debated (Preuss, 1995; Uylings et al., 2003). The characterisation of a PFC has historically been the existence of a granular layer IV, which is lacking in rodents. However based on the early work of Rose and Woolsey, the PFC is now typically defined as the area of the cortex that receives reciprocal connectivity with the medial dorsal thalamic nuclei (Rose & Woolsey, 1948). The current consensus, based on structural and functional studies, is that the rodent medial prefrontal cortex (mPFC) is roughly homologous to the primate dorsolateral frontal cortex (areas 8, 9, 46) (Uylings et al., 2003). In this thesis work has been focussed on understanding the network functions within the mouse mPFC. Mice as opposed to rats were chosen as an animal model for these studies, as little evidence in the literature suggests an obvious difference in mPFC function between rats and mice, and the use of mice permits utilisation of transgenic strains.

1.1.4 The mouse prefrontal cortex

The mouse PFC consists of 3 major regions, the medial, ventral, and lateral PFC (Van De Werd et al., 2010) (Fig. 1.2). The medial PFC is by far the most studied region of the mouse PFC based on its functional similarities to the primate PFC (Uylings et al., 2003), and consequently the mPFC is the focus of this thesis. Based on cytoarchitecture the mPFC is divided into three major regions; the cingulate region 1 (Cg1), prelimbic (PrL) and infralimbic (IL) cortex (Paxinos & Franklin, 2004) (Fig. 1.2). The rodent mPFC is often divided along its dorsal ventral axis, due to deferent efferent projections and functions. The dorsal mPFC encompasses the Cg1 and PrL, while the ventral mPFC includes the IL cortex (Heidbreder & Groenewegen, 2003). Within each of these mPFC regions are the five cortical layers named layers I - VI with the omission of layer IV that is not found in the rodent mPFC (Van De Werd et al., 2010). The PrL has been the focus of substantially more research compared to other mPFC regions, due to its role in many cognitive behaviours that closely correlate to processes mediated by the dorsolateral PFC in primates and humans, such as working-memory and attention. For these reasons the prelimbic cortex is the

mPFC region of focus in this thesis. Due to the contrasting behavioural functions found between nearby mPFC regions , experiments in this thesis are exclusively conducted in the PrL. However, the majority of studies in the literature do not differentiate between mPFC subregions, and so the remainder of this thesis will describe findings from the mPFC in general, unless otherwise stated.

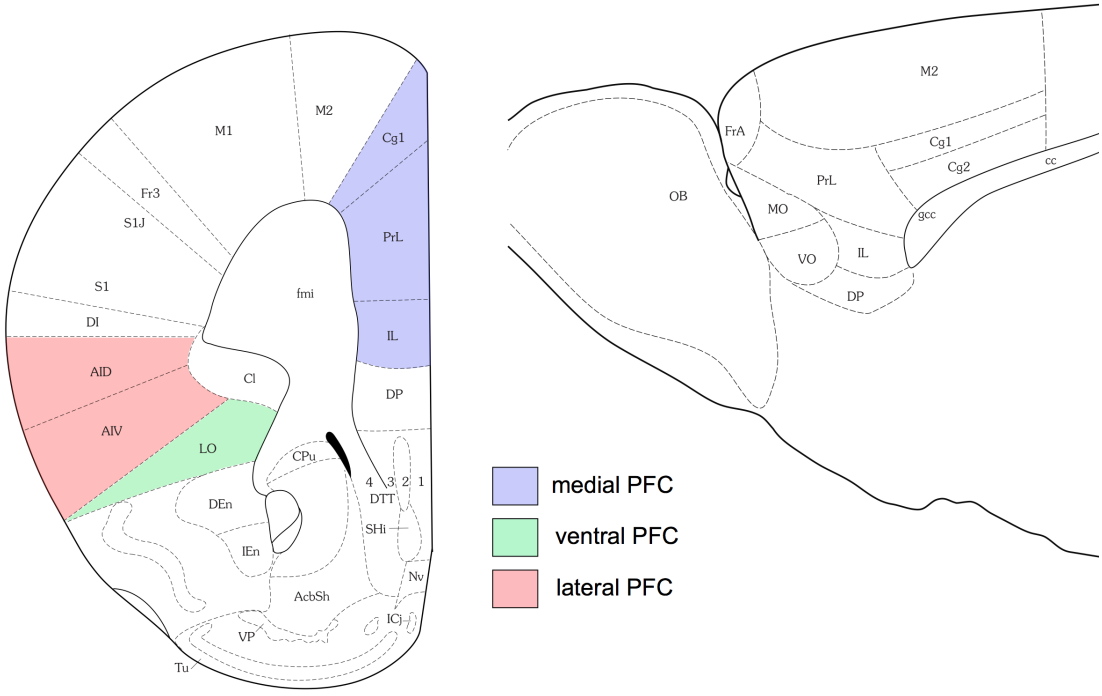

Figure 1.2 The mouse prefrontal cortex

Brain map of the mouse prefrontal cortex. Coronal slice (left) highlights the medial, ventral and lateral PFC regions. The medial PFC contains the cingulate region 1 (cg1) prelimbic (PrL) and infralimbic (IL) regions. A sagittal slice showing the location of the medial PFC regions. Image adapted from Paxinos & Franklin, (2004).

1.2 The medial prefrontal cortex

1.2.1 mPFC architecture and cell types

The mPFC consists of cortical layers containing a mixture of cortical neurons that make up the mPFC microcircuit. Layer I, the most superficial layer, contains inhibitory interneurons, apical dendrites from other cortical neurons and afferent fibres from other brain regions. Within layers II/III reside pyramidal neurons with

apical dendrites that terminate in layer I. These layers also contain a high number of intracortical and subcortical afferent fibres and the apical dendrites from other layers. Layer II/III also contains a variety of inhibitory interneuron subtypes. Layers V and VI contain pyramidal neurons whose apical dendrites span the length of the cortical layers terminating in layer I (Van De Werd et al., 2010). These pyramidal neurons are generally termed output neurons as they typically have long-range subcortical and intracortical projections. Both layers V and VI also contain a mixture of inhibitory interneuron subtypes (Poorthuis et al. 2012) (Fig. 1.3).

Excitatory pyramidal neurons make up 80% of the total neurons and inhibitory interneurons the remaining 20%. Both neuron types are generally classified by their location within the cortical layers, however can be further subdivided based on their intrinsic properties and intracortical and subcortical projections.

1.2.1.1 Inhibitory interneurons within the mPFC

The inhibitory interneurons within the mPFC are the more diverse cell type. These neurons can be classified based on their morphology, molecular markers (including somatostatin (SOM), parvalbumin (PV), vasoactive intestinal peptide (VIP)), and their biophysical properties (including action potential firing rate, membrane properties) (DeFelipe et al., 2013; Petilla Interneuron Nomenclature Group et al., 2008). It is hard to group these interneurons into defined classes due to their overlapping characteristics. However the biophysical properties such as fast-spiking (FS) vs. non-fast spiking (NFS) are useful characteristics to classify interneurons as these are easily identified with electrophysiology and can provide clues to their function within the network.

Within the mPFC, PV-expressing FS interneurons and the SOM expressing and NFS interneurons are the most studied. These interneurons are found throughout all cortical layers and primarily inhibit pyramidal neurons, but can also reciprocally inhibit other inhibitory interneurons (Rudy et al., 2011). It is thought that FS interneurons are responsible for regulating the action potential firing of excitatory pyramidal neurons via targeting their soma and proximal

dendrites and are activated by both local, and projection neurons (Kvitsiani et al., 2013). Conversely NFS interneurons mainly target dendritic shafts and spines and so can regulate the integration of afferent inputs to pyramidal neurons. In addition these interneurons can also regulate the activity of other, predominantly FS interneurons, via reciprocal inhibition (Kvitsiani et al., 2013).

1.2.1.2 Excitatory pyramidal neurons within the mPFC

The glutamatergic pyramidal neurons within the mPFC are less diverse than mPFC interneurons, however they too can be categorised, based on their location within the cortical layers and projection targets. Pyramidal neurons within layers II/III primarily connect to other local pyramidal and interneurons within the mPFC but can also project to other nearby cortical regions. Layer V and VI pyramidal neurons are mainly projecting pyramidal neurons, these neurons can either project subcortically vai the pyramidal tracts, termed pyramidal tract (PT) neurons or intracortically via the cerebral commissure termed intratelenecephalic (IT) neurons (Molnár & Cheung, 2006). PT and IT neurons seem to process different types of information from different afferent inputs via their ability to sample inputs with differing windows of integration (Dembrow et al., 2015). In addition the major subcortical projecting, PT neurons, are activated by IT neurons and inhibited by FS interneurons, suggesting their output is tightly regulated (Dembrow & Johnston, 2014; Lee et al., 2014).

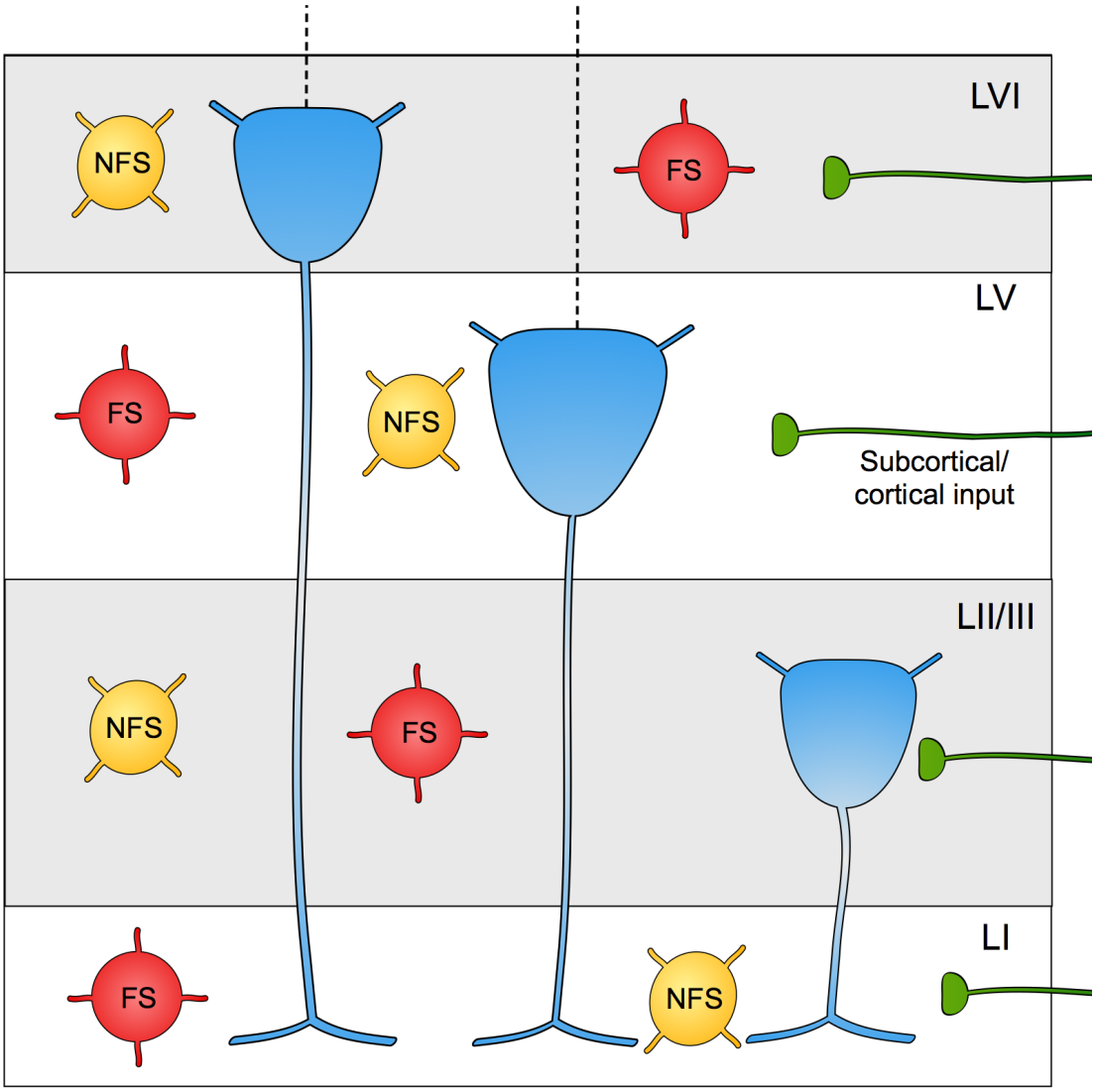

Figure 1.3 Layer architecture and neurons within the mouse mPFC

The prelimbic cortex consists of layers I-VI with the omission of layer IV. Excitatory pyramidal neurons (blue) are found in all cortical layers except layer I. Pyramidal neurons in layer V and VI typically project to subcortical regions whilst Layer II/III neurons typically project to other cortical regions. All layers contain a variety of inhibitory interneurons, both fast spiking (FS) and non-fast spiking (NFS). Afferent inputs from other brain regions innervate all layers.

1.2.2 mPFC inputs, outputs and information flow

1.2.2.1 Efferent and afferent connections to the mPFC

As mentioned, mPFC pyramidal neurons can project to both subcortical and cortical regions. Subcortically projecting layer V/VI output neurons posses a diverse array of efferent outputs to a large number of other brain regions, including the BLA, striatum, thalamus, lateral septum, hypothalamus, VTA, raphe nucleus, basal forebrain and brain stem regions amongst others. In addition neurons within layer II/III also provide efferent projections, primarily to other cortical regions and the amygdala (Gabbott et al., 2005; Sesack et al., 1989).

In addition to these efferent pathways the mPFC also receives a diverse number of afferent inputs from many different cortical and subcortical regions. Of the intracortical afferents, the mPFC receives excitatory inputs from adjacent ipsilateral cortical regions such as the infralimbic cortex, but also receives inputs from an array of contralateral cortical regions, including the contralateral mPFC (Hoover & Vertes, 2007). These cortico-cortico connections are not layer specific with both superficial and deep layers receiving excitatory input (DeNardo et al., 2015; Little & Carter, 2012). In addition, the mPFC receives glutamatergic inputs from subcortical regions including the ventral hippocampus and basolateral amygdala (BLA), whilst a dense innervation is observed from multiple thalamic nuclei including the medial dorsal nucleus (MD). Other less dense subcortical innervation is found from the hypothalamus and nucleus accumbens (DeNardo et al., 2015; Hoover & Vertes, 2007), whilst evidence also suggests glutamatergic innervation from the ventral tegmental area (VTA) (Gorelova et al., 2012). Thalamic and hippocampal inputs innervate both superficial and deep cortical layers (DeNardo et al., 2015; Jay & Witter, 1991; Little & Carter, 2012), whilst the BLA afferents primarily innervate layer II/III (Little & Carter, 2013). How these subcortical and cortico-cortico afferents regulate the mPFC network is still unclear. It is known that thalamic, ventral hippocampal and BLA afferents can all regulate the activity of both pyramidal neurons and inhibitory interneurons, (Gabbott et al., 2006; Little & Carter, 2013; Parent et al., 2010), and therefore participate in a complex regulation of mPFC network activity.

Some of the major pathways to the mPFC have been studied for their role in mediating certain cognitive behaviours. For example the BLA-mPFC pathway is particularly important for emotional control (Herry et al., 2008). The BLA inputs in to the mPFC are shown to encode learnt fear responses and anxiety related behaviours. A recent *in vivo* optogenetics study demonstrated that activation of the BLA-mPFC pathway enhances anxiogenic behaviour in the elevated plus maze and open field test, whilst optogenetic inhibition of the same pathway induced anxiolytic behaviours (Felix-Ortiz et al., 2016).

Studies in which the hippocampus was lesioned in one hemisphere and the mPFC in the other hemisphere demonstrate the hippocampal-mPFC pathway is critical for working-memory tasks such as the radial arm maze task (Floresco et al., 1997), with these two regions synchronising their activity during such processes (O'Neill et al., 2013). This pathway is also implicated in reward learning, recognition memory and contextual-fear. As such the hippocampal-PFC pathway is implicated in multiple cognitive disorders such as schizophrenia, post traumatic stress disorder and depression (Godsil et al., 2013).

The thalamo-cortical pathway in which reciprocal excitatory connections are found between the thalamus and cortex enables the thalamus to receive and process sensory information. The mPFC receives dense innervation from MD but the exact role for this pathway is unclear, the pathway is known to be important for integration of different afferent inputs to the PFC, with the MD inputs shown to gate the inputs from the hippocampus (Floresco & Grace, 2003). In addition MD inputs can also regulate the integration of inputs and influence the direct firing output of principle cells via a feedforward inhibitory mechanism. It was found that thalamic inputs target pavalbumin expressing fast-spiking interneurons. This feedforward inhibition consequently limits the time window in which excitatory inputs can be integrated and action potentials discharged by pyramidal neurons in the mPFC (Delevich et al., 2015). The pathway also appears to be key to many of the cognitive functions mediated by the PFC, such as attention and working memory, and learning of new information (Mitchell & Chakraborty, 2013; Parnaudeau et al., 2013).

1.2.2.2 Cortical microcircuit and information flow

The mPFC encompasses a large number of different cortical cell types, which are fed with inputs from subcortical and cortical regions across multiple layers. How this information is processed within the mPFC network is poorly understood, however in other cortical regions, such as the sensory cortices, circuit connections and information flow models have been proposed (Douglas & Martin, 2004). In these models afferent inputs are received by cortical layer IV neurons, these neurons then transmit information to pyramidal neurons in layer II/III, at this level inputs from other cortical regions may be integrated via horizontal cortical connections. After processing, information is fed to layer V pyramidal neurons. Layer V feeds forward to layer VI and subcortical regions and feeds back to layer II/III. Layer VI neurons also send information sub-cortically and feeds back to layer IV finishing the cortical loop (Fig. 1.4).

This microcircuit has multiple stages in which information can also be regulated by local inhibitory interneurons. In addition both excitation and inhibition of the cortical network can be regulated by horizontal communication from other cortical regions and this allows for coordinated cortical processing across different regions of the cortex (Douglas & Martin, 2004).

These models are however based on regions of the cortex that possess a cortical layer IV, which is not present in the mPFC. Instead the mPFC receives inputs across all layers meaning the flow of information in the mPFC may be different to the one proposed here. However in the mPFC, it is generally agreed that there is a similar hierarchical system in which information is processed from superficial to deep cortical layers which then provides output to subcortical structures (DeNardo et al., 2015). For these reasons understanding how deep layer mPFC neurons are regulated, provides indication of the net consequence of the cortical processing in the mPFC network in regards to subcortical output, as such layer V pyramidal neurons were chosen as the major focus of this thesis.

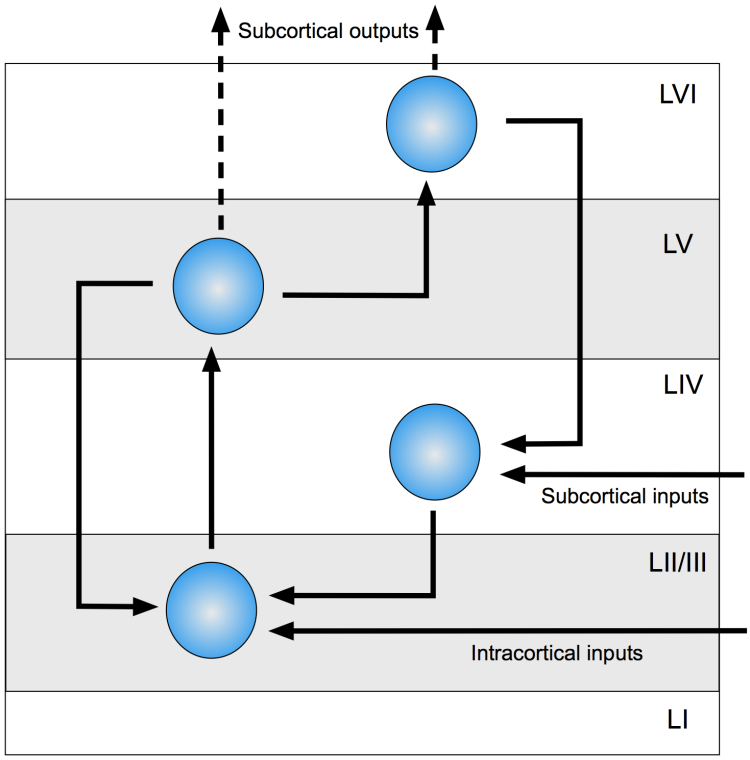

Figure 1.4 Information flow within the cortical microcircuit

Proposed model of the information flow between excitatory neurons (blue) within the cortex, based on visual cortex. Information is received and processed in superficial layers which then propagates to deeper cortical layers, with feedback back to superficial layers and output to subcortical regions. Note that the medial PFC lacks input layer IV. Image based on (Douglas & Martin, 2004).

1.3 Synaptic plasticity at excitatory synapses

As we have seen, pyramidal neurons within mPFC receive an array of synaptic connections from both subcortical brain regions and local microcircuit neurons. These synapses can be both excitatory and inhibitory, with the balance between the two ultimately determining the neuron's depolarisation state and neuronal output. The number of active excitatory synapses at any one time can increase the excitation of the neuron but so to can the relative 'strength' of the synapse, a property of the synapse that can be altered via the process of synaptic plasticity. Synaptic plasticity within the mPFC allows neurons to successfully process and store information, and is fundamental for many of the cognitive processes mediated by the mPFC (Laroche et al., 2000).

Synaptic plasticity involves the short-term or lasting alteration in the efficacy of the synaptic signal across a synapse. This process is dynamic and includes both enhancement ('strengthening'), or reduction ('weakening') of the synaptic output. The strengthening and the weakening of synaptic communication are assigned the terms long-term potentiation (LTP) and long-term depression (LTD) respectively. Both LTP and LTD allows neurons to alter the connectivity with other neurons over a protracted period of time, which allows neurons to dynamically store information. As such, synaptic plasticity is the leading candidate for the molecular mechanisms of learning and memory.

One of the fundamental characteristics of synaptic plasticity is often captioned as 'neurons that fire together, wire together.' This statement describes the principles of Hebbian-synaptic plasticity, which was first theorised by Donald Hebb (Hebb, 1949). Hebb's model reasoned that coincident activation of pre- and postsynaptic neurons would lead to the strengthening of the connection between these two neurons. Work that followed several decades later discovered that this process was mediated via the molecular process of synaptic plasticity (Bliss & Lomo, 1973), and central to the majority of the synaptic plasticity mechanisms is the N-methyl-D-aspartate receptor (NMDAR) (Bliss & Collingridge, 1993; Collingridge et al., 1983; Malenka & Nicoll, 1993).

The majority of our understanding of LTP and LTD is based on studies in the hippocampus, with relatively few studies examining the intricate details of mPFC plasticity. Although other mechanisms exist, and will be mentioned, the majority of LTP and LTD findings within the mPFC have been shown to be NMDAR dependent. Therefore the following section will give a general overview of the mechanisms of NMDAR-LTP and LTD, followed by additional studies conducted in the mPFC.

1.3.1 NMDAR-LTP

The NMDAR is a member of the ionotropic glutamate receptors, including the 2-amino-3-(3-hydroxy-5-methyl-isoxazol-4-yl) propanoic acid (AMPA) and kainate receptors, and is found in synaptic and extra-synaptic locations throughout the

CNS (Paoletti et al., 2013). What makes the NMDAR fundamental in many forms of synaptic plasticity is its ability to only conduct ions upon coincident activation of pre- and postsynaptic neurons. Central to this mechanism is the NMDAR's voltage dependent block, mediated by extracellular magnesium ions that obstruct the pore of the ion channel (Mayer et al., 1984). Within a synapse, if both pre- and postsynaptic neurons are activated, the depolarised postsynaptic membrane potential will relieve the postsynaptic NMDAR of its voltage block, and presynaptic release of glutamate will bind to and open the NMDAR - as such the NMDAR detects pre- and post synaptic activation. In contrast if the postsynaptic neuron is not already depolarised, presynaptic glutamate release will bind to the NMDAR, but the Mg^{2+} block will prevent any ionic conductance.

For this process, NMDARs rely on postsynaptic co-expression of other excitatory ion channels, such as AMPARs. Glutamate binding to AMPARs results in the influx of primarily Na^{+} ions that contribute to the depolarisation required to relieve NMDARs from their voltage dependent block. If the presynaptic activity is high, the subsequently released glutamate will bind to and activate the NMDARs. NMDARs are highly permeable to calcium (Cull-Candy & Leszkiewicz, 2004), and this elevation of postsynaptic calcium through the NMDAR is crucial for initiating and determining the magnitude, and polarity, of postsynaptic plasticity (Lynch et al., 1983; Malenka et al., 1988). In addition to the NMDAR-mediated calcium rise, other sources of calcium can contribute. In hippocampal CA1 neurons, NMDAR-LTP is also known to require the additional elevation of calcium from intracellular stores via IP_3 acting at IP_3 receptors (Harvey & Collingridge, 1992), whilst the depolarisation of the postsynaptic membrane may also activate voltage gated calcium channels (VGCC) that can contribute to postsynaptic calcium (Wyllie et al., 1994).

1.3.1.1 Induction and expression of NMDAR-LTP

The elevation of calcium through these mechanisms, leads to activation of various signalling molecules and intracellular signalling cascades that ultimately lead to increases in the synaptic strength. The initial synaptic alterations can

last for several minutes and are defined as early-LTP. These alterations can either return to basal levels, or can be stabilised for longer periods of hours to days, defined as late-LTP. Distinct cellular processes govern early and late LTP and are briefly described below (Lynch, 2004).

Early-LTP is dependent on activation of protein kinases, one of the most important being the calcium/calmodulin dependent protein kinase II (CaMKII). Other kinases such as protein kinase C (PKC), protein kinase A (PKA), and mitogen-activated protein kinase or extracellular signal-regulated kinase (MAPK/ERK) are also implicated in the mechanisms of early-LTP, summarised in figure 1.5 and reviewed by M. A. Lynch, (2004). However CAMKII is central to nearly all mechanisms of LTP induction. CAMKII gene deletion and molecular inhibition of CAMKII inhibit LTP both *in vitro* and *in vivo* (Malinow et al., 1989; Silva, Stevens, et al., 1992; Silva, Paylor, et al., 1992), whilst introduction of constitutively activated CAMKII alone is sufficient to induce LTP (Pettit et al., 1994).

CAMKII is a multi-subunit protein complex that is dynamically activated by intracellular calcium/calmodulin. Elevated calcium concentrations leads to CAMKII auto-phosphorylation, which enables the enzyme to remain constitutively active, even after the initial induction of plasticity. This ability to remain constitutively active allows CAMKII to act as a molecular switch for LTP (Shonesy et al., 2014). Although the molecular targets of activated CAMKII are vast, in general CAMKII activation and its downstream targets mediate two key mechanism for early-LTP expression. Firstly, CAMKII and other kinases directly phosphorylate existing postsynaptic AMPARs, with CAMKII directly increasing AMPAR conductance by phosphorylation of the GluA1 subunits ser-831 residue (Barria et al., 1997; Derkach et al., 1999). Secondly, CAMKII activity leads to the trafficking and stabilisation of a non-synaptic pool of AMPARs to the postsynaptic membrane (Shi et al., 1999), thought to primarily be mediated via the lateral movement of perisynaptic AMPARs to the postsynaptic membrane (Makino & Malinow, 2009). This increased number of AMPARs, in addition to their higher conductance leads to a marked increase in sensitivity of the postsynaptic membrane to glutamate, and thus a ‘strengthened’ synapse (Fig. 1.5).

Late-LTP describes the longer-term changes in synaptic efficacy that are dependent on protein synthesis and gene transcription. Late-LTP is generally seen as the extension of early-LTP, and protein kinases activated in early-LTP activate the cellular signalling pathways involved in L-LTP. One critical signalling pathway involved in the Late-LTP is the MAPK/ERK pathway. The MAPK/ERK signalling cascade is complex and can be activated by a host of other signalling molecules including, CAMKII, PKA and PKC (Lynch, 2004). ERK is implicated in both the early and late phase of LTP and inhibition of ERK, via the MEK inhibitor, PD98059 prevents the long lasting changes in synaptic plasticity (English & Sweatt, 1997). Late-LTP involves long lasting structural changes, including increased dendritic spine number and spine volume. ERK plays a key role here and ERK levels correlate with increased spine number, and new spine formation is inhibited by preventing ERK activation via the MEK inhibitor, U0126 (Wu et al., 2001). ERK also phosphorylates key transcription factors such as cAMP response element-binding protein (CREB). Phosphorylated CREB, reviewed by Josselyn & Nguyen, (2005), ultimately leads to transcription of multiple synaptic plasticity genes such as the immediate early genes *zif268* and *arc* and *c-fos* that contribute to the lasting alterations in L-LTP.

1.3.2 NMDAR dependent LTD

LTD is the weakening of synaptic efficacy. Compared to LTP less research has been conducted in studying LTD, with the majority of studies conducted in the hippocampus.

Most forms of LTD follow the Hebbian rules of plasticity and require the coincident pre- and postsynaptic activation, as such many forms of LTD are dependent on NMDAR activation. However in addition to NMDAR mediated LTD, mGluR dependent LTD is also a prominent mechanism of synaptic depression within the hippocampus and other brain regions (Kemp & Bashir, 2001). LTD is dependent on postsynaptic increases in calcium, and shares many of the same sources of calcium to LTP, including influx through NMDARs, VGCCs and intracellular stores (Fig. 1.5). As postsynaptic calcium elevations

are required for both LTP and LTD a mechanism must exist by which postsynaptic calcium can regulate these contrasting processes. Such a mechanism was first proposed by Lisman (1989). Lisman (1989) suggested that the polarity of the synaptic plasticity was dictated by postsynaptic calcium concentration and that, upon a less intense activation of pre and post synaptic neurons, a lower level of postsynaptic calcium would fail to induce LTP, but instead induce LTD. Therefore low/moderate levels of calcium leads to LTD whilst high levels of calcium leads to LTP Therefore low/moderate levels of calcium levels (Malenka & Bear, 2002). This difference in calcium concentration regulates the balance in protein kinase and phosphatase activation, with LTP depending on protein kinases, and LTD depending on protein phosphatases (Lynch, 2004).

Like LTP there is a very complex signalling process involved in LTD that is still to be fully unravelled for each synapse, but one of the key phosphatases implicated in LTD is the calcium/calmodulin dependent phosphatase, calcineurin (PP2B). Importantly PP2B has a much higher affinity for calcium/calmodulin than does CAMKII, and is thus activated at lower calcium concentrations to trigger LTD. Activation of PP2B leads to dephosphorylation and thus inactivation of inhibitor 1 (I1) which leads to disinhibition of protein phosphatase 1/2 (PP1/2) that acts to dephosphorylate key proteins, leading to LTD (Fig. 1.5). PP2B and PP1/2 are crucial for LTD and inhibitors of these proteins prevent LTD (Mulkey et al., 1994). The targets for dephosphorylation of PP1/2 are primarily the same proteins targeted for phosphorylation by LTP mediated kinases (Blitzer et al., 1998). Indeed, PP1 can inactivate CAMKII itself to help facilitate LTD and potentially preventing LTP induction (Ma et al., 2015). In addition to CAMKII, PP1 can dephosphorylate AMPAR GluA1 subunit at ser-845 leading to reduced receptor transmission (Munton et al., 2004), and can also mediate the down regulation of AMPARs from the synaptic membrane by activating endocytosis mechanisms (Beattie et al., 2000). In addition to molecular changes, LTD also induces opposing effects to LTP in synaptic structure including dendritic shrinkage and dendritic spine loss (Nägerl et al., 2004; Zhou et al., 2004).

In addition to the postsynaptic mechanisms of synaptic plasticity expression, synaptic efficacy can also be altered via presynaptic mechanisms. These mechanisms bring about lasting changes in the release of neurotransmitter. These changes can be brought about via presynaptic receptors or can involve the retrograde transport of secondary messengers from the postsynaptic neuron such as nitric oxide (NO) and endocannabinoids. The many mechanisms of presynaptic plasticity are reviewed in detail by Ying Yang & Calakos, (2013).

1.3.3 LTP and LTD within the mPFC

Compared to the hippocampus synaptic plasticity within the mPFC remains relatively understudied. Afferent inputs and local cortical networks within the mPFC are heterogeneous, meaning the synaptic plasticity mechanisms of defined synapes within the mPFC is difficult. The majority of brain slice electrophysiology studies investigating mPFC plasticity *in vitro* have looked at intra mPFC plasticity by stimulating fibres in layers II/III and recording from deeper layer V. Studies taking this approach have found that local synaptic plasticity within the mPFC also follows the rules of Hebbian synaptic plasticity (Couey et al., 2007; Meredith et al., 2007), and that this process is reliant on elevations in postsynaptic calcium (Hirsch & Crepel, 1992; Otani et al., 2002; Zhao et al., 2005). The majority of studies also demonstrate that LTP within the mPFC is NMDAR dependent, with NMDAR antagonists blocking the formation of mPFC LTP in both the mouse and rat (Couey et al., 2007; Hirsch & Crepel, 1992; Meredith et al., 2007; Zhao et al., 2005). In addition to local mPFC LTP several studies have investigated more defined neuronal pathways. *In vivo* recordings in the mPFC whilst stimulating the ventral hippocampus of the rat revealed that hippocampal-mPFC synapses also exhibit LTP, in an NMDAR dependent mechanism (Jay et al., 1995), whilst *in vitro* stimulation of a hippocampal-mPFC pathway also elicits NMDAR-dependent LTP (Parent et al., 2010). In addition, thalamus-mPFC, amygdala-mPFC and contralateral mPFC-mPFC synapses have all been shown to exhibit LTP *in vivo* (Gemmell & O'Mara, 2000; Herry & Garcia, 2002; Maroun & Richter-Levin, 2003).

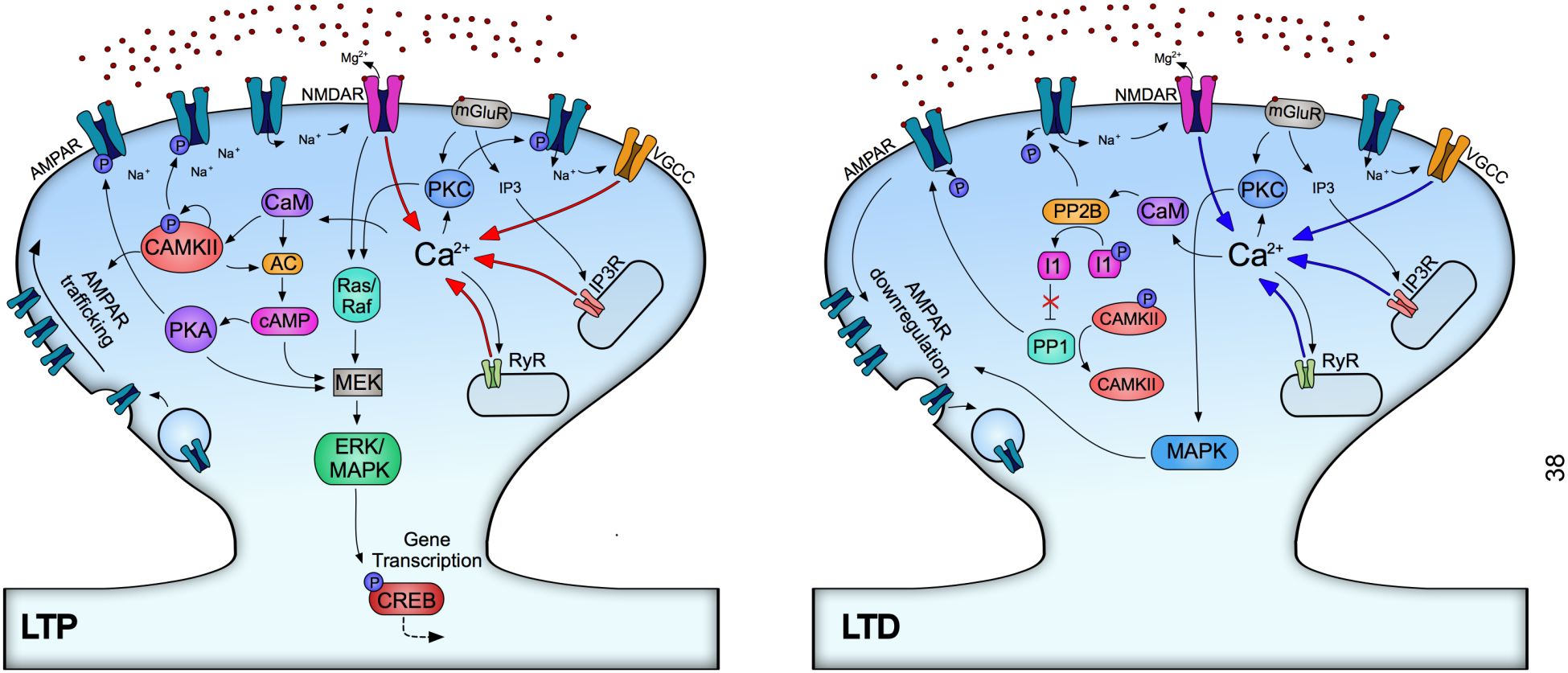

Figure 1.5 Postsynaptic long-term potentiation and depression

Summary of the major postsynaptic mechanisms of long-term potentiation (LTP) (left) and long-term depression (LTD) (right). LTP is induced upon high levels of postsynaptic calcium (red arrows), which instigate CAMKII mediated increase in AMPAR trafficking and AMPAR phosphorylation to increase channel conductance and gene transcription. mGluR activation can also contribute to these mechanisms by increasing intracellular calcium and activating PKC. LTD is induced upon moderate levels of postsynaptic calcium (blue arrows), which activates PP2B (calcineurin) leading to activation of PP1 and inactivation of CAMKII. PP1 and PP2B can dephosphorylates AMPARs leading to receptor internalisation. mGluR activation can also lead to LTD via increasing intracellular calcium and via activating MAPK pathway ultimately leading to receptor internalisation.

NMDAR-LTP however is not the only form of LTP within the mPFC and some research suggests metabotropic glutamate receptors also participate in mPFC LTP. Application of the group 1 mGluR agonist DHPG in combination with a theta burst stimulation, converts a subthreshold LTP into a stable potentiation measured via alterations in layer V population spikes (Morris et al., 1999). In addition theta burst stimulation to mPFC slices incubated with the broad-spectrum mGluR antagonist MCPG fails to induce LTP. Under control conditions this theta burst stimulation induces an NMDAR dependent LTP, suggesting that this mGluR dependent LTP within the mPFC also requires NMDAR activation (Vickery et al., 1997).

In addition to LTP, synapses within the mPFC are able to undergo LTD. mPFC LTD is also dependent on postsynaptic calcium (Hirsch & Crepel, 1992), but the induction requirement for mPFC LTD is less clear. Ma et al., (2015) show in mice brain slices that mPFC LTD can be evoked by low-frequency stimulation (LFS) of layer II/III in a mechanism dependent on NMDARs. Interestingly they show that this LTD can be inhibited by overexpression of CAMKII, suggesting these mechanisms are likely to be similar to those described above in the hippocampus. Consistent with an NMDAR dependent mechanism for LTD, *in vivo* studies show that a LFS applied to the hippocampus leads to LTD within the mPFC in rats, that can be blocked by the local application of the NMDAR antagonist AP7 to the mPFC (Lopes-Aguiar et al., 2013). However others have shown that stimulus-induced LTD can also occur in an NMDAR independent manner, instead relying on muscarinic AChR activation or mGluR activation (Caruana et al., 2011; Hirsch & Crepel, 1991; Lafourcade et al., 2007).

mGluRs also seem to play a role in LTD induction within the mPFC. The mGluR1 antagonists, AIDA and LY367385 but not the mGluR5 antagonist MPEP, block an NMDAR independent form of LTD evoked by pairing pre and post synaptic depolarisations within the mPFC (Guzman et al., 2010). In the rat mPFC slice, application of the group II mGluR agonist, DCG-IV, induces a stable LTD in the absence of LFS, via a mechanism that requires NMDAR activation (Otani et al., 2002), although at high concentrations of DCG-IV, LTD is induced independently from NMDAR activation (C.-C. Huang & Hsu, 2008). In

a similar fashion, LTD can also be evoked by other agonists in the absence of LFS, including NA (acting at α1 and α2 NA receptors) (Marzo et al., 2010), and selective mAChR agonists (acting at M1 mAChRs) (Caruana et al., 2011), in mechanisms that are NMDAR dependent and independent respectively. Another NMDAR independent LTD mechanism is induced by a sub-threshold LFS to layers II/III and requires background dopamine acting on both D1 and D2 receptors (Y. Y. Huang et al., 2004). Indeed dopamine appears to play a key role in modulating the levels of both LTP and LTD within the mPFC and is reviewed by Otani et al., (2015).

1.3.4 Synaptic plasticity in mPFC dependent memory and neurological disease

The mPFC is thought to be the loci of several forms of learning and memory that enable it to mediate certain cognitive processes (Jung et al., 2008), which implicates the importance of synaptic plasticity within this region. For example the mPFC has been well studied for its role in consolidation and extinction learning for both fear and drug associated memories (Van den Oever et al., 2010; Zhao et al., 2005). For extinction of fear memories, it has been demonstrated that repetitive exposure to a tone, previously conditioned to a eyelid shock results in extinction of fear behaviour, this extinction coincided with an extinction mediated LTP at the hippocampal to mPFC synapse. Added to this LTP and extinction learning could be blocked by the MAPK/ERK inhibitory PD098059 locally delivered to the mPFC, demonstrating that extinction of fear memories induces LTP within the mPFC (Hugues et al., 2006). In addition, synaptic plasticity within the mPFC is also thought to be critical for declarative forms of memory such as recognition memory. For example, object-in-place recognition memory requires NMDAR activation within the mPFC, lesions to the mPFC impair this type of recognition memory whilst blocking synaptic plasticity, with an NMDAR antagonist, impairs the acquisition of short-term and long-term memory required for the task (Barker et al., 2007; Barker & Warburton, 2008). In addition synaptic plasticity within the mPFC is also thought to be important for

performance in working-memory tasks, specifically at the hippocampal to mPFC synapses (Laroche et al., 2000).

Further highlighting the importance of studying mPFC synaptic plasticity, several disease states (detailed in table 1.1) are associated with aberrant synaptic plasticity in the PFC. In Alzheimer's disease the short-term and working-memory deficits are thought to be mediated by impaired PFC synaptic plasticity (Germano & Kinsella, 2005). This is demonstrated in several Alzheimer's disease mice lines that show impaired mPFC stimulus-induced LTP compared to wildtype mice. Such transgenic lines include the APP/PS1 and AβPPPS1-21 mice that express mutated amyloid precursor protein and presenilin-1, (two key proteins implicated in Alzheimer's disease) (Battaglia et al., 2007; Lo et al., 2013). Schizophrenia is also implicated with aberrant synaptic plasticity evidenced by the majority of susceptibility genes being synaptic plasticity related (reviewed by Harrison & Weinberger, (2005)). Animal model of schizophrenia in which neurodevelopment is disrupted, leads to augmented level of LTP within the hippocampal-mPFC pathway (Goto & Grace, 2006), whilst impaired neuroplasticity is also highlighted by reduced spine density in the PFC of schizophrenia patients (Lewis & Gonzalez-Burgos, 2008). Finally mPFC synaptic plasticity is also implicated in addiction to illicit drugs (Van den Oever et al., 2010). Animals models of addiction show that mPFC activity is implicated in relapse to drug seeking behaviours, with findings showing that acute synaptic plasticity within the mPFC is responsible for reinstatement to drug seeking (Van den Oever et al., 2008).

Sections 1.2 and 1.3 have highlighted that the mPFC constitutes a complex network of excitatory and inhibitory neurons that receive connections from a range of brain regions. In addition these synaptic connections within the mPFC network can be altered in efficacy via synaptic plasticity – a mechanism that is key for several cognitive processes. The mechanism of mPFC synaptic plasticity is made more complex when we consider the numerous neuromodulatory systems that modulate excitatory and inhibitory neurotransmission. One of the key neuromodulators is acetylcholine, this neuromodulator is known to regulate synaptic plasticity within several brain regions including the mPFC (Couey et al., 2007; Gu et al., 2012; Mansvelder

and McGehee 2000). What's more is acetylcholine is also implicated in the many cognitive processes and disease states mediated by the mPFC. Consequently understanding the contribution acetylcholine modulation has on mPFC network activity and plasticity is an important area of study, and is the focus of this thesis. The remainder of this introduction will describe the acetylcholine modulation system and highlight its function in the regulation of mPFC network activity and synaptic plasticity.

1.4 The acetylcholine neuromodulation system

Acetylcholine (ACh) has fundamental roles in both the peripheral and central nervous systems, in the peripheral nervous system ACh acts as the major neurotransmitter at the neuromuscular junction whilst in the CNS it is a critical neuromodulator that can regulate cellular activity in a plethora of different brain regions.

Within the brain there are two distinct cellular populations of cholinergic projection neurons, located in the basal forebrain and the brainstem region. The brainstem cholinergic region termed the mesopontine tegmentum area is made up of the pedunculopontine nucleus (PPT) and the lateraldorsal tegmental nucleus (LDT), these two regions serve to source acetylcholine most prominently to the thalamus but also to the VTA, hypothalamus and the cerebellum. This acetylcholine innervation is vitally important in the circadian rhythms, wakefulness and consciousness (Woolf & Butcher, 2011), and through their connections with the thalamus and the basal forebrain is thought to be important for attention (Rostron et al., 2008). The basal forebrain cholinergic region comprises of the medial septum (MS), the vertical limb of the diagonal band of broca (VDB), the nucleus basalis of meynert (NBM) and the substantia innominata (SI). The SI provides ACh to the olfactory bulb and amygdala whilst the MS is the major cholinergic pathway to the hippocampus mediating its important role in learning and memory. The VDB and the NBM provide the majority of the cortical ACh, where ACh innervation can be found across the entire cortical mantle (Fig. 1.6) (Bigl et al., 1982; Woolf & Butcher, 2011).

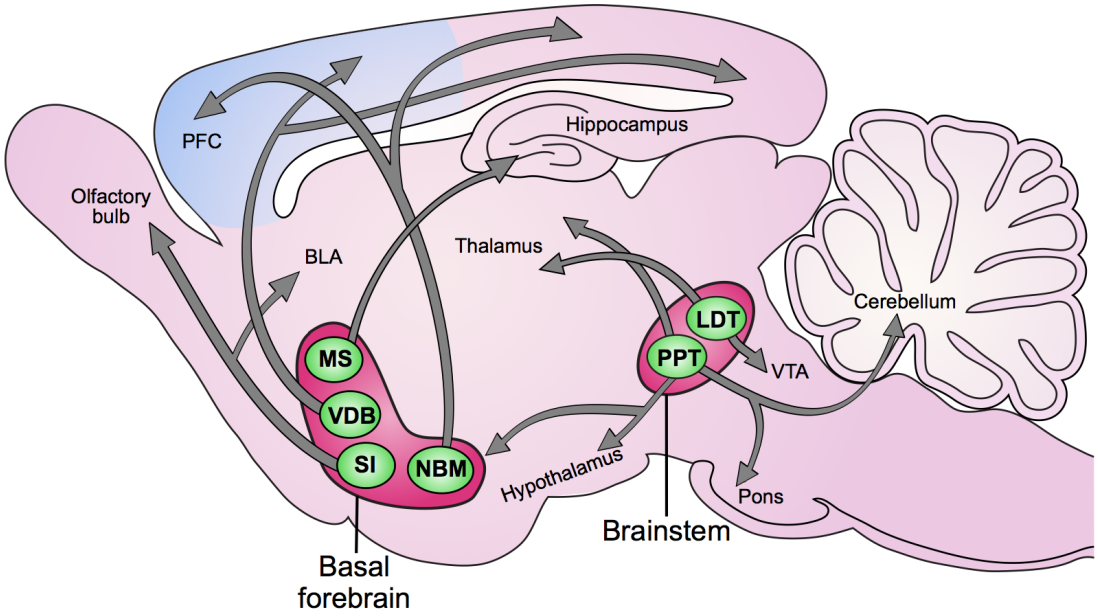

Figure 1.6 Acetylcholine innervation within the rodent brain.

Two major sources of acetylcholine shown here in the rat brain originate from the basal forebrain and brain stem regions. The basal forebrain region contains acetylcholine nuclei from the medial septum (MS), the vertical limb of the diagonal band of broca (VDB), the nucleus basalis of meynert (NBM) and the substantia innominata (SI). The brain stem (mesopontine tegmentum area) contains the acetylcholine nuclei, the pedunculopontine nucleus (PPT) and the lateraldorsal tegmental nucleus (LDT). These acetylcholine sources innervate a range of different cortical and subcortical brain regions.

1.4.1 Acetylcholine innervation of the mPFC

The cholinergic innervation to the mPFC originating in the basal forebrain is evenly distributed throughout all cortical layers, whilst certain regions of the basal forebrain appear to target different regions/layers of the mPFC (Bloem, Schoppink, et al., 2014). Upon reaching the mPFC cholinergic afferents display a varicose pattern of innervation forming both synaptic and non-synaptic connections within the cortex (Lendvai & Vizi, 2008), although direct synaptic contacts are rare (Descarries et al., 1997). The long held belief is that ACh is released in a dispersed volume transmission system, based on the extra-synaptic location of ACh receptors and their localisation to non-ACh releasing synapses. This volume transmission is consistent with ACh's role as a neuromodulator, however recent lines of evidence suggests that direct synaptic communication via ACh is also important in regulating network activity, in

particular specific subtypes of inhibitory interneurons have been shown to respond directly to synaptic ACh release, leading to regulation of nearby cortical neurons (Arroyo et al., 2012). The classic volume transmission hypothesis of ACh release is still under debate - volume transmission leads to slow increases in ACh concentrations that are largely regulated by acetylcholinesterase concentrations, however evidence *in vivo* has demonstrated that phasic rapid increases in ACh are critical for the mPFC's ability to perform certain cognitive functions implicated in attention such as cue detection (Gritton et al., 2016; Parikh et al., 2007). This evidence has highlighted that volume transmission is most likely not the only ACh release mechanism, and that deterministic release is critical for cortical function (Sarter et al., 2009).

1.4.2 Acetylcholine receptor subtypes

ACh acts as the endogenous ligand for a range of different ACh receptor subtypes enabling ACh to have broad effects on its cellular target. ACh receptors are divided into nicotinic acetylcholine receptors (nAChR), which are the main focus of interest in this thesis, and muscarinic receptors. Muscarinic acetylcholine receptors (mAChRs) are G-protein receptors with 5 subtypes (M1-M5) within the CNS. These couple to cellular signalling pathways via activation of Gq and Gi alpha subunits, enabling mAChRs to mediate slow cellular processes. These effects can be both excitatory, mediated by M1, 3, 5 mAChRs or inhibitory via M2, 4 mAChRs.

nAChRs, the major focus of this thesis, are ionotropic receptors and are able to mediate fast excitatory effects. The nAChRs have had a rich history in shaping the understanding of fundamental neuroscience. Much of the early work understanding neurotransmitter release and transmission was conducted by Sir Bernard Katz studying nAChR function in the neuromuscular end plate tissue preparation (del Castillo & Katz, 1954). The same preparation also led the way to the advent of patch clamp electrophysiology, with the first single channel recording being performed with the nAChR (Neher & Sakmann, 1976). Since then our understanding of the structure and function of nAChRs has progressed. Within the CNS nAChRs generally mediate neuromodulatory

actions via their expression at neuronal extra-synaptic sites such as at presynaptic terminals (Livingstone & Wonnacott, 2009). However they also play a role in traditional synaptic communication at asymmetric synapses, and can be expressed on non-neuronal locations such as astrocytes (Lendvai & Vizi, 2008).

The nAChR subgroup is composed of a diverse range of functional pentameric ion channels. Much of this diversity is attributed to the multiple combinations of subunits that can make up a nAChR. With three β (β2-β4) and nine α (α2-α10) subunits there are a variety of subunit combinations possible (Zoli et al., 2015). The nAChRs assemble as either heteromeric or homomeric complexes. Heteromeric nAChRs consist of at least two α subunits and a combination of β subunits, whilst homomeric nAChRs consist of five α subunits (of either α7-α9). Out of the functional nAChRs subunit combinations the most abundant within the CNS are the heteromeric α4β2 (Gotti et al., 2006), and the homomeric α7 nAChRs – with the α7 nAChR being the major focus of this thesis.

1.4.3 nAChR distribution throughout the brain

nAChRs are expressed throughout the human nervous system in both the peripheral and central nervous systems. Most of our understanding of nAChR expression comes from rodent studies, studies using single subunit KO mice along with radioligand binding, immunocytochemistry and in situ hybridisation, have enabled the precise localisation of nAChR protein and mRNA levels, helping us understand which nAChRs are expressed, and where, within the brain (Pistillo et al., 2015). As mentioned, the most abundant nAChRs are the homomeric α7 and heteromeric α4β2 containing nAChRs. Most of the studies on localisation of the α7 nAChR is based on radioliogand binding of α-Bungarotoxin (selective ligand to α7 nAChR subunit). From these studies it is known that α7 nAChRs are expressed heavily throughout the rodent brain, in particularly in the cortex, hippocampus and subcortical limbic regions (Gotti et al., 2006). In agreement with α4β2 nAChR expression being the most prominent, β2 or α4 KO mice show a substantially reduced level of nAChR total

binding with α4β2* receptors thought to represent 90% of the total high affinity nAChR binding throughout the brain (Zoli et al., 2015). Other common heteromeric nAChRs include the α3β2 which is highly expressed in the medial habenula, dorsocaudal medulla oblongata and the pineal gland, and the α4β4 expressed in the medial lateral habenula (Zoli et al., 1998). For an overview of the locations of nAChRs within the rodent brain see figure 1.7 and Gotti et al., (2006).

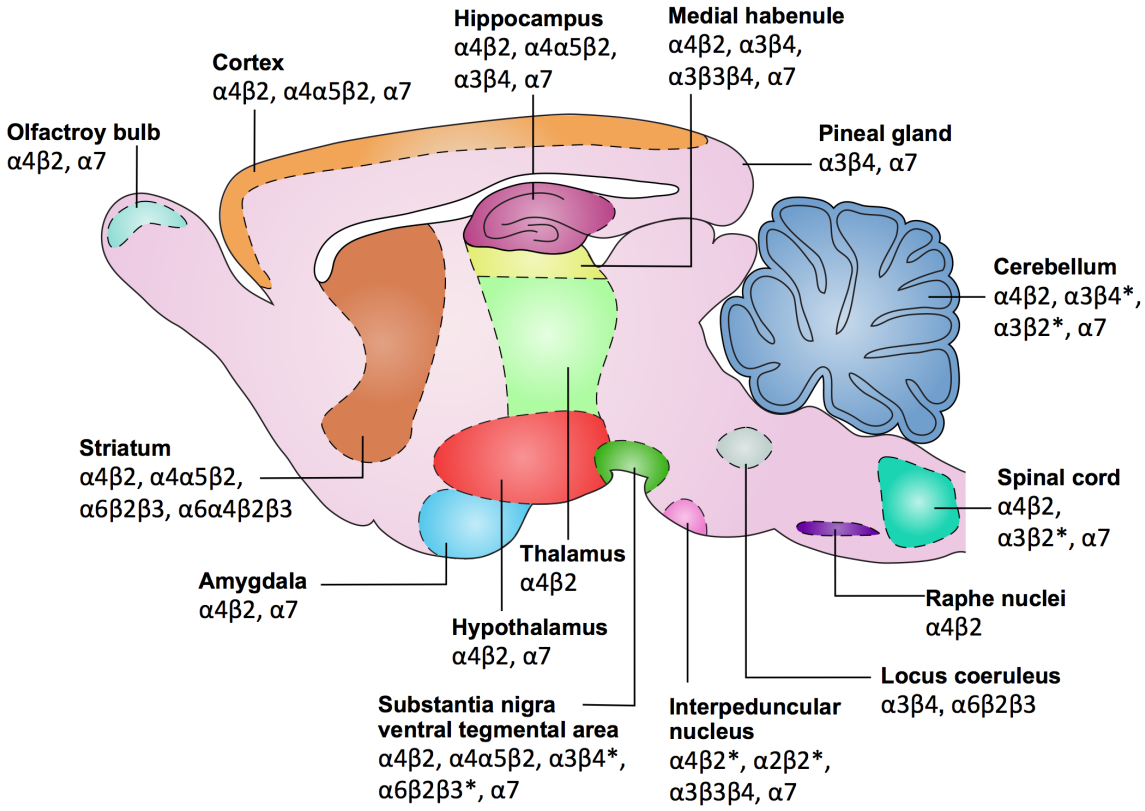

Figure 1.7 nAChR localisation within the rodent brain

Location of the major nAChR subtypes within the rodent brain (shown here as rat brain) Throughout the entire brain the homomeric α7 nAChR and heteromeric α4β2 nAChR ate the most abundant. nAChR locations and image recreated from (Gotti et al., 2006).

1.4.4 nAChR structure and function

Substantial work has gone into studying the structure of nAChR subunits, and much of our understanding is based on the structure, gene sequence and biochemistry of the torpedo nAChR, found in the electrical organ of the torpedo (Unwin, 2005). It is now understood that each nAChR subunit contains a long ~200 amino acid extracellular N-terminal domain, four transmembrane spanning domains (T1-T4), a short cytoplasmic loop between T3 and T4 and a short extracellular c-terminal domain (Fig. 1.8).

The extracellular N-terminal domain contains the 'cys-loop', which is a characteristic of other similar 'cys-loop' receptors such as $5HT_3$, $GABA_A$, and glycine receptors. Distinguishing α subunits from β subunits are two vital cysteine residues contained within the C-loop of the N-terminal domain. This C-loop within the α subunit forms the agonist binding site which occurs at the subunit interface of an α subunit, as such different receptor combinations have different number of agonist binding sites (Albuquerque, et al., 2009).

The TM domains consist of 4 tightly packed alpha helixes, which in combination with other subunits create the pore of the ion channel. T2 makes up the surface of the internal pore of the receptor and is critical for ion selectivity and gating of the receptor. In the receptors closed position the T2 forms a closed hydrophobic pore whilst upon ligand binding and a series of conformational changes leads to a rotation of the T2 helix to create an open hydrophilic pore (Albuquerque, et al., 2009). The amino acids that line the pore in the open conformation determine the receptors ion selectivity. In general the nAChRs are non-selective cation channels permeable to Na^+, K^+ and Ca^{2+}. However different subunit combinations can alter the relative permeability of these ions, in particular the homomeric α7 nAChRs has a higher permeability to calcium which can be attributed to different charged amino acids within the selectivity filter of the pore (Fucile, 2004). This high calcium permeability of the α7 nAChR enables this receptor to partake in a variety of cell processes and signalling pathways and consequently the α7 nAChR has gained a lot of research interest and is the focus of the work in this thesis.

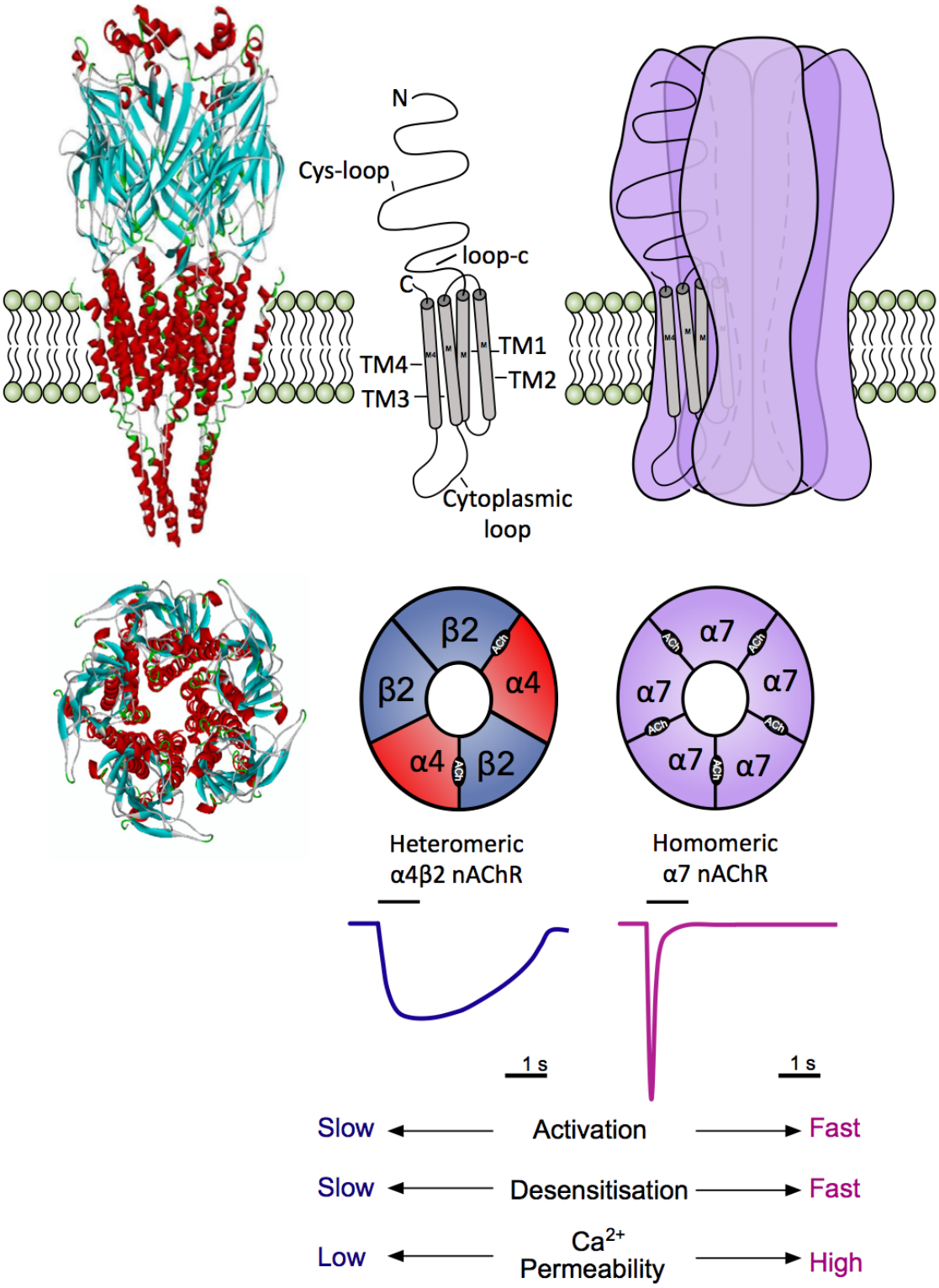

Figure 1.8 Structure and functional properties of nAChRs

Structure and function of nAChRs. Molecular model of the $\alpha 7$ nAChR, diagram of the major components of nAChR subunit including the 4 transmembrane domains and extracellular and intracellular loops (top). Heteromeric and homomeric nAChRs subunit combinations, with agonist binding site between alpha subunits (middle). $\alpha 4\beta 2$ and $\alpha 7$ nAChRs have diverse channel characteristics including different rates of activation, desensitisation and permeability to calcium. Current traces represent typical whole-cell currents for each receptor (bottom). Parts of figure adapted from Dineley et al., (2015)

Another functional property of the all nAChRs attributed to different subunit combinations, is the rate of activation and desensitisation of the receptor. nAChRs are observed in three conformational states; resting (closed), open and desensitised. Upon agonist binding to the agonist binding site, the receptor transitions from the resting state to the open state, allowing flux of ions through open receptor pore. α7 nAChRs posses a rapid transition to the open state upon agonist binding and results in a very fast influx of ions, in comparison the heteromeric α4β2 nAChR has a slower opening rate leading to a slower influx of ions (Fig. 1.8) (Dineley et al., 2015). In the open agonist bound state the agonist can unbind allowing the receptor to return to its resting state, or under higher agonist concentrations the agonist can remain bound leading to the transition of the receptor into the non-conducting desensitised conformation (Giniatullin et al., 2005). The rate of desensitisation of the receptor is again dependent on the subunit combination with α7 nAChRs desensitising within milliseconds of agonist exposure. This rapid desensitisation has made studying this process challenging as desensitisation rate is quicker than the peak measurement of current in oocytes (Papke & Thinschmidt, 1998). α4β2 nAChRs have a slower rate of desensitisation (seconds). The different opening and desensitising rates of these receptor subtypes produces the characteristic fast and slow ion currents for α7 and α4β2 nAChRs respectively (Fig. 1.8).

In addition to the rapid desensitisation to high concentrations of agonist, under lower concentrations of agonist nAChRs transition into an additional desensitised state termed high affinity desensitisation (Giniatullin et al., 2005). This desensitisation arises upon low agonist occupancy of the receptor leading to a stable desensitised conformation of the receptor. As high affinity desensitisation is achieved upon low agonist concentrations, this infers that under physiological conditions of volume transmission in which the concentrations of tonic ACh are low, nAChRs might be basally desensitised. The exact mechanisms by which desensitisation of nAChRs modulate physiological functions of endogenous ACh transmission is not clear. However under exposure to the nAChR agonist nicotine, differential desensitisation of nAChRs on inhibitory interneurons and glutamatergic terminals leads to activation of dopaminergic neurons within the VTA, leading to activation of the neural reward pathway (Mansvelder et al., 2002). This highlights that prolonged

exposure to exogenous agonists might have the opposite effect to that which is expected of an agonist, which is important to consider upon use of nAChR agonists as a therapeutic treatment. This has led to the development of allosteric modulators that bind to the receptor to alter receptor function and in some cases prevent desensitisation. As a lot of the work in this thesis uses an α7 nAChR positive allosteric modulator they will be described in more detail below.

1.4.5 Positive allosteric modulators

Positive allosteric modulators are molecules that bind to the receptor at a distinct region other than the agonist binding site and alter the energy barriers between various conformational states of the receptor. α7 nAChR positive allosteric modulators have gained a lot of attention as potential therapeutic compounds, these molecules alone have no intrinsic activity but in the presence of an agonist are able to enhance the agonist response. For α7 nAChRs, PAMs come in two forms, Type-I and Type-II; both are thought to bind within an intra-subunit cavity between the four transmembrane helixes of the α7 nAChR subunit (Chatzidaki & Millar, 2015; Collins et al., 2011). Type-I PAMs such as NS1738, once bound, lower the activation barrier between resting and open conformation, resulting in an increased peak current in response to agonist binding (Timmermann et al., 2007). Type-II PAMs, such as PNU-120596 in addition to enhancing peak current, also prevent receptor desensitisation and rescue already desensitised receptors to a non-desensitised state (Hurst et al., 2005). This prevention of desensitisation is presumably via increasing the energy barrier between open and desensitised states (Chatzidaki & Millar, 2015).

Type-II positive allosteric modulators such as PNU-120596 are also useful in studying receptor function within a neuronal network. Because α7 nAChRs are prone to desensitisation, application of α7 nAChR agonists can render the receptors desensitised even before an effect can be measured, making it challenging to investigate α7 nAChR function. The use of PNU-120596 can

prevent and reverse α7 nAChR desensitisation and thus allow the receptor to be studied in its active form, in the absence of desensitisation. In addition, because PNU-120596 has no intrinsic activity and requires presence of an α7 nAChR agonist, PNU-120596 applied alone will selectively potentiate the activity of α7 nAChRs exposed to endogenously released ACh. Therefore the use of α7 nAChR PAMs can help elucidate the actions of endogenous ACh acting at α7 nAChRs within a complex neuronal network, for these reasons PNU-120596 is utilised in this thesis.

1.5 α7 nAChRs in medial prefrontal cortex

1.5.1 α7 nAChRs in mPFC mediated cognitive behaviour

Using behavioural tasks, many of the cognitive processes assigned to the mPFC have been modelled in rodents, including cognitive processes such as working-memory and attention. Consequently it has become clear that ACh within the mPFC plays a fundamental role in these cognitive tasks, with one of ACh's targets being the α7 nAChR. The involvement of α7 nAChRs in some of these processes will be briefly discussed below.

The mPFC is critical for the process of attention, which can be modelled well in the rodent. The 5 choice serial reaction time test (5-CSRTT), which assesses, visual-spatial attention, is the most commonly used. The test measures correct, incorrect and missed responses (often nose pokes) to a sensory cue. Upon mPFC lesions the number of cue misses (omissions) increases, indicative of a decreased attentional performance (Broersen & Uylings, 1999; Chudasama & Muir, 2001). During attention, moments before an accurate cue detection, there is a notable decrease in mPFC neuronal activity (Totah et al., 2009), which is thought to reduce the levels of noise to allow mPFC neurons to accurately process the sensory cues and successfully respond (Poorthuis & Mansvelder, 2013). These processes are thought to be mediated by ACh release into the mPFC. Indeed lesions to the source of mPFC ACh in the basal forebrain, leads to impairment in the 5-CSRTT (Muir et al., 1994), and stimulation of these ACh

inputs can enhance attention performance (St Peters et al., 2011). Work from Martin Sarter's laboratory has intricately demonstrated that during cue detection, waves of phasic ACh are released into the mPFC (Parikh et al., 2007) and optogenetic inhibition or excitation of these cholinergic transients leads to impairment or facilitation in cue detection (Gritton et al., 2016).

Studies aiming to investigate the role of nAChRs in these processes indicate that at least some of the attention performance is attributed to α7 nAChRs. Systemic nicotine administration is shown to decrease the number of omissions in the 5-CSRTT in mice which is thought to partially be attributed to α7 nAChRs (Hahn et al., 2011; Young et al., 2004). What's more KO mice of the α7 nAChRs exhibit reduced attention performance compared to WT mice (Young et al., 2007). Moreover, systemic administration of the selective α7 nAChR agonist, RG3487, is shown to enhance performance in a related sustained visual attention task (Rezvani et al., 2009). However the precise involvement of α7 nAChRs is not clear, as other selective α7 nAChR agonists had no effect on attentional performance in the 5-CSRTT (Hahn et al., 2003), and other α7 nAChR KO studies found no impairment in attentional performance (Guillem et al., 2011). These discrepancies have been suggested to be due to differences in the attentional load of the task in which α7 nAChRs may play a more important role.

In addition to attention the mPFC plays important roles in working-memory, which as mentioned previously is the ability to retain and process information for a short time period, to enable the execution of a specific task (Goldman-Rakic, 1995). Working-memory is often assessed via delay response tasks in which presentation of a cue is followed by a delay and then a task related behavioural response. Lesions to the mPFC in the rodent leads to impairment in these working-memory tasks (Kolb et al., 1994). During the delay period of the task, neurons within the mPFC are shown to have recurrent spiking activity, thought to be mediated by the mPFC's microcircuit and interconnectivity with the thalamus and hippocampus (Goldman-Rakic, 1995; Griffin, 2015).

ACh plays an important role in working-memory and there is clear evidence for α7 nAChRs activity during this process. Lesions of the cholinergic inputs to the

PFC reduces working memory performance in non-human primates (Croxson et al., 2011). KO α7 nAChR mice tested in the delayed matching-to-place Morris water-maze and were impaired in comparison to their WT siblings (Fernandes et al., 2006). In addition systemic administration of several α7 nAChR agonists including AR-R1779, GTS-21 and ABT-107 enhances working-memory performance in rats and non-human primates (Bitner et al., 2010; Briggs et al., 1997; Levin et al., 1999). However these systemically administered compounds means the precise role of mPFC α7 nAChRs in working-memory remains uncertain. An interesting finding showed that α7 nAChRs in the dorsolateral PFC in non-human primates could enhance NMDAR mediated currents (Yang Yang et al., 2013). These NMDAR currents have been hypothesised to allow the mPFC neurons to maintain the sustained neuronal activity during working-memory (Goldman-Rakic, 1995), and might implicate mPFC α7 nAChRs in the mechanisms of working-memory.

In addition to attention and working-memory, the mPFC and α7 nAChR activation is implicated in performance in the novel object recognition (NORT) and attention set shifting tasks (ASST), which are cognitive tests for spatial working-memory and cognitive flexibility. In a rodent model of the cognitive deficits in schizophrenia, performance in the ASST is impaired, which is thought to be brought about via mPFC deficits. Interestingly recent data shows that α7 selective agonists, compound A and SSR180711 systemically administered enhanced performance in this task (Wood et al., 2016), whilst others show the same effect with the α7 nAChR PAM, PNU-120596, in both the ASST and NORT (Nikiforuk et al., 2016).

1.5.2 α7 nAChRs implicated in disease

With nAChRs playing a key role in mediating cognitive functions within the mPFC, it is no surprise that nAChRs and in particular α7 nAChRs are also implicated in the cognitive disorders associated with the mPFC shown in table 1.1.

In Alzheimer's disease, a loss of cholinergic tone is observed within the mPFC and the subsequent reduction in nAChR signalling is thought to contribute to the substantial loss of synaptic function within the region (Lombardo & Maskos, 2015). Indeed amyloid-β, one of the candidates mediating major neuronal loss, aggregates most highly in nAChR expressing regions. In addition amyloid-β has a high affinity to the α7 nAChRs, which *in vitro* has been shown to substantially alter α7 nAChR function (Parri et al., 2011; Wang et al., 2000). As a consequence, combatting the altered α7 nAChR activity has become a potential therapeutic target for the treatment of Alzheimer's disease (Vallés et al., 2014).

α7 nAChRs are also heavily implicated in schizophrenia. Mutation in the α7 nAChR subunit gene *CHRNA7* is found in a cohort of schizophrenia sufferers who display an impaired sensory processing phenotype (Leonard & Freedman, 2006), and post-mortem analysis reveals a severe reduction in α7 nAChRs in schizophrenic brains including the PFC (Martin-Ruiz et al., 2003). Added to this is the observation that schizophrenia suffers often consume nicotine (mainly through smoking) which is thought to compensate for the reduced α7 nAChR signalling (D'Souza & Markou, 2012). Indeed, highlighting the role of impaired α7 nAChR signalling is that several proof of concept clinical trials testing α7 nAChR agonists in schizophrenia have had success (Olincy et al., 2006; Preskorn et al., 2014).

Added to this, work from other laboratories (Feng et al., 2011), and ours have found that α7 nAChRs through their effects on synaptic plasticity may be implicated in the process of relapse to drug seeking of addictive drugs such as morphine (Wright et al. 2016 unpublished data). This is demonstrated by the ability of systemic and local infusions of the α7 nAChR antagonist MLA to the hippocampus ability to reduce the level of reinstatement to previously extinguished conditioned place preference to morphine.

1.5.3 α7 nAChRs regulating cellular and network functions

It is clear from animal studies, and in some cases human trials, that α7 nAChRs are implicated in the cognitive processes mediated by mPFC function, whilst α7 nAChRs are also implicated in the etiology or treatment strategy of several neurological diseases. To better understand the involvement of α7 nAChRs in mPFC activity and disease, it is essential to understand how they regulate the complex network interactions within the mPFC. The following sections will describe how, depending on their cellular locations, α7 nAChRs can regulate different cellular functions.

The precise location of the α7 nAChR within the cell often determines its role. α7 nAChRs within the mammalian brain rarely mediate direct fast synaptic transmission within a synapse. Instead α7 nAChRs are most often found presynaptically either just before or within the presynaptic bouton, or postsynaptically on dendrites, axons and the soma of different neuronal subtypes.

As mentioned previously α7 nAChRs have a high permeability to calcium (Fucile, 2004), enabling this receptor to activate cell signaling cascades that far outlast the duration of their fast depolarising currents. Indeed, α7 nAChRs are shown to have a higher (relative) calcium permeability compared to NMDARs (Séguéla et al., 1993). This high calcium permeability allows the α7 nAChRs to partake in a range of cellular processes both pre- and postsynaptically.

1.5.3.1 Presynaptic α7 nAChRs

α7 nAChRs are expressed at, or near, the presynaptic terminal of multiple afferent inputs to various brain regions and this presynaptic location enables α7 nAChRs to alter neurotransmitter release of many different neurotransmitters including ACh (Marchi & Raiteri, 1996; Summers & Giacobini, 1995), dopamine (Luetje, 2004; F. M. Zhou et al., 2001), noradrenaline (Clarke & Reuben, 1996; Westphalen et al., 2009), serotonin (Li et al., 1998; Summers & Giacobini,

1995), glutamate (Gray et al., 1996; Role & Berg, 1996) and GABA (Alkondon et al., 1997; Léna & Changeux, 1997). Vesicular neurotransmitter release is intricately linked with the level of presynaptic calcium and α7 nAChRs bring about increases in presynaptic calcium in multiple ways. In mossy-fibre terminals of the hippocampus the direct calcium influx through α7 nAChRs alone has been shown to be sufficient to induce transmitter release (Gray et al., 1996). In addition presynaptic calcium influx through α7 nAChRs can be further increased via initiating calcium induced calcium release via both ryanodine, and IP_3 receptors on the endoplasmic reticulum, both mechanisms of which have been shown to enhance transmitter release (Dajas-Bailador et al., 2002; Sharma & Vijayaraghavan, 2003; Cheng & Yakel, 2014). And finally, the depolarising nature of the α7 nAChR current is able to activate VOCC which provides another method of enhancing transmitter release (Dajas-Bailador et al., 2002; Rathouz & Berg, 1994; B.-W. Wang et al., 2006). The increase in presynaptic calcium mediated via these mechanisms is able to trigger transmitter release directly but can also modulate transmitter release via activation of signaling molecules, with presynaptic α7 nAChR activity linked with PKA, CAMKII and the ERK/MAPK pathways that can directly mediate changes in presynaptic release machinery (Cheng & Yakel, 2014; Dickinson et al., 2008; Sharma et al., 2008; B.-W. Wang et al., 2006).

1.5.3.2 Postsynaptic α7 nAChRs

Postsynaptic expression of α7 nAChRs mediate a variety of cellular functions on multiple timescales. The immediate effect of activation of the cationic α7 nAChRs is the direct depolarisation of the postsynaptic neuron and, although cholinergic synapses are rare, α7 nAChRs are found within both GABA and glutamate synapses (Lendvai & Vizi, 2008), enabling these receptors to directly contribute to synaptic depolarisation, whilst α7 nAChRs expressed on both the soma and dendrites of neurons can also contribute to membrane potential and signal integration (McKay et al., 2007).

In addition to the direct role of α7 nAChRs in influencing neuronal excitability, the receptor's calcium permeability enables them to also modulate neuronal signaling across a longer timescale. Activating cell signaling cascades and modulating gene transcription enables α7 nAChR to engage in multiple neuronal processes such as learning and memory and neuroprotection (Dajas-Bailador et., 2002). For example selective α7 nAChR agonist PNU-282987 has been shown to increase expression of the immediate early gene *c-fos* in the rat frontal cortex (Hansen et al., 2007), whilst in PC12 cells the same agonist in combination with the α7 nAChR PAM PNU-120596 activates the ERK/MAP pathway via CAMKII activation, leading to increases in phosphorylated CREB a key transcription factor implicated in learning and memory (Gubbins et al., 2010; Kouhen et al., 2009). α7 nAChRs are also play a role in neuroprotection, where activation of α7 nAChRs leads to activation of PI3K, Akt and consequently Bcl-2 and also via activation of JAK-2/Stat-3 pathway ultimately leading to cell survival (Arredondo et al., 2006; Kihara et al., 2001). α7 nAChRs involvement in such cellular processes has led to α7 nAChRs becoming therapeutic targets for neurological diseases such as Parkinson's and Alzheimer's disease (Dineley et al., 2015; Quik et al., 2015).

1.5.4 Location of α7 and non-α7 nAChRs in the rodent mPFC

The cellular function of α7 nAChRs largely depends on the neuronal compartment in which they are expressed, but the overall effect on network function also depends on which type of neuron they are expressed on. Within the mPFC both heteromeric α4β2 and homomeric α7 nAChR are expressed (Fig. 1.9), and multiple studies have aimed to elucidate the cell types that express certain nAChRs. The general approach to determine their location has been to record from different cell types from different layers whilst either globally or locally applying non-selective nAChR agonists, alone, or in the presence of selective nAChR antagonists or using subtype selective KO mice.

Within layer I all inhibitory interneurons (predominantly NFS interneurons) are sensitive to activation of both α7 and non-α7 nAChRs (Christophe et al., 2002).

Within layers II/III α7 nAChRs are found somatically expressed on FS and NFS inhibitory interneurons whilst α4β2 nAChRs are found on NFS and somatostatin expressing interneurons (Poorthuis et al., 2012). Within layer V, α7 and α4β2 nAChRs are expressed on NFS interneurons whilst FS interneurons only possess α7 nAChRs, however the expression of nAChRs on FS interneurons has not been observed by others (Couey et al., 2007; Gulledge et al., 2007) so their location here is still uncertain. In contrast to interneurons, pyramidal neurons within layer II/III do not express nAChRs, and in layer V α7 nAChRs have been shown to be expressed on the soma and dendrites of layer V pyramidal neurons (Poorthuis et al., 2012), but again this has not been oberved by others (Hedrick & Waters, 2015). Within layer VI only α4β2 nAChRs are found on inhibitory interneurons whilst pyramidal neurons posses both α4β2 and α4β2α5 receptors (Proulx et al., 2014).

In addition to somatically expressed nAChRs, nAChRs are also shown to be expressed presynaptically. Aracri et al., (2010), demonstrate that heteromeric nAChRs, presumably α4β2 nAChRs, are expressed presynaptically on interneuron terminals to both pyramidal neurons and other interneurons. And others have shown that α4β2 nAChRs are expressed on thalamic inputs to the mPFC (Lambe et al., 2003). The expression of presynaptic α7 nAChRs within the mPFC is uncertain, the majority of electrophysiology studies have found no evidence for presynaptic α7 nAChRs (Aracri et al., 2013; Lambe et al., 2003; Poorthuis et al., 2012) although see (Lench et al., 2008), whilst other biochemical methodologies have provided evidence for presynaptic α7 nAChRs (Dickinson et al., 2008; Lubin et al., 1999).

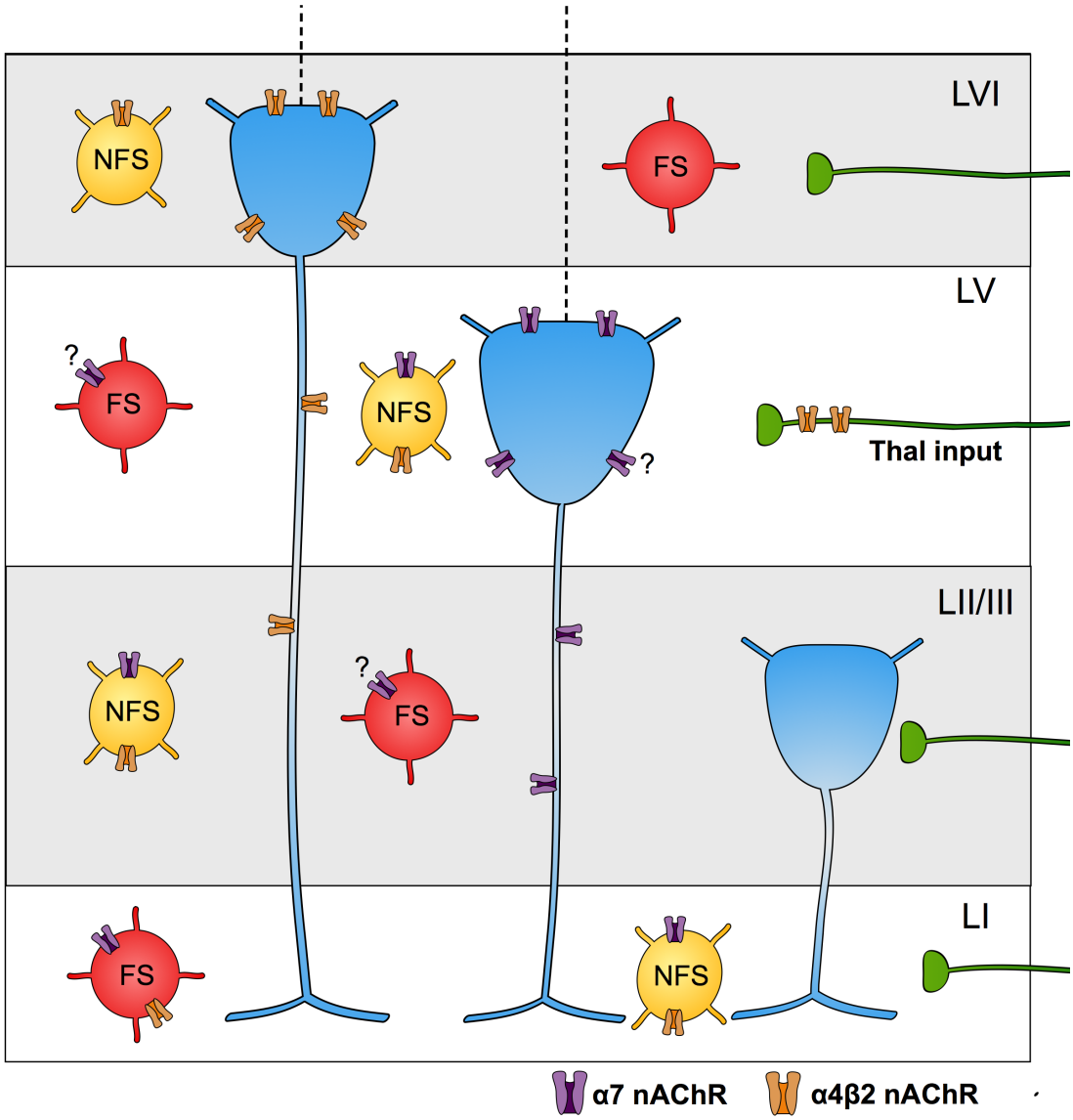

Figure 1.9 nAChR location within the mPFC

Location of $\alpha 7$ and $\alpha 4\beta 2$ nAChRs within the prelimbic cortex. Homomeric $\alpha 7$ nAChRs are found on non-fast-spiking (NFS) and fast-spiking (FS) inhibitory interneurons within all layers except layer VI and are also found on layer V pyramidal neurons. Heteromeric $\alpha 4\beta 2$ nAChRs are found in all NFS interneurons and layer VI pyramidal neurons and also on layer I FS interneurons and expressed preterminally on inputs from the thalamus. Question mark (?) represents findings that have not been replicated by some studies, and so localisation remains uncertain.

1.5.5 α7 nAChR and non-α7 nAChR regulation of the mPFC network activity

As described and seen in figure 1.9 nAChRs within the mPFC network are expressed on both excitatory pyramidal neurons and terminals, but also on inhibitory GABAergic interneurons across all layers. With this information, it would appear that ACh regulation of the mPFC network appears to be complex. Another level of complexity comes from the different modes of cholinergic release within the cortex, with both volume transmission and phasic release thought to be important (Sarter et al., 2009).

Studies that have investigated the effect of global administration of ACh or nicotine to the mPFC network have shown that a key effect is an enhancement in excitatory glutamate release. Nicotine and ACh have both been shown to increase spontaneous release of glutamate onto layer V pyramidal neurons (Lambe et al., 2003), thought to mediated via preterminal α4β2 nAChRs on thalamic inputs rather than presynaptic α7 nAChRs. Others have also shown that ACh enhanced spontaneous glutamate release onto layer V and layer VI pyramidal neurons, but had no effect at layer II/III neurons (Poorthuis et al., 2012). Pyramidal neurons in layer V-VI also contain postsynaptic nAChRs, which are not found in pyramidal neurons in more superficial layers. Thus it appears that ACh acting at nAChRs has the overall effect of promoting excitation predominantly in deeper layers of the cortex.

Matters are made more complex when we consider the activity of inhibitory interneurons in response to nAChRs activation. ACh and nicotine application directly excites interneurons within layer I via postsynaptic α4β2 and α7 nAChRs (Christophe et al., 2002), whilst nicotine also increases spontaneous glutamatergic input to these neurons (Tang et al., 2015). Layer V FS and NFS interneurons also receive increased glutamatergic input upon addition of nicotine (Couey et al., 2007). The postsynaptic nAChRs on inhibitory interneurons means that they can be activated directly by ACh, although ACh preferentially activates NFS rather than FS interneurons (Christophe et al., 2002; Gulledge et al., 2007). This ACh induced activation of interneurons consequently leads to inhibition of pyramidal neurons, via enhanced

spontaneous inhibitory currents onto layer II/III and V pyramidal neurons, but not layer VI pyramidal neurons (Poorthuis et al., 2012).

The overall pattern of activation in response to nAChR activation is an increase in excitatory input to deep cortical layers and a recruitment of inhibitory interneurons that predominantly inhibit superficial pyramidal neurons and layer V pyramidal neurons. Poorthuis et al., (2012), demonstrate this by observing layer specific activation via single cell calcium signaling in response to bath applied ACh. Poorthuis et al., show that the net consequence is predominant excitation of pyramidal neurons in deep layers but not superficial layers. In this regard it is hypothesised that ACh's role, via recruitment of interneurons, is to inhibit superficial pyramidal neurons, that send and receive intra-cortical connections, thus filtering out inputs to 'reset' the network and allow processing of inputs from subcortical structures such as the thalamus (Kruglikov & Rudy, 2008; Poorthuis et al., 2012).

Much more research is needed to understand the role of nAChR activation in regulating the cortical network. The use of non-selective nAChR agonists in these studies means the individual contribution of α7 nAChRs in regulating mPFC network activity is still not clear, and global activation of agonists provides little information on nAChRs response to endogenously released ACh. But what is clear is that nAChRs play a key role in shaping the neuronal network of the mPFC.

1.6 α7 nAChR mediated synaptic plasticity

As mentioned in section 1.3, neurons within the mPFC are able to undergo synaptic plasticity, in the forms of both LTP and LTD. The critical factor determining synaptic plasticity within these regions is the elevation of calcium, predominantly in the postsynaptic neuron. We have seen so far in this introduction that α7 nAChRs are unique in having a high permeability to calcium, comparable to that of the NMDAR. This gives α7 nAChRs the opportunity to modulate the levels of synaptic plasticity in various ways, either

by directly contributing to the levels of postsynaptic calcium through postsynaptic expression, by increasing excitatory transmitter release via their presynaptic expression or by regulating the levels of inhibition via their expression on interneurons.

α7 nAChRs involvement in synaptic plasticity has been realised in several brain regions, but the role α7 nAChRs play in modulating plasticity within the mPFC is less clear. The mechanisms by which α7 nAChRs, can modulate synaptic plasticity within other brain regions will be highlighted below followed by what is known about α7 nAChRs contribution to mPFC plasticity.

1.6.1 α7 nAChR mediated plasticity within other brain regions

Within the VTA, α7 nAChR activation has been shown to induce LTP at glutamatergic synapses on dopaminergic neurons. 24 hours following a systemic administration of nicotine resulted in an up regulation of AMPARs within DA neurons which was both α7 nAChR and NMDAR dependent (Gao et al., 2010). Follow up experiments from the same laboratory showed exposure of VTA brain slices to nicotine also led to increases in the AMPA/NMDA receptor ratio and paired pulse ratio in DA neurons - an effect absent in the presence of an α7 nAChR antagonist and in α7 KO mice (Jin et al., 2011). These studies, along with others, demonstrate that α7 nAChRs expressed presynaptically on glutamatergic terminals increases the levels of glutamate available to activate NMDARs and thereby enhance the levels of LTP (Jin et al., 2011; Mao et al., 2011; Mansvelder & McGehee, 2000).

Similar observations have been shown in the hippocampus. The selective α7 nAChR agonist SSR190711 enhanced the levels of LTP at Schaffer collateral to CA1 synapses (Kroker et al., 2011). Furthermore, application of ACh to dendrites of CA1 pyramidal neurons resulted in an increase in miniature excitatory post synaptic current (mEPSC) frequency, that when paired with postsynaptic depolarisation could induce LTP in a subset of cells, an effect presumed, but not tested, to be mediated by presynaptic α7 nAChRs (Ji et al.,

2001). Similar observations have been found for presynaptic α7 nAChRs at mossy fibre terminals. Selective activation of α7 nAChRs with a selective agonist led to an increase in glutamate release via an α7 nAChR induced increase in presynaptic calcium leading to enhanced postsynaptic activity of CA3 neurons (Cheng & Yakel, 2014). These presynaptic α7 nAChRs at mossy fibre terminals can also induce short-term plasticity in a presynaptic mechanism that involves activation of presynaptic CAMKII (Sharma et al., 2008).

In addition to modulating transmitter release α7 nAChR's calcium permeability means the receptor can also directly contribute to the levels of postsynaptic calcium and thus modulate LTP via postsynaptic mechanisms. Ji et al., (2001) show that, at the Schaffer collateral - CA1 synapse, direct application of ACh to the soma of CA1 pyramidal neurons evoked an α7 nAChR mediated current. When this α7 nAChR current coincided with pre- and postsynaptic glutamate signalling a short-term plasticity was converted into long-term plasticity. Findings that highlight the increased calcium through α7 nAChRs can directly contribute to the mechanisms of LTP (Ji et al., 2001). Other studies have also demonstrated this, and shown that both pre- and postsynaptic α7 nAChRs at CA3-CA1 synapses are required for induction of a postsynaptic calcium and NMDAR dependent, short- and long-term plasticity (Gu et al., 2012).

Via their calcium permeability it is clear that α7 nAChRs can directly enhance the levels of LTP by either directly or indirectly increasing the level of postsynaptic calcium. However, as mentioned above, α7 nAChRs are also not restricted to expression within excitatory neurons and are also found within inhibitory neurons. Therefore, α7 nAChRs by activating inhibitory interneurons can promote the inhibition of the postsynaptic neurons undergoing synaptic plasticity and thus modulate the levels of LTP. This idea is supported by studies in the hippocampus, Ji et al., (2001) show that ACh applied to interneurons results in inhibition of nearby CA1 pyramidal neurons. If this interneuron activation coincides with weak and strong LTP induction then short-term plasticity could be blocked and long-term potentiation reduced respectively. Although the nAChR subtype mediating this interneuron mediated effect was

not tested in this study, subsequent studies have demonstrated that CA1 interneurons readily express somatic α7 nAChRs (Kalappa et al., 2010).

1.6.2 α7 nAChR mediated plasticity within the mPFC

With numerous studies highlighting the role of α7 nAChRs in other brain regions, few studies have provided direct evidence that α7 nAChRs in the mPFC can modulate synaptic plasticity. As mentioned in section 1.3.3 the mPFC shares many of the mechanisms of LTP that have been investigated in the hippocampus, namely a Hebbian coincident activation, postsynaptic calcium elevations and NMDAR dependence. In this regard it is not unreasonable to predict that α7 nAChRs within the mPFC may also be involved in regulating mPFC synaptic plasticity. Several studies have provided evidence for a potential involvement for α7 nAChR regulation of plasticity but none have demonstrated a direct role for α7 nAChRs. The studies that have investigated this have focussed on nAChRs in general and have not distinguished between receptor subtypes.

1.6.2.1 α7 nAChR modulation of mPFC LTP

The involvement of nAChRs in general in mPFC plasticity has been provided by studies in which nicotine has been systemically administered to rodents. Brunzell et al., (2003) demonstrated that chronic nicotine exposure in mice resulted in increases in phosphorylated CREB and ERK, two key proteins regulated during the process of synaptic plasticity. Others have shown that acute systemic administration of nicotine leads to increased levels of Arc and c-Fos mRNA in adult and adolescent rat mPFC, demonstrating nicotine can induce increased transcription of plasticity related-genes (Schochet et al., 2005). Alterations in mPFC synaptic plasticity in response to nicotine exposure has also been measured with electrophysiology. Goriounova & Mansvelder, (2012b) demonstrated that chronic nicotine exposure in adolescent rats leads to

a short-term decrease and long-term increase in spike timing dependent plasticity (STDP) in layer V pyramidal neurons. Others have shown that intracerebroventricular injections of nicotine in rats can enhance the levels of LTP within the thalamus-mPFC pathway *in vivo* (Bueno-Junior et al., 2012). Finally, recent human studies show that nicotine administered to patients via patches, could reduce the levels of transcranial direct current stimulation (tDCS)-induced LTP in a calcium dependent manner, although this was in the nearby motor cortex (Lugon et al., 2015).

Based on these studies nicotine appears to play a role in mPFC plasticity, although the findings appear to be complex with both increases and decreases in plasticity in response to nicotine. What none of the above studies have attempted is to elucidate is the roles played by specific nAChR subtypes, and so the involvement for α7 nAChRs in mPFC plasticity remain uncertain. One study that does attempt to differentiate between receptor subtypes is the study by Couey et al., (2007). Couey and colleagues found that nicotine increases the threshold for spike timing dependent plasticity within layer V pyramidal neurons within the mPFC. Nicotine, administered to the slice, converted LTP into LTD in a mechanism dependent on nAChRs expressed on inhibitory interneurons. Similar to mechanisms shown in the hippocampus (Ji et al., 2001), activation of inhibitory interneurons resulted in increased inhibition of pyramidal neurons, which Couey and colleagues demonstrate led to decreased levels of dendritic calcium and thus reduced plasticity. The nicotine-induced inhibition of pyramidal neurons and reduction in LTP, was brought about by increases in spontaneous inhibitory post synaptic currents (sIPSCs) onto these neurons. In an attempt to determine which nAChR subtype was responsible, experiments measuring sIPSCs were conducted in the presence of the α7 nAChRs antagonist MLA and the global nAChR antagonist MEC. In these experiments MLA only prevented nicotine's effect on sIPSCs in 1 of 4 neurons, whilst MEC prevented the effect in 5 of 7 neurons tested. The authors go onto suggest that nicotine brings about its effect on LTP via a mixed population of both α7 nAChRs and other nAChRs.

Even after considering this study it still seems unclear what roles α7 nAChRs partake in mPFC plasticity. What remains uncertain is if α7 nAChRs alone can alter mPFC LTP or whether other receptor subtypes are required, and it is also

not known if the effects shown by Couey and colleagues represent the effects mediated by endogenous ACh or are unique to the exogenous agonist nicotine.

1.6.2.2 α7 nAChR modulation of mPFC LTD

Few studies have been carried out to investigate a role for α7 nAChRs in LTD. Within the hippocampus CA1 region, ACh applied onto the dendrites of CA1 pyramidal neurons acts at nAChRs to produce LTP or LTD in an NMDAR dependent manner, with the timing of ACh application critical for the induction of either LTP or LTD (Ge, 2005). Others show in the CA3-CA1 synapse that nicotine can enhance the levels of LFS induced LTD, in a mechanism dependent on α7 nAChRs but also non-α7 nAChRs. Interestingly the same group also show that the α7 nAChR antagonist MLA alone can reduce the levels of LTD, suggesting that endogenous signalling through the α7 nAChR can prevent LTD formation (Fujii & Sumikawa, 2001; Nakauchi & Sumikawa, 2014).

Within the mPFC the same study that showed that nicotine can enhance the thalamic-mPFC LTP *in vivo* also found that nicotine suppressed the formation of LTD, although the involvement of α7 nAChRs was not determined (Bueno-Junior et al., 2012). Further, as mentioned above, both Couey et al., (2007) and Goriounova & Mansvelder, (2012b) show that nicotine converts spike timing dependent LTP into LTD, but again the involvement of α7 nAChRs is unclear.

Overall, even though α7 nAChRs have the clear potential in modulating network activity and synaptic plasticity within the mPFC, their precise effects in the mPFC are yet to be elucidated. Many studies have researched the effects of nAChR activation in network activity and plasticity but have focused on the effects of nicotine, principally due to its link with cigarette smoking. However in doing so, the individual contributions of nAChR subtypes have been difficult to ascertain. Studying the effects of nicotine is of course of importance to increase our understanding of the effects of cigarette smoking. However understanding how endogenous ACh release acting at α7 nAChRs can regulate network

activity and plasticity is also important to increase our understanding of the physiological roles of ACh release. Defining a role for α7 nAChRs in these processes and how they might be regulated by endogenous ACh is not only important for our basic understanding of the functioning of the PFC, but also in our understanding of how α7 nAChRs may be involved in the disease states in which α7 nAChR signalling is compromised. With these considerations in mind the aims of this thesis are detailed below.

1.7 Thesis aims

Test the hypothesis that prelimbic cortex synaptic plasticity can be modulated by activity at α7 nAChRs. This was investigated via the use of extracellular field recordings and stimulus-induced synaptic plasticity within the prelimbic cortex, in response to an array of selective α7 nAChR compounds.

To investigate in detail how the activity at α7 nAChRs can influence excitatory and inhibitory neurotransmission within the prelimbic cortex. This was investigated by performing whole-cell patch clamp experiments, primarily in layer V pyramidal neurons and measuring excitatory and inhibitory neurotransmission onto these neurons in response to α7 nAChR activation and antagonism.

To determine a more precise localisation for α7 nAChRs within the prelimbic cortex network. This was carried out using whole-cell patch clamp electrophysiology in combination with pharmacology, and optogenetics.

Chapter 2:

Methods

Chapter 2: Methods

2.1 Animal housing and welfare

Male wildtype C57BL/6J mice were used for the majority of the experiments in this thesis and were bred at the University of Bath. In some electrophysiology experiments male transgenic GAD67-GFP C57BL/6J mice were used (Tamamaki et al., 2003). These mice bred at the University of Bath were hemizygous for the transgene and were genotyped from wildtype littermates at birth with a non-invasive visualisation of brain fluorescence. Both wildtype and transgenic mice were weaned at P21 and then housed in cages of 4 mice. Mice were housed in a 12 hour light/dark cycle (lights on at 6am) with unlimited access to food and water with cages cleaned weekly. For the majority of electrophysiology experiments mice were used at between 5-6 weeks old.

All protocols and procedures were carried out in accordance with the UK Animals (Scientific Procedures) Act 1986, the European Communities Council Directive 1986 (86/609/EEC), the ARRIVE guidelines (Kilkenny et al., 2010) and the University of Bath ethical review document. All efforts were made to minimise animal suffering and to limit the number of animals used.

2.2 Brain slice preparation

Male C57BL/6 mice, were anaesthetised via intraperitoneal injection of 160 mg/kg ketamine and 20 mg/kg xylazine and then decapitated. Brains were immediately removed and submerged in ice-cold cutting solution saturated with 95% O_2/ 5% CO_2. Coronal brain slices (285 μm thickness for patch clamp recordings and 350–400 μm thickness for field recordings), 1.54-2.34 mm anterior to bregma) containing the mPFC were obtained using a vibratome (DSK, DTK-1000). The two hemispheres of the brain slice were then separated with a razor blade and then incubated at 32 °C for 30 min in artificial cerebrospinal fluid (aCSF) saturated with 95% O_2/ 5% CO_2. Slices were

maintained at room temperature for at least a further 30 min before commencing the experiment.

Experiments in which a hippocampal-cortical pathway was stimulated required coronal slices cut at an approximate 10° angle (Parent et al., 2010) achieved manually when dissecting the PFC. 285 μm coronal brain slices were prepared as above, and slices containing the hippocampal afferent fibre bundle used for these experiments.

For optogenetic experiments brain slices were prepared from older (9-12 week old) mice. In these mice 285 μm brain slices were prepared in ice-cold cutting solution saturated with 95% O_2/ 5% CO_2. The two hemispheres of the brain slice separated and then incubated at 35 °C in a protective recovery, NMDG solution (Ting et al., 2014), for approximately 5 min this overcame poor slice health obtained from older animals using conventional slicing techniques mentioned above. Slices were then held at room temperature for at least 1 hour in aCSF saturated with 95% O_2/ 5% CO_2 before experimentation. For each optogenetic experiment, 300 μm brain slices containing the injection site were also prepared and visualised under fluorescent microscopy to determine the accuracy of the injection location (see Section 2.5).

2.3. Extracellular field recordings

Individual slices (350-400 μm) were transferred to a humidified interface recording chamber with a continuous flow rate of 1.5-2 ml/min aCSF saturated with 95% O_2/ 5% CO_2 at 35 °C. Recording electrodes with a 2-5 MΩ resistance were filled with aCSF and placed in the layer V region of the prelimbic cortex. A Teflon coated platinum/iridium bipolar stimulating electrode (FHC) 125 μm tip diameter with a 150 μm tip separation was placed perpendicular to the midline in layer II/III of the prelimbic cortex.

Field excitatory post synaptic potentials (fEPSPs) were evoked via 0.1 ms square current pulse, generated by a MASTER-8 (A.M.P.I.) pulse generator and

delivered via a constant current stimulation isolation unit (DS2A, Digitimer). Stimuli were initially evoked at 0.2 Hz until a suitable fEPSP was obtained, which was sufficiently separated from the stiumulation artefact and had a clear monosynapic downward phase that was not contaminated with a population spike. On acquiring a suitable fEPSP they were evoked at 0.05 Hz to minimise synaptic fatigue. A current intensity response curve was conducted for each experiment and a stimulus intensity that gave 50% maximum response was used for the entire recording. fEPSPs were recorded via an Axoclamp-2A amplifier (Axon Instruments) and digitised at a sample rate of 10 kHz (CED Micro 1401 analogue-digital converter).

The linear gradient, 20 – 80 % of the downward slope, of the fEPSP was used as a measure of the fEPSP magnitude. For all fEPSP plasticity experiments a 20 min stable baseline was recorded ensuring no continuous increase or decrease in the fEPSP slope. Long-term potentiation (LTP) was induced via a high frequency theta burst stimulation (4 bursts 10 s apart, each burst contained 7 trains 140 ms apart, each train contained 4 pulses at 100 Hz.). Long-term depression (LTD) was induced via a low frequency tetanus at 3 Hz for 15 min (total of 2700 stimuli) (Fig. 2.1).

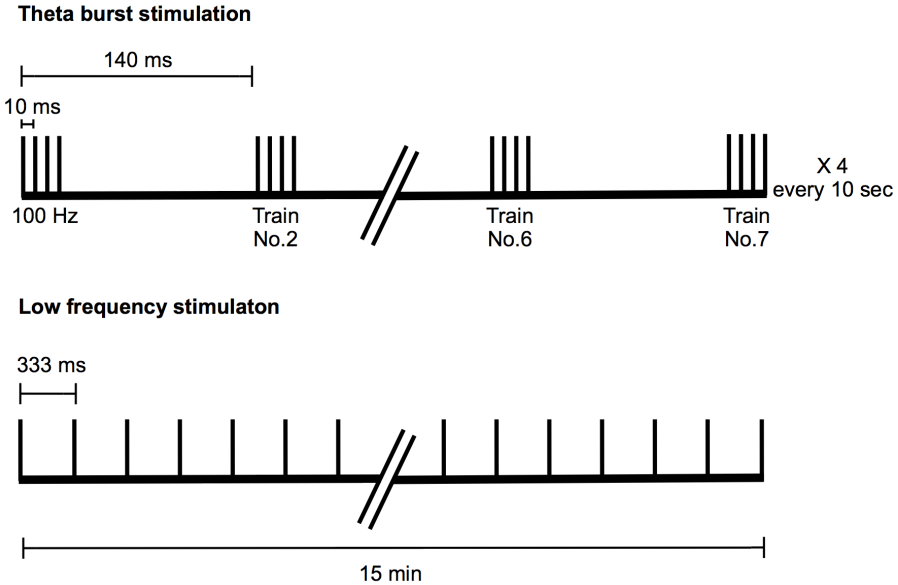

Figure 2.1 Theta burst and low frequency stimulation used for synaptic plasticity induction

Theta burst stimulation used to induce LTP was repeated 4X unless otherwise stated. 3 Hz low frequency stimulation was used to induce LTD. Vertical lines represent a single square pulse of 0.1 ms.

2.4 Whole cell patch-clamp experiments

Slices (285-300 µm) were transferred to a submerged chamber with a continuous flow rate of 2-3 ml/min aCSF saturated with 95% O_2/ 5% CO_2 at 32 °C. Slices were visualised using oblique optics on an Olympus BX51WI upright microscope. Prelimbic layer V pyramidal neurons were identified as being approximately 300-500 µm from the slice midline and possessing a pyramidal neuron morphology (Van De Werd et al., 2010). Recording electrodes with a 2-5 MΩ resistance were fabricated using a micropipette puller (Sutter-instruments, P-97). For the Whole cell voltage clamp recordings, intracellular recording solution A was used and for current clamp recordings intracellular solution B was used (section 2.10). Recordings were amplified and filtered at 2 kHz (Axopatch 200A amplifier, Axon Instruments), and digitised with a sampling rate of 10 kHz (Digidata 1440 A, Axon Instruments). For all patch clamp experiments, series resistance was measured throughout experiments and data were excluded if series resistance changed by 25%. For intracellular solution A, a liquid junction potential of ~12 mV was calculated using pCLAMP software (Axon instruments) and accounted for during the experiments.

2.4.1 Spontaneous and miniature current recordings

All recordings of spontaneous and miniature excitatory post-synaptic currents (EPSCs) and inhibitory post-synaptic currents (IPSCs) unless stated, were performed in the absence of GABAergic or glutamatergic blockers, to ensure the continued presence of local network activities. To achieve this, holding voltages were alternated throughout the recordings from -60 mV to 0 mV (respectively the reversal potentials of $GABA_A$ and AMPA receptor-mediated currents) (Semyanov & Kullmann, 2000). For spontaneous and miniature EPSC and IPSC experiments, drugs were bath applied via perfusion to the slice for at least 5 min before a 1 min analysis of spontaneous currents for each drug application. A 5 min drug application was deemed a sufficient incubation time based on previous experiments in which drugs applied as positive controls elicited a maximum response within a minute of bath application. Miniature

EPSCs and IPSCs (mEPSC, mIPSC) were recorded in the presence of the Na^+ channel antagonist tetrodotoxin (TTX, 1 μM) to block network activity and action-potential-driven neurotransmitter release.

2.4.2 Evoked EPSC recordings

Stimulated EPSCs were evoked via a stimulus pulse (0.05 Hz, 0.15 ms) using a teflon coated platinum/iridium bipolar stimulating electrode (FHC) 125 μm tip diameter with a 150 μm tip separation placed in layers II/III. Stimuli were generated by WinWCP software and delivered via a constant current stimulation isolation unit (DS2A, Digitimer). Stimulus intensities that gave 25-50% maximum response were used for the entire recording. Responses were then averaged to give an average response per minute. Evoked EPSC paired pulses were evoked via paired stimulus pulses with an interstimulus interval of 50 ms, at least 10 responses were then averaged and paired pulse ratio calculated as the amplitude of peak 2 / the amplitude of peak 1. For experiments involving the activation of the hippocampal-mPFC afferent fibre bundle a custom bipolar stimulating electrode was fabricated from a fine (50 μm diameter) Teflon coated tungsten wire to give a tip separation of approximately 50-100 μM. For these experiments the stimulating electrode was placed across the fibre bundle and single stimuli evoked as above. For all stimulated recordings neurons were held at -60 or -70 mV.

2.4.3 Current clamp recordings of inhibitory interneurons

Whole cell current clamp recordings of interneurons were conducted in brain slices obtained from transgenic GAD67-GFP C57BL/6 mice. These experiments conducted on an Olympus BX51WI upright microscope with an Olympus U-LH100HG fluorescent light source under DIC optics. Layer V inhibitory interneurons were identified via their GFP fluorescence and position relative to the midline. Recorded interneurons were further characterised by a series of 10

300 ms current steps starting at -150 pA in increments of +50 pA. Fast spiking and non-fast spiking inhibitory interneurons were then identified via inspection of their firing frequency to a +150 pA depolarising current step. Interneurons were held at their resting membrane potential for the duration of the experiment and drugs were perfused onto the slice for at least 5 min before changes in membrane potential were measured. Membrane potential changes were calculated as an average baseline membrane potential in the absence of action potentials for the final minute of drug application. Cells were discarded if their resting membrane potential before drug application was higher than -60 mV.

2.4.4 Optogenetic electrophysiology recordings

To evoke optogenetic dependent release of glutamate within the slice, LED light with a wavelength of 475nM was delivered to the underside of the slice. The custom designed light source consisted of a round glass lensed LED (Thor labs) attached to micromanipulator positioned between the microscope condenser and coverslide containing the sample. The LED provided a broad aperture of light (roughly 5 mm diameter) directed to the apical side of the recorded neuron. Light stimuli were generated via a computer (WinWCP software) connected to an LEDD1B, LED variable current driver (Thor labs) used to control light intensity. For initial experiments conducted at Vrije University, light evoked EPSCs were evoked via a fluorescent light source directed through the objective of a Olympus BX51WI microscope using an optical shutter and driver VCM-D1 (Uniblitz) connected to a computer controlled by pClamp software (Axon).

For all optogenetic whole-cell voltage clamp recordings experiments, light evoked EPSCs were evoked at 0.05 Hz via a 2-5 ms square light pulse. Light intensity was adjusted and where possible area of illumination to the slice altered to minimise polysynaptic responses. In all cases in which a light intensity response curve was obtainable, a light intensity that gave a response approximately 50% of maximum was used for the remainder of the experiment. For the majority of optogenetic recordings intracellular solution A was used, all

neurons were held at -60 or -70 mV, in the absence of $GABA_A$ receptor blockade.

2.5 Optogenetic viruses

Several optogenetic viruses were used for optogenetic activation of glutamate release these include:

AAV2/8-Syn-ChrimsonR-tdTomato – red shifted opsin activated with red light 660 nm under the synapsin promoter (used for pan-neuronal expression) with tdTomato fluorescent reporter.
AAV5-CamKIIa-hChR2-EYFP – second generation (H134R) channel rhodopsin under the calmodulin dependent kinase IIα promoter (used for expression in excitatory pyramidal neurons) activated with blue light at 450 nm with a eYFP fluorescent reporter.
AAV5-CAG-ChR2-GFP – First generation channelrhodopsin under the ubiquitous synthetic CAG promoter (used for high levels of gene expression in mammalian cells) activated with blue light at 450 nm with GFP as a fluorescent reporter.

2.6 Optogenetic surgeries

4-5 week old male wildtype C57BL/6J mice were used for all optogenetic surgeries. Mice were weighed at the start of surgeries and then anaesthetised with isoflurane, mice had fur removed from the scalp and were then mounted onto a stereotaxic frame (Kopf) under continuous anaesthesia with isoflurane. Mice were administered the non-steroidal anti-inflammatory drug, carprieve 5 mg / kg s.c. for pain relief, the eye lubricant, Lacrolube ointment (Allergan) to eyes and local anaesthetic cream (ELMA cream) to the incision site. Once under suitable levels of anaesthesia tested via pedal reflex an incision was made, and lambda and bregma co-ordinates were calculated to ensure mice were positioned with a flat skull within the stereotaxic frame. Each mouse underwent a unilateral (mPFC) or bilateral (all other brain regions) injection into

a single brain region. The following injection site co-ordinates in mm relative to bregma, were used based on the co-ordinates of a mouse brain atlas (Paxinos & Franklin, 2004): ventral hippocampus: AP -3.3, ML ±3.25, DV-3.7. BLA: AP -1.5, MV ±2.75, DV -4.7. Thalamus: AP -1.8, ML ±0.6, DV -3.6. mPFC: AP +1.9, ML ±0.6, DV -2.3. VTA: AP +3.1, ML ±0.5, DV -4.5. A 35g bevelled NanoFil stainless steel needle (WPI) connected via tubing to a 10 μl Nanofil syringe (WPI) was backfilled with virus. Burr holes ~1 mm diameter, were drilled in the skull at the calculated injection site and injection needle inserted to the desired brain co-ordinate. 0.5 μl of virus (per injection site) was perfused over 5 min using the automated syringe pump (Harvard apparatus) and allowed to diffuse for an additional 5 min before the injection needle was slowly retracted. After injections were completed, the skull was cleaned, the incision closed with sutures and iodine wound spray applied. Mice received 0.1 ml / 10 g s.c. saline to prevent dehydration and were allowed to recover from anaesthesia in a clean cage under careful supervision. Mice were monitored and weighed post operatively and every day thereafter for a minimum of 7 days to ensure successful recovery. Mice were re-housed in groups of 4, 2 days post-operatively, until use for electrophysiology experiments approximately 4-6 weeks later.

2.7 Brain slice fixation and imaging

Brain slices used for fluorescent imaging were obtained via vibratome slicing as described in section 2.1. 100-300 μm slices were transferred to a 24 well plate, fixed in 4% paraformaldehyde (PFA) for > 24 hrs at 4 °C. PFA was removed and replaced with phosphate buffered saline (PBS) 3 times and washed via agitation for at least 45 min, replacing PBS every 15 min. Slices were then mounted onto coverslides with a 9:1 glycerol:PBS mounting media containing 5 mg / ml ascorbic acid pH 8.5 to prevent fluorescent quenching. For wide-field fluorescent imaging of injection sites and interneuron fluorescence individual images were taken at 5x or 10x magnification using a Leica DMI4000 B inverted microscope and post-hoc stitched together using Autopano giga 2.9 (KOLOR) software.

2.8 Materials

Methyllycaconitine (MLA), donepezil, TTX and 6,7-dinitroquinoxaline-2,3-dione (DNQX) were purchased from Abcam Scientifica. PNU-120596 and PNU-282987 were provided by Pfizer Inc. USA. All other drugs and compounds were purchased from Sigma Aldrich. All viruses used were purchased from Penn Vector Core (University of Pennsylvania).

2.9 Data analysis

All electrophysiological data were acquired and analysed using WinEDR and WinWCP software (Strathclyde University). fEPSP and eEPSC mean baseline was calculated by averaging the final 5 min time points of the baseline before theta burst stimulation or drug application, and used to normalise the data. fEPSP and eEPSC data were excluded if baseline recordings showed an obvious increase or decrease in response over time. For LTP/LTD data statistical comparison was made between conditions at a single time point 60 min post theta burst/low frequency stimulation. Changes in evoked EPSCs upon prolonged drug application were statistically compared between time point 10 min (control) and 40 min (drug). For all hippocampal fibre and optogenetic evoked EPSC experiments average EPSC values were taken as an average of all traces across the entire 10 min drug application. Rise times and rate of rise were measured between 10 – 90% of the rising phase of the EPSC whilst decay times were analysed as time taken to 50% decay. For comparison of light evoked monosynaptic responses from different afferent fibres, an average monosynaptic trace for each cell was generated and tau decay measured by fitting a single decay exponential curve; equation [1], using WinEDR software.

Equation [1] $y(x) = A.exp\left[\frac{-x}{tau}\right]$

Miniature and spontaneous EPSCs and IPSCs were detected using a threshold of 3-7 pA and manually inspected to eliminate false events. Spontaneous and miniature EPSC and IPSC frequencies, amplitudes, rise time and decay time

were analysed via the nonparametric Kolmogorov-Smirnov test (K-S test) with p values adjusted for multiple comparisons. The same number of events were taken for each cell so as not to skew results towards cells with higher frequencies. Significant differences from control obtained via K-S test are represented as asterisks on histograms and assigned when $p \leq 0.01$. sEPSC rise times were calculated as time between 10 – 90 % of maximum current while decay times taken as time for current to decay 50%. Representative spontaneous current traces were calculated by averaging at least 50 individual current traces for each condition. EPSCs were fit to both a single and double exponential decay curve and in general fit best to a double exponential decay curve.

Excitatory to inhibitory ratios were calculated by dividing the number of sEPSC events/min by the number of sIPSC events/min. Differences were statistically compared by repeated measures one-way ANOVA. All other data were analysed via paired or unpaired Student's *t*-tests, ANOVAs, or one sample t-tests and significance assigned when $p \leq 0.05$.

2.10 Solutions

Artificial Cerebrospinal Fluid (aSCF)

125 mM	Sodium Chloride
2.5 mM	Potassium Chloride
1.2 mM	Monosodium Phosphate
1.2 mM	Magnesium Chloride
2.4 mM	Calcium Chloride
21.4 mM	Sodium Bicarbonate
11.1 mM	D-Glucose
0.1 mM	Ascorbic Acid

Giving an osmolarity of approximately 322 mOsm/L, pH 7.4

Cutting Solution

20 mM	Sodium chloride
2.5 mM	Potassium chloride
1.6 mM	Monosodium phosphate
7 mM	Magnesium chloride
0.5 mM	Calcium chloride
60 mM	Sodium Bicarbonate
24 mM	D-Glucose
85 mM	Sucrose

Giving an osmolarity of approximately 305 mOsm/L, pH 7.4

NMDG 'protective recovery' solution

93 mM	N-methyl-D-glucamine (NMDG)
2.3 mM	Potassium chloride
1.2 mM	Monosodium phosphate
30 mM	Sodium bicarbonate
20 mM	4-(2-hydroxyethyl)-1-piperazineethanesulfonic acid (HEPES)
25 mM	Glucose
12 mM	N-acetyl-L-cysteine
2 mM	Sodium ascorbate
3 mM	Sodium pyruvate
10 mM	Magnesium sulphate
0.5 mM	Calcium chloride

Giving an osmolarity of approximately 330 mOsm/L adjusted pH to 7.4 (with HCL)

Intracellular recording solution A. (Voltage clamp)

120 mM	Caesium Methanesulphonate
10 mM	Sodium Chloride
2 mM	Magnesium Chloride
10 mM	4-(2-hydroxyethyl)-1-piperazineethanesulfonic acid (HEPES)
0.5 mM	Ethyline glycol tetraaceitic acid (EGTA)
5 mM	*N*-(2,6-Dimethylphenylcarbamoylmethyl) triethylammonium bromide (QX314)
2 mM	Mg-ATP
0.25 mM	Na-GTP

Giving an Osmolarity 275 mOsm/L adjusted pH to 7.4 (with CsOH)

Intracellular recording solution B. (Current clamp)

120 mM	Potassium gluconate
20 mM	Potasium Chloride
2 mM	Magnesium Chloride
10 mM	4-(2-hydroxyethyl)-1-piperazineethanesulfonic acid (HEPES)
5 mM	Mg-ATP
0.2 mM	Na-GTP

Giving an Osmolarity 280 mOsm/L adjusted pH to 7.4 (with KOH)

Chapter 3:

α7 nAChR regulation of synaptic plasticity within the prelimbic cortex

Chapter 3: α7 nAChR regulation of synaptic plasticity within the prelimbic cortex

3.1 Introduction

Cortical synaptic plasticity, including both LTP and LTD, is known to be regulated by the levels of postsynaptic calcium (Koester & Sakmann, 1998; Sjöström & Nelson, 2002), with higher levels leading to LTP and lower Ca^{2+} levels leading to LTD (Neveu & Zucker, 1996; Hansel et al., 1997) (see section 1.3). α7 nAChRs have a high permeability to calcium and so a mechanism by which these receptors may influence plasticity is not unreasonable. Indeed in the hippocampus α7 nAChRs are known to influence the levels of plasticity in the hippocampus (see section 1.6.1).

nAChRs modulation of synaptic plasticity in the mPFC is less well studied than in the hippocampus, however evidence does suggest these receptors do play a role in mPFC plasticity mechanisms (see section 1.6.2). *In vitro* brain slice experiments show that nicotine can alter the threshold for pyramidal neurons spike-timing dependent plasticity (Couey et al., 2007), and *in vivo* electrophysiology experiments in rats show nicotine can alter thalamo-cortical LTP and LTD (Bueno-Junior et al., 2012). Although an apparent role for nAChRs in regulating mPFC plasticity has been established, the use of non-selective nAChR agonists within previous studies means the individual roles of nAChR subtypes in these processes are not clear.

Evidence from the hippocampus, demonstrates that α7 nAChRs have the potential to be key modulators of synaptic plasticity due to their high calcium permeability, and cellular localisation. However no studies have directly studied the direct effect α7 nAChRs activation or antagonism has on mPFC synaptic plasticity, and so it is unknown if this receptor alone is able to modulate mPFC synaptic plasticity.

To address this gap in our understanding, this thesis chapter aimed to determine a potential role for α7 nAChRs in modulating the levels of LTP and LTD within the dorsal mPFC prelimbic cortex. To achieve this aim brain slices

containing the PrL from 5 week old mice were used to conduct extracellular field recording experiments. By evoking and recording field excitatory post synaptic potentials (fEPSPs), in combination with specific stimulation protocols, synaptic plasticity, (including both LTP and LTD), could be measured. Application of pharmacological compounds selective for the α7 nAChR during these synaptic plasticity recordings could then be employed, to investigate any contribution α7 nAChRs provide to the modulation of PrL synaptic plasticity.

3.2 Results

3.2.1 Optimisation of stimulus-induced LTP and LTD within the prelimbic cortex

Initial experiments were carried out to optimise an extracellular field recording protocol to induce LTP within the PrL. Brain slices containing the PrL region of the mPFC were prepared from 5 week old mice (see methods). A metal bipolar stimulating electrode was placed within layers II/III, while a recording electrode was placed in layer V of the PrL (Fig. 3.1A). Efforts were made to ensure that electrode placement was consistent between experiments in an attempt to stimulate a similar population of fibres. In doing so the variability between experiments was minimised.

An example of a field EPSP trace is shown in figure 3.1. This response was reversibly abolished by the non-selective glutamate receptor antagonist kynurenic acid (10 mM) in all slices tested (n = 6), demonstrating that the fEPSP was mediated via glutamate (Fig 3.1B). To ensure each electrical stimulation was evoking the same population of fibres, a short train of stimulations at a frequency of 50 Hz was applied. This 50 Hz train reliably produced fEPSPs that decreased in amplitude with increased stimulation number, indicative of short-term synaptic depression. This occurred in all slices tested (n = 9), suggesting that the fEPSPs were likely monosynaptic (Hempel et al., 2000; Huang et al., 2004) (Fig. 3.1C). For all experiments the slope of the fEPSP was used as a measure of the synaptic response. Although the

amplitude of the fEPSP is often less variable than the slope of the fEPSP, this measurement is less representative of synaptic transmission as it is can be contaminated by a population spike from the soma of nearby pyramidal cells (Selig & Malenka, 1997).

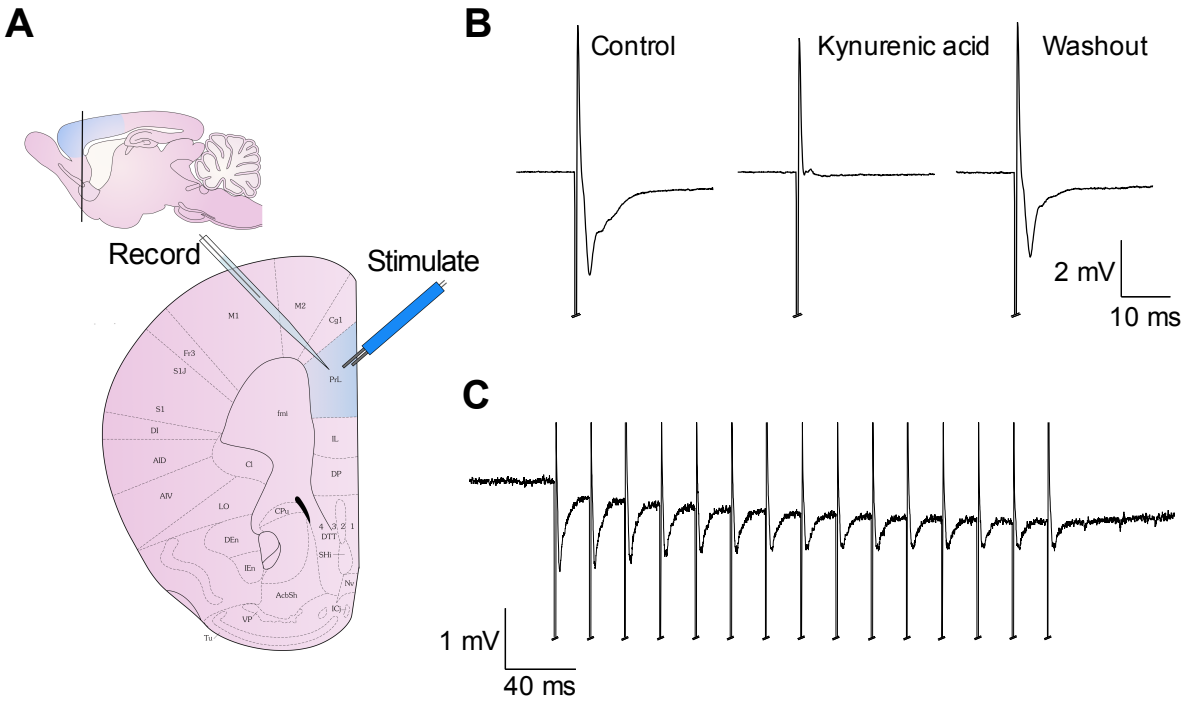

Figure 3.1 fEPSC recordings within the mouse prelimbic cortex

*(**A**) Extracellular field excitatory postsynaptic potentials (fEPSP) were evoked via a bipolar stimulating electrode placed perpendicular to the midline in layer II/III of the PrL (blue) of coronal brain slices (350-400 μm thickness) approximately +2.0 mm anterior from bregma. A recording electrode was placed in parallel to the stimulating electrode in layer V. (**B**) fEPSPs, evoked at 0.05 Hz in response to control aCSF and aCSF containing kynurenic acid (10 mM), before washout with control aCSF, fEPSP were abolished in all slices tested (n = 6). (**C**) fEPSPs were reliably evoked, following 50 Hz stimulation in all slices tested (n = 9).*

When performing synaptic plasticity experiments, a stimulus intensity to response relationship was first obtained by incrementally increasing the stimulation intensity until a maximal response was obtained. A stimulation intensity giving a response approximately 50% of maximum was then used throughout the remainder of the experiment. This allowed for both increases and decreases in synaptic efficacy to be observed after subsequent LTP or LTD induction protocols.

For LTP experiments, a stable 20 min fEPSP baseline was obtained before a theta burst stimulation was administered to the brain slice (see methods section 2.3). This theta burst stimulation reliably produced increases in the synaptic response measured by a change in slope of the fEPSP (Fig. 3.2A). The level of the synaptic potentiation is important to consider when performing LTP experiments so as to ensure any reduction or enhancement in LTP in response to drug application could be observed. It was found that by increasing the number of repetitions of the theta burst stimulation, the average potentiation level of the synaptic response, post theta burst stimulation, could be increased. A single theta burst, gave little to no potentiation of the fEPSP slope (101.2 ± 3.1%, n = 4), however repeating the theta burst stimulation 2 times gave an average potentiation of 117 ± 7.2%, (n = 4) while repeating the stimulation 4 and 5 times gave a larger potentiation of 126 ± 6.3% (n = 4) and 140 ± 9.7% (n = 4) respectively. Both a 4 and 5 times theta burst stimulation gave a significant enhancement in synaptic potentiation (one-sample t-test $p < 0.05$) whereas a 1 and 2 times theta burst stimulation failed to significantly alter the level of potentiation (Fig. 3.2B). As the 4 times theta burst stimulation gave an intermediate potentiation level that could be enhanced or reduced this stimulation protocol was used for the majority of the subsequent LTP experiments.

Long-term potentiation within the brain can be achieved via a variety of plasticity mechanisms (section 1.3). The most common LTP mechanism in the mPFC is NMDAR dependent LTP. To investigate if the LTP obtained with theta burst stimulation was NMDAR dependent, LTP recordings were conducted (by a fellow PhD student Vicki Wright) in the presence of the NMDAR antagonist D-AP5 (50 μM). When D-AP5 was bath applied to the slice 10 min before and during a theta burst stimulation the level of potentiation increased to only 109 ± 2.7% (n = 2), whereas control recordings in the absence of D-AP5 resulted in a significantly induced potentiation of 141 ± 11.4% (one-sample t-test $p < 0.05$) (Fig. 3.2C). Although the sample size for D-AP5 application was low, it would appear that NMDAR blockade prevented the induction of LTP.

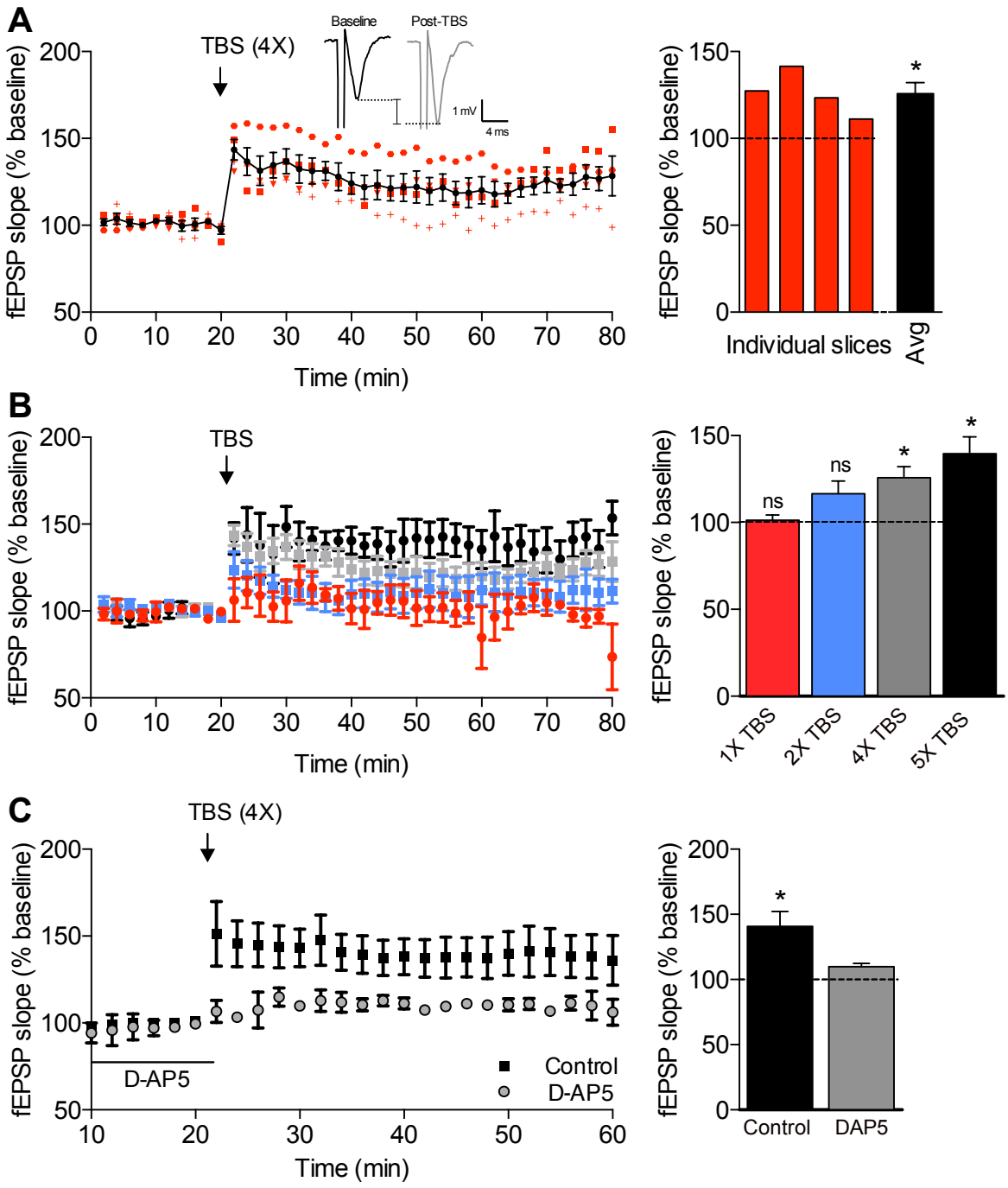

Figure 3.2 Optimisation of theta burst induced long-term potentiation within the prelimbic cortex

*Extracellular field EPSPs (fEPSP) were recorded in layer V upon electrical stimulation of layers II/III. After a 20 min stable baseline, long-term potentiation was induced via theta burst stimulation. (**A**) A theta burst repeated 4 times induced a stable from of LTP average potentiation shown in black, individual experiments shown in red. (n = 4). (**B**) LTP induced by a series of theta burst repetitions (1x n = 4; 2x n = 4; 4x n = 4; 5x n = 4). (**C**) LTP induction with a 4x theta burst stimulation in control aCSF (n = 4), and in response to 10 min application of NMDAR antagonist DAP5 (10 μM) before and during the theta burst stimulation (n = 2). Time courses (left) show fEPSP slope at each timepoint normalised to baseline. Histograms (right) show averaged potentiation across all timepoints post theta burst stimulation, which were used to determine significant induction of LTP, assessed via a one-sample t-test. Statistical significance assigned if p<0.05. Data represented as mean ± S.E.M.*

In some experiments a low frequency stimulation was used in an attempt to induce LTD within the slice (see methods section 2.3). This protocol however failed to reliably induce long-term depression. In response to a low frequency stimulation, of the 7 slices tested, 3 produced a reduced level of synaptic strength whereas 4 slices produced no change or slight increases in the level of synaptic strength (Fig. 3.3). Although LTD was not induced with this protocol, it could be used as a sub-threshold induction of LTD in further experiments.

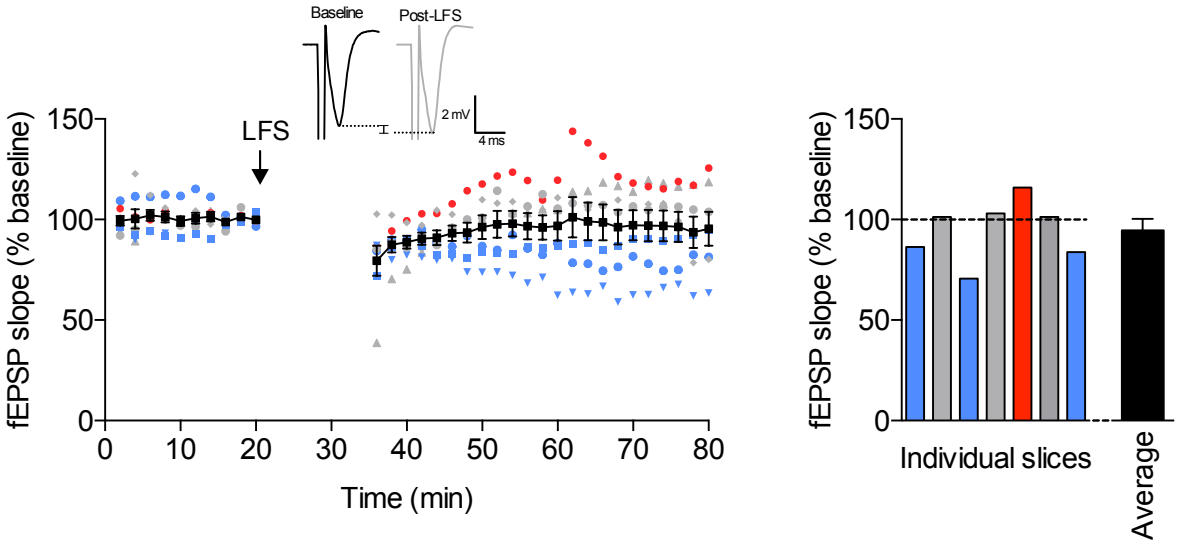

Figure 3.3 Subthreshold low frequency stimulation protocol used to induce long-term depression within the prelimbic cortex

*Extracellular field EPSPs (fEPSP) were recorded in layer V upon electrical stimulation of layers II/III. After a 20 min stable baseline, long-term depression was induced via a 15 min low frequency stimulation. (**A**) The level of potentiation after low frequency stimulation was variable with some slices undergoing LTD (blue) whilst others had no change (grey) and slight increases in potentiation (red), resulting, on average, in a subthreshold induction of LTD (n = 7). Time courses (left) show fEPSP slope at each timepoint normalised to baseline with average potentiation shown in black. Histograms (right) show averaged potentiation across all timepoints post low frequency stimulation. Data represented as mean ± S.E.M.*

3.2.2 α7 nAChR antagonism inhibits the level of LTP but enhances the level of LTD

To investigate if the endogenous activation of α7 nAChRs contributes to the mechanisms of LTP within the PrL the α7 nAChR selective antagonist MLA (100 nM) was bath applied to the slice 10 minutes before and during the theta burst stimulation. This concentration of MLA was based on its use in similar fEPSP experiments (Fujii et al., 2000; Söderman et al., 2011). MLA application resulted in a significant reduction in the level of LTP at later stages of the experiment, suggesting that the endogenous activation of α7 nAChRs is needed to sustain a stable form of long-term potentiation within the slice (Fig. 3.4A). To ensure the effect seen was not caused via MLA reducing the baseline extracellular field response, 100nM MLA was applied to the slice in the absence of a theta burst stimulation. In this experiment MLA produced no significant alteration in the fEPSP. (Fig. 3.5).

To corroborate the involvement of α7 nAChRs in LTP modulation, another PhD student (Vicki Wright), performed similar experiments with the highly specific, α7 nAChR irreversible antagonist α-bungarotoxin. Perfusion of α-bungarotoxin onto the slice during experiments was avoided, to prevent the peptide adhering to the perfusion and recording equipment. Instead slices were incubated with α-bungarotoxin for at least 1 hour prior to experiments allowing for α-bungarotoxin's slow rate of action to sufficiently antagonise α7 nAChRs. Brain slices were then transferred to the recording chamber and LTP recordings conducted in control aCSF, under these conditions α7 nAChRs would remain antagonised throughout the experiment due to α-bungarotoxin's irreversible binding. Brain slices treated with 300 nM α-bungarotoxin produced a significantly lower level of LTP compared to untreated slices (Fig. 3.4B). These data verify that endogenous ACh acting at α7 nAChRs are implicated in the modulation of LTP within the PrL.

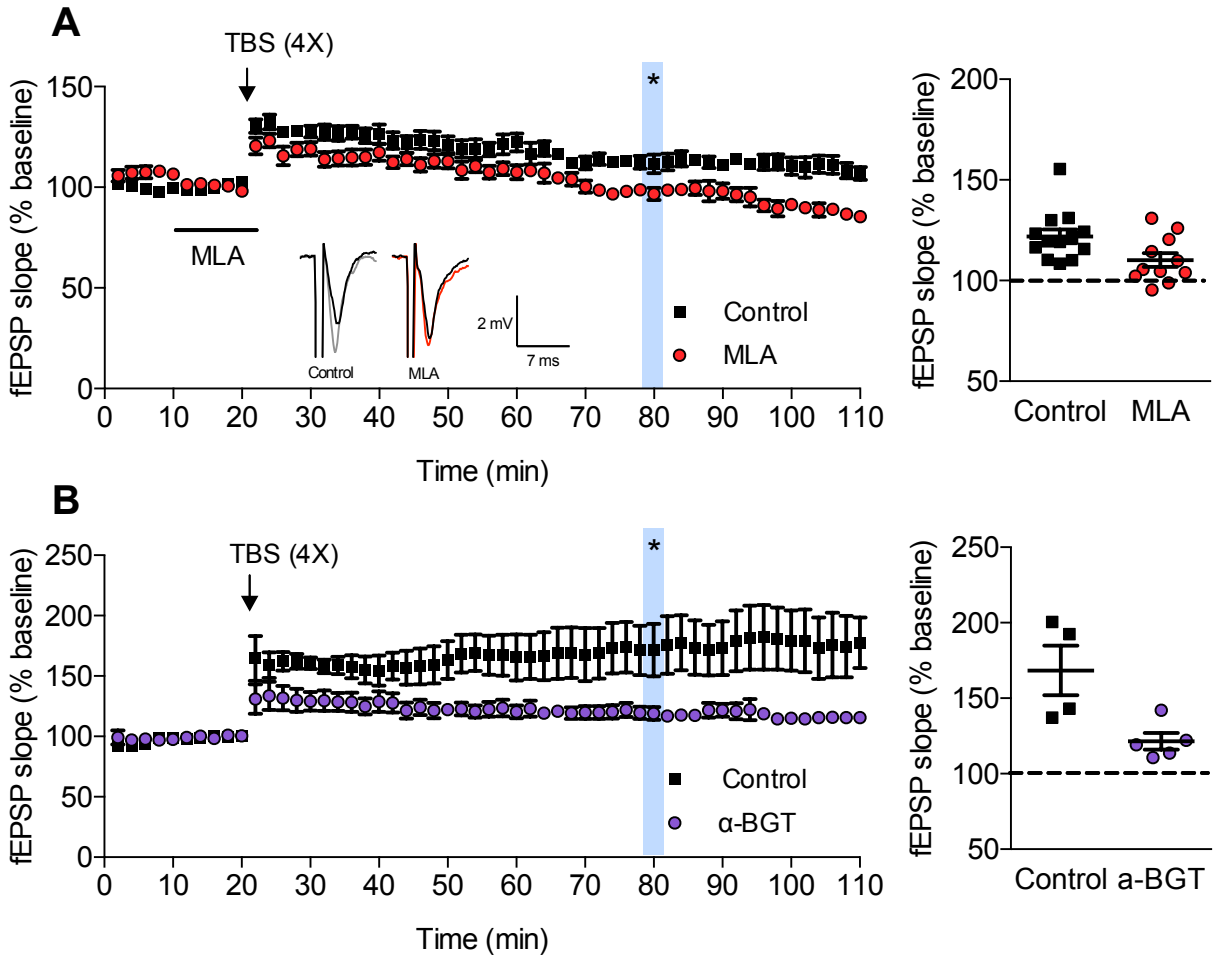

Figure 3.4 Modulation of long-term potentiation in response to α7 nAChR antagonism

*Extracellular field EPSPs (fEPSP) were recorded in layer V upon electrical stimulation of layers II/III. After a 20 min stable baseline, long-term potentiation was induced via a 4x theta burst stimulation (**A**) Recordings were made in the absence (control n = 7-13) and presence of a 10 min bath application of the α7 nAChR antagonist MLA (100 nM; n = 5-11). (**B**) Slices were incubated with the irreversible α7 nAChR antagonist α-bungarotoxin (300 nM) for >1 hr before LTP was induced via theta burst stimulation (n = 5), control slices (n = 4). Time courses (left) show fEPSP slope at each timepoint normalised to baseline. Potentiation plots (right) represent averaged potentiation across all timepoints post TBS for each slice. Statistical significance between control and drug assessed at timepoint 60 minutes post theta burst via unpaired t-test and statistical significance assigned if p ≤ 0.05. Data represented as mean ± S.E.M.*

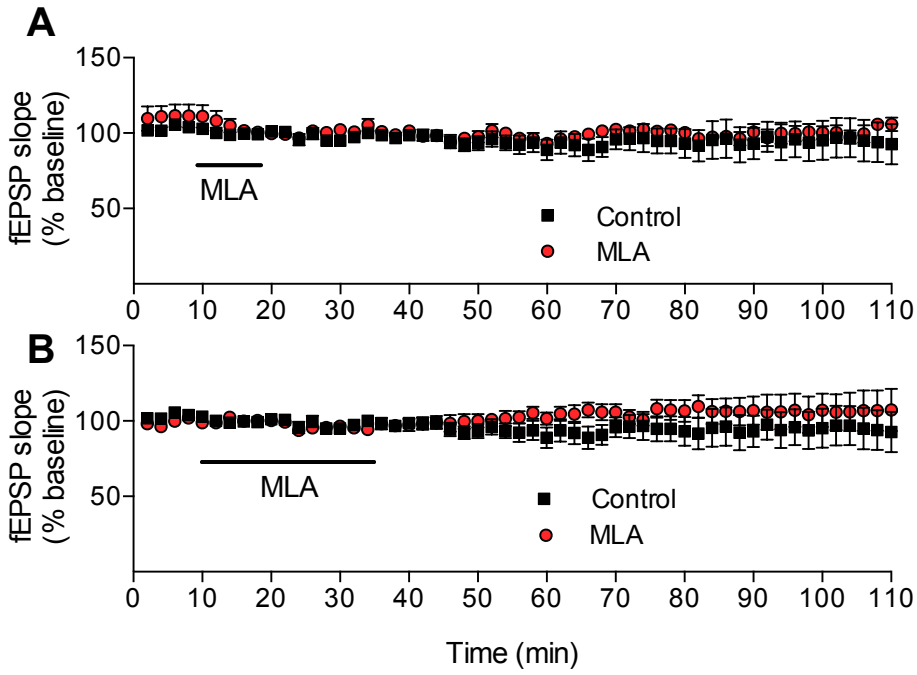

Figure 3.5 fEPSP modulation in response to α7 nAChR antagonism

*Extracellular field EPSPs (fEPSP) were recorded in layer V upon electrical stimulation of layers II/III. (**A**) After a 10 min stable baseline, the α7 nAChR antagonist MLA (100nM) was applied to the slice for 10 min (n = 3-5) (control; = 5-8). (**B**) After a 10 min stable baseline, the α7 nAChR antagonist MLA (100nM) was applied to the slice for 25 min (n = 5-6) (control; = 5-8). Time courses show fEPSP slope at each timepoint normalised to first 10 min baseline. Statistical significance between control and drug assessed at timepoint 60 minutes post drug washout via unpaired t-test and statistical significance assigned if p ≤ 0.05. Data represented as mean ± S.E.M.*

Experiments shown in figure 3.3 demonstrate that a LFS produced a mixed response in plasticity including LTD, LTP and no potentiation. To investigate if antagonism of α7 nAChRs might modulate the synaptic depression in response to a LFS, to produce a more reliable induction of LTD within the PrL., MLA (100nM) was applied to the brain slice 10 min before and during the same 15 min 3 Hz LFS, used in figure 3.3. Compared to control slices in which the LFS failed to induce a pronounced LTD, in the presence of MLA the LFS resulted in a stable form of synaptic depression (Fig. 3.6). This synaptic depression as a result of α7 nAChR antagonism, was deemed statistically significant from baseline (one-sample t-test $p < 0.05$) and statistically different to control slices post LFS (Unpaired t-test $p < 0.05$). To ensure that α7 nAChR antagonism was not affecting the baseline fEPSP response MLA was applied to the slice for the

corresponding time frame in the absence of a low frequency stimulation, during which no significant alteration in the baseline was observed (Fig. 3.5B).

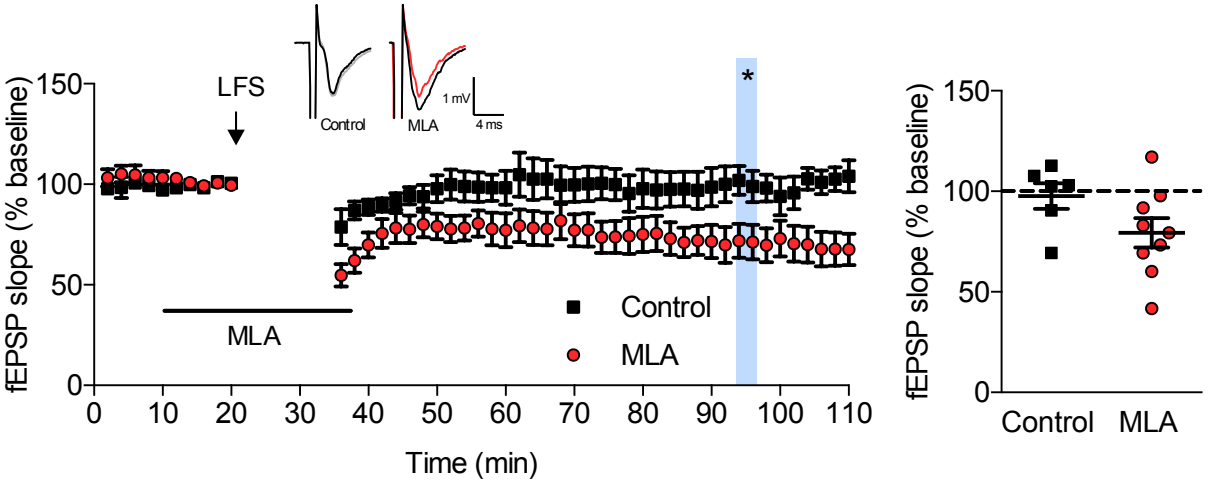

Figure 3.6 Modulation of long-term depression in response to α7 nAChR antagonism

Extracellular field EPSPs (fEPSP) were recorded in layer V upon electrical stimulation of layers II/III. After a 20 min stable baseline, long-term depression was induced via a low frequency stimulation. Recordings were made in the absence (control n = 6) and presence of the α7 nAChR antagonist MLA (100 nM) (n = 6-8) bath applied for 10 min before and during the 15 min low frequency stimulation. Time courses (left) show fEPSP slope at each timepoint normalised to baseline. Potentiation plots (right) represent averaged synaptic depression across all timepoints post LFS. Statistical significance between control and MLA was assessed at timepoint 60 min post LFS via unpaired t-test and statistical significance assigned if p ≤ 0.05. Data represented as mean ± S.E.M.

The findings that MLA and α-bungarotoxin can reduce LTP whilst MLA could enhance LTD demonstrate that preventing endogenous ACh activating α7 nAChRs before and during the initiation of synaptic plasticity leads to reduction in the overall output of synaptic strength. Endogenous ACh would thus appear to have a direct role in promoting PrL synaptic strength during synaptic plasticity by acting at α7 nAChRs.

3.2.3 α7 nAChR activation with exogenous ligands inhibits the levels of LTP but has no effect on LTD

Experiments conducted by other laboratories have shown that activation of nicotinic receptor can alter the levels of LTP within the PrL, however the contribution of α7 nAChRs remains untested (Bueno-Junior et al., 2012; Couey et al., 2007). In this thesis α7 nAChR antagonism reduced stimulus-induced LTP, and so it was hypothesised that activation of α7 nAChRs would result in an increase in stimulus-induced LTP.

To investigate this hypothesis the selective α7 nAChR agonist PNU-282987, co-applied with the α7 nAChR type II PAM, PNU-120596 (co-applied to prevent α7 nAChR desensitisation), were used to investigate if activation of α7 nAChRs could enhance LTP. Surprisingly, it was found that PNU-282987 (300 nM) and PNU-120596 (10 μM), applied 20 min before and during a theta burst stimulation, led to a significant reduction in the level of LTP compared to control (Fig. 3.7A). An extended drug application (20 min instead of 10 min) was used to ensure that there was no reduction in the baseline observed upon drug application (see section 4.2.2.2).

Exogenous activation of α7 nAChRs by this combination of drugs produced a similar reduction in LTP as seen with antagonism with MLA (Fig. 3.4). MLA also led to the induction of a pronounced LTD, so next the effect of exogenous activation of α7 nAChRs during a LFS was investigated to observe if α7 nAChR activation could also induce a stable synaptic depression. Unlike MLA however, co-application of PNU-282987 (300 nM) and PNU-120596 (10 μM) did not result in formation of LTD, as seen in control recordings (Fig. 3.7B).

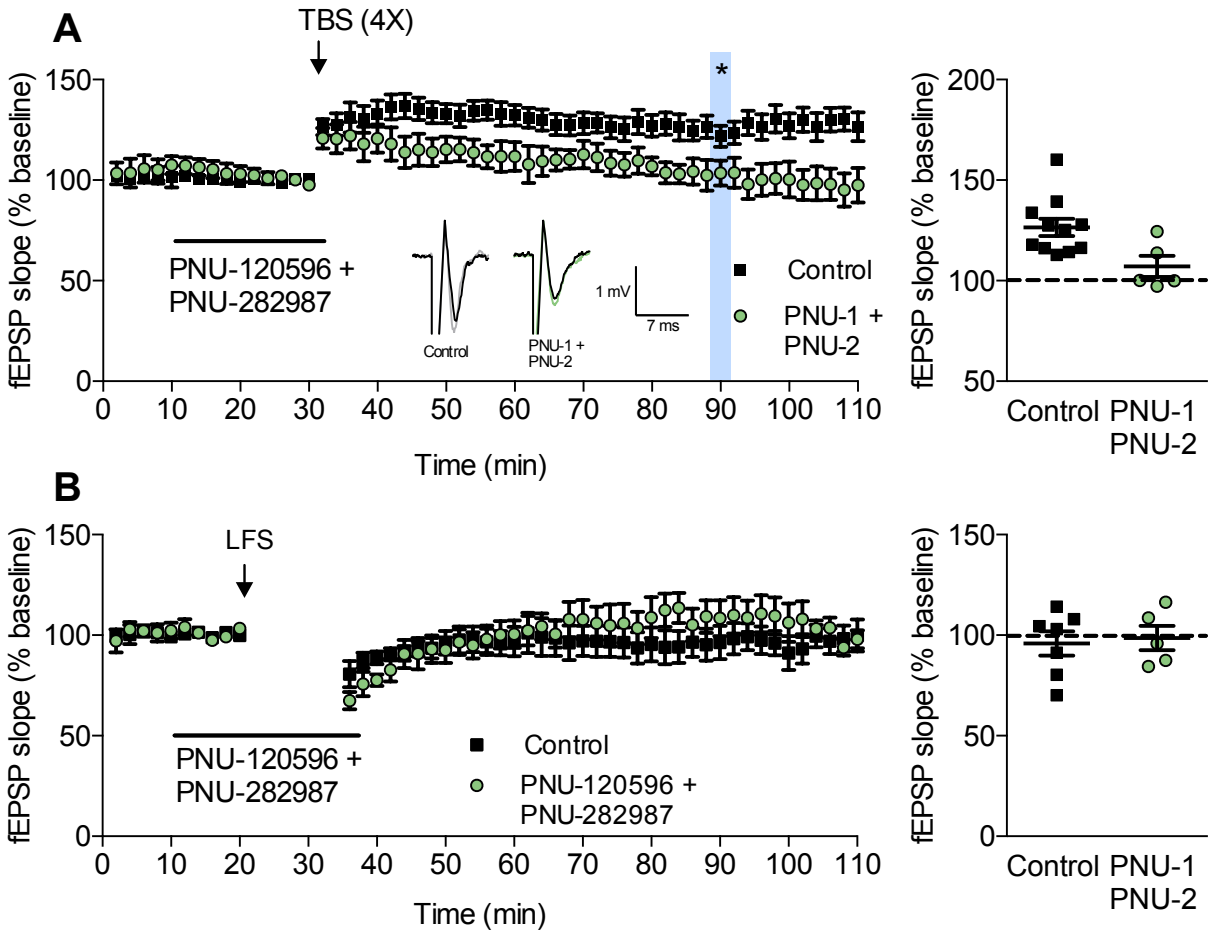

Figure 3.7 Modulation of long-term potentiation and depression in response to α7 nAChR activation and antagonism

*Extracellular field EPSPs (fEPSP) were recorded in layer V upon electrical stimulation of layers II/III. After a 20 min stable baseline long-term potentiation or depression were induced via theta burst or low frequency stimulation (**A**) LTP recordings were made in the absence (control; n = 7-11) and presence of a 20 min application of the α7 nAChR PAM PNU-120596 (10 μM) and agonist PNU-282987 (300 nM) (n = 5). (**B**) LTD recordings were made in the absence (control; n = 7) and presence of the α7 nAChR PAM and agonist, PNU-120596 (10 μM) and PNU-282987 (300 nM) (n = 4-5) bath applied for 10 min before and during the 15 min low frequency stimulation. Time courses (left) show fEPSP slope at each timepoint normalised to baseline. Potentiation plots (right) represent averaged potentiation across all timepoints post TBS/LFS for each slice. Statistical significance between control and PNU-1 + PNU-2 was assessed at timepoint 60 minutes post TBS/LFS via unpaired t-test and statistical significance assigned if p ≤ 0.05. Data represented as mean ± S.E.M.*

3.2.4. Positive allosteric modulation of α7 nAChRs does not alter the level of LTP

Antagonism of the endogenous actions of acetylcholine at α7 nAChRs with MLA reduced the levels of stimulus-induced LTP in the PrL (Fig. 3.4A), whereas activation of α7 nAChRs with an exogenous agonist also reduced the levels of stimulus-induced LTP (Fig. 3.7A). These paradoxical findings might be explained due to differences in receptor localisation or reflect the different population of receptors that are activated during endogenous acetylcholine release vs. α7 nAChRs activated via application of an exogenous agonist. It was therefore hypothesised that enhancing the endogenous activity of the α7 nAChRs, rather than activating the α7 nAChRs exogenously, would result in an increase in synaptic potentiation.

To test this hypothesis the α7 nAChR PAM, PNU-120596, was applied alone in the absence of the selective agonist PNU-282987. As PNU-120596 not only reverses the desensitisation, but also prolongs the average open state and conductance of the α7 nAChR (Hurst et al., 2005), administrating PNU-120596 alone should amplify any endogenous activity at the α7 nAChRs. Surprisingly PNU-120596 (10 μM) applied 10 minutes before and during a 4 times theta burst stimulation resulted in no significant alteration in the levels of synaptic potentiation compared to control recordings (Fig. 3.8A). A possible explanation for this finding could be that the intensity of the 4 times theta burst stimulation used to induce LTP was too strong, leading to a near maximal level of potentiation, masking any further increase in synaptic strength. To test this idea both a 1 and 2 times theta burst stimulation were used to provide a reduced level of control synaptic potentiation (see section 3.2.1). It was found that PNU-120596 (10 μM) applied to the slice 10 minutes before and during a 2 times theta burst stimulation gave no alteration in the level of synaptic potentiation compared to control (Fig. 3.8B). The same was found with a 1 times theta burst stimulation (Fig. 3.8C). These findings suggest that even with a weaker LTP induction protocol enhancing the activity of endogenous ACh at α7 nAChRs, does not lead to an enhancement of PrL LTP.

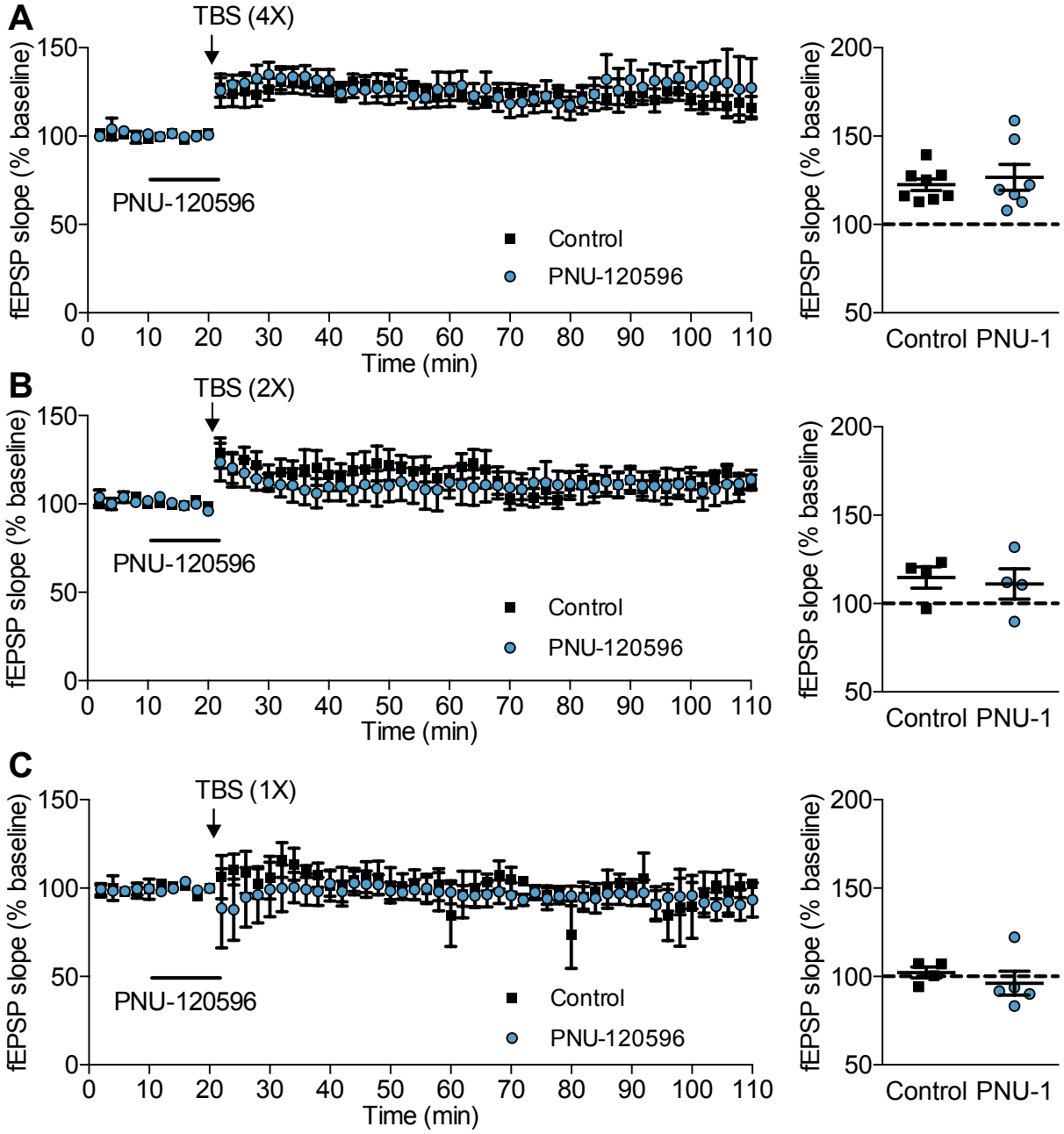

Figure 3.8 Modulation of long-term potentiation in response to positive allosteric modulation of α7 nAChRs

*Extracellular field EPSPs (fEPSP) were recorded in layer V upon electrical stimulation of layers II/III. After a 20 min stable baseline long-term potentiation was induced via a variety of theta burst. (**A**) LTP induced via a 4x theta burst stimulations in the absence (control; n = 4-8) and presence (n = 4-7) of a 10 min application of the α7 nAChR PAM PNU-120596 (10 μM). (**B**) LTP induced via a 2x theta burst stimulations in the absence (control; n = 4) and presence (n = 4) of a 10 min application of the α7 nAChR PAM PNU-120596 (10 μM). (**C**) LTP induced via a 1x theta burst stimulations in the absence (control; n = 2-4) and presence (n = 5) of a 10 min application of the α7 nAChR PAM PNU-120596 (10 μM). Time courses (left) show fEPSP slope at each timepoint normalised to baseline. Potentiation plots (right) represent averaged potentiation across all timepoints post TBS for each slice. Statistical significance between control and drug was assessed at timepoint 60 minutes post theta burst via unpaired t-test and statistical significance assigned if p ≤ 0.05. Data represented as mean ± S.E.M.*

Studies have shown that the length of time α7 nAChRs are exposed to PNU-120596 can alter the drugs efficacy, with PNU-120596 enhancing peak current between 0 - 10 min, after which the peak-current begins to decline (Williams et al., 2011). In addition, experiments in section 4.2.2.2 (Fig. 4.11) of this thesis, suggest that 10 min of PNU-120596 may result in a slightly reduced level of α7 nAChR potentiation compared to 5 min application. Experiments were therefore conducted in which PNU-120596 was applied to the slice for 5 min (instead of 10 min), before and during a theta burst stimulation, to potentially reveal an increase in the level of potentiation. However it was found that PNU-120596 (10 μM) applied to the slice 5 min before and during a 2 times theta burst stimulation still failed to significantly increase in the level of LTP (Fig. 3.9). These results therefore suggest that positive allosteric modulation of α7 nAChRs, in the absence of exogenous agonists is unable to modulate the levels of LTP within the PrL

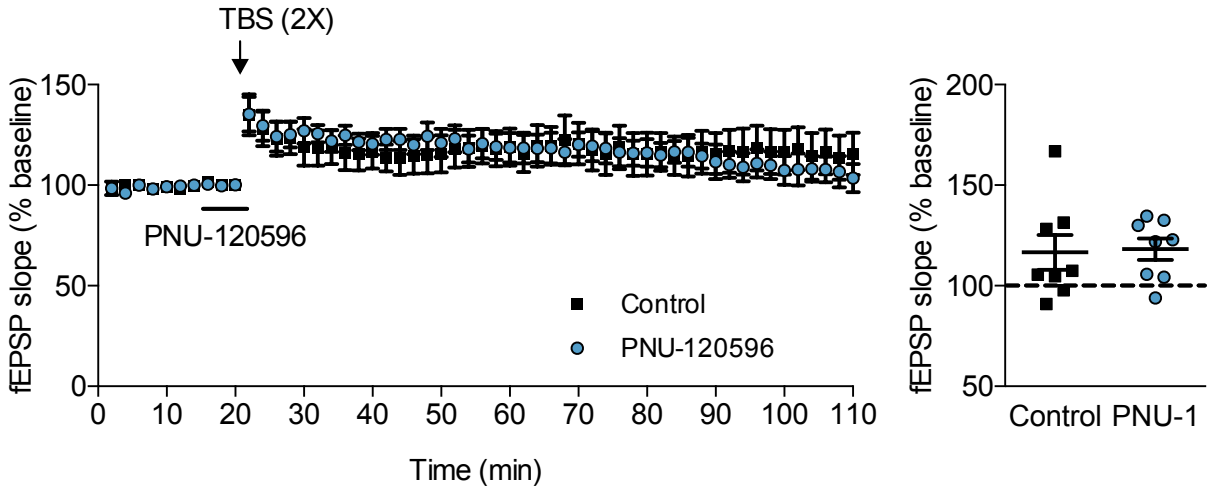

Figure 3.9 Modulation of long-term potentiation in response to a shortened exposure to α7 nAChR positive allosteric modulation.

Extracellular field EPSPs (fEPSP) were recorded in layer V upon electrical stimulation of layers II/III. After a 20 min stable baseline long-term potentiation was induced via a 2x theta burst stimulation. LTP induced in the absence (control; n = 7-8) and presence of a 5 min application of the α7 nAChR PAM PNU-120596 (10 μM) (n = 7-8). Time courses (left) show fEPSP slope at each timepoint normalised to baseline. Potentiation plots (right) represent averaged potentiation across all timepoints post TBS for each slice. Statistical significance between control and PNU-120596 was assessed at timepoint 60 minutes post theta burst via unpaired t-test and statistical significance assigned if p<0.05. Data represented as mean ± S.E.M.

3.3 Summary

The aim of this chapter was to investigate the potential contribution that activity at the α7 nAChR has in the initiation and maintenance of synaptic plasticity within the PrL. First a protocol that would enable the measurement of stimulus-induced synaptic plasticity was optimised. A range of α7 nAChR-selective compounds were then employed to investigate if α7 nAChRs have a functional role in PrL plasticity. The pharmacological mechanisms of the agonist and potentiator compounds also enabled the investigation into differences between endogenous and exogenous activation of α7 nAChRs in PrL plasticity mechanisms.

It was found that inhibiting the effects of endogenous acetylcholine at α7 nAChRs with the antagonists MLA and α-bungarotoxin resulted in a reduction in stimulus-induced LTP within the PrL. Surprisingly it was found that activating α7 nAChRs with an agonist in the presence of an allosteric modulator also reduced the levels of LTP. These findings were in contrast to the effects found when enhancing the effects of endogenous acetylcholine with a positive allosteric modulator. Here, as expected, there was no reduction in the levels of plasticity, but unexpectedly an enhancement in the levels of plasticity was also not observed, even with variety of different LTP induction protocols.

Experiments also aimed to investigate α7 nAChR modulation of LTD within the PrL slice. Although a low frequency stimulation failed to induce stable LTD within control slices, it was found that blocking the activity of endogenous ACh at α7 nAChRs with MLA, induced a stable form of LTD. This effect was not seen when α7 nAChRs were activated with the α7 nAChR PAM and selective agonist.

The most striking finding within this chapter is that both antagonism and activation of the α7 nAChR results in a similar decrease in LTP. Interestingly the paradoxical finding with LTP was not observed when studying LTD, instead, α7 nAChR inhibition induced LTD, whilst global activation of α7 nAChRs had no

effect on LTD. This suggests that α7 nAChRs exhibit a complex modulation on plasticity, that may involve distinct network and cellular mechanisms.

The mechanisms of synaptic plasticity are vast, however a balance in the level of excitation or inhibition of the neurons undergoing synaptic plasticity often governs the threshold and extent of synaptic plasticity. α7 nAChRs are expressed in multiple cell types across multiple layers within the cortex (see section 1.5.4) and so activation and antagonism of α7 nAChRs is likely to have a complex influence on the levels of PrL excitation and inhibition. In addition, global activation of all α7 nAChRs within the PrL appears to have a contrasting outcome on PrL plasticity compared to endogenously activated α7 nAChRs. Therefore to better understand the mechanisms behind α7 nAChRs contribution towards PrL plasticity, one needs to understand the effect activation, modulation and antagonism of the α7 nAChR has on the overall excitation and inhibition of the PrL network. The following chapters will therefore aim to investigate how α7 nAChRs can alter the network activity of the PrL.

Chapter 4:

α7 nAChR modulation of the excitatory and inhibitory network activity in the prelimbic cortex

Chapter 4: α7 nAChR modulation of the excitatory and inhibitory network activity in the prelimbic cortex

4.1 Introduction

In the previous chapter it was shown that α7 nAChRs can modulate the levels of prelimbic cortex stimulus-induced plasticity. Plastic changes in a neuron can be governed by the neuron's excitable state, which is often governed by the relative balance in excitatory to inhibitory inputs onto the neuron (Paulsen & Moser, 1998; Song et al., 2000). Therefore studying the outcome on excitatory and inhibitory signalling within the PrL network in response to α7 nAChR activation and antagonism was undertaken in order to provide a better understanding of the mechanisms by which α7 nAChRs can influence PrL plasticity.

On a broader scale α7 nAChR activity has been implicated in the cognitive processes assigned to the mPFC, and are also implicated in multiple disease states such as schizophrenia, Alzheimer's disease, ADHD and addiction (section 1.5) These cortical processes and disorders are also thought to be influenced by the balance in excitation within the PFC network (John & Berg, 2015; Yizhar et al., 2011). Investigating how α7 nAChR activity can modulate excitatory and inhibitory neurotransmission in the PrL is therefore important in understanding the mechanism by which ACh signalling at α7 nAChRs might be implicated in normal and abnormal functioning of the PFC.

Work by others, as detailed in section 1.5.5 has investigated the role of nAChRs in regulating the mPFC network activity. These studies have used either nicotine or ACh to provide evidence that nAChRs can enhance both excitation and inhibition within the prelimbic cortex (Poorthuis et al., 2012; Aracri et al., 2010). However the use of non-selective agonists means the individual contribution of α7 nAChRs in regulating mPFC network activity still remains unclear. The aim of this thesis chapter was to address this issue by using the selective α7 nAChR agonist, positive allosteric modulator and antagonists, used in chapter 3, to determine a more precise role for α7 nAChRs in modulating

excitation and inhibition within the PrL. Along side this, the potential differences between endogenous vs. exogenous α7 nAChR activation could also be investigated. These studies will help us piece together α7 nAChRs physiological function within the PrL network.

To achieve this aim, whole-cell patch clamp recordings were made from layer V pyramidal neurons within the prelimbic cortex and spontaneous inhibitory and excitatory postsynaptic currents in addition to evoked excitatory currents were recorded in response to different types of α7 nAChR activation. α7 nAChRs network modulation in response to endogenous ACh could be investigated using the selective α7 nAChR PAM PNU-120596 and antagonist MLA. This could be then be compared to α7 nAChR neuromodulation in response to exogenous agonist activation via the use of the selective α7 nAChR agonist PNU-282987 alone, and in combination with PNU-120596.

4.2 Results

4.2.1 Measurement and optimisation of excitatory and inhibitory post-synaptic currents

To investigate how α7 nAChRs could modulate the spontaneous excitatory and inhibitory network activity of the prelimbic cortex, spontaneous excitatory and inhibitory post synaptic currents (sEPSC & sIPSC) were measured via whole-cell voltage clamp recordings in layer V pyramidal neurons. Drugs influencing α7 nAChR activation were then examined for their effects on spontaneous currents.

To investigate the effect that α7 nAChR activity has on the PrL network, blockade of excitatory and inhibitory signalling was avoided, keeping the network pharmacologically intact. An intact network would enable the net consequence α7 nAChR intervention to be studied. To achieve this, a method was adapted from Semyanov & Kullmann, (2000) to allow measurement of both sEPSCs and sIPSCs from the same neuron.

The method utilised a caesium-based intracellular recording solution containing the Na^+ channel antagonist QX-314 and a low chloride ion concentration. This enabled the measurement of inward, inhibitory chloride currents at depolarised holding voltages and excitatory, AMPAR-mediated currents at resting membrane potentials, both in the absence of postsynaptic action potential firing. In theory, neurons voltage clamped at the reversal potential of chloride (GABAergic) currents (approximately -60 mV), would exhibit downward excitatory currents, whilst neurons held at the approximate reversal potential of AMPAR-mediated currents (approximately 0 mV), would exhibit upward inhibitory currents. To confirm this, sEPSCs and sIPSCs were pharmacologically isolated and the frequency of spontaneous currents recorded at different holding potentials.

First $GABA_A$ receptors were blocked with picrotoxin (50 μM) in order to eliminate sIPSCs after which, sEPSCs were recorded at a series of holding voltages. The predicted sEPSC reversal potential was confirmed to be

approximately 0 mV: at this holding voltage no sEPSCs were recorded, whilst at more hyperpolarised holding potentials sEPSCs were reliably observed (Fig. 4.1A). Next, in different cells, ionotropic glutamate receptors were blocked with kynurenic acid (10 mM) and sIPSCs recorded at different holding voltages. As predicted the sIPSC reversal potential was approximately -60 mV at which no sIPSCs were recorded, whilst at depolarised holding voltages sIPSCs were reliably recorded (Fig. 4.1A). These measurements confirmed that sEPSCs and sIPSCs could be isolated and independently measured by altering the neurons holding voltage between -60 mV and 0 mV, which would enable both to be measured from the same cell.

4.2.2 Modulation of spontaneous excitatory and inhibitory signalling by α7 nAChRs

Using the methodology established in section 4.2.1, experiments were conducted to test if α7 nAChR activity contributes to prelimbic excitation or inhibition. By measuring the change in frequency, amplitude, rise and decay time of spontaneous currents in response to different drugs affecting α7 nAChR activation, information into how these receptors might regulate the release of excitatory and inhibitory neurotransmitters could then be deduced. To achieve this, different combinations of the α7 nAChR PAM, agonist and antagonist (used in chapter 3) were bath-applied to the slice for 5 min whilst recording sEPSCs and sIPSCs from layer V pyramidal neurons (Fig. 4.1B). The α7 nAChR PAM PNU-120596 (10 μM) was first bath applied alone, then PNU-120596 was co-applied with the α7 nAChR selective agonist PNU-282987 (300 nM) and finally the α7 nAChR antagonist MLA (100 nM) was applied in the presence of PNU-120596 and PNU-282987. This protocol design is shown in figure 4.1B.

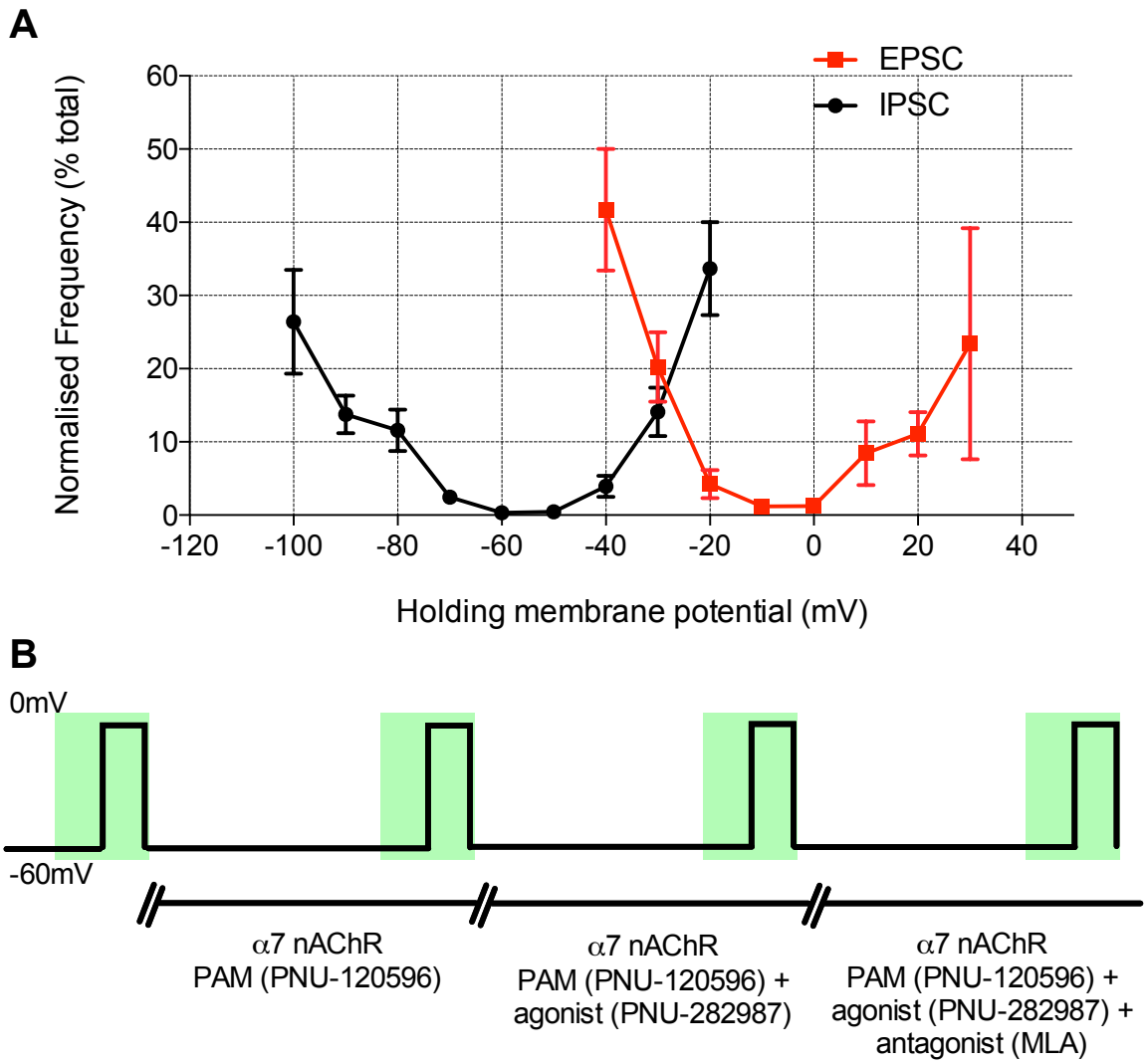

Figure 4.1 Optimisation of a protocol to measure sEPSCs and sIPSCs within the same neuron

*Whole-cell voltage clamp experiments were conduced to measure sEPSC and IPSC from layer V pyramidal neurons. (**A**) sIPSC and sEPSC were recorded in the presence of 10 mM kynurenic acid (n = 5) or 50 μM picrotoxin (n = 2-5) respectively at holding voltages between -100 and +30 mV, revealing a reversal potential for sIPSCs and sEPSCs to be -60 mV and 0 mV respectively. (**B**) By switching the holding voltage of the neuron to the measured reversal potential, allowed measurement of sEPSCs and sIPSCs from the same neuron in response to α7 nAChR activation. During these experiments drugs were bath applied to the slice and allowed to equilibrate for 5 min before analysis of 1 min of events at -60 mV and 1 min of events at 0 mV (green shading). Data in A represents mean ± S.E.M current frequency at each holding voltage was normalised as a percentage of the total frequency (events / min) in that cell*

4.2.2.1 α7 nAChR modulation of spontaneous excitatory currents

Bath application of the α7 nAChR PAM alone significantly enhanced the frequency of sEPSCs (Fig. 4.2A,C). This suggests that enhancing the endogenous activity at α7 nAChRs can promote excitation of layer V pyramidal neurons. Interestingly, when the α7 nAChR PAM and the α7 nAChR agonist were subsequently co-applied, the frequency of sEPSCs significantly decreased compared with the α7 nAChR PAM alone. These findings suggest exogenous agonist mediated activation of α7 nAChRs has an opposing effect on excitation than endogenous activation of the receptor. Upon addition of MLA (100 nM) no further effect on the frequency was observed, although the sEPSC frequency in the presence of MLA was statistically lower than control (Fig. 4.2A,C).

In addition to sEPSC frequency, sEPSC amplitudes were also measured to investigate if α7 nAChR activity may lead to alterations in postsynaptic sensitivity to the released neurotransmitter. The α7 nAChR PAM alone had no effect on amplitude, however upon co-application with the α7 nAChR agonist the sEPSC amplitude significantly decreased compared to control (Fig. 4.2B,C). This decrease in amplitude was not reversed upon application of MLA. In the presence of MLA the sEPSC amplitude was also statistically lower than control. Changes in sEPSC amplitude can be interpreted as an altered postsynaptic sensitivity to the released neurotransmitter or a change in the amount of neurotransmitter released (Auger & Marty, 2000). This suggests that co-application of the α7 nAChR PAM and agonist produces an overall reduction in the excitability of layer V pyramidal neurons, observed as both a decrease in sEPSC frequency and amplitude.

To confirm that the effect seen with the PAM was mediated by α7 nAChRs, additional experiments were conducted in which MLA was applied directly after PNU-120596. In this experiment the significant increase in sEPSC frequency in response to the α7 nAChR PAM (10 μM) was reversed in the presence of the MLA (100 nM) (Fig. 4.3).

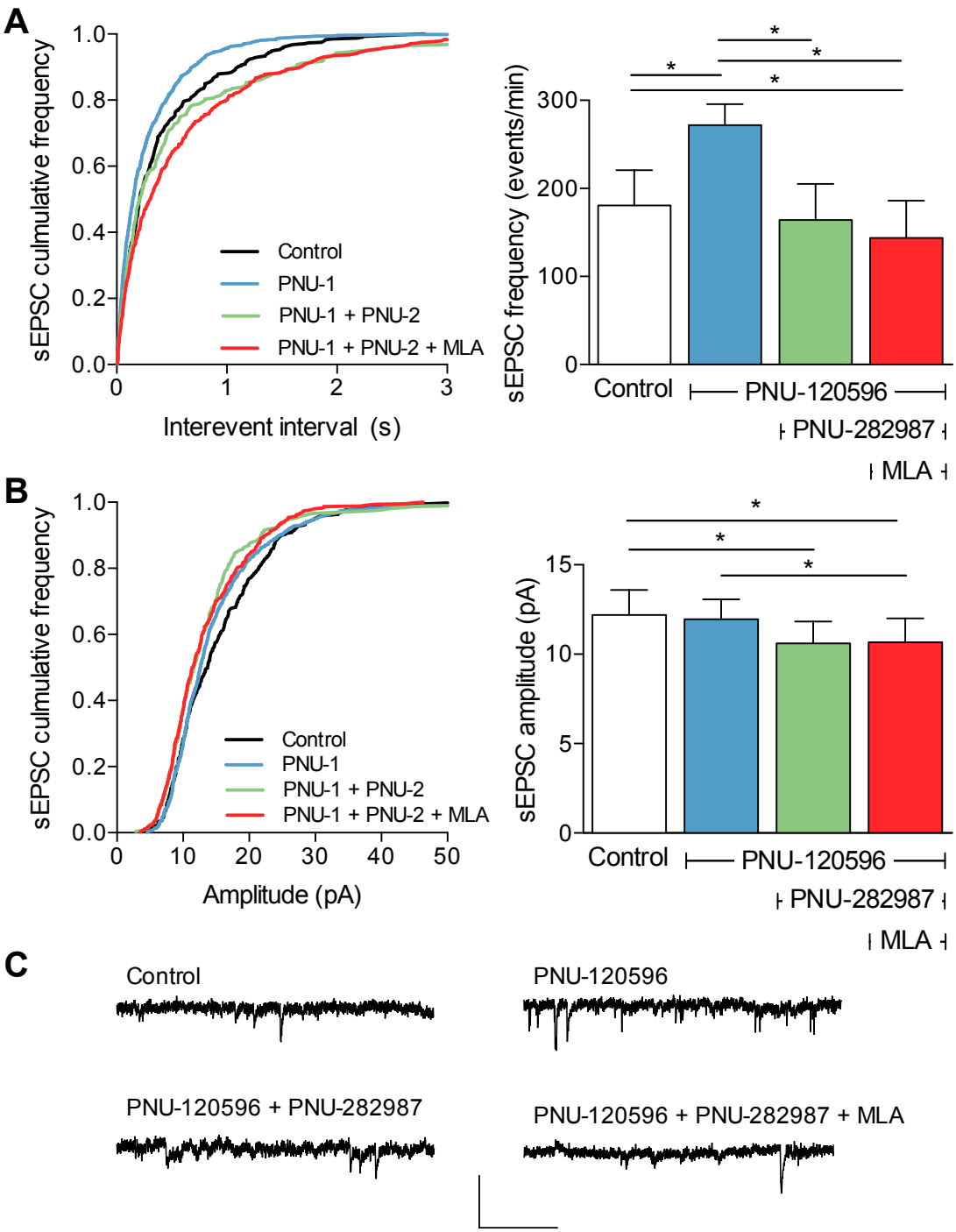

Figure 4.2 Frequency and amplitude of sEPSCs in response to α7 nAChR activation and antagonism

Voltage clamp recording were made from layer V pyramidal neurons. Whilst neurons were held at -60 mV sEPSCs were recorded in response to continual bath perfusion of control aCSF and then aCSF containing the α7 nAChR-selective PAM PNU-120596 (10 μM), the α7 nAChR PAM and selective agonist PNU-282987 (300 nM) and finally the α7 nAChR PAM + agonist and antagonist MLA (100 nM). ***(A)*** *sEPSCs frequency (interevent interval) and (****B****) sEPSC amplitudes were analysed, ranked and plotted in a cumulative frequency plot (left) total events per minute (A) and average amplitude (B) were also calculated and plotted as mean ± S.E.M in a summary histogram (right). Statistical difference shown in the histogram is based on results of K-S tests of data shown in the corresponding cumulative frequency plots. * significantly different, p ≤ 0.01; n = 7. (****C****) Representative current traces showing sEPSCs during each drug application. Scale bar: 30 pA and 0.5 sec.*

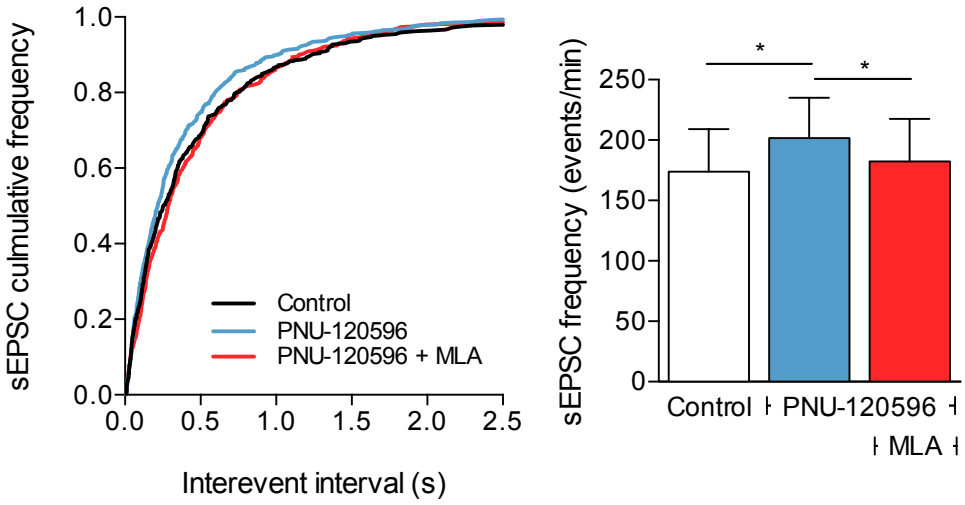

Figure 4.3 Increased frequency of sEPSCs in response to α7 nAChR PAM is directly reversed via α7 nAChR antagonism

*Voltage clamp recording were made from layer V pyramidal neurons. Whilst neurons were held at -60 mV sEPSCs were recorded in response to continual bath perfusion of control aCSF and then aCSF containing the α7 nAChR-selective PAM PNU-120596 (10 μM), followed by the α7 nAChR PAM and antagonist MLA (100 nM). sEPSCs frequency was analysed as interevent interval, ranked and plotted in a cumulative frequency plot (left) total events per minute were also calculated and plotted as mean ± S.E.M in a summary histogram (right). Statistical difference shown in the histogram is based on results of K-S tests of data shown in the cumulative frequency plot. * significantly different, p ≤ 0.01; n = 9*

The rise and decay times of sEPSCs were also measured, as changes in these current parameters can be an indicator of the proximal location of the activated synapse in relation to the soma of the recorded neuron (Magee, 2000; Smith et al., 2003; Han et al., 2013; Johnston & Brown, 1983; S. H. Williams & Johnston, 1991). Longer (slower) rise and decay times correspond to synapses at distal dendrites, while shorter (faster) rise and decay times represent synapses at more proximal locations, an effect caused via dendritic filtering as a result of the cable properties of dendrites within a neuron. As layer V pyramidal neurons span the length of the cortical layers these current properties are of interest to study. Changes in these values could indicate that synapses at distal dendrites in superficial layers may be differentially regulated by α7 nAChRs compared to synapses at proximal dendrites within layer V.

sEPSC rise and decay times were unaltered by application of α7 nAChR PAM alone. On addition of the α7 nAChR selective agonist, sEPSC decay times significantly increased compared to control but no effect was seen with the sEPSC rise time. Addition of the α7 nAChR antagonist MLA significantly increased both the sEPSC rise and decay times compared to control (Fig. 4.4A-C). This slower/longer rise and decay time in response to MLA could indicate α7 nAChR antagonism leads to reduced synaptic release from more proximal excitatory synapses. However if true, one might expect a decrease in rise and decay time upon activation of α7 nAChRs, which was not seen. In fact upon activation of α7 nAChRs with PAM and agonist there was an increase in sEPSC decay time (Fig. 4.4A-C).

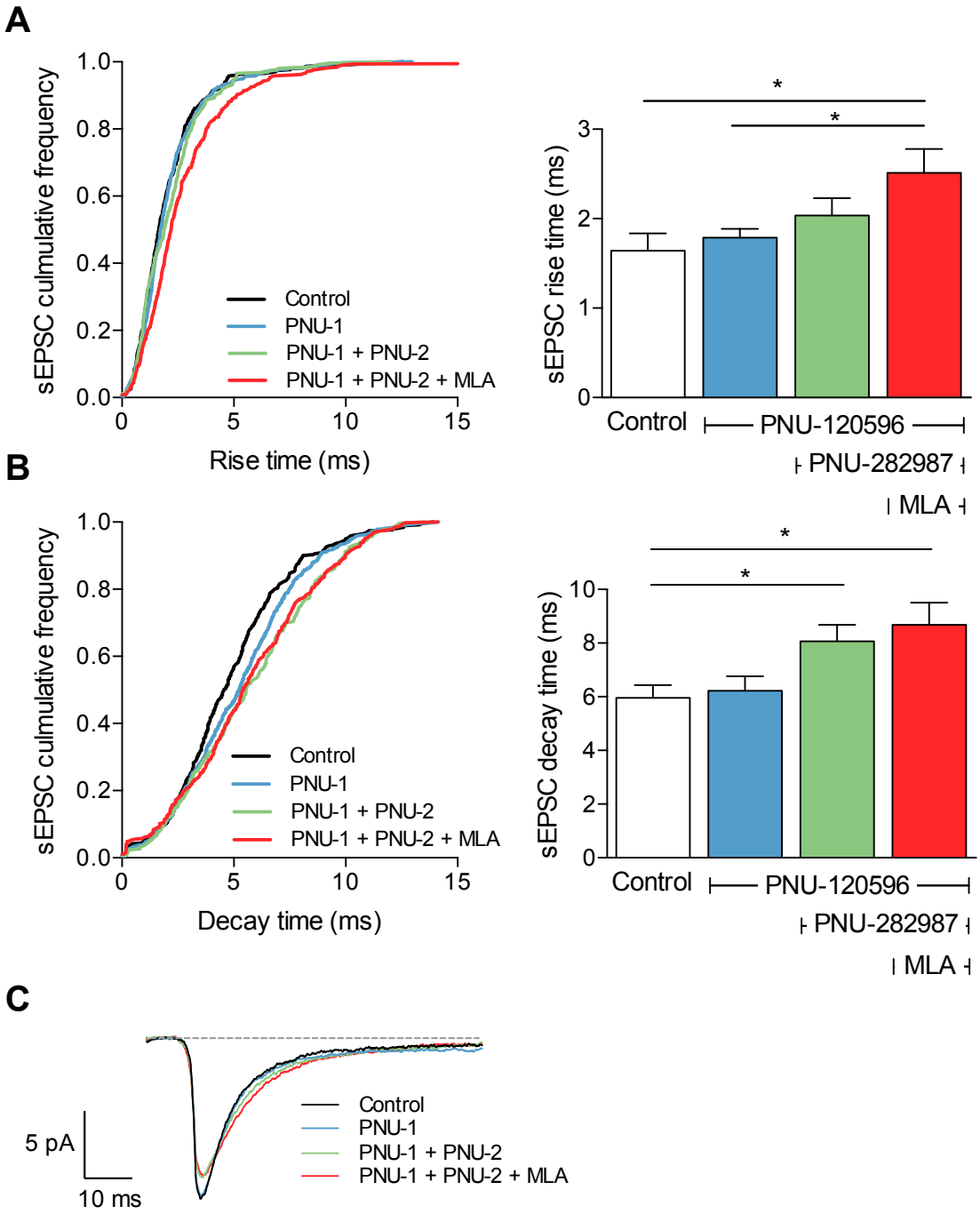

Figure 4.4 Rise and decay times of sEPSCs in response to α7 nAChR activation and antagonism

Voltage clamp recording were made from layer V pyramidal neurons. Whilst neurons were held at -60 mV sEPSCs were recorded in response to continual bath perfusion of control aCSF and then aCSF containing the α7 nAChR-selective PAM PNU-120596 (10 μM), the α7 nAChR PAM and selective agonist PNU-282987 (300 nM) and finally the α7 nAChR PAM + agonist and antagonist MLA (100 nM). ***(A)*** *sEPSCs rise time and (****B****) sEPSC decay time were analysed, ranked and plotted in a cumulative frequency plot (left) average rise time (A) and decay time (B) were also calculated and plotted as mean ± S.E.M in a summary histogram (right). Statistical difference shown in the histogram is based on results of K-S tests of data shown in the corresponding cumulative frequency plots. * significantly different, p ≤ 0.01; n = 7. (****C*** *For each drug treatment individual sEPSCs were averaged to give an average trace per cell, traces from all cells were then averaged to give an overall representative sEPSC trace.*

As shown in previous figures, α7 nAChR antagonism with MLA produces changes in sEPSC frequency, amplitude, rise and decay times compared to control. These findings were observed after the previous addition of the α7 nAChR PAM and agonist and so to investigate the effect of α7 nAChR antagonism alone, further sEPSCs were recorded from cells in which MLA was applied to the slice in the absence of other α7 nAChR-selective drugs.

In these experiments MLA (100 nM) caused a slight overall decrease in sEPSC frequency: a clear decrease was seen in 3 out of 6 neurons, on average, this was not statistically significant from control ($p = 0.04$; K-S test (significance assigned a $p<0.01$)) (Fig. 4.5A). In contrast to previous observations application of MLA did not result in statistically significant changes in sEPSC amplitudes ($p = 0.30$; K-S test) or rise times ($p = 0.13$; K-S test) (Fig. 4.5B,C). There was however a significant increase in the decay time of the sEPSC in response to MLA (Fig. 4.5D,E).

The results obtained from experiments in which MLA was applied alone are not completely consistent with the findings in previous experiments. A possible explanation could be due to alterations in EPSC parameters over the length of the recording. The protocol used for experiments shown in figures 4.2 and 4.1 was approximately 35-40 min, with MLA applied in the final 5 min. The recorded currents may be distorted over this time course due to neuron deterioration or loss of adequate voltage clamp. To ensure neurons recorded for this length of time produced stable current properties with time, sEPSCs were recorded and analysed at matched timepoints in the absence of α7 nAChR modulation.

The sEPSC frequency over time was unchanged at any of the corresponding timepoints (Fig. 4.6A), confirming that the measurement of sEPSC frequency over time is reliable. sEPSC amplitude, rise time and decay time, were stable over time until the final timepoint, (timepoint 4) at which the sEPSC amplitudes significantly decreased (Fig. 4.6B), and sEPSC rise and decay time significantly increased compared to control (Fig. 4.6C,D). As timepoint 4 corresponds to the final bath application of MLA, this suggests that the significant alterations in sEPSC amplitude, rise and decay times, shown in figures 4.2B and 4.4 may not be reliable.

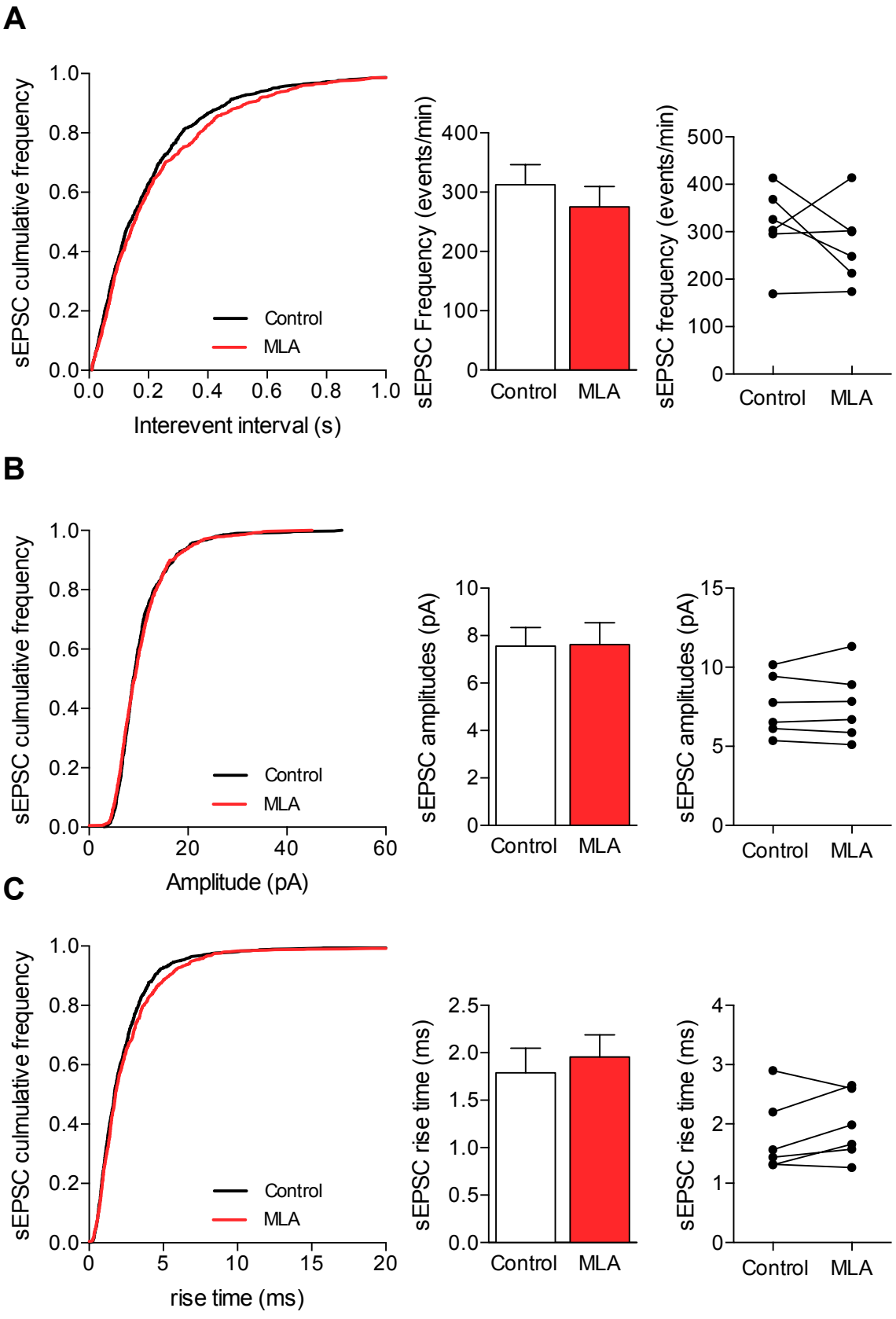
A
sEPSC culmulative frequency
1.0
0.8
0.6
0.4
0.2
0.0
0.0 0.2 0.4 0.6 0.8 1.0
Interevent interval (s)
Control
MLA
sEPSC Frequency (events/min)
400
300
200
100
0
Control MLA
sEPSC frequency (events/min)
500
400
300
200
100
0
Control MLA
B
sEPSC culmulative frequency
1.0
0.8
0.6
0.4
0.2
0.0
0 20 40 60
Amplitude (pA)
Control
MLA
sEPSC amplitudes (pA)
10
8
6
4
2
0
Control MLA
sEPSC amplitudes (pA)
15
10
5
0
Control MLA
C
sEPSC culmulative frequency
1.0
0.8
0.6
0.4
0.2
0.0
0 5 10 15 20
rise time (ms)
Control
MLA
sEPSC rise time (ms)
2.5
2.0
1.5
1.0
0.5
0.0
Control MLA
sEPSC rise time (ms)
4
3
2
1
0
Control MLA

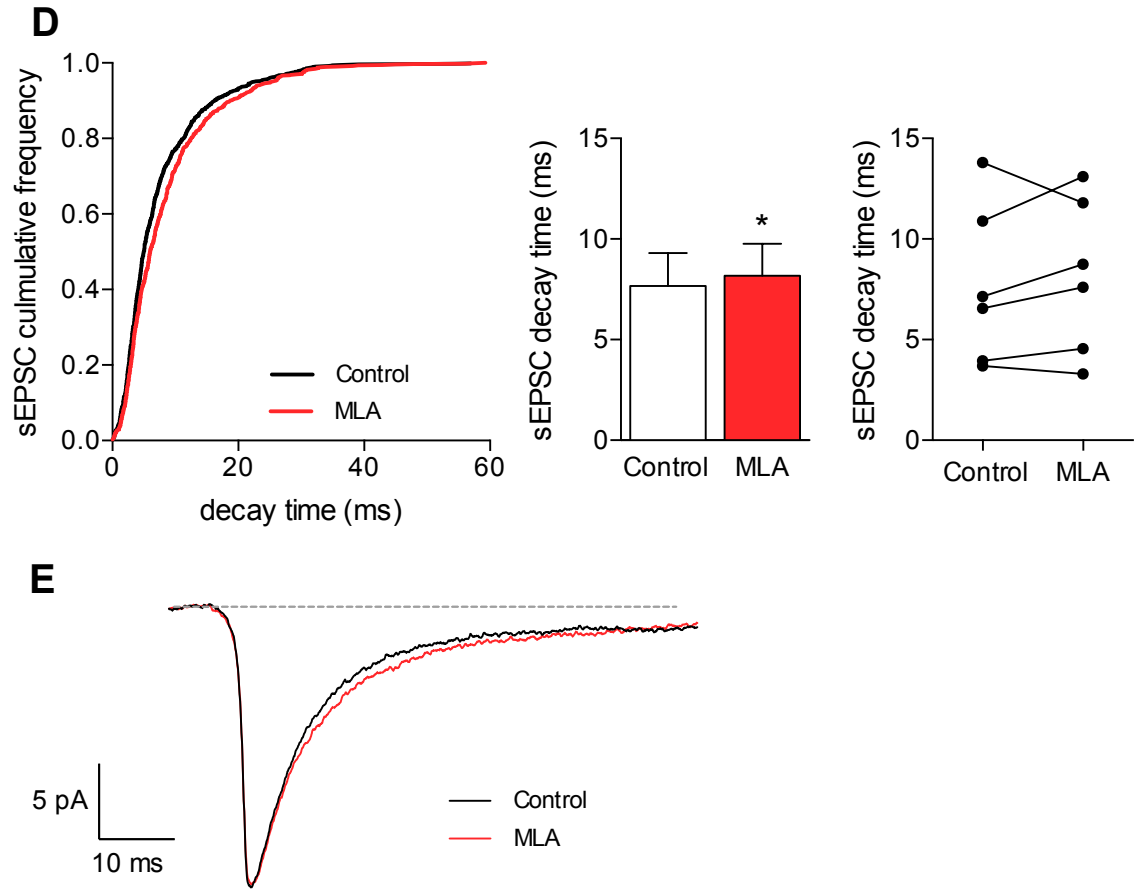

Figure 4.5 Changes in sEPSC properties in response to α7 nAChR antagonism

*Voltage clamp recording were made from layer V pyramidal neurons. Whilst neurons were held at -60 mV sEPSCs were recorded in response to continual bath perfusion of control aCSF followed by a 5 min application of aCSF containing the α7 nAChR antagonist MLA (100 nM). (**A**) sEPSC frequency (interevent interval), (**B**) sEPSC amplitude, (**C**) sEPSC rise time and (**D**) sEPSC decay time was analysed for each EPSC, ranked and plotted in a cumulative frequency plot (left). Average events per min, amplitudes, rise time and decay time were also calculated for each cell and plotted (right) and shown as mean ± S.E.M in a summary histogram (middle) Statistical difference shown in the histogram is based on results of K-S tests of data shown in the corresponding cumulative frequency plots. * significantly different, p ≤ 0.01; n = 6. (**C**) For each drug treatment individual sEPSCs were averaged to give an average trace per cell, traces from all cells were then averaged to give an overall representative sEPSC trace.*

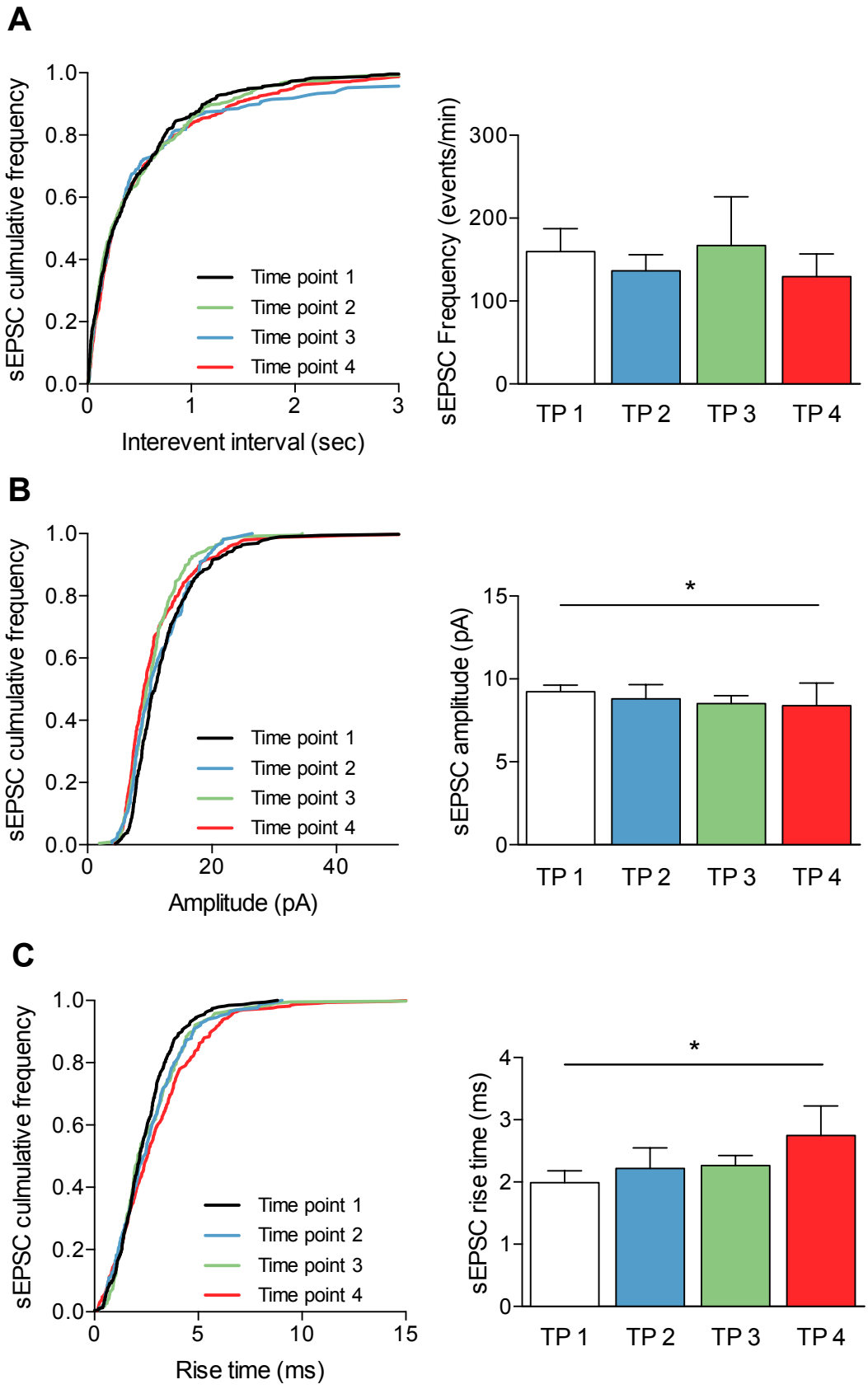
A
sEPSC culmulative frequency
1.0
0.8
0.6
0.4
0.2
0.0
0
1
2
3
Interevent interval (sec)
Time point 1
Time point 2
Time point 3
Time point 4
sEPSC Frequency (events/min)
300
200
100
0
TP 1
TP 2
TP 3
TP 4
B
sEPSC culmulative frequency
1.0
0.8
0.6
0.4
0.2
0.0
0
20
40
Amplitude (pA)
Time point 1
Time point 2
Time point 3
Time point 4
sEPSC amplitude (pA)
15
10
5
0
*
TP 1
TP 2
TP 3
TP 4
C
sEPSC culmulative frequency
1.0
0.8
0.6
0.4
0.2
0.0
0
5
10
15
Rise time (ms)
Time point 1
Time point 2
Time point 3
Time point 4
sEPSC rise time (ms)
4
3
2
1
0
*
TP 1
TP 2
TP 3
TP 4

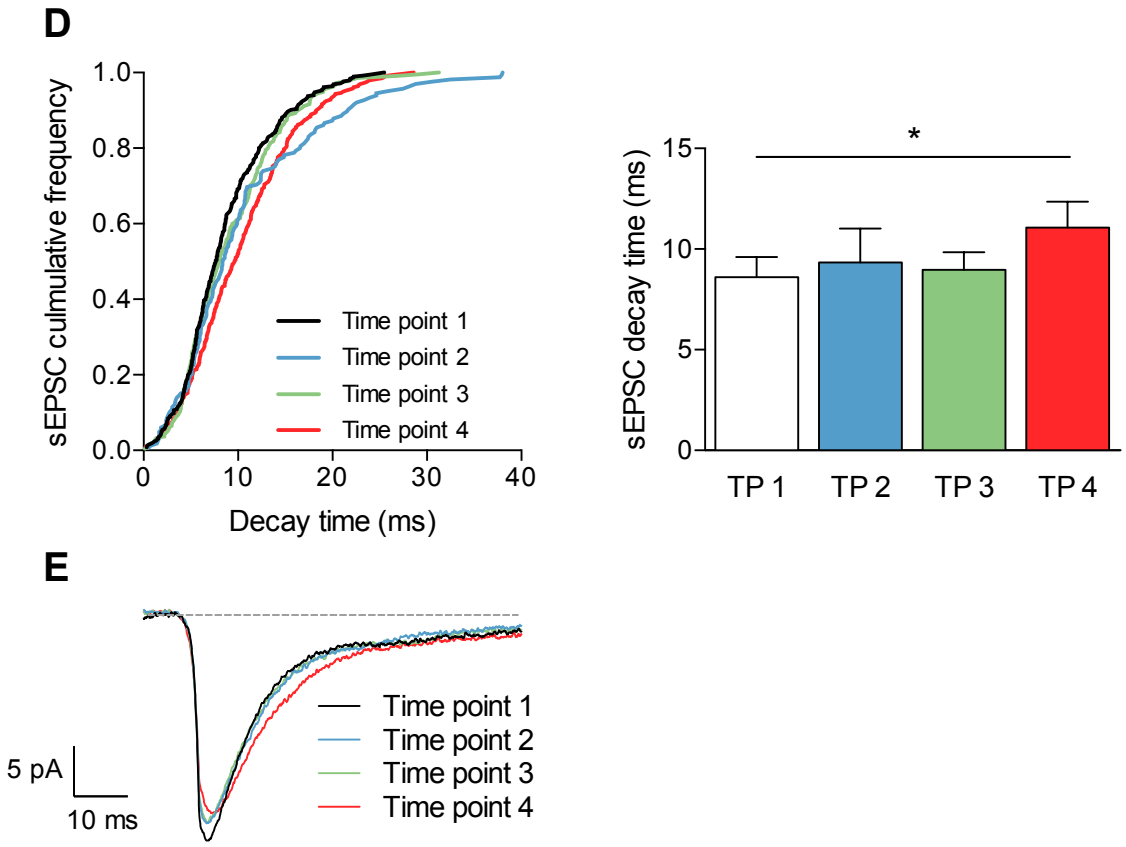

Figure 4.6 sEPSC frequency, amplitude rise and decay times over time in the absence of α7 nAChR modulation

*Voltage clamp recording were made from layer V pyramidal neurons. Whilst neurons were held at -60 mV sEPSCs were recorded during a continual bath perfusion of control aCSF, sEPSC were then analysed at four timepoints (TP) 7 min apart corresponding to the three drug applications in previous experiments (**A**) sEPSC frequency (interevent interval), (**B**) sEPSC amplitude, (**C**) sEPSC rise time and (**D**) sEPSC decay time was analysed for each EPSC, ranked and plotted in a cumulative frequency plot (left). Average events per min, amplitudes, rise time and decay time were also calculated for each cell and plotted (right) and shown as mean ± S.E.M in a summary histogram (middle) Statistical difference shown in the histogram is based on results of K-S tests of data shown in the corresponding cumulative frequency plots. * significantly different, p ≤ 0.01; n = 5. (**C**) For each timepoint individual sEPSCs were averaged to give an average trace per cell, traces from all cells were then averaged to give an overall representative sEPSC trace.*

4.2.2.2 α7 nAChR modulation of spontaneous inhibitory currents

Measurement of the inhibitory sIPSCs from the same layer V neurons shown in figures 4.2 and 4.4, revealed substantially different effects of α7 nAChR activation on inhibitory input. α7 nAChR positive allosteric modulation with PNU-120596 (10 μM) did not alter the sIPSC frequency, whereas co-application of PNU-120596 with the α7 nAChR agonist PNU-282987 (300 nM) significantly increased sIPSC frequency compared to control. This increase in inhibition was subsequently reversed upon application of MLA (100 nM) (Fig. 4.7A,B). In separate experiments MLA applied directly to the slice in the absence of PNU-120596 or PNU-282987, had no effect on the baseline sIPSC frequency (Fig. 4.8) and no change in sIPSC frequency were observed over time in the absence of α7 nAChR drugs (Fig. 4.9)

These findings demonstrate that α7 nAChR activity can modulate the inhibition of layer V pyramidal neurons. Interestingly inhibition was only enhanced in response to co-applications of α7 nAChR agonist and PAM and not the PAM alone. This suggests that enhancing endogenous activity at α7 nAChRs with the α7 nAChR PAM alone is insufficient to enhance inhibition of layer V pyramidal neurons, in contrast to the effect seen with sEPSCs shown in figure 4.2A.

Due to the high sIPSC frequency in response to PNU-120596 and PNU-282987 co-application, individual inhibitory currents merged with neighbouring currents (Fig. 4.7B). It was therefore not possible to isolate individual currents to accurately measure sIPSC amplitudes, rise or decay times in response to α7 nAChR activation.

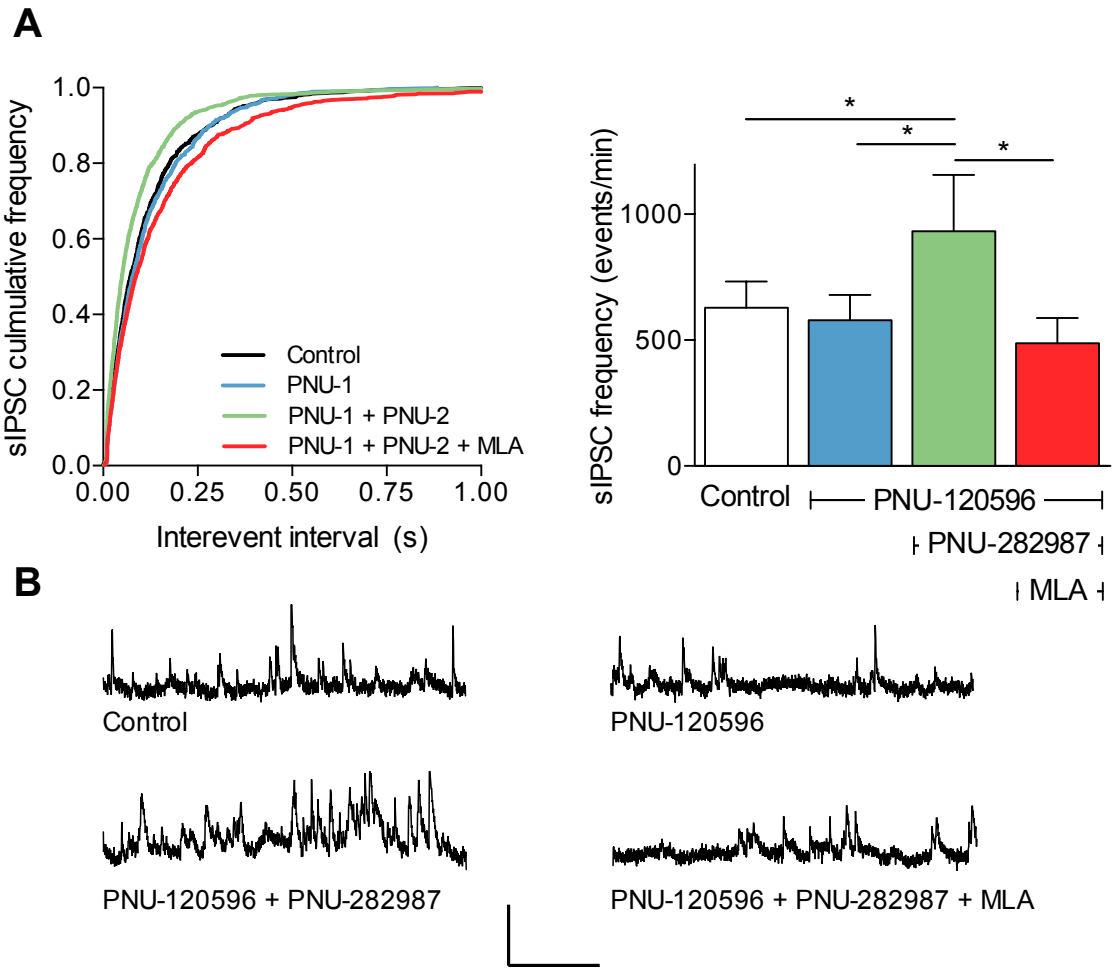

Figure 4.7 Frequency of sIPSCs in response to α7 nAChR activation and antagonism

Voltage clamp recording were made from layer V pyramidal neurons. Whilst neurons were held at 0 mV sIPSCs were recorded in response to continual bath perfusion of control aCSF and then aCSF containing the α7 nAChR-selective PAM PNU-120596 (10 μM), the α7 nAChR PAM and selective agonist PNU-282987 (300 nM) and finally the α7 nAChR PAM + agonist and antagonist MLA (100 nM). ***(A)*** *sIPSC interevent intervals were analysed, ranked and plotted in a cumulative frequency plot (left) total events per minute were also calculated and plotted as mean ± S.E.M in a summary histogram (right). Statistical difference shown in the histogram is based on results of K-S tests of data shown in the corresponding cumulative frequency plots. * significantly different, p ≤ 0.01; n = 7. (****C****) Representative current traces showing sIPSCs during each drug application. Scale bar: 30 pA and 0.5 sec.*

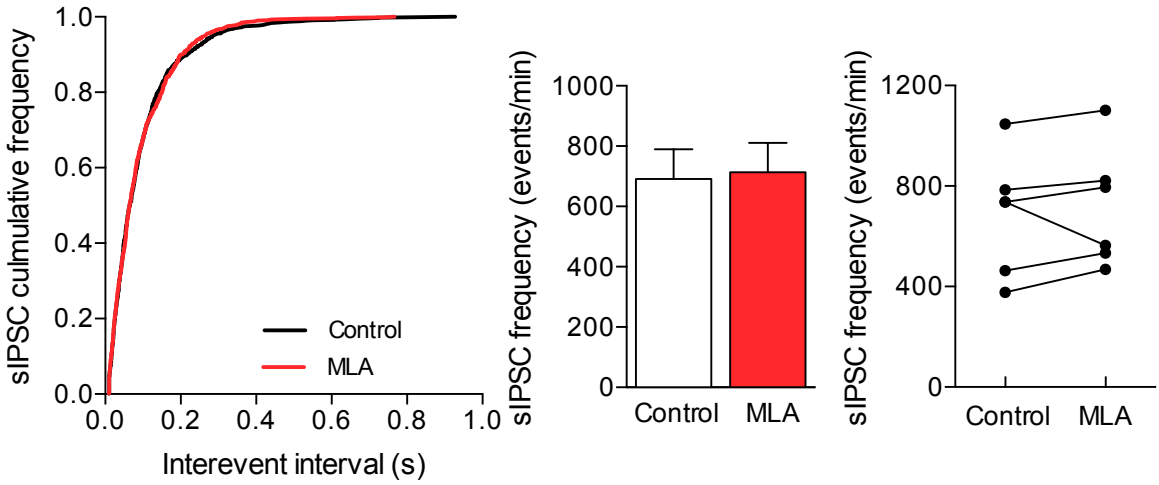

Figure 4.8 Frequency of sIPSCs in response to direct α7 nAChR antagonism

Voltage clamp recording were made from layer V pyramidal neurons. Whilst neurons were held at 0 mV sIPSCs were recorded in response to continual bath perfusion of control aCSF and then 5 min application of aCSF containing the α7 nAChR antagonist MLA (100 nM). sIPSC interevent intervals were analysed, ranked and plotted in a cumulative frequency plot (left) total events per minute were calculated for each cell and plotted (right) and shown as mean ± S.E.M in a summary histogram (middle). K-S tests of data shown in the cumulative frequency plot found no statistical difference in sIPSC frequency. n = 6.

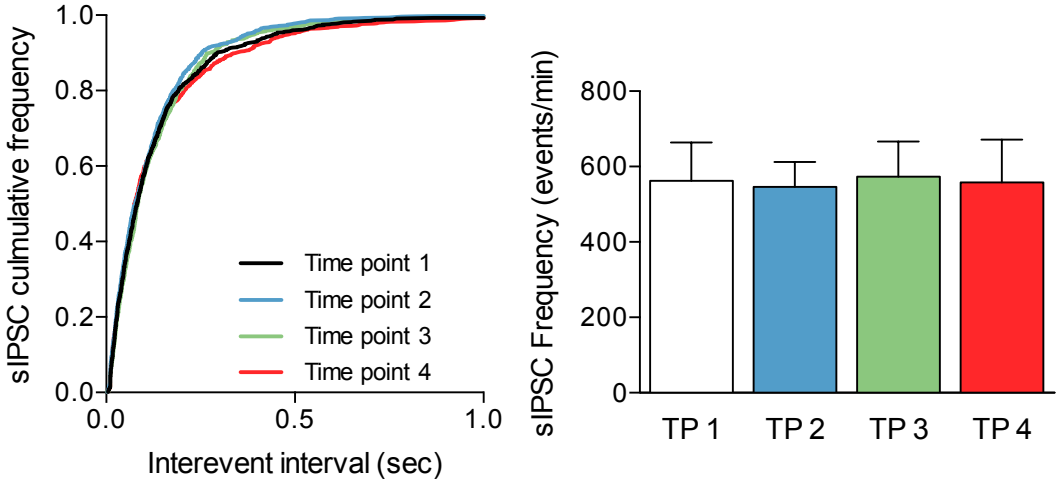

Figure 4.9 sIPSC frequency change over time in the absence of α7 nAChR modulation

Voltage clamp recording were made from layer V pyramidal neurons. Whilst neurons were held at 0 mV, sIPSCs were recorded during a continual bath perfusion of control aCSF. sIPSC were then analysed at four timepoints (TP) 7 min apart corresponding to the three drug applications in previous experiments. sIPSC interevent intervals were analysed, ranked and plotted in a cumulative frequency plot (left) total events per minute were also calculated and plotted as mean ± S.E.M in a summary histogram (right) K-S tests of data shown in the cumulative frequency plot found no statistical difference in sIPSC frequency between timepoints. n = 6.

The α7 nAChR agonist PNU-282987 in the afore mentioned experiments was applied in the presence of the α7 nAChR PAM PNU-120596, to prevent α7 nAChR desensitisation. To investigate if the increase in inhibition and decrease in excitation (Fig. 4.7 and 4.2A) seen with co-application of α7 PAM and agonist could be achieved with the agonist alone, PNU-282987 (300 nM) was applied directly to the slice for 5 min and both sEPSC and sIPSCs measured. Interestingly sEPSC and sIPSC frequencies were unaltered upon PNU-282987 application (Fig. 4.10A,B). This suggests the effects observed with the α7 nAChR agonist in figures 4.2 and 4.7 are dependent on the presence of the α7 nAChR PAM.

The α7 nAChR PAM PNU-120596 used in these experiments has been reported to have an altered efficacy depending on the length of time it is exposed to α7 nAChRs (Williams et al., 2011). A possibility thus arises that the observed increase in inhibition and decrease in excitation achieved upon PNU-120596 and PNU-282987 co-application may be the result of the prolonged exposure of the α7 nAChRs to PNU-120596 and is independent of PNU-282987. To rule out this possibility, sIPSCs and sEPSCs were measured in response to prolonged PNU-120596 application, replicating previous experiments but in the absence of PNU-282987. Prolonged application of PNU-120596 (10 μM) resulted in no significant increase in the sIPSC frequency (Fig. 4.11B). PNU-120596 after 5 min significantly increased sEPSC frequency, as found previously, however after 10 min application of PNU-120596 the sEPSC frequency was no longer significantly higher than control (Fig. 4.11A). As no further increase in sIPSCs were observed upon prolonged activation of the α7 nAChR PAM, the effects observed in figures 4.2 and 4.7 in response to α7 nAChR PAM and agonist co-application appear to be dependent on the presence of the α7 nAChR agonist PNU-282987.

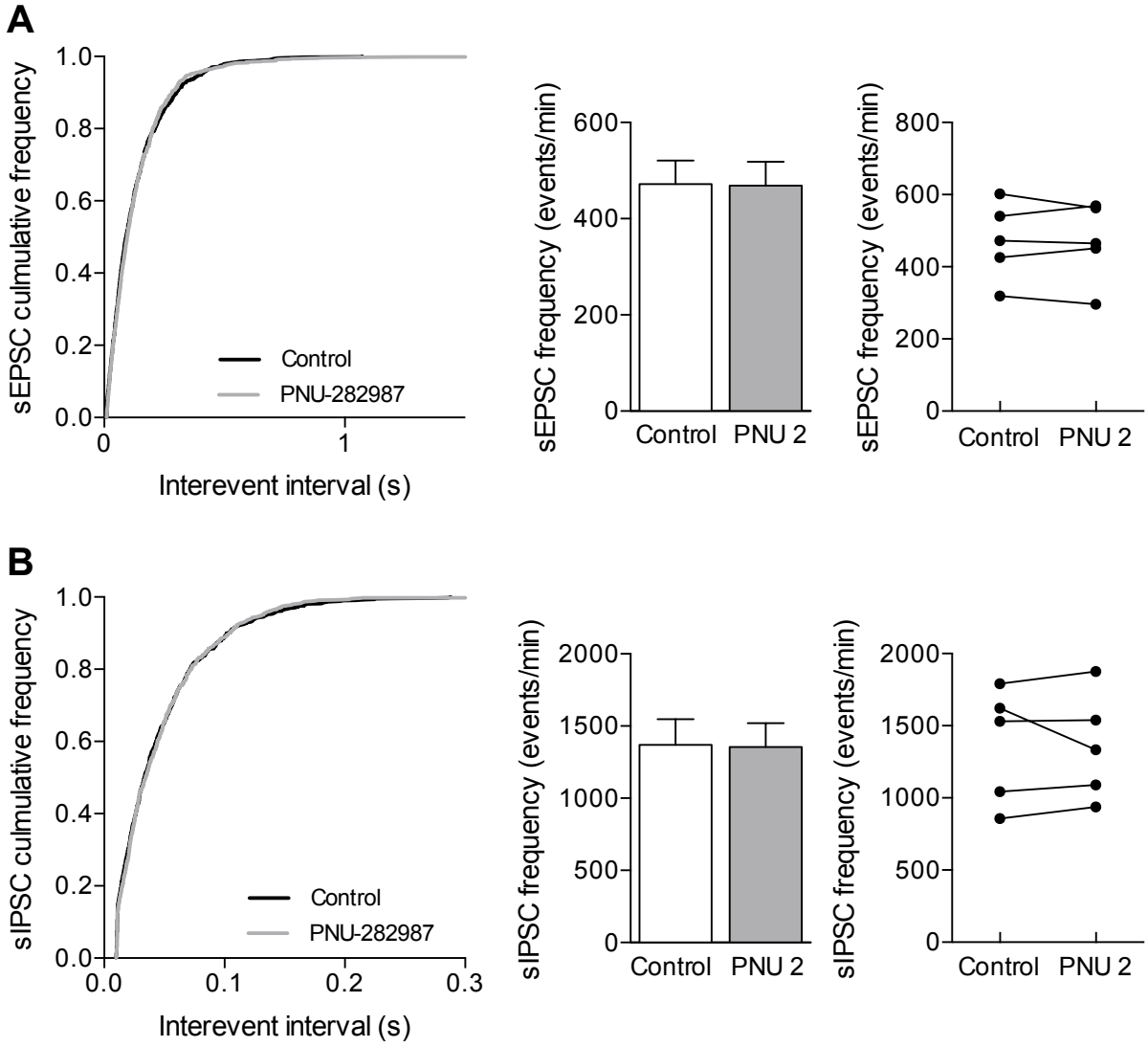

Figure 4.10 sEPSC and sIPSC frequency in response to α7 nAChR agonist activation in the absence of a positive allosteric modulator

*Voltage clamp recording were made from layer V pyramidal neurons that were held at -60 mV and then 0mV to record sEPSCs and sIPSCs from the same cell. Spontaneous currents were recorded in response to continual bath perfusion of control aCSF and then 5 min application of aCSF containing the α7 nAChR agonist PNU-282987 (300 nM) (PNU-2). (**A**) sEPSC and (**B**) sIPSC interevent intervals were analysed, ranked and plotted in a cumulative frequency plot (left) total events per minute were calculated for each cell and plotted (right) and shown as mean ± S.E.M in a summary histogram (middle). K-S tests of data shown in the cumulative frequency plot found no statistical difference in either sEPSC or sIPSC frequency. n = 5.*

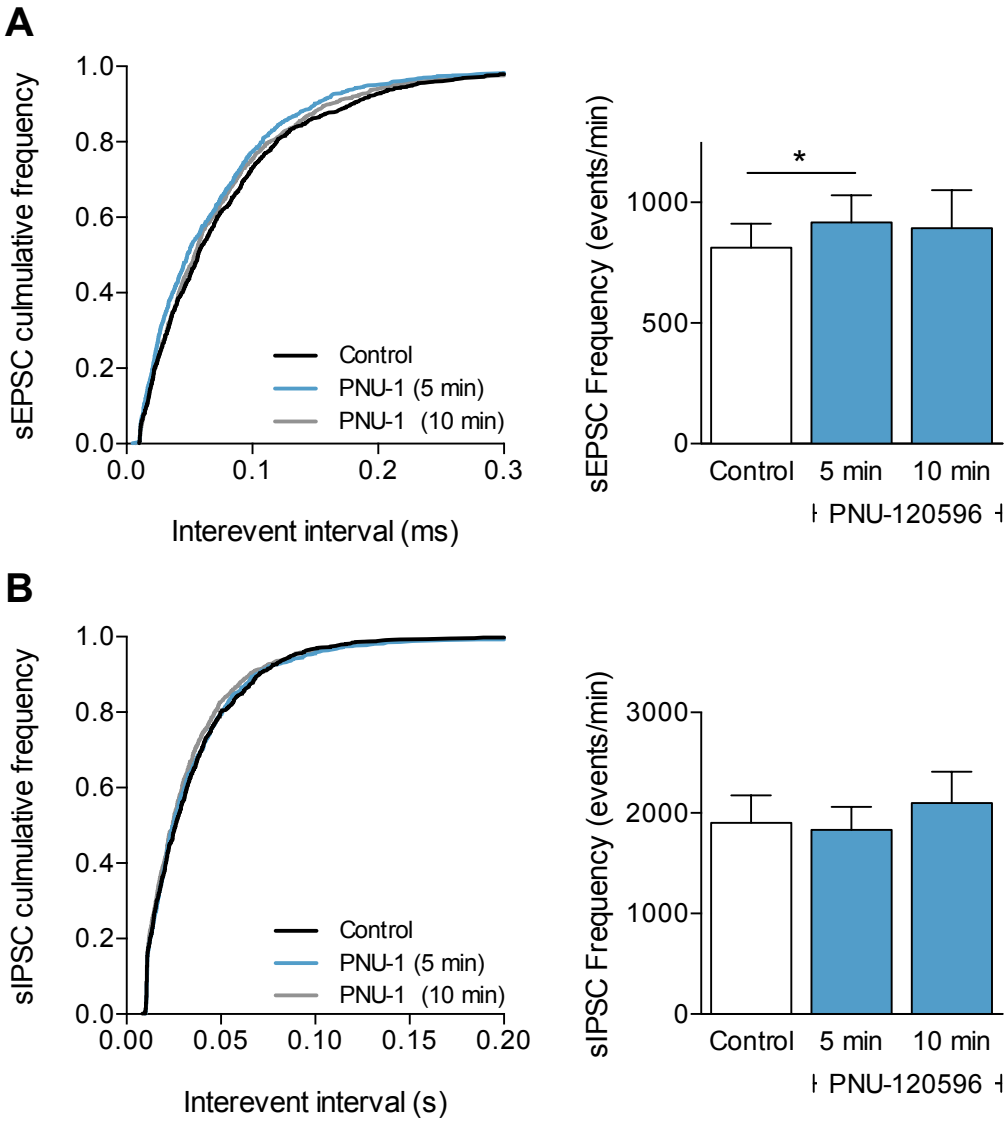

Figure 4.11 sEPSC and sIPSC frequency in response to prolonged α7 nAChR positive allosteric modulation

*Voltage clamp recording were made from layer V pyramidal neurons that were held at -60 mV and then 0mV to record sEPSCs and sIPSCs from the same cell. Spontaneous currents were recorded in response to continual bath perfusion of control aCSF and then 10 min application of aCSF containing the α7 nAChR PAM PNU-120596 (10 μM). (**A**) sEPSC and (**B**) sIPSC interevent intervals were analysed at 5 min and 10 min after drug application, data was then ranked and plotted in a cumulative frequency plot (left) total events per minute were calculated for each cell and plotted as mean ± S.E.M in a summary histogram (right) Statistical difference shown in histograms is based on results of K-S tests of data shown in the corresponding cumulative frequency plots. * significantly different, p ≤ 0.01; n = 5.*

α7 nAChRs can enhance the level of spontaneous excitation but also enhance the level of spontaneous inhibition onto layer V pyramidal cells. The balance in excitation and inhibition is important in determining the neuron's overall excitable state and output, and is shown to be important for mediating normal neuronal function, whilst imbalances in the E/I ratio is implicated in numerous neurological diseases (John & Berg, 2015; Yizhar et al., 2011). As the methodology used in the experiments thus far was designed to enable the measurement of excitatory and inhibitory signalling onto the same neuron, the excitatory to inhibitory neurotransmission ratio (E/I ratio) can be determined, revealing the overall network consequence of α7 nAChR modulation. Data obtained from figures 4.2 and 4.7 were used to calculate the E/I ratios by dividing sEPSCs and sIPSC frequencies within the same cell. Upon application of α7 nAChR PAM alone, the E/I ratio significantly increased compared to control (Fig. 4.12), showing an overall net increase in excitatory neurotransmission. Upon co-application of the α7 nAChR PAM and agonist this enhancement in the E/I ratio was significantly reversed (Fig. 4.12), consistent with a switch from overall enhanced excitatory drive to a predominantly inhibitory drive.

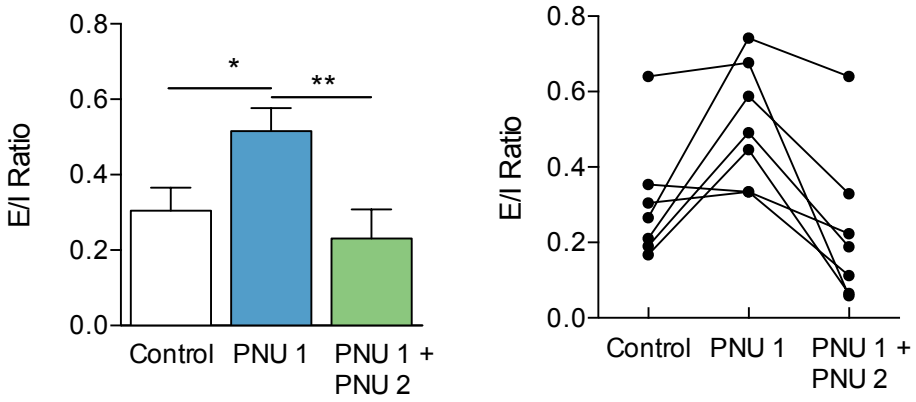

Figure 4.12 Excitatory / inhibitory ratio in response to different types of α7 nAChR activation

*Voltage clamp recording were made from layer V pyramidal neurons that were held at -60 mV and then 0mV to record sEPSCs and sIPSCs from the same cell. Spontaneous currents were recorded in response to continual bath perfusion of control aCSF and then aCSF containing the α7 nAChR-selective PAM PNU-120596 (10 μM) followed by aCSF containing the α7 nAChR PAM and selective agonist PNU-282987 (300 nM). E/I ratios were calculated by dividing the frequency (events per min) of sEPSCs by the frequency of sIPSC. E/I ratio changes of individual neurons were plotted (right) and averaged and shown as mean ± S.E.M in summary histograms (left). Significance was assigned via one-way repeated measures ANOVA with Dunnett's post hoc test, p ≤ 0.05 * and p ≤ 0.01 **: n = 7. Data used from figures 4.2A and 4.7.*

4.2.3 α7 nAChRs modulation of excitatory and inhibitory neurotransmission is mediated via independent processes

Studies investigating the effects of nicotine on inhibitory neurotransmission in the mPFC suggest that nicotine can increase inhibition of pyramidal cells directly and also via a feedforward inhibition mechanism. This feedforward inhibition mechanism is brought about via a nicotine-induced increase in glutamate release onto mPFC interneurons via the activation of α4β2 nAChRs expressed on thalamo-cortical inputs (Aracri et al., 2010; Couey et al., 2007; Lambe et al., 2003), consequently leading to inhibition of pyramidal neurons. To determine if the increase in sIPSCs frequency upon co-application of the α7 nAChR PAM and agonist may be a result of a similar feedforward inhibition mechanism, sIPSCs were recorded in response to α7 nAChR activation in the absence of glutamatergic signalling.

The AMPA/kainate receptor antagonist DNQX (10 μM) was applied to the slice to remove excitatory inputs within the network. Any increase in sIPSC frequency upon α7 nAChR activation could then be assigned to direct effects at GABAergic interneurons. Similar to previous experiments (Fig. 4.7), in the presence of DNQX, co-application of PNU-120596 (10 μM) and PNU-282987 (300 nM) caused a significant increase in sIPSC frequency, which was significantly reduced by MLA (100 nM) (Fig. 4.13). This increase in inhibition to PNU-120596 and PNU-282987 in DNQX was comparable to original experiments in the absence of DNQX (Fig. 4.7). In this experiment PNU-120596 and PNU-282987 resulted in 138 ± 20% (mean ± S.E.M) increase in sIPSC frequency compared to control, comparable to the 147 ± 26% increase in sIPSC frequency to PNU-120596 and PNU-282987 in the absence of DNQX ($p = 0.80$; t-test). This suggests that α7 nAChR activation can directly enhance the activity of GABAergic interneurons and is not dependent on a feedforward inhibition mechanism.

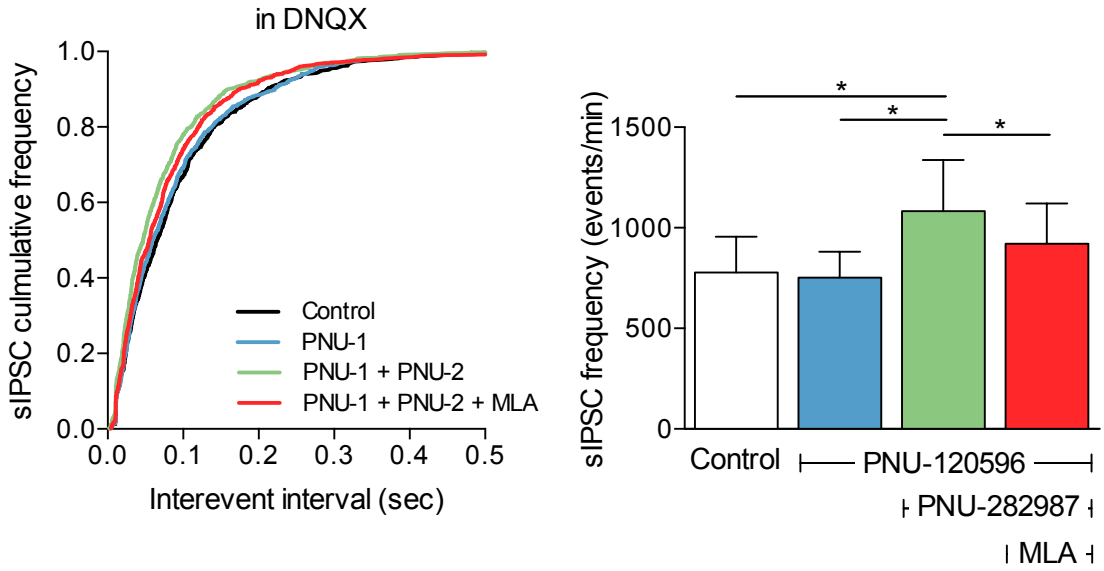

Figure 4.13 sIPSC frequency in the absence of glutamatergic neurotransmission in response to α7 nAChR activation and antagonism

*Voltage clamp recording were made from layer V pyramidal neurons in the presence of the AMPA receptor antagonist DNQX (10 μM). Whilst neurons were held at 0 mV sIPSCs were recorded in response to continual bath perfusion of control aCSF containing DNQX and then aCSF containing the α7 nAChR-selective PAM PNU-120596 (10 μM), the α7 nAChR PAM and selective agonist PNU-282987 (300 nM) and finally the α7 nAChR PAM + agonist and antagonist MLA (100 nM) all in the presence of DNQX. sIPSC interevent intervals were analysed, ranked and plotted in a cumulative frequency plot (left) total events per minute were also calculated and plotted as mean ± S.E.M in a summary histogram (right). Statistical difference shown in the histogram is based on results of K-S tests of data shown in the corresponding cumulative frequency plots. * significantly different, p ≤ 0.01; n = 6.*

In addition to feedforward inhibition, cortical interneurons participate in reciprocal inhibition of other inhibitory interneurons, and it has been suggested that nicotinic activation of interneurons promotes such mechanisms (Aracri et al., 2010). It was therefore interesting to investigate if the α7 nAChR-mediated increase in excitation observed is independent of inhibitory neurotransmission. To test this possibility sEPSCs were recorded in the presence of the $GABA_A$ receptor antagonist picrotoxin (50 μM). Upon picrotoxin application, producing reliably stable sEPSC recordings was difficult. Repetitive bursts of excitatory activity were observed in the absence and presence of α7 nAChR drugs (Fig. 4.14C and 4.15B). This made it difficult to accurately record sEPSC activity.

It was found that in the presence of picrotoxin, application of the α7 nAChR PAM alone or together with the α7 nAChR agonist resulted in no alteration to sEPSC frequency. However upon application of MLA sEPSC frequency was significantly reduced compared to control (Fig. 4.14A). This was unexpected, and upon closer inspection of individual cell frequencies it appeared that half of the recorded cells produced a continual decrease in frequency, while the other half of cells exhibited the predicted frequency change (Fig. 4.14B).

Interestingly upon co-application of the α7 nAChR PAM and agonist there was an increased tendency of sEPSC burst activity. In addition to this, in the presence of the α7 nAChR PAM and agonist the majority of cells exhibited large fluctuations in the holding current of the cell (Fig. 4.14C), which could be reversed upon MLA application. Although not definitive, these observations provide evidence that in the absence of inhibition, activation of the α7 nAChRs with a PAM and agonist can enhance the excitability of the layer V pyramidal neurons as was originally predicted (also see Fig. 4.23)

Due to the lack of effect seen in the presence of picrotoxin and the observation that some neurons exhibited a continual decrease in frequency, a hypothesis was formed that picrotoxin may be leading to a continual decrease in the basal sEPSC frequency over time, which may have masked any effect of α7 nAChRs on excitation. To test this, a time-matched control similar to that depicted in figure 4.6 was conducted in the presence of picrotoxin. It was indeed found that in the presence of picrotoxin (50 μM) the average sEPSC frequency significantly decreased over time (Fig. 4.15A), suggesting that the data shown in figure 4.14A may not be reliable and any interpretation may not be valid.

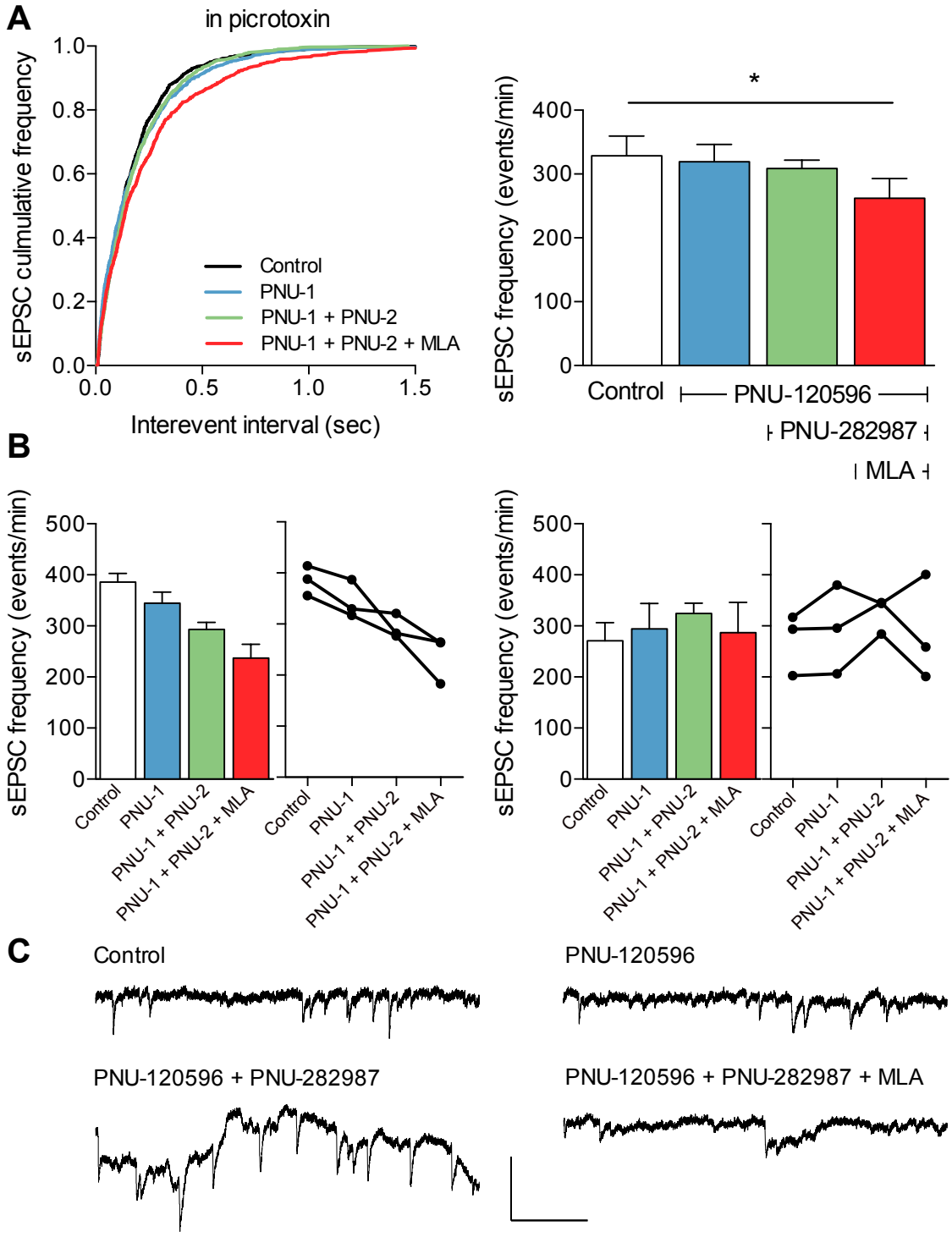

Figure 4.14 sEPSC frequency in the absence of GABAergic neurotransmission in response to α7 nAChR activation and antagonism

*Voltage clamp recording were made from layer V pyramidal neurons in the presence of the $GABA_A$ receptor antagonist picrotoxin (50 μM). Whilst neurons were held at -60 mV sEPSCs were recorded in response to continual bath perfusion of control aCSF containing picrotoxin and then aCSF containing the α7 nAChR-selective PAM PNU-120596 (10 μM), the α7 nAChR PAM and selective agonist PNU-282987 (300 nM) and finally the α7 nAChR PAM + agonist and antagonist MLA (100 nM) all in the presence of picrotoxin. (**A**) sEPSC interevent intervals were analysed, ranked and plotted in a cumulative frequency plot (left) total events per minute were also calculated and plotted as mean ± S.E.M in a summary histogram (right). (**B**) cells from (A) were split into two*

*groups one showing a continual decrease in response (left) whilst the other possessing a more typical response to drug application (right). Data shown as mean ± S.E.M in summary histogram and individual cell value plots for each drug treatment. Statistical difference shown in the histogram is based on results of K-S tests of data shown in the corresponding cumulative frequency plots. * significantly different, p ≤ 0.01; n = 6. (**C**) sEPSC traces in response to drug application demonstrate the destabilisation of the recording baseline in the presence of PNU-120596 and PNU-282987. Scale bar: 30 pA and 0.5 sec.*

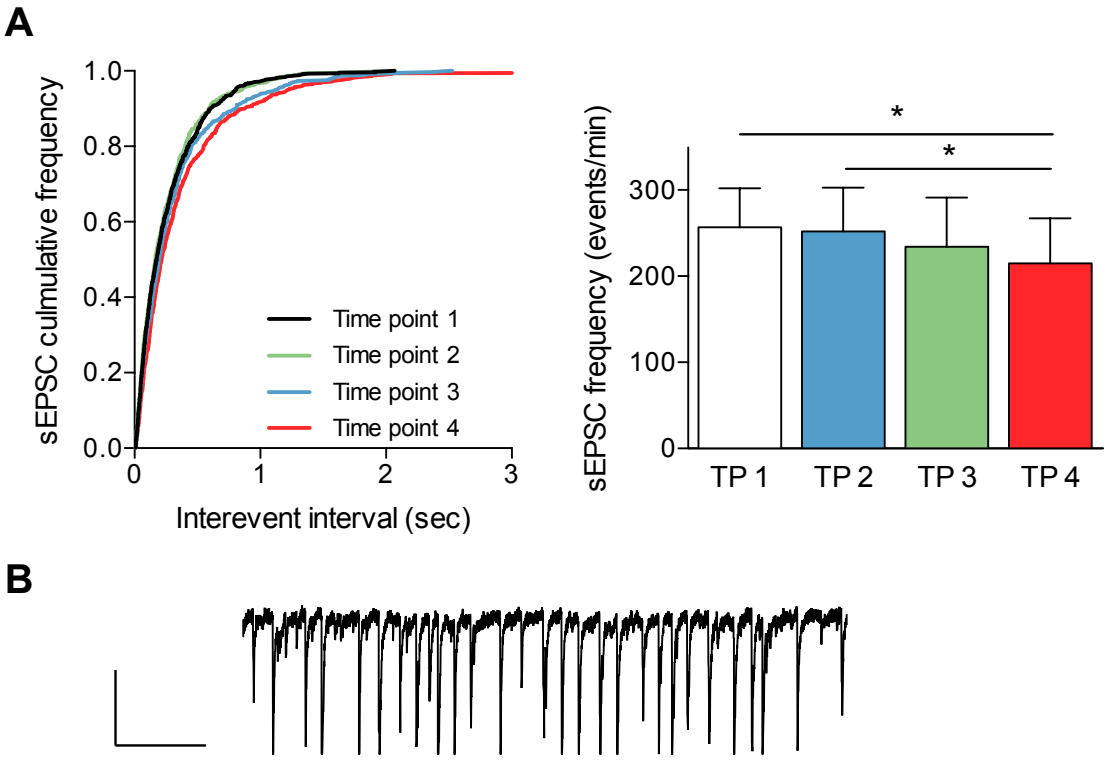

Figure 4.15 sEPSC frequency over time in the presence of picrotoxin

*Voltage clamp recording were made from layer V pyramidal neurons in the presence of the $GABA_A$ receptor antagonist picrotoxin (50 μM). Whilst neurons were held at -60 mV, sEPSCs were recorded during a continual bath perfusion of control aCSF containing picrotoxin. sEPSC were then analysed at four timepoints (TP) 7 min apart corresponding to the three drug applications in previous experiments. (**A**) sEPSC interevent intervals were analysed, ranked and plotted in a cumulative frequency plot (left) total events per minute were also calculated and plotted as mean ± S.E.M in a summary histogram (right) Statistical difference shown in the histogram is based on results of K-S tests of data shown in the corresponding cumulative frequency plot. * significantly different, p ≤ 0.01; n = 6. n = 6. (**B**) sEPSC traces demonstrating the tendency of neurons to release rapid bursts of spontaneous activity. Scale bar: 30 pA and 0.5 sec.*

4.2.4 Determining the subcellular location of α7 nAChRs within the prelimbic cortex

The findings in this chapter suggest that activation of α7 nAChRs can enhance both excitatory and inhibitory neurotransmitter release via mechanisms that appear to be independent of one another. The next objective was to identify the cellular localisation of α7 nAChRs on excitatory and inhibitory neurons, to provide a more defined mechanism to how differential activation of α7 nAChRs can regulate neurotransmission within the PrL.

It is known that α7 nAChRs are expressed somatically on multiple types of inhibitory interneurons across multiple layers of the cortex (Gulledge et al., 2007; Poorthuis et al., 2012). Heteromeric α4β2 but not homomeric α7 nAChRs, are thought to be expressed presynaptically on GABAergic terminals in the prelimbic cortex (Aracri et al., 2010). However like many studies investigating nAChRs, nicotine has been the primary non-selective agonist used. Experiments were therefore conducted to confirm the predictions from these studies, by exploiting selective α7 nAChR compounds, whilst providing details into how the different modes of α7 nAChR activation can regulate inhibitory interneurons within the prelimbic cortex.

First, to determine whether α7 nAChRs are located on nerve terminals of GABAergic interneurons, miniature IPSCs (mIPSC) were recorded from layer V pyramidal neurons. mIPSC experiments were recorded in the presence of the Na^+ channel antagonist tetrodotoxin (TTX) (1 μM), applied to block action potential firing. By preventing action potential firing, action potential-dependent transmitter release is abolished, so any changes in mIPSC frequency can be attributed to presynaptic mechanisms, whilst changes in mEPSC amplitude are indicative of postsynaptic alterations. It was found that the α7 nAChR PAM PNU-120596 (10 μM) alone and co-application of PNU-120596 with the selective nAChR agonist PNU-282987 (300nM) failed to alter either the frequency or amplitude of mIPSCs (Fig. 4.16 and 4.17). These results provide no evidence for presynaptic α7 nAChRs on mPFC interneurons.

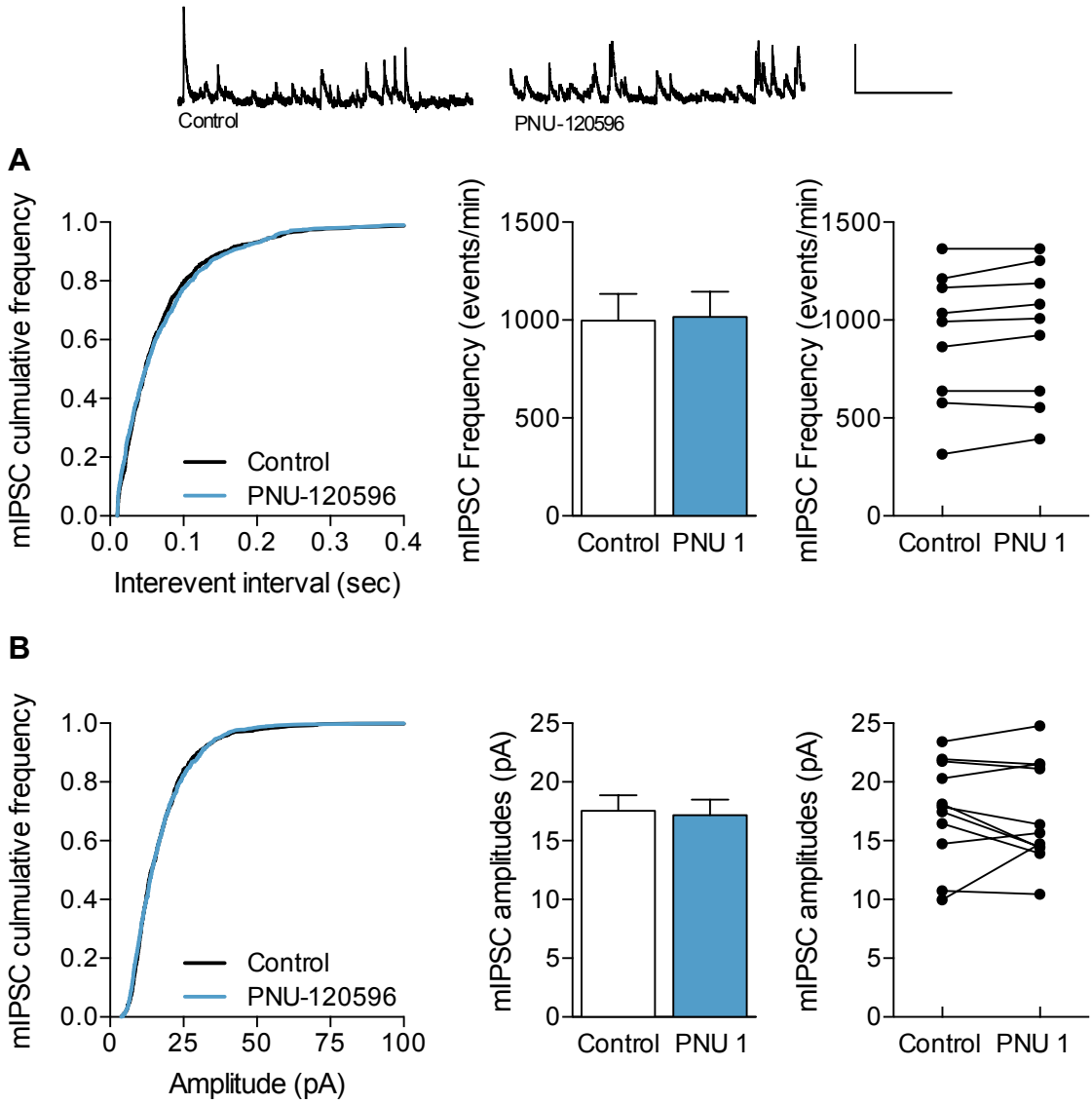

Figure 4.16 mIPSC frequency and amplitude in response to α7 nAChR positive allosteric modulation alone

*Voltage clamp recording were made from layer V pyramidal neurons in the presence of tetrodotoxin (1 μM) to block action potentials. Neurons were held at 0 mV and mIPSCs were recorded in response to continual bath perfusion of control aCSF and then 5 min application of aCSF containing the α7 nAChR PAM PNU-120596 (10 μM). (**A**) mIPSC interevent intervals and (**B**) mIPSC amplitudes were analysed, ranked and plotted in a cumulative frequency plot (left) total events per minute and average amplitudes were also calculated for each cell and plotted (right) and shown as mean ± S.E.M in a summary histogram (middle). K-S tests of data shown in the cumulative frequency plot found no statistical difference in either mIPSC frequency of amplitude; n = 11. Example mIPSCs are represented in traces (top); scale bar: 30 pA and 0.5 sec*

.

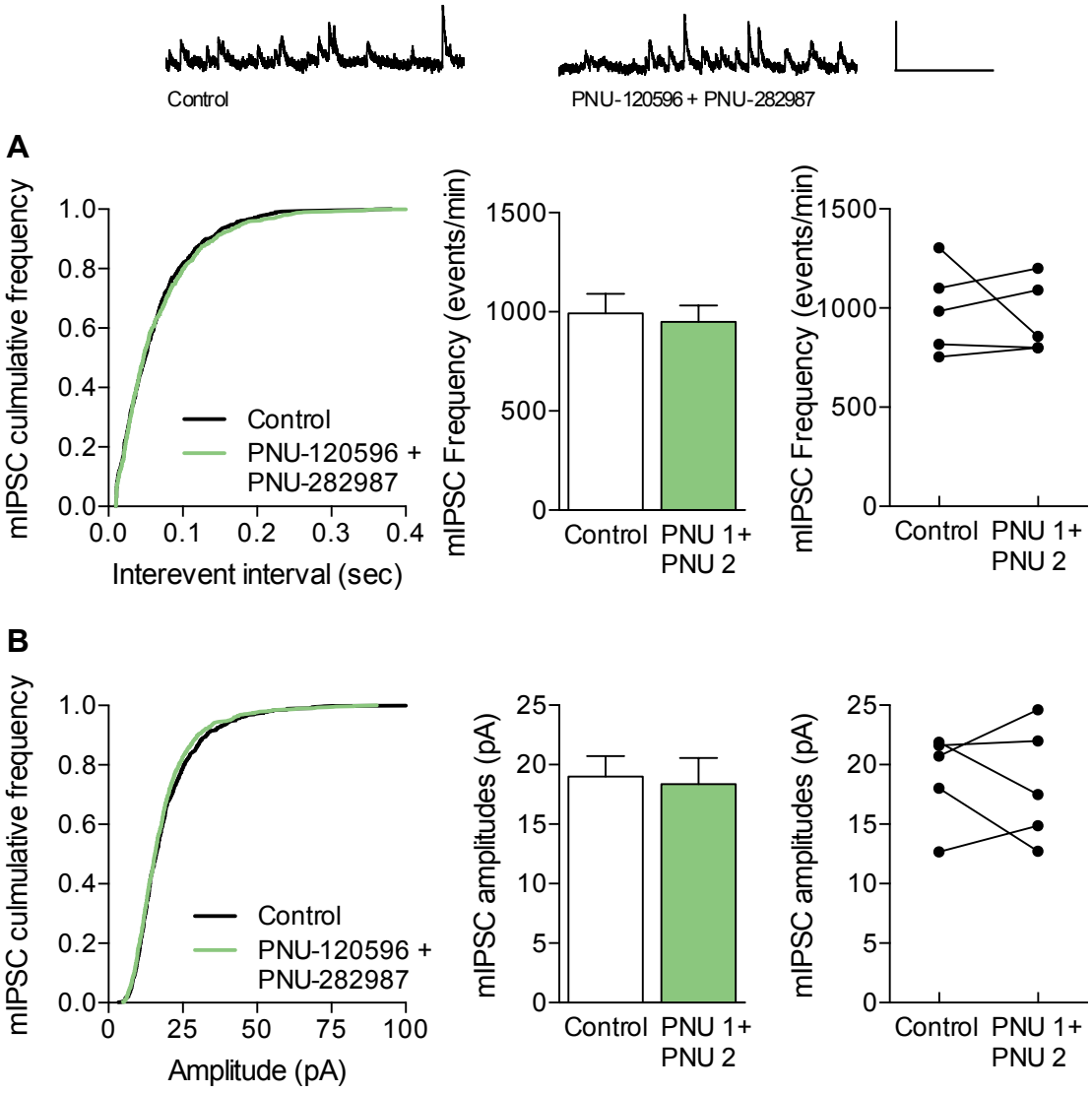

Figure 4.17 mIPSC frequency and amplitude in response to α7 nAChR activation with a selective agonist and positive allosteric modulator

*Voltage clamp recording were made from layer V pyramidal neurons in the presence of tetrodotoxin (1 μM) to block action potentials. Neurons were held at 0 mV and mIPSCs were recorded in response to continual bath perfusion of control aCSF and then 5 min application of aCSF containing the α7 nAChR PAM PNU-120596 (10 μM) and agonist PNU-282987 (300 nM). (**A**) mIPSC interevent intervals and (**B**) mIPSC amplitudes were analysed, ranked and plotted in a cumulative frequency plot (left) total events per minute and average amplitudes were also calculated for each cell and plotted (right) and shown as mean ± S.E.M in a summary histogram (middle). K-S tests of data shown in the cumulative frequency plot found no statistical difference in either mIPSC frequency of amplitude; n = 5. Example mIPSCs are represented in traces (top); scale bar: 30 pA and 0.5 sec.*

Ruling out the possibility of both a glutamate-dependent increase in inhibition (Fig. 4.13), and enhanced inhibition from direct actions at presynaptic terminals in the absence of action potentials, it was hypothesised that the increase in inhibitory input onto pyramidal cells seen with α7 nAChR PAM and agonist co-application was dependent on activation of somatic α7 nAChRs residing on the GABAergic interneurons. To test this hypothesis whole-cell current clamp recordings were made from layer V fast and non-fast spiking inhibitory interneurons. In doing so the direct depolarisation and action potential firing of these interneurons in response to bath application of α7 nAChR targeted drugs could be determined. To ensure that recordings were taken solely from inhibitory interneurons, these experiments were conducted using cortical slices from C57/BL6 GAD67-GFP transgenic mice (Tamamaki et al., 2003). These mice, hemizygous for the GAD67-GFP transgene, produce green fluorescent protein (GFP) under the GAD67 promoter, whose WT gene expresses the glutamate decarboxylase enzyme required for GABA synthesis. All inhibitory interneurons synthesising GABA could therefore be identified for electrophysiological recording using fluorescence microscopy. Depolarising current steps were also used to confirm the identity and subtype of inhibitory interneurons from their characteristic action potential firing patterns. An example of a cortical brain slice taken from a GAD67-GFP transgenic mouse is shown in figure 4.18. Here positive GAD67-GFP interneurons are clearly seen within all layers of the prelimbic cortex.

Upon current clamp recordings of these interneurons there was no observed change in depolarisation of either fast or non-fast spiking interneurons in response to the α7 nAChR PAM PNU-120596 (10 μM) or MLA (100 nM) (Fig. 4.19B,C and 4.20B,C), indicating that tonic endogenous activation of α7 nAChRs appears not to occur at these interneurons. In contrast a significant depolarisation of non-fast spiking (NFS), but not fast spiking (FS), interneurons in response to co-application of the α7 nAChR PAM and agonist PNU-282987 (300 nM) was observed (Fig. 4.20E and 4.19E). This depolarisation was sufficient to overcome the action potential threshold and action potential discharge was observed within these NFS interneurons (Fig. 4.20D). This provides evidence that α7 nAChRs, residing on cell bodies of a population of

layer V inhibitory interneurons can directly alter the levels of inhibitory signalling within the prelimbic cortex.

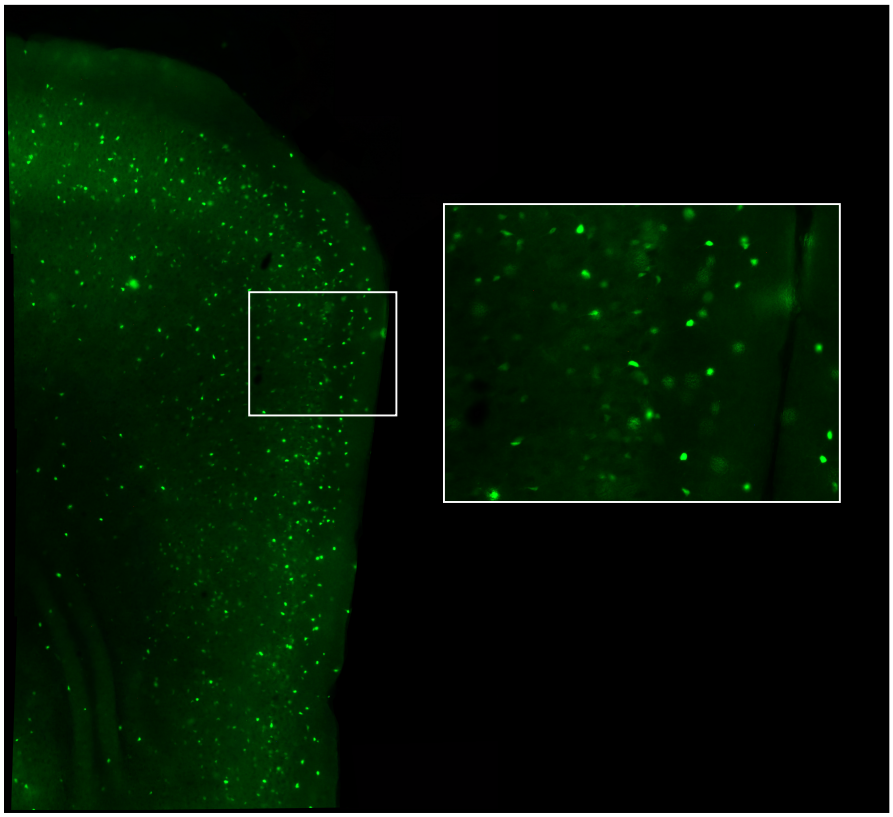

Figure 4.18 GABAergic interneurons expressing GFP in mPFC brain slice from GAD67-GFP transgenic mouse

Example of a PFA fixed brain slice (300 μm thickness) from a 5 week old GAD67-GFP transgenic mouse used for the electrophysiological identification of GABAergic inhibitory interneurons. GFP fluorescence can be seen across all layers of the mPFC indicating a high level of inhibitory interneurons. Inset shows a magnified section of the dorsal prelimbic region.

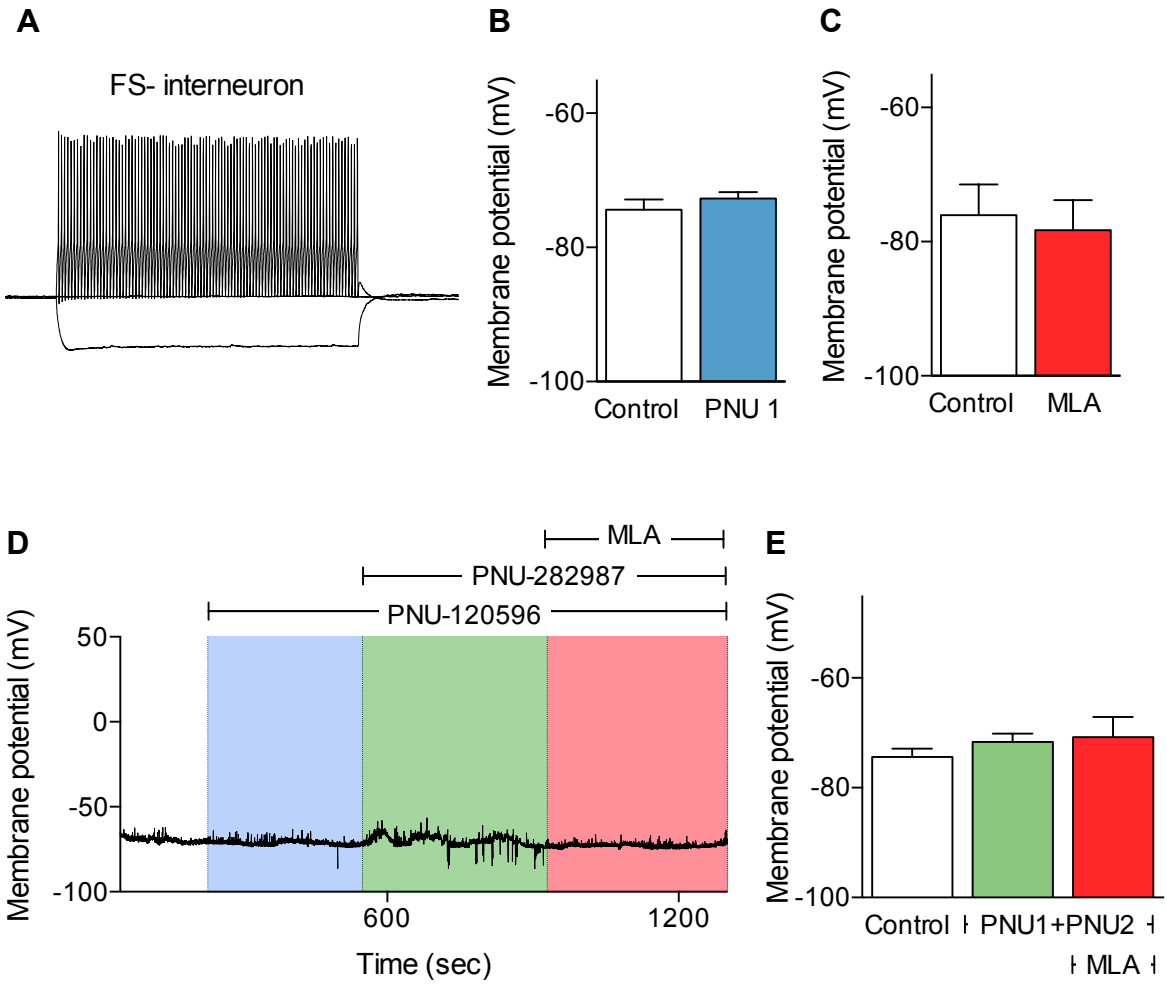

Figure 4.19 Current clamp recordings from fast spiking inhibitory interneurons in response to α7 nAChR activation

*Current clamp recording were made from layer V fast-spiking inhibitory interneurons identified by GFP fluorescence from a GAD-GFP transgenic mice. (**A**) Fast-spiking interneurons were characterised via the high frequency of action potential firing upon injection of 300 ms 150 pA depolarising and hyperpolarising current step. (**B-E**) Interneurons were held at their resting membrane potential and α7 nAChR compounds bath applied to the slice for at least 5 min, measurements of membrane potential were taken as an average of the baseline potential for the final minute of drug application (excluding any action potential discharge) (**A**) membrane potential was measured in response to application of the α7 nAChR PAM PNU-120596 (10μM) alone (n = 5) and (**B**) the α7 nAChRs antagonist MLA (100 nM) alone (n = 3). (**E**) After prior bath application of PNU-120596 alone (shown in B), PNU-120596 (10 μM) was co-applied with the α7 nAChR agonist PNU-282987 (300 nM) before the final addition of the α7 nAChR antagonist MLA (100 nM) (n = 5). (**D**) Example recording demonstrating the change in membrane potential in response to different α7 nAChR drug applications. Data in histograms represented as mean ± S.E.M.*

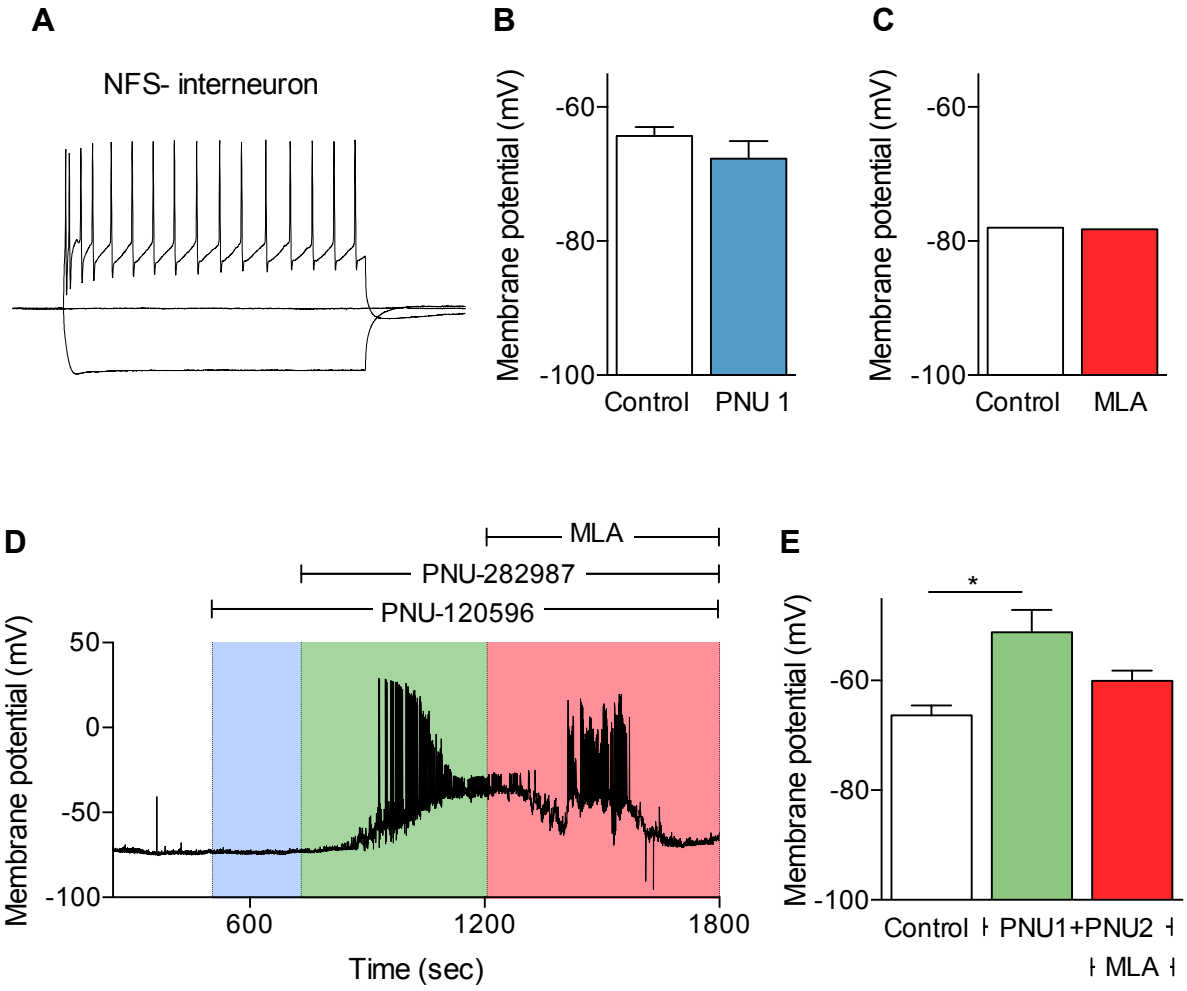

Figure 4.20 Current clamp recordings from fast spiking inhibitory interneurons in response to α7 nAChR activation

*Current clamp recording were made from layer V non-fast-spiking inhibitory interneurons identified by GFP fluorescence from a GAD-GFP transgenic mice. (**A**) Non-fast-spiking interneurons were characterised via the low frequency of action potential firing upon injection of 300 ms 150 pA depolarising and hyperpolarising current step. (**B-E**) Interneurons were held at their resting membrane potential and α7 nAChR compounds bath applied to the slice for at least 5 min, measurements of membrane potential were taken as an average of the baseline potential for the final minute of drug application (excluding any action potential discharge) (**A**) membrane potential was measured in response to application of the α7 nAChR PAM PNU-120596 (10μM) alone (n = 3) and (**B**) the α7 nAChRs antagonist MLA (100 nM) alone (n = 1). (**E**) membrane potential was measured in response to PNU-120596 (10 μM) co-applied with PNU-282987 (300 nM) before the final addition of the MLA (100 nM) (n = 5). In some cells PNU-120596 was bath applied prior to addition of PNU-282987 and in other cases PNU-282987 was applied prior to addition of PNU-120596 (**D**) Example recording demonstrating the change in membrane potential and action potential firing in response to different α7 nAChR drug applications. Data represented as mean ± S.E.M in histograms. * significantly different from control, p ≤ 0.05, one-way repeated measures ANOVA with Dunnett's post hoc test.*

In a proportion of NFS inhibitory neurons shown in figure 4.20E (3 out of 5 cells), the α7 nAChR PAM PNU-120596 was applied alone prior to co-application with the α7 nAChR agonist PNU-282987. In the other 2 cells PNU-282987 was applied prior to the PNU-120596. Interestingly when applied alone PNU-282987 induced what appear to be α7 nAChR mediated small, transient step-like depolarisations (Fig. 4.21). Similar α7 nAChR mediated depolarisations have been observed by others within CA1 pyramidal neurons in the hippocampus (Kalappa et al., 2010). This suggests that after agonist application alone, α7 nAChRs appear to still function and are not fully, or continually, desensitised as previous experiments suggested (Fig. 4.10). Interestingly in both cells, subsequent addition of the α7 nAChR PAM resulted in a large depolarisation and action potential firing (Fig. 4.21). This indicates that substantial and prolonged interneuron depolarisation and subsequent inhibition of layer V pyramidal neurons, requires the reversal of desensitisation and/or the enhanced α7 nAChR conductance achieved via positive allosteric modulation and agonist activation of α7 nAChRs.

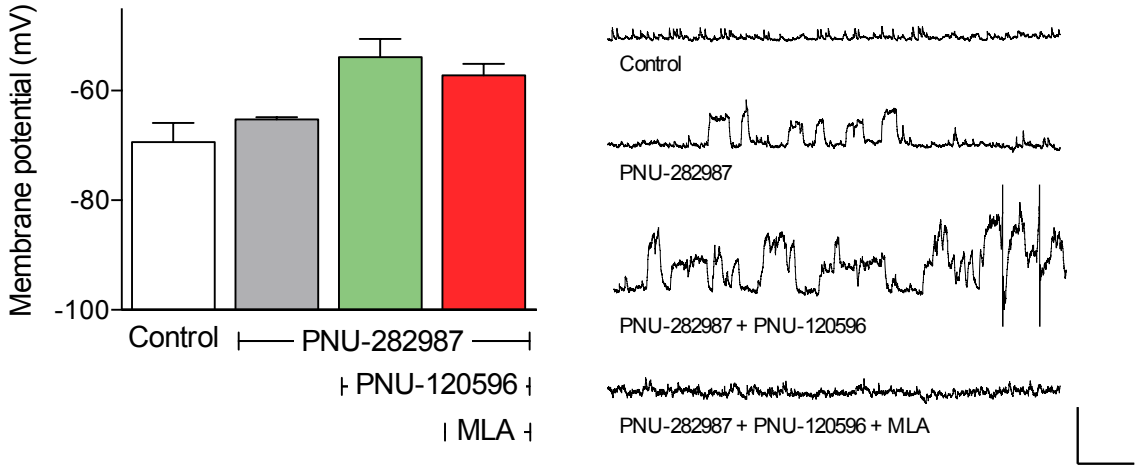

Figure 4.21 Current clamp recordings from non-fast spiking inhibitory interneurons in response to direct α7 nAChR activation with a selective agonist

Current clamp recording were made from layer V non-fast-spiking inhibitory interneurons. Interneurons were held at their resting membrane potential and α7 nAChR compounds bath applied to the slice for at least 5 min, measurements of membrane potential were taken as an average of the baseline potential for the final minute of drug application (excluding any action potential discharge). Membrane potential was measured in response to application of the α7 nAChR agonist PNU-282987 (300 nM) alone, before co-application of PNU-282987 with the α7 nAChR PAM PNU-120596 (10 μM) before addition of the α7 nAChR antagonist MLA (100 nM) (n = 2). Data represented as mean ± range in histogram (Left). Example voltage recording traces (right) highlight the step like voltage depolarisations in response to the α7 nAChR agonist PNU-282987 alone, which are enhanced by addition of the α7 nAChR PAM PNU-120596 and abolished in MLA. Scale bar; 10 mV and 2.5 sec.

The data presented in this chapter have shown that positive allosteric modulation of α7 nAChRs can enhance the frequency of sEPSCs onto layer V pyramidal neurons in cortical slices of mouse brain (Fig. 4.2A). It is hypothesised that this increase in sEPSC frequency is brought about via the actions of α7 nAChRs expressed on the presynaptic terminals of glutamatergic inputs that synapse onto layer V pyramidal neurons. An alternative hypothesis is that this enhanced sEPSC frequency may be mediated via activation of α7 nAChRs residing postsynaptically on mPFC pyramidal neurons leading to a direct increase in excitation of these neurons. Evidence for postsynaptic expression of α7 nAChRs on layer V pyramidal neurons is unclear. Our

experiments gave no evidence of somatic currents induced by α7 nAChR activation in agreement with Hedrick and Waters, (2015), however other groups have recorded somatic α7 nAChR currents on layer V neurons (Poorthuis et al., 2012).

To test the hypothesis that presynaptic α7 nAChRs are able to enhance the level of layer V excitation, mEPSC recordings were conducted in the presence of tetrodotoxin. As tetrodotoxin prevented an increase in α7 nAChR mediated GABA release, by abolishing action potential firing and thus preventing somatic α7 nAChR induced interneuron excitability (Fig. 4.17), this strategy enabled the effects of presynaptic α7 nAChRs on excitatory transmission to be observed in isolation.

Application of the α7 nAChR PAM PNU-120596 (10 μM) significantly increased mEPSC frequency with no effect on mEPSC amplitude (Fig. 4.22). These data suggest that α7 nAChRs are located on nerve terminals of afferent glutamatergic inputs.

Interestingly co-application of PNU-120596 (10 μM) and PNU-282987 (300 nM) in the presence of TTX resulted in a substantial fluctuation of membrane current in recorded cells similar to that seen in the presence of picrotoxin (Fig. 4.14C). This was presumably due to high levels of glutamate release in the absence of inhibitory modulation, although this was not directly tested. However upon application of a lower (submaximal) concentration of PNU-282987 (30 nM) together with PNU-120596 (10 μM), these issues were overcome and stable recordings were obtainable and revealed a significant increase in the frequency of mEPSCs with no change in miniature EPSC amplitude (Fig. 4.23). Together these data suggest that exogenous activation of α7 nAChR with the agonist and PAM is capable of enhancing presynaptic glutamate release, but this effect is attenuated via α7 nAChR activation of inhibitory interneurons in a functionally intact network, as observed in spontaneous EPSCs experiments (Fig. 4.2A).

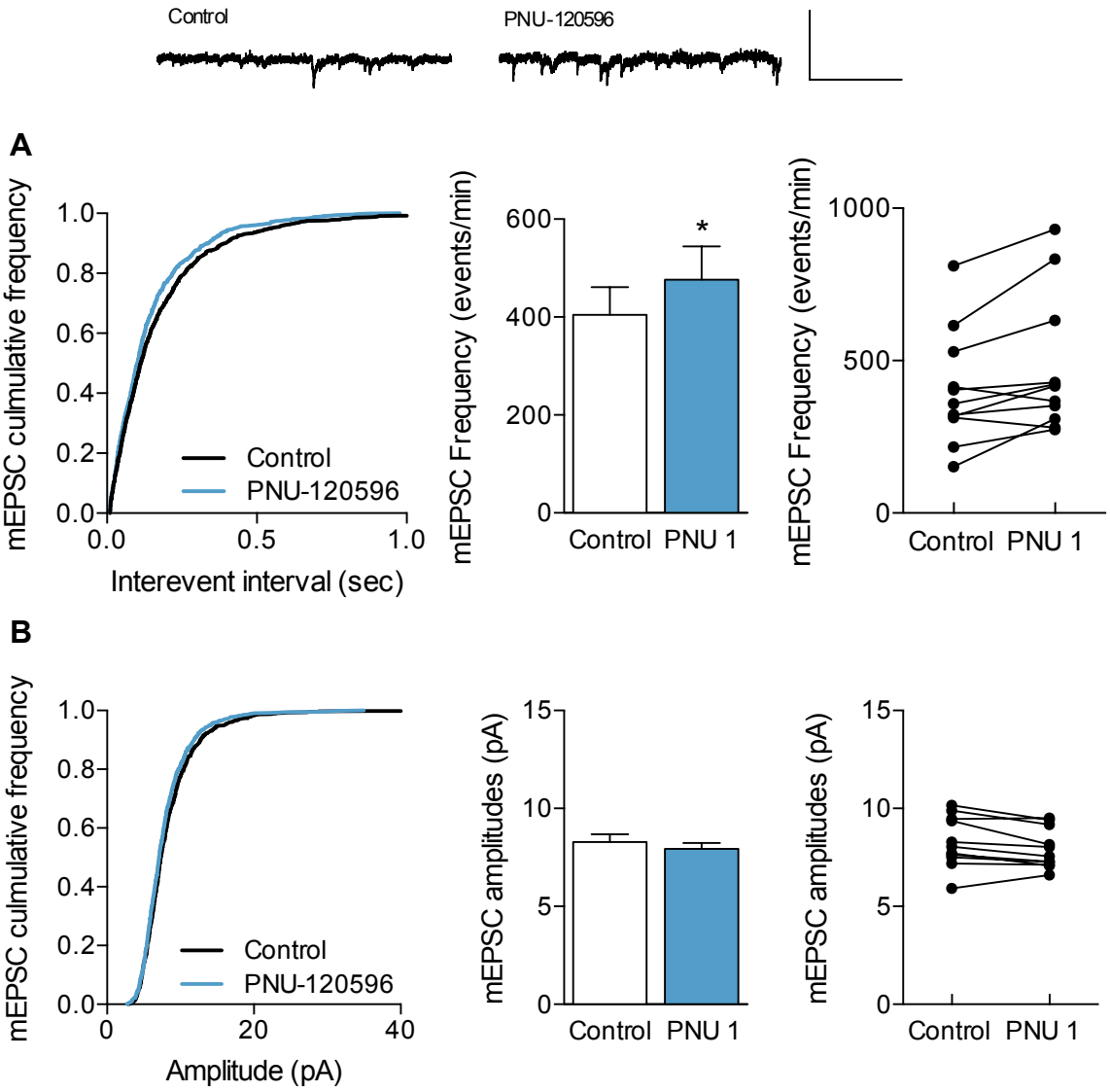

Figure 4.22 mEPSC frequency and amplitude in response to α7 nAChR positive allosteric modulation alone

*Voltage clamp recording were made from layer V pyramidal neurons in the presence of tetrodotoxin (1 μM) to block action potentials. Neurons were held at -60 mV and mEPSCs were recorded in response to continual bath perfusion of control aCSF and then 5 min application of aCSF containing the α7 nAChR PAM PNU-120596 (10 μM). (**A**) mEPSC interevent intervals and (**B**) mEPSC amplitudes were analysed, ranked and plotted in a cumulative frequency plot (left) total events per minute and average amplitudes were also calculated for each cell and plotted (right) and shown as mean ± S.E.M in a summary histogram (middle). Statistical difference shown in histograms is based on results of K-S tests of data shown in the corresponding cumulative frequency plots. * significantly different, p ≤ 0.01; n = 11. Example mEPSCs are represented in traces (top); scale bar: 30 pA and 0.5 sec.*

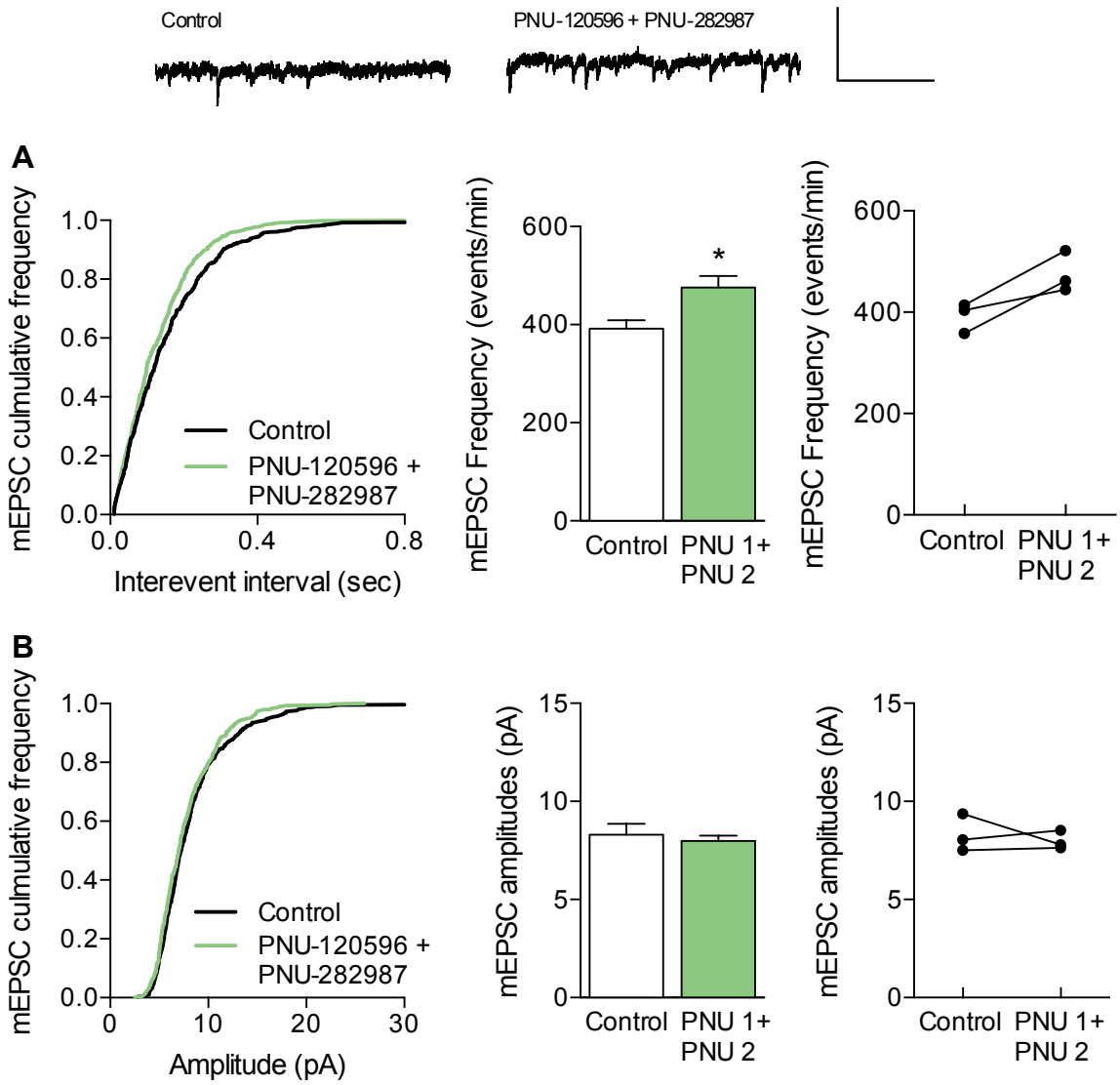

Figure 4.23 mEPSC frequency and amplitude in response to α7 nAChR activation with a selective agonist and positive allosteric modulator

*Voltage clamp recording were made from layer V pyramidal neurons in the presence of tetrodotoxin (1 μM) to block action potentials. Neurons were held at -60 mV and mEPSCs were recorded in response to continual bath perfusion of control aCSF and then 5 min application of aCSF containing the α7 nAChR PAM PNU-120596 (10 μM) and a reduced concentration of α7 nAChR agonist PNU-282987 (30 nM). (**A**) mEPSC interevent intervals and (**B**) mEPSC amplitudes were analysed, ranked and plotted in a cumulative frequency plot (left) total events per minute and average amplitudes were also calculated for each cell and plotted (right) and shown as mean ± S.E.M in a summary histogram (middle). Statistical difference shown in histograms is based on results of K-S tests of data shown in the corresponding cumulative frequency plots. * significantly different, p ≤ 0.01; n = 3. Example mEPSCs are represented in traces (top); scale bar: 30 pA and 0.5 sec*

4.2.5 Tonic endogenous cholinergic tone preferentially modulates excitatory but not inhibitory neurotransmission

The results presented so far have shown that activation of α7 nAChRs can bring about enhancements in both excitation and inhibition, doing so via independent mechanisms. This is seemingly achieved via different modes of α7 nAChR activation: activation of all α7 nAChRs throughout the slice, via the combined action of the α7 nAChR agonist and PAM, leads to an increase in inhibitory signalling onto layer V pyramidal neurons, whereas application of the α7 nAChR PAM alone selectively enhances excitatory signalling onto layer V neurons. As the α7 nAChR PAM administered alone will only enhance α7 nAChR signalling at locations exposed to endogenous ACh, the difference observed could reflect a spatial relationship between cholinergic afferents and glutamatergic nerve terminals. Afferent ACh fibres within the brain slice, having been severed from their cell body, are unlikely to exhibit activity-driven/phasic ACh signalling but may undergo spontaneous tonic release, these results may suggest that tonically released endogenous ACh within the brain slice, preferentially activates presynaptic α7 nAChRs that modulate glutamate release, rather than α7 nAChRs on the cell bodies of GABAergic interneurons.

To test the hypothesis that endogenous ACh signalling within the brain slice may preferentially promote increased layer V pyramidal neuron excitation, sEPSC and sIPSC recordings were conducted in response to enhanced endogenous ACh, achieved by preventing ACh enzymatic breakdown, with the acetylcholinesterase inhibitor donepezil. Donepezil (10 μM) alone did not significantly alter the frequency of sEPSCs or sIPSCs (Fig. 4.24A). However, in the presence of the α7 nAChR PAM PNU-120596 (10 μM), donepezil significantly increased the sEPSC frequency, compared to both control and to α7 nAChR PAM alone (Fig. 4.24B). This enhancement was reversed by MLA (100 nM). In contrast, PNU-120596 did not alter the sIPSC frequency, with or without donepezil (Fig. 4.23C). These findings are consistent with the observations in figure 4.5A, where antagonism of endogenous activity at α7 nAChRs with MLA appeared to reduced sEPSC frequency, but had no effect on sIPSC frequency. In addition, no alteration in the inhibitory interneuron

membrane potential was observed in the presence of either MLA or α7 nAChR PAM (Fig. 4.19B,C and Fig 4.20B,C).

These data support the hypothesis that endogenous tonic release of ACh acting at α7 nAChRs is able to selectively enhance excitatory neurotransmission, but not inhibitory neurotransmission, in layer V of the prelimbic cortex.

4.2.6 Modulation of evoked excitatory neurotransmission by α7 nAChRs within the prelimbic cortex

The work described in this thesis chapter has sought to understand how α7 nAChR activity may modulate the network activity of the prelimbic cortex with an aim of providing a mechanism by which α7 nAChRs can alter the levels of PrL synaptic plasticity observed in chapter 3. In doing so the spontaneous activity of both excitatory and inhibitory neurotransmission has been measured in response to α7 nAChR modulation. Although these measures can assign α7 nAChRs a functional role in controlling excitation and inhibition, spontaneous recordings may not correlate directly with measures of stimulus-induced synaptic plasticity. Spontaneous activity corresponds to the background tonic release of neurotransmitters and neuromodulators, whereas stimulus evoked recordings used during extracellular field recordings in chapter 3, leads to a more synchronous action potential-dependent release of neurotransmission. α7 nAChRs may regulate these two different forms of transmitter release differently. In addition the local levels of ACh are likely to be different between spontaneous and evoked recordings. With spontaneous activity one may expect low levels of tonically released ACh. In contrast, electrical stimulation is likely to activate an array of local and afferent fibres, leading to an enhanced level of a multitude of different neurotransmitters and modulators including ACh.

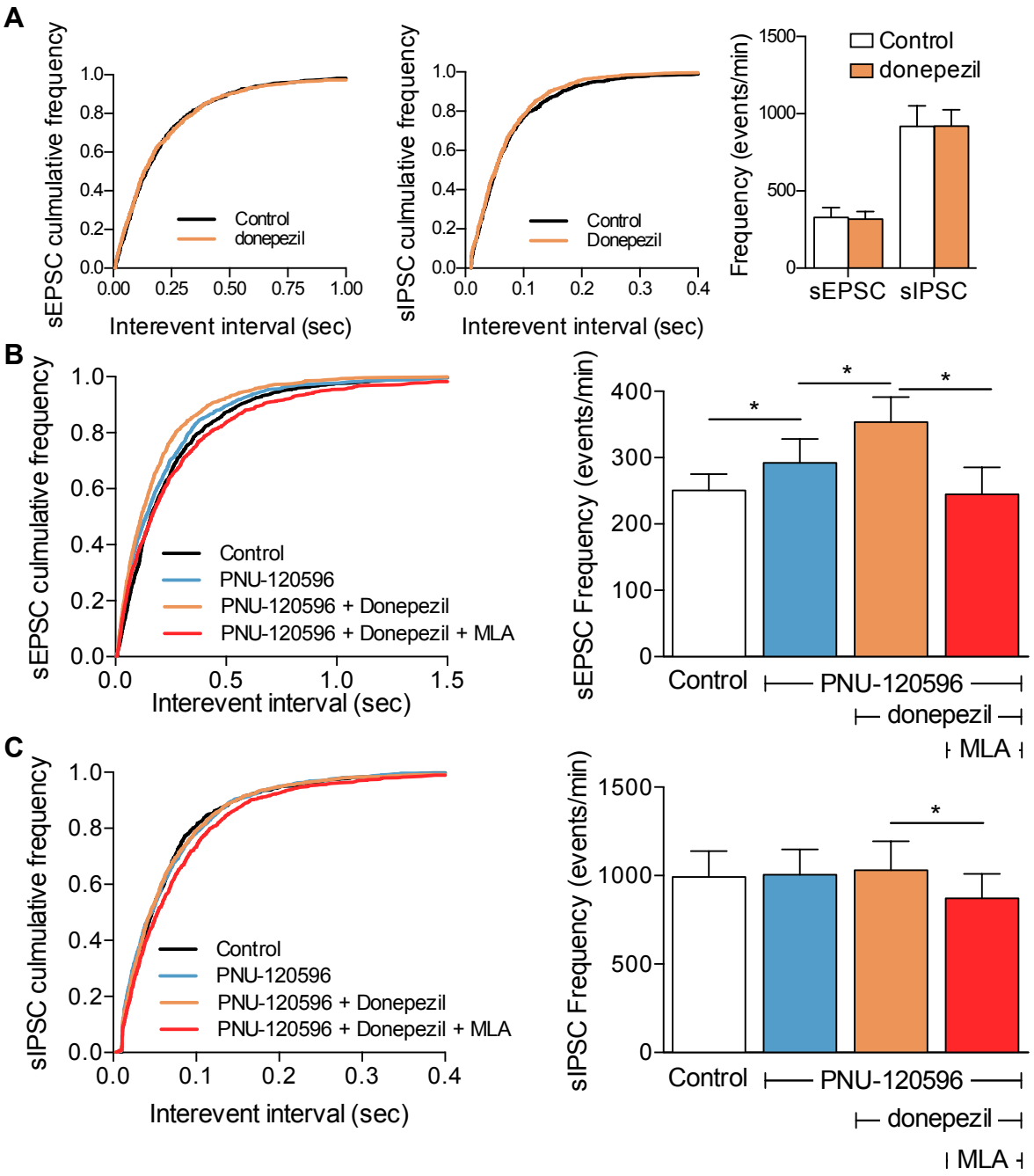

Figure 4.24 mEPSC frequency and amplitude in response to α7 nAChR activation with a selective agonist and positive allosteric modulator

*Voltage clamp recording were made from layer V pyramidal neurons that were held at -60 mV and then 0mV to record sEPSCs and sIPSCs from the same cell. (**A**) sEPSCs and sIPSCs were recorded in response to control aCSF and then 5 min application of aCSF containing the acetylcholinesterase inhibitor donepezil (10 μM) alone. (**B**) sEPSC and (**C**) sIPSCs were recorded in response to control aCSF then aCSF containing the α7 nAChR-selective PAM PNU-120596 (10 μM), then the α7 nAChR PAM and donepezil (10 μM) and finally the α7 nAChR PAM + donepezil and α7 nAChR antagonist MLA (100 nM). sEPSC and sIPSC interevent intervals were analysed, ranked and plotted in a cumulative frequency plots (left/middle) total events per minute were also calculated and shown as mean ± S.E.M in a summary histograms (right). Statistical difference shown in histograms is based on results of K-S tests of data shown in the corresponding cumulative frequency plots. * significantly different, p ≤ 0.01; n = 6.*

To better understand if α7 nAChRs are able to modulate action potential mediated glutamate release, evoked excitatory postsynaptic currents (eEPSCs) were measured. Whole-cell voltage clamp recordings from layer V pyramidal neurons were conducted in response to bipolar electrical stimulation of afferent fibres and local mPFC neurons within layer II/III of the prelimbic cortex (similar in method to extracellular fEPSP recordings in chapter 3). eEPSCs were evoked by holding layer V neurons at -60 mV, in the absence of $GABA_A$ receptor blockade. This produced a monosynaptic glutamatergic EPSC sensitive to DNQX (10 μM). The α7 nAChR PAM PNU-120596, co-application of α7 nAChR PAM + agonist PNU-282987 and the α7 nAChR antagonist MLA were applied to the slice for prolonged periods of time in separate experiments, to observe the effects these drugs have on the amplitude of evoked responses.

Upon prolonged bath application of the of α7 nAChR antagonist MLA (100 nM) the amplitudes of eEPSCs were significantly decreased (Fig. 4.25A), suggesting that endogenous cholinergic activity at α7 nAChRs can promote the level of glutamate release. With this observation and results of previous sEPSC measurements (Fig. 4.2A), it was predicted that positive allosteric modulation of α7 nAChRs would enhance the levels of evoked glutamate. However, surprisingly, application of PNU-120596 (10 μM) alone failed to alter eEPSC amplitudes (Fig. 4.25C). Positive allosteric modulation of the α7 nAChRs, although able to enhance spontaneous glutamate release, was not able to further enhance evoked glutamate levels. These data are consistent with findings in chapter 3 where positive allosteric modulation of α7 nAChRs did not alter the levels of LTP (section 3.2.4). Upon co-application of α7 nAChR PAM PNU-120596 (10 μM) and α7 nAChR agonist PNU-282987 (300 nM) a significant reduction in the eEPSC amplitudes was observed (Fig. 4.25B). This decrease in evoked glutamate is presumably due to an enhanced level of inhibition within the network as seen in figure 4.7A, and is consistent with α7 nAChR PAM + agonist application reducing mPFC plasticity (section 3.2.3).

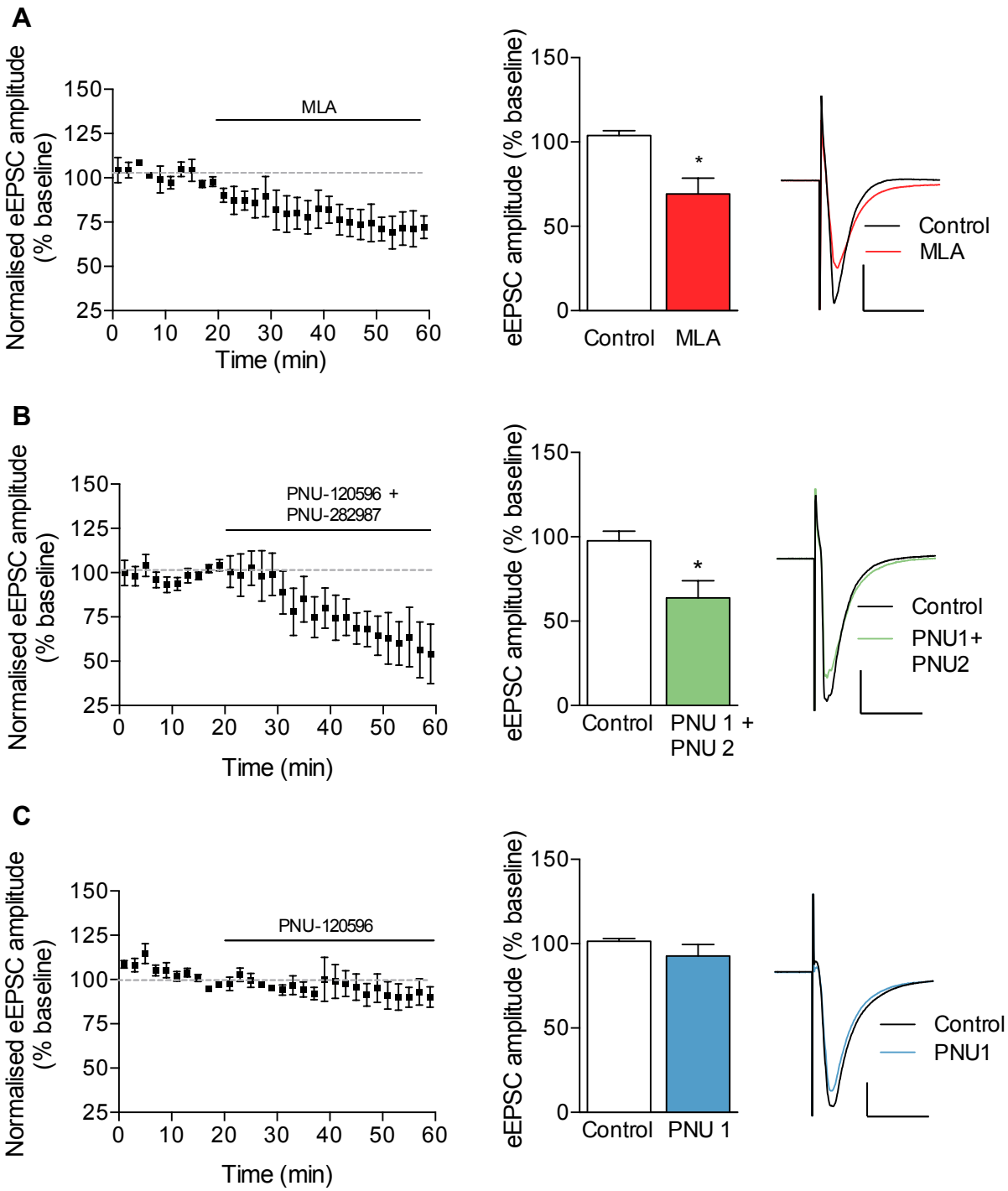

Figure 4.25 Evoked EPSC amplitude in the presence of α7 nAChR activation and antagonism

*Voltage clamp recording were made from layer V pyramidal neurons and eEPSCs evoked via stimulation of in layers II/III at 0.05 Hz. A 20 min stable baseline of eEPSC was obtained before a prolonged bath application of (**A**) the α7 nAChR antagonist MLA (100 nM) (n = 4), (**B**) co-application of the α7 nAChR PAM PNU-120596 (10 μM) and agonist PNU-282987 (300 nM) (n = 5) and (**C**) α7 nAChR PAM PNU-120596 (10 μM) alone (n = 3). Time-courses (left) show amplitude of eEPSC normalised to baseline. Histograms (middle) represents averaged data at time points 10 min (control) and 40 min (drug) * significantly different from control, p ≤ 0.05, paired t-test. All data represents mean ± S.E.M Traces (right) show averaged eEPSC from all cells; scale bar: 25 pA and 100 ms.*

Spontaneous and miniature EPSC experiments in section 4.2.4 demonstrate that presynaptic α7 nAChRs are located on glutamatergic nerve terminals, whilst α7 nAChRs are also observed on the cell bodies of GABAergic interneurons. Additional experiments suggest that endogenous ACh preferentially activates α7 nAChRs on nerve terminals to increase glutamate release. To test this hypothesis paired pulse ratio experiments were conducted to investigate if the reduction in evoked EPSCs upon addition of MLA, is brought about by ACh acting at presynaptic α7 nAChRs.

Evoked EPSC paired pulse recordings involve a paired stimulation of nerve inputs with a defined inter-stimulus duration, usually between 25-100 ms (Gemmell & O'Mara, 2000; Zhang, 2004). Upon paired stimulation the second evoked response can be larger (paired pulse facilitation) or smaller (paired pulse depression) than the first. The ratio between the amplitudes of these two responses provides a measure of the probability of neurotransmitter release. For example if an input has a high probability of neurotransmitter release the first stimulus leads to a high degree of transmitter release, depleting presynaptic neurotransmitter stores, then upon the second stimulus less transmitter is available for release, resulting in a smaller response than the first. Conversely an input with a low probability of release, when stimulated will release a low to moderate level of neurotransmitter, presynaptic transmitter stores are depleted by a lesser extent, and more transmitter is released on the second stimulus as a result of additive presynaptic Ca^{2+} intracellular levels (Debanne et al., 1996; Katz & Miledi, 1968). Any alteration in this ratio on the addition of a receptor agonist/antagonist is evidence to suggest that the targeted receptor can influence the presynaptic release of neurotransmitter.

Upon 50 ms paired pulse stimulation, a reliable paired pulse facilitation was obtained (Fig. 4.26A). Upon 10 min application of MLA (100 nM) a significant increase in the paired pulse ratio compared to control was observed (Fig. 4.26B). Antagonism of presynaptic α7 nAChRs thus appears to reduce the probability of glutamate release. Paired pulse recordings were also conducted in the presence of the α7 nAChR PAM PNU-120596 (10 μM) alone and co-application of α7 nAChR PAM and agonist PNU-282987 (300 nM). Upon 10 min co-application of α7 nAChR PAM and agonist no significant alteration in the

paired pulse ratio was observed, suggesting that the reduction in eEPSC seen in figure 4.25B is unlikely to be due to presynaptic effects. Previous experiments show α7 nAChR PAM can enhance presynaptic glutamate release (Fig. 4.22) so it would not be surprising if the α7 nAChR PAM alone could alter the paired pulse ratio, however no significant change in the paired pulse ratio was observed upon 10 min application of the PNU-120596 (Fig. 4.26D). The lack of effect seen with the α7 nAChR PAM may reflect the differences in α7 nAChR regulation of spontaneous and evoked glutamate release, with the negative finding consistent with the lack of effect that the α7 PAM has on eEPSC amplitudes and plasticity.

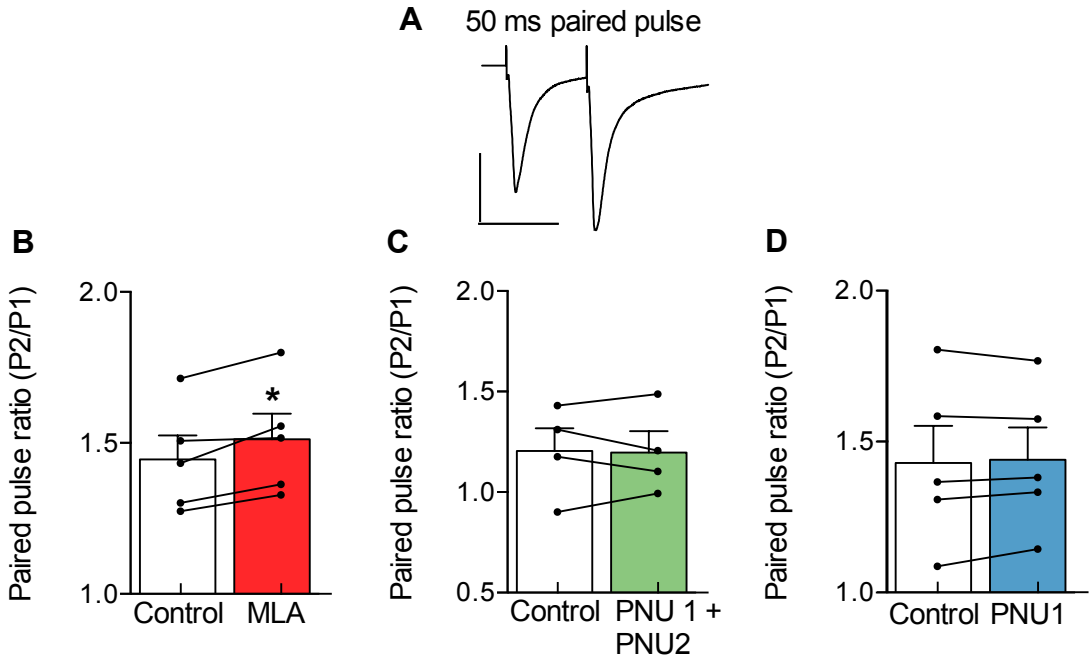

Figure 4.26 Paired pulse ratios of eEPSCs in the presence of α7 nAChR activation and antagonism

*Voltage clamp recording were made from layer V pyramidal neurons and paired eEPSCs were evoked at 0.05 Hz from layers II/III via a paired stimulation with a 50 ms interpulse interval (**A**) Example paired pulse response which typically gave paired pulse facilitation in the majority of neurons. The amplitude of both eEPSCs were measured and paired pulse ratio calculated by dividing the second by the first pulse. (**B**) Paired pulse ratios were measured before and after a 10 min bath application of MLA (100nM) (n = 5), (**C**) co-application of the α7 nAChR PAM PNU-120596 (10 μM) and α7 nAChR agonist PNU-282987 (300 nM) (n = 4) and (**D**) α7 nAChR 10 μM PAM PNU-120596 (10 μM) alone (n = 5). Individual paired pulse changes are shown (right) these were averaged to give mean ± S.E.M paired pulse ratios shown in histogram (left). * significantly different from control, p ≤ 0.05, paired t-test.*; scale bar: 25 pA and 100 ms

4.4 Summary

The aim of this chapter was to investigate the potential for α7 nAChRs to modulate excitatory and inhibitory neurotransmission within the prelimbic cortex. In doing so, the localisation of these receptors could be confirmed and the mechanisms by which they regulate network activity could be ascertained. In addition, endogenous activation of the α7 nAChRs could also be studied. The main findings within this chapter are detailed below.

Via the use of the α7 nAChR PAM PNU-120596 it has been shown endogenous ACh activating α7 nAChRs increases the spontaneous release of glutamate onto layer V pyramidal neurons. This increase in excitation is not dependent on action potentials, suggesting that endogenous ACh acts on presynaptic α7 nAChR on glutamatergic terminals.

Interestingly the α7 nAChR-mediated increase in glutamate release in the presence of PNU-120596 is not further potentiated, but reversed, on addition of the selective α7 nAChR agonist PNU-282987. A decrease in the excitability of the recorded pyramidal neurons in response to PNU-120596 and PNU-282987 suggests a more complicated regulation of network activity. Indeed, the decrease in excitation on addition of PNU-120596 and PNU-282987 is found to coincide with an enhanced level of inhibitory neurotransmission onto layer V pyramidal neurons. This increase in inhibition is independent of glutamate signalling but is dependent on action potential firing, suggesting that α7 nAChRs are likely expressed on the soma of inhibitory interneurons. Recording from inhibitory interneurons confirmed this and it was found that α7 nAChR activation with a selective PAM and agonist leads to depolarisation and action potential firing of NFS but not FS inhibitory interneurons.

The different effects seen in the presence of the α7 nAChR PAM alone and in the presence of a selective α7 nAChR agonist, suggest there may be a difference in the receptor population that endogenous tonic release of ACh within the brain slice is acting on. This idea was tested by enhancing the concentration of endogenous ACh via addition of the acetylcholinesterase inhibitor donepezil. Donepezil further enhanced excitatory input to layer V

pyramidal neurons in the presence of α7 nAChR PAM, but had no effect on inhibitory input. This, along with findings that neither MLA nor PNU-120596 altered the membrane potential of inhibitory interneurons, suggest that in the system being studied, tonically released ACh preferentially activates presynaptic α7 nAChRs on glutamatergic terminals rather than α7 nAChRs on inhibitory interneurons.

The effect that α7 nAChR activity has on more pronounced glutamate release, more akin to the type of co-ordinated transmitter release observed during stimulus-induced synaptic plasticity, was also investigated. Contrasting findings were observed here, MLA alone induced a profound decrease in evoked glutamate release, whereas earlier findings showed that MLA alone caused only a very slight reduction in spontaneous glutamate release. Paired pulse recordings suggest that this effect is via a presynaptic mechanism. Positive allosteric modulation of α7 nAChRs surprisingly did not alter evoked glutamatergic events, unlike its effect on spontaneous glutamatergic events. These data suggest the modulatory effect of α7 nAChRs on pronounced and spontaneous glutamate levels are diverse and are discussed in more detail in chapter 6.

The findings of this thesis chapter provides several lines of evidence that α7 nAChR expressed on presynaptic terminals can modulate the level of glutamate release within the PrL, which had been previously suggested by others (Lubin et al., 1999; Yang Yang et al., 2013; Dickinson et al., 2008). As detailed in section 1.2.2 the mPFC receives afferent inputs from a variety of brain regions, which of these afferent fibres express presynaptic α7 nAChRs is unknown, the focus of the next thesis chapter is to investigate this.

Chapter 5:

Localisation of presynaptic α7 nAChRs in the prelimbic cortex

Chapter 5: Localisation of presynaptic α7 nAChRs in the prelimbic cortex

5.1 Introduction

In the previous chapter experiments demonstrate that α7 nAChRs are located presynaptically on glutamatergic terminals and promote the presynaptic release of glutamate onto layer V pyramidal neurons.

The evidence provided so far for presynaptic α7 nAChRs are provided by two key observations. Firstly, α7 nAChRs activation results in an (action potential independent) increase in spontaneous EPSC frequency. Secondly, α7 nAChR antagonism during electrical stimulation of layers II/III resulted in a reduced eEPSC amplitude coinciding with a reduction in glutamate release probability. However spontaneous EPSC recordings sample all synapses onto the recorded neuron and electrical stimulation of layer II/III (although presumably evoking release only from local layer II/III inputs) has no specificity to which fibres are activated. Consequently a question that still remains is: Which afferent fibres innervating the prelimbic cortex possess presynaptic α7 nAChRs? The aim of this thesis chapter is to help address this question.

The mPFC receives direct excitatory innervation from a diverse group of connecting brain regions (Hoover & Vertes, 2007) (see section 1.2.2). In general these afferent fibres innervate the mPFC across all layers with the majority of afferent innervation from the ventral hippocampus, BLA, thalamus and contralateral mPFC, residing in both layers V and II/III (DeNardo et al., 2015; Jay & Witter, 1991; Little & Carter, 2012) (see section 1.2.2.1). Although the afferent innervation from these brain regions appear not to be localised to specific layers they do project information that is critical for the many cognitive processes assigned to the mPFC (section 1.2.2.1). Whether any of these excitatory inputs to the PrL are modulated by α7 nAChRs is unknown, if they do, this might be an important mechanism by which ACh signalling modulates some of the cognitive processes assigned to this brain region, and is therefore important to investigate.

To elucidate which specific inputs are modulated by α7 nAChRs, a different experimental approach is needed to the ones used so far. Along with electrophysiology other classical methods to study presynaptic receptors include, synaptosome studies, brain slice immunohistochemistry and electron microscopy. However, with these experimental approaches, it is generally not possible to selectively investigate specific inputs. Using electrophysiology, several approaches can be used to try and overcome this problem:

- Lesions of discrete brain regions can be performed to eliminate specific afferent inputs.
- In some cases defined fibre tracts within the brain slice can be electrically stimulated to selectively activate specific inputs.
- In some cases, certain receptors selectively expressed on specific afferent fibres can be pharmacologically targeted to selectively 'shut down' an input.

In the PrL, it would be possible to ablate specific inputs using lesioning. It is also possible to selectively activate hippocampal inputs electrically (Parent et al., 2010), and to silence thalamic inputs using pharmacology (Lambe et al., 2003) However, it is not currently possible to investigate inputs from other brain regions using pathway-specific electrical activation or pharmacology. An alternative methodology that can be used is optogenetics.

Optogenetics, an increasingly utilised technology in neuroscience uses gene delivery methodology, to enable the regulated expression of light sensitive ion-channels (or GPCRs) in specific cell types (Boyden et al., 2005). A common optogenetic method is to introduce a viral vector into discrete brain regions often by stereotaxic injection of a virus containing the vector. The most common virus used for this approach is the adeno-associated virus (AAV) of which there are several serotypes each with differing characteristic levels of transduction (Watakabe et al., 2015). The viral vector can be designed to possess a DNA sequence encoding 3 primary elements.

1. DNA sequence that enables cell type specific transcription. Often, cell type specific promoters or recombination technologies such as the Cre-lox system (Rein & Deussing, 2012).
2. DNA sequence that encodes a light sensitive ion-channel (sometimes referred to as opsins). These come in a variety of types, and can be excitatory or inhibitory ion-channels and are gated by specific wavelengths of light.
3. A reporter gene to identify successful ion-channel expression, often a fluorescent marker, such as GFP, eYFP or TdTomato.

Upon delivery of the virus to the targeted brain region, the targeted neuronal population, upon successful transduction, will begin to express the light sensitive ion-channel, which is transported and localised to the membranes throughout the entire neuron, including its efferent fibres. The most commonly used opsin is channelrhodopsin (ChR2), which is gated by blue light (peak wavelength of 450 nM) (Nagel et al., 2003). Upon channel opening with a short flash of blue light, the cation permeable ChR2, excites the host neuron often leading to action potential firing. This methodology thus enables activation of a specific neuronal population with flash of light.

For the question being addressed in this thesis chapter, optogenetics can be utilised to selectively express opsins into the glutamatergic neurons that project to the PrL. This would allow for specific afferent fibres to be selectively activated by light during brain slice electrophysiology experiments. In selectively activating specific afferent inputs their regulation by α7 nAChRs can be assessed.

The aim of this thesis chapter is to investigate the precise localisation of α7 nAChRs in the PrL. To achieve this, several different methodologies were used: A. Pharmacological suppression of thalamic inputs allowing α7 nAChR effects on spontaneous signalling to be studied in the absence of thalamic mediated events. B: Electrical stimulation of the hippocampal-mPFC excitatory pathway to investigate α7 nAChRs modulation of hippocampal-mPFC evoked glutamate signalling. C: Optogenetics to investigate α7 nAChRs modulation of light

evoked glutamate from multiple brain regions (hippocampus, thalamus, amygdala, contralateral PFC) onto layer V pyramidal neurons of the PrL.

5.2 Results

5.2.1 Pharmacological suppression of thalamic inputs

μ-opioid receptors have been shown to supress the release of spontaneous glutamate from thalamic afferent fibres onto layer V cortical neurons (Marek & Aghajanian, 1998). Within the cortex, radioligand binding data suggests that μ-opioid receptors have a similar localisation to the projecting thalamic afferent fibres within the cortex (McLean et al., 1986). This cortical μ-opioid receptor binding along with the μ-opioid receptor mediated suppression of excitatory transmission, can be attenuated via thalamic lesions (Marek et al., 2001), data that suggests that μ-opioid receptors are expressed selectively on thalamic inputs. Previous studies have utilised the μ-opioid receptor agonist [D-Ala^2, N-MePhe^4, Gly-ol]-enkephalin (DAMGO) as a tool to infer the location of both $5HT_{2A}$ and α4β2 nAChRs on thalamic inputs to layer V mPFC pyramidal neurons (Lambe et al., 2003; Marek & Aghajanian, 1998).

This methodology was adopted for experiments in this thesis, to investigate if the α7 nAChR mediated enhancement in glutamate release is altered upon the suppression of thalamic inputs to the PrL. It was predicted that suppression of thalamic inputs with DAMGO may result in either attenuation or enhancement of α7 nAChR mediated effect. If α7 nAChR are expressed on thalamic inputs, supressing these inputs could prevent the α7 nAChR mediated potentiation of glutamate release. Conversely if α7 nAChRs are not expressed on thalamic inputs, addition of DAMGO should lead to a reduction in the level of spontaneous glutamate release, and the lower basal sEPSC frequency. This reduction in 'noise' might uncover a more prominent α7 nAChR effect as the signal to noise ratio is enhanced.

Upon addition of DAMGO (3 μM), the frequency of sEPSCs significantly decreased by 25 ± 10 % compared to control (Fig. 5.1). Upon subsequent addition of the α7 nAChR PAM PNU-120596 (10 μM) the sEPSC frequency was unchanged, indicating that activation of μ-opioid receptors attenuated the α7 nAChR mediated increase in spontaneous glutamate release perhaps due to their localisation on thalamic inputs. Addition of the opioid antagonist naltrexone (3 μM) reversed the effect of DAMGO and significantly enhanced the sEPSC frequency compared to DAMGO + PNU-120596. Interestingly however naltrexone in the presence of DAMGO + PNU-120596 did not further potentiate the sEPSC frequency compared to baseline levels.

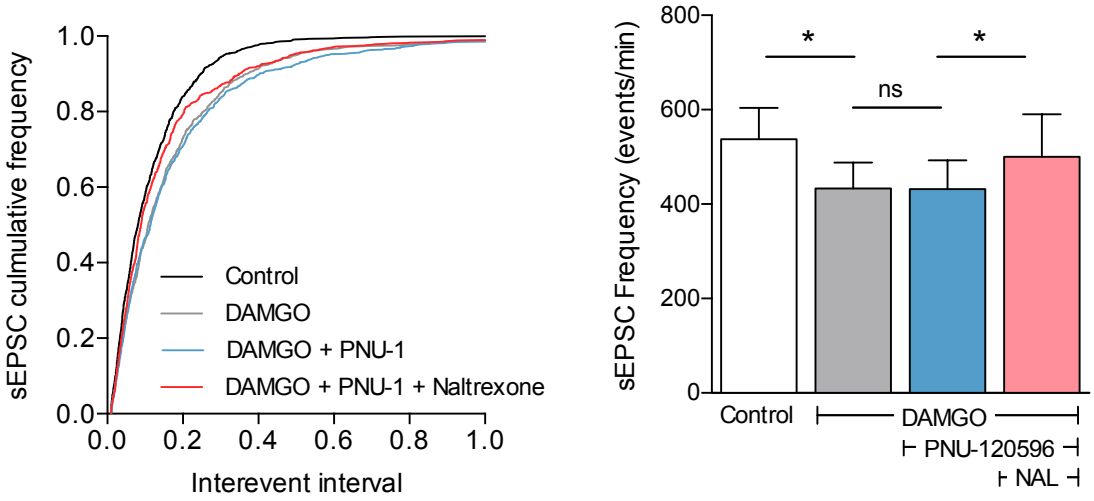

Figure 5.1 μ-opioid receptor dependent attenuation of α7nAChR mediated excitation

*Voltage clamp recording were made from layer V pyramidal neurons. Whilst neurons were held at -60 mV sEPSCs were recorded in response to continual bath perfusion of control aCSF and then aCSF containing the μ-opioid agonist DAMGO (3μM) alone followed by DAMGO in the presence of the α7 nAChR PAM PNU-120596 (10 μM), followed DAMGO + PNU-120596 and the opioid antagonist naltrexone (3 μM). sEPSCs frequency was analysed as interevent interval, ranked and plotted in a cumulative frequency plot (left) total events per minute were also calculated and plotted as mean ± S.E.M in a summary histogram (right). Statistical difference shown in the histogram is based on results of K-S tests of data shown in the cumulative frequency plot. * significantly different, p ≤ 0.01; n = 6*

5.2.2 Stimulated glutamate release from afferent pathways originating from the hippocampus

Within an acute brain slice the identification and selective electrical stimulation of afferent pathways is challenging. In some acute brain slice preparation such as the hippocampal slice, specific fibre pathways have been well characterised for example the CA3 to CA1 pathway. Within the mPFC brain slice selective stimulation of one of the many afferent fibres is often not possible. However Parent et al., (2010) have characterised a fibre bundle that resides within the mPFC brain slice that can be stimulated to selectively evoke glutamate from hippocampal afferent fibres. They report a method where an angled dissection of mPFC coronal brain slices can preserve a fibre bundle, originating from the ventral hippocampus that upon electrical stimulation induces monosynaptic release of glutamate onto layer V pyramidal neurons.

The methodology of Parent et al., (2010) was utilised to investigate if α7 nAChRs modulate the basal synaptic transmission of ventral hippocampal afferent inputs. mPFC brain slices were obtained as previously described (section 2.2) with the exception of an approximately 10° angled coronal cut whilst dissecting the frontal cortex from the whole brain as described in Parent et al., (2010) and shown in figure 5.2A. Posterior mPFC slices (+1.42 to +1.70 mm from bregma), possessed a prominent fibre bundle similar to that observed in Parent et al., (2010). Single pulse stimulation of these afferent fibres during whole-cell voltage clamp recordings of layer V pyramidal neurons held at -60 mV in the absence of GABAergic blockade produced monosynaptic EPSCs that were reversibly abolished in the presence of kynurenic acid (10mM) (Fig. 5.2B).

The hippocampal-mPFC pathway to cortical pyramidal neurons is primarily excitatory (Ghoshal & Conn, 2015), however there is also evidence for direct activation of local mPFC inhibitory interneurons, that can partake in feedforward inhibition of pyramidal neurons (Dégenètais et al., 2003; Jay et al., 1996; Parent et al., 2010; Tierney et al., 2004). To investigate a potential feedforward inhibitory pathway, layer V pyramidal neurons were held at 0 mV to measure eIPSC responses. In some cases eIPSCs were observed (reduced by addition of picrotoxin), whilst in the majority of neurons tested inhibitory currents were

not observed (Fig. 5.2C). Evidence of a direct GABAergic pathway between the vHip and the PrL has not been described and so the inhibitory currents observed are likely to occur via excitatory hippocampal afferents activating local PrL interneurons.

Initial experiments aimed to remove any inhibitory components to study the effect α7 nAChR may have on excitatory signalling in isolation. However blockade of inhibitory signalling via the addition of picrotoxin resulted in large polysynaptic excitatory currents upon electrical stimulation, likely due to reverberative excitation within the PrL. Therefore it was decided to keep inhibitory signalling intact and record neurons at the reversal potential of GABAergic currents (-60 mV). Under these conditions experiments were performed to investigate if α7 nAChRs could modulate the basal glutamatergic transmission of the hippocampal afferent pathway. EPSCs were evoked continuously at 0.05 Hz and a stable 20 min baseline of EPSCs was recorded prior to consecutive 10 min applications of the α7 nAChR PAM PNU-120596 (10 μM) alone, PNU-120596 in the presence of the α7 nAChR agonist PNU-282987 (300 nM) upon the final addition of the α7 nAChR antagonist MLA (100 nM). It was found that the EPSC amplitude, rate of rise and 10 -90 % rise time remained unaltered in response to any of the applied drugs (Fig. 5.3A-C), providing no evidence for direct α7 nAChR-mediated modulation of basal neurotransmission of hippocampal-PrL pathway.

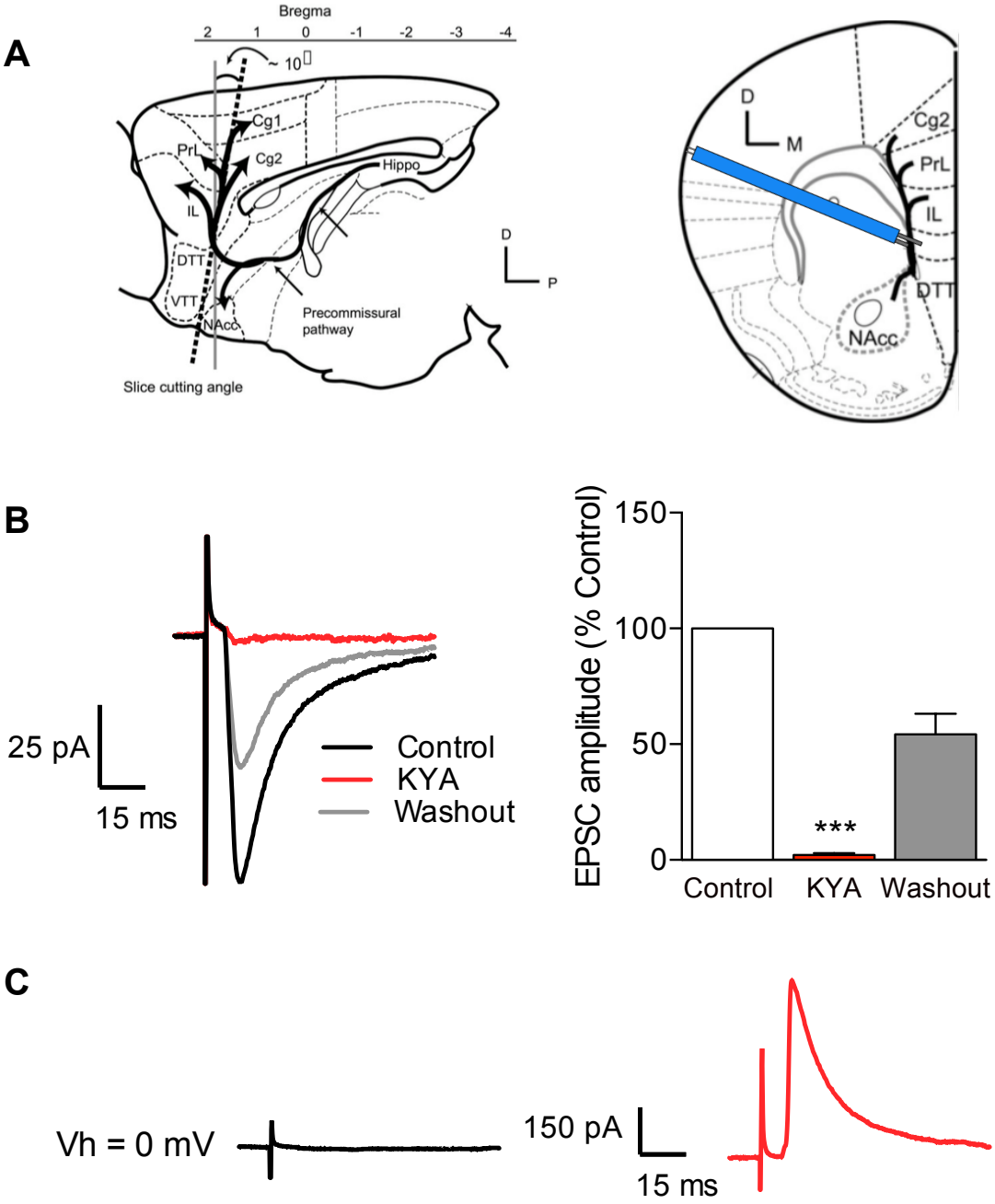

Figure 5.2 Stimulation of afferent fibre bundle originating from the hippocampus

Modified brain slice preparation from the mPFC to isolate the afferent fibre bundle originating from the ventral hippocampus as described by (Parent et al., 2010) *(**A**) Angled dissection of the mPFC at approximately 10° (angled anterior to bregma) (left), enabled preparation of 300 nm slices that obtained an afferent fibre bundle originating from the hippocampus. Stimulating electrode (blue) was positioned across the ventral region of these fibres and used to excite these fibres (right). (**B**) Single, stimulating pulses evoked EPSCs recorded in PrL layer V pyramidal neurons held at -60 mV. Bath application of the glutamate receptor antagonist kynurenic acid (10 mM) was applied before washout of the drug, EPSC amplitudes were analysed and normalised to control EPSC and shown in histogram (right) (**C**) Stimulation of afferent fibres whilst holding the neurons at 0 mV resulted in either no response (left) or a prominent outward current (which could be reduced by picrotoxin) (left). Statistical difference in (B) one sample t-test * significantly different, p ≤ 0.001; n = 3. Images in (A) adapted from Parent et al., (2010)*

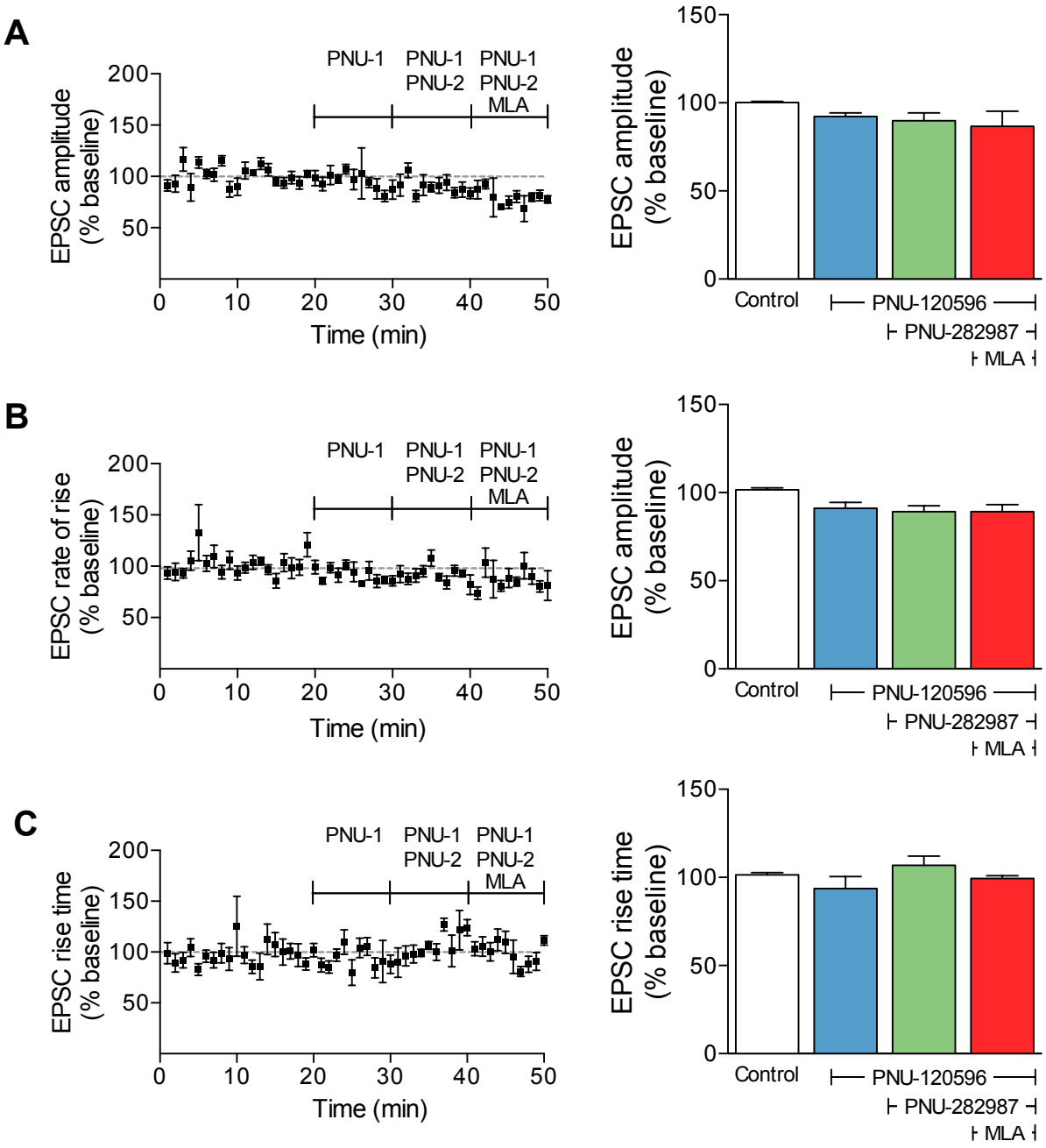

Figure 5.3 Evoked EPSC from hippocampal afferent fibres in response to α7 nAChR activation and antagonism

*Voltage clamp recordings were made from layer V pyramidal neurons in the PrL. Neurons were held at -60 mV and EPSCs were evoked from hippocampal afferents by stimulating afferent fibre bundle. A stable EPSC baseline of at least 10 min was obtained in control aCSF before 10 min bath applications of the α7 nAChR PAM PNU-120596 (10 μM) (PNU-1) alone, the α7 nAChR PAM and agonist PNU-282987 (300 nM) (PNU-2), followed by application of the α7 nAChR PAM, agonist and MLA (100 nM). (**A**) Light evoked EPSC amplitudes, (**B**) rate of rise and (**C**) rise time were analysed. Time-courses (left) show EPSCs normalised to baseline. Histograms (right) represents averaged data across entire 10 min drug application. All data shown as mean ± S.E.M. Significance assessed via multiple repeated measures ANOVA's with Dunnett's post hoc tests between each treatment and control, no significant difference was found to any of the conditions; n = 4.*

5.2.3 Optogenetic stimulation of glutamate release from afferent inputs of the thalamus

With the exception of the defined pathway between the ventral hippocampus and mPFC (Parent et al., 2010), no other afferent pathway, to our knowledge, can be isolated for selective electrical stimulation within the mPFC brain slice. An alternative approach to electrical stimulation is the use of optogenetics (see section 5.1). Via injections of a viral construct into discrete brain regions, specific neuronal pathways can be genetically targeted for the selective expression of a light activated ion-channel (opsin), e.g. channelrhodopsin. This approach used in combination with conventional brain slice electrophysiology would enable selective release of glutamate from specific afferent pathways with light. This approach could then be used to investigate if α7 nAChRs can modulate glutamate release from specific inputs.

Due to the methodology of optogenetics, experiments are typically performed in older animals. It is therefore important that any observations made in previous experiments, using younger animals, are validated in older animals. So far experiments shown in this thesis have been conducted using brain slices obtained from 5 - 6 week old mice. For optogenetic experiments an adequate expression level of the light sensitive opsin typically requires a post surgery expression duration of 4-6 weeks. Consequently mice would only be suitable for brain slice experimentation at 9-12 weeks old (based on surgery conducted in 5 week old mice). α7 nAChRs expression levels are known to increase within the cortex during development (Fuchs, 1989; Zhang et al., 1998), and although α7 nAChR expression levels are thought to plateau during adolescence, α7 nAChR function may alter with age. It was therefore important to ensure that the effect of α7 nAChR modulation on excitation and inhibition seen in 5-6 week old mice was still present in older mice.

Therefore experiments in which sEPSC/IPSC were recorded in response to α7 nAChRs activation (Fig. 4.2 and Fig. 4.7) were repeated in 10 - 12 week old mice. Similar to previous experiments, the frequency of sEPSCs was significantly enhanced upon the addition of the α7 nAChR PAM PNU-120596 (10 μM) (Fig. 5.4A), whilst sIPSC frequency was unaltered with PNU-120596

alone but was significantly enhanced upon the addition of the α7 nAChR PAM and agonist PNU-282987 (300 nM) and subsequently reversed by addition of MLA (100nM) (Fig. 5.4B). Interestingly upon addition of the α7 nAChR PAM + agonist, sEPSCs became too unstable to analyse, similar to the observation in section 4.2.3. As α7 nAChRs mediate similar effects in older mice, optogenetic experiments were carried out to further investigate the location of α7 nAChRs within the cortex.

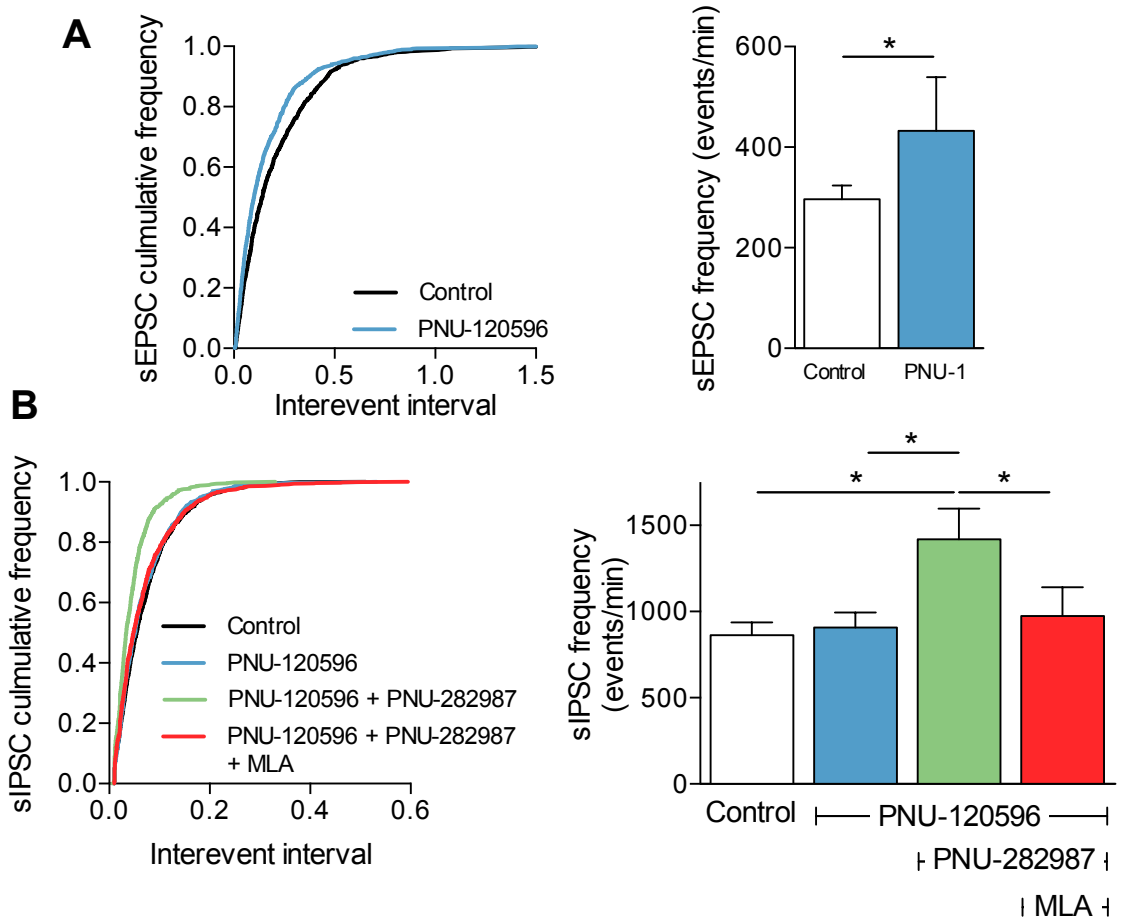

Figure 5.4 Evoked EPSC from Hippocampal afferent fibres in response to α7 nAChR activation and antagonism

mPFC brain slices were prepared in from 10-11 week old C57BL/6 mice Voltage clamp recording were made from layer V pyramidal neurons. Neurons were held at -60 mV and then 0 mV to record sEPSCs and sIPSCs from the same cell. Spontaneous currents were recorded in response to continual bath perfusion of control aCSF and then aCSF containing the α7 nAChR-selective PAM PNU-120596 (10 μM), the α7 nAChR PAM and selective agonist PNU-282987 (300 nM) and finally the α7 nAChR PAM + agonist and antagonist MLA (100 nM). ***(A)*** *sEPSCs and* ***(B)*** *sIPSC frequency (interevent interval) was analysed, ranked and plotted in a cumulative frequency plots (left) total events per minute were also calculated and plotted as mean ± S.E.M in a summary histograms (right). Statistical difference shown in the histogram is based on results of K-S tests of data shown in the corresponding cumulative frequency plots. * significantly different, p ≤ 0.01; n = 5.*

A variety of different brain regions send glutamatergic projections to the mPFC, all of which could potentially posses presynaptic α7 nAChRs. Based on their notable glutamatergic pathways to the PrL, inputs from the ventral hippocampus, contralateral mPFC, VTA, BLA and thalamus were chosen as targets for optogenetic control. Preliminary experiments, were conducted at Vrije University in Amsterdam in Prof. Huib Mansvelder's laboratory, to assess the suitability of these targeted pathways for optogenetic-mediated glutamate release within the PrL. Initial experiments focused on the pathways from the thalamus, VTA and BLA, as technical difficulties in which an inappropriate viral construct was delivered, meant that inputs from the ventral hippocampus and contralateral mPFC could not be assessed.

The optogenetic viral vector chosen for these initial experiments was the AAV5 - CAMKIIα - hChR2 - eYFP (see methods 2.5). The successful transfection of this viral construct would enable the expression of ChR2 in Ca^{2+}/calmodulin-dependent protein kinase 2 alpha (CAMKIIα) expressing cells, primarily used for optogenetic control of glutamatergic excitatory neurons (Dittgen et al., 2004; Rein & Deussing, 2012). Animal surgery and bilateral viral transfusion into either the BLA, VTA or thalamus was conducted in 5 week old male mice. After 4-6 weeks of viral expression, mPFC brain slices were obtained for electrophysiology experiments. Of the three brain regions targeted with this virus only animals injected into the thalamus resulted in sufficient expression of ChR2 to produce reliable glutamatergic responses onto layer V pyramidal neurons within the PrL. Animals injected into the BLA or VTA failed to produce glutamatergic responses in any of the layer V or layer II/III prelimbic cortex pyramidal neurons tested (2 animals per region; VTA n = 7 cells, BLA n = 10 cells).

Due to the limited number of animals that received thalamic injections with the AAV5 - CAMKIIα - hChR2 - eYFP virus construct, additional mice, injected in the thalamus with a different optogenetic virus (as part of a separate PhD project from another student) were also used for these studies. This AAV2/8 - Syn - Chrimson - tdTomato virus, under the control of the synapsin promoter, drives expression of Chrimson, an excitatory ion channel gated with red light with a peak activation at 590 nM (Klapoetke et al., 2014). Similar to the previous

experiments using the ChR2 virus, thalamic injections of the Syn – Chrimson – tdTomato virus, provided sufficient expression in thalamic afferents to produce reliable light evoked EPSCs in layer V pyramidal neurons of the PrL. Both ChR2 and Chrimson activation induced EPSCs that increased in magnitude upon increasing light intensity (Fig. 5.5A). When comparing responses from the two opsins, EPSCs from both opsins had comparable rate of rise and decay times, whilst excitation of ChR2 evoked larger EPSCs with an average amplitude of 582 ± 124 pA compared to Chrimson (295 ± 73 pA), although this difference was not statistically different (Fig. 5.5B). EPSCs obtained via excitation of ChR2 were completely abolished by kynurenic acid (10 mM) suggesting these response were glutamatergic in nature. Due to similar EPSC waveforms, the Chrimson evoked EPSCs were presumed to be glutamatergic, however the limited number of available brain slices meant this could not be pharmacologically verified.

To assess if α7 nAChR activation could modulate the release of glutamate from thalamic inputs, single EPSCs were recorded from layer V pyramidal neurons held at -60 mV in the absence of inhibitory blockade. EPSCs were evoked via a 2 ms light pulse at an intensity that produced a 50% maximal response. A stable 20 min EPSC baseline, recorded at 0.05 Hz, was acquired before consecutive 10 min bath applications of the α7 nAChR PAM PNU-120596 alone (10 μM), PNU-120596 in the presence of the α7 nAChR agonist PNU-282987 (300 nM) and finally application of both PNU-120596 and PNU-282987 and the α7 nAChR antagonist MLA (100 nM). As both the ChR2 and the Chrimson virus produced similar glutamatergic responses, data obtained using both methods were pooled and are shown in figure 5.6. Upon application of the PNU-120596 alone the EPSC amplitude, rate of rise and 10 - 90 % rise time were unaltered. However upon co-application of the PNU-120596 and PNU-282987, the EPSC amplitude was significantly enhanced compared to baseline levels, the EPSC rate of rise also appeared to increase, although not significantly, whereas the rise time remained unchanged (Fig. 5.6A-C). The final addition of MLA appeared to reverse the increase in EPSC rate of rise and amplitude, although in both cases there was not a statistically significant reduction between PNU-120596 and PNU-282987 co-application and MLA. MLA did however reduce the EPSC amplitude to a level no longer significantly larger than control.

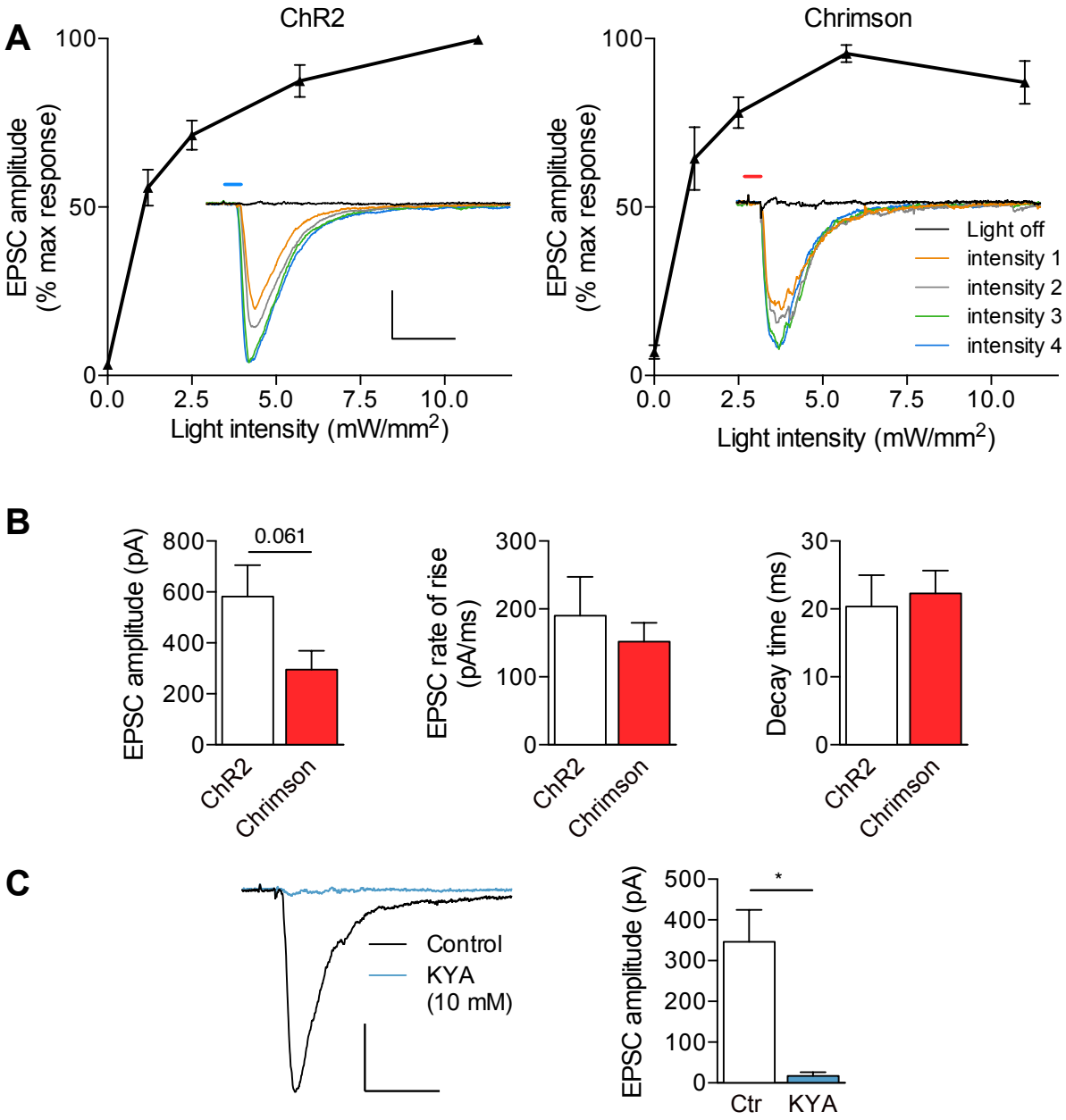

Figure 5.5 Light evoked EPSC from thalamus afferent fibres in response to α7 nAChR activation and antagonism

*Mice were injected with either CAMKIIα-ChR2-eYFP or Syn-Chrimson-tdTomato into the thalamus. Voltage clamp recording were made from layer V pyramidal neurons in the PrL. Neurons were held at -60 mV and light evoked EPSCs were evoked at 0.05 Hz by a single or 50 ms paired pulse 2 ms blue or red light. (**A**) Light evoked EPSCs were evoked at 4 different light intensities from animals injected with CAMKIIα-ChR2 virus (left) and Syn-Chrimson virus (left). EPSCs were analysed and normalised to max response, inset shows example traces at each light intensity. (**B**) EPSCs at maximal amplitude were analysed for amplitude, rate of rise and decay time and shown in histograms (For (A) and (B); ChR2; n = 4 cells; 2 animals, Chrimson n = 6 cells; 2 animals). (**C**) ChR2 EPSCs were completely abolished by kynurenic acid (10 mM) (n = 3) (Chrimson EPSCs were not tested) All data shown as mean ± S.E.M. Data analysed via t-test * significantly different, p ≤ 0.05. Scale bars; 150 pA, 15 ms.*

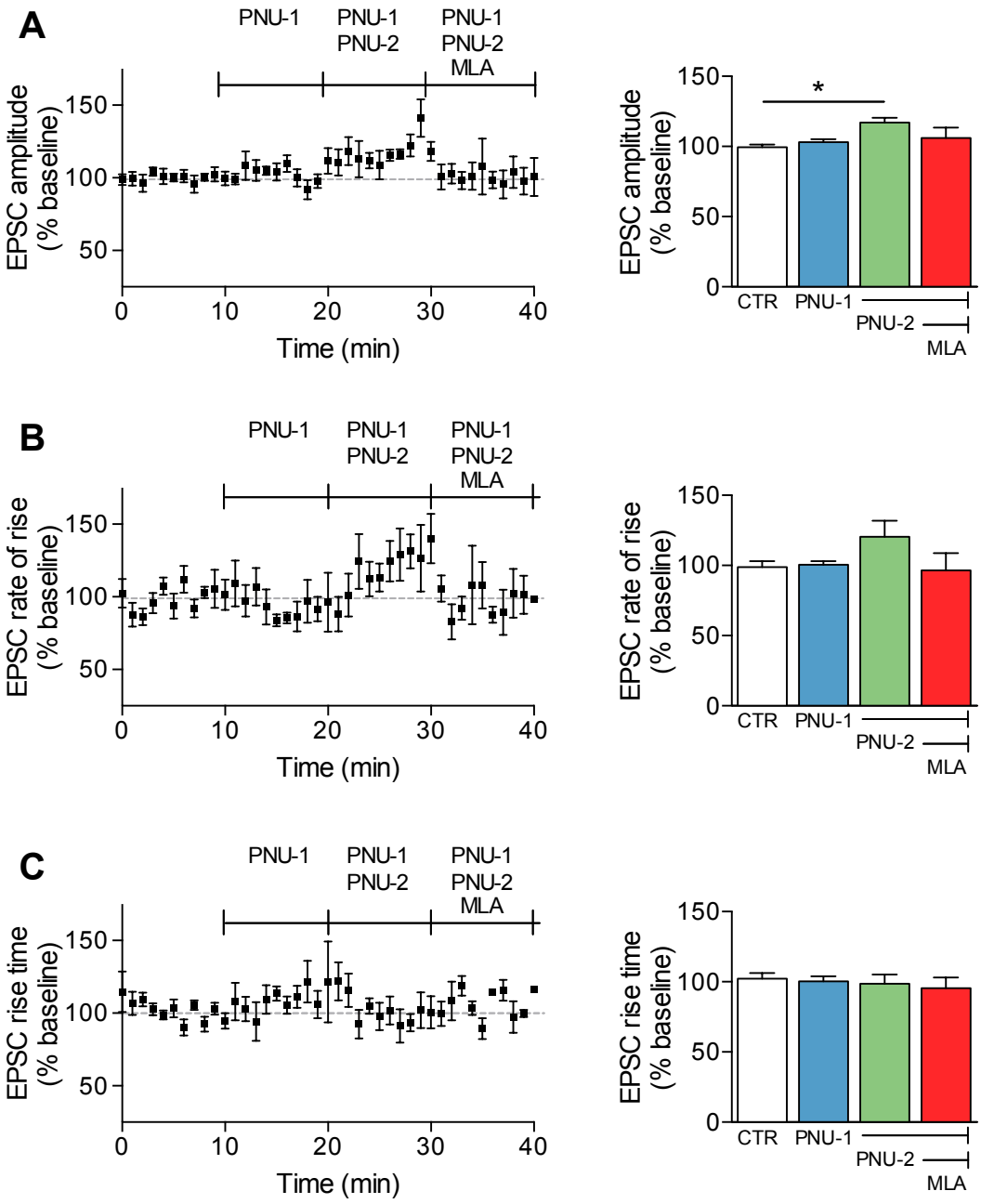

Figure 5.6 Light evoked EPSC from thalamic afferent fibres in response to α7 nAChR activation and antagonism

*Experiments conducted in mice bilaterally injected in the thalamus with the CAMKIIα-ChR2-eYFP or Syn-Chrimson-tdTomato virus. Voltage clamp recordings were made from layer V pyramidal neurons in the PrL. Neurons were held at -60 mV and light evoked EPSCs were evoked at 0.05 Hz by a single or 50 ms paired pulse 2 ms blue light. A stable EPSC baseline of at least 10 min was obtained in control aCSF before 10 min bath applications of the α7 nAChR PAM PNU-120596 (10 μM) (PNU-1) alone, the α7 nAChR PAM and agonist PNU-282987 (300 nM) (PNU-2), followed by application of the α7 nAChR PAM, agonist and MLA (100 nM). (**A**) Light evoked EPSC amplitudes, (**B**) rate of rise and (**C**) 10 – 90 % rise time were analysed. Time-courses (left) show EPSCs normalised to baseline. Histograms (right) represents averaged data across entire 10 min drug application. All data shown as mean ± S.E.M. Significance assessed via repeated measures ANOVA's with bonforroni post hoc tests to compare between each treatment group; * significantly different, p ≤ 0.05; n = 4.*

5.2.3 Optogenetic release of glutamate from afferent inputs to the mPFC from thalamus, contralateral mPFC, ventral hippocampus and basolateral amygdala

To further characterise the glutamatergic inputs to the PrL, optogenetic investigations were continued at the University of Bath. In previous experiments light stimulation of glutamate release was not achieved upon optogenetic control of BLA and VTA inputs. Although ChR2 expressing inputs in these experiments may have been targeting other non-pyramidal cells, such as interneurons, the most probable cause of the lack of responses was due to an inadequate ChR2 expression. Low ChR2 expression could be caused via a number of factors, including the density of CAMKIIα expressing neurons and time given for ChR2 expression. In a bid to overcome the lack of ChR2 expression a AAV5 CAG-ChR2-GFP optogenetic viral construct was used that contains the ubiquitous CAG promoter to drive ChR2 expression (Little & Carter, 2013). The CAG promoter, an artificial promoter made of the β-actin promoter region and the chicken cytomegalovirus (CMV) enhancer element, is used to drive high levels of expression in mammalian cells (Niwa et al., 1991). This construct should provide higher levels of expression of ChR2 than the previous cell type specific CAMKIIα driven virus. As the CAG promoter is not cell type specific, non-glutamatergic projections to the PrL from the targeted brain regions might inadvertently be recruited by the CAG expression system. The VTA as part of the mesolimbic pathway sends a pronounced dopaminergic projection to the PrL. As this dopaminergic pathway is likely to be recruited via the CAG promoter it was decided the VTA would not be targeted. Conversely the BLA, ventral hippocampus, thalamus and contralateral mPFC primarily project to the PrL via glutamatergic afferent pathways (DeNardo et al., 2015; Hoover & Vertes 2007) and so targeting these regions with the AAV5 CAG-ChR2-GFP virus should enable the selective control of glutamate release. Bilateral viral injections of AAV5 CAG-ChR2-GFP were made into the thalamus, ventral hippocampus and BLA, whilst unilateral injections were made into the contralateral dmPFC. After 4-6 weeks of expression brain slices were obtained for electrophysiology, with each injection location visually inspected by fluorescent microscopy to ensure accurate injection site expression.

5.2.3.1 Optogenetic release of glutamate from afferent inputs to the mPFC from contralateral mPFC

Brains slices from mice receiving unilateral mPFC viral injections (Fig. 5.7A), were acquired after 4 weeks of viral expression and whole cell voltage clamp recordings from layer V pyramidal neurons were made in the contralateral PrL. Upon single pulse stimulation with a 2 ms light pulse, clear EPSC responses were observed (Fig. 5.7B). Individual neurons received mixed responses with light stimulation of cortical afferents evoking both mono and polysynaptic EPSCs. To measure the kinetics of these mPFC-mPFC synapses monosynaptic responses (50 % maximal) were taken and fit with a single exponential decay curve (see section 2.9). The average EPSC amplitude, latency, rise time, rate of rise and tau decay of these EPSCs are shown in figure 5.7. The magnitude of these EPSCs increased with increasing light intensities (Fig. 5.8A) and the selective glutamatergic nature of the response was shown as EPSCs were reversibly abolished by kynurenic acid (10 mM) (Fig. 5.8B). Whilst at a range of paired pulse intervals, a reliable paired pulse depression was observed, suggesting a relatively high probability of release from these synapses (Fig. 5.8C).

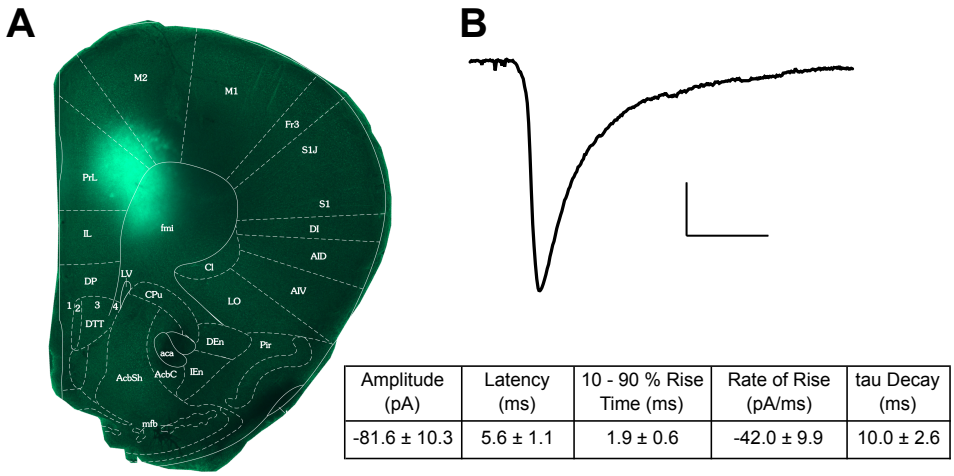

Amplitude (pA)	Latency (ms)	10 - 90 % Rise Time (ms)	Rate of Rise (pA/ms)	tau Decay (ms)
-81.6 ± 10.3	5.6 ± 1.1	1.9 ± 0.6	-42.0 ± 9.9	10.0 ± 2.6

Figure 5.7 CAG-ChR2-GFP expression within the dmPFC and averaged monosynaptic EPSC from contralateral mPFC LV pyramidal neuron

*(**A**) Example fixed brain slice showing the expression of CAG-ChR2-GFP injected into the contralateral mPFC after 4 weeks expression. (**B**) Averaged light evoked monosynapic EPSC recorded from layer V pyramidal neuron in the contralateral PrL (top) was fitted with a single exponential decay curve and averaged EPSC parameters calculated and shown in table (bottom) (n = 5). Scale bar; 20 pA, 15 ms.*

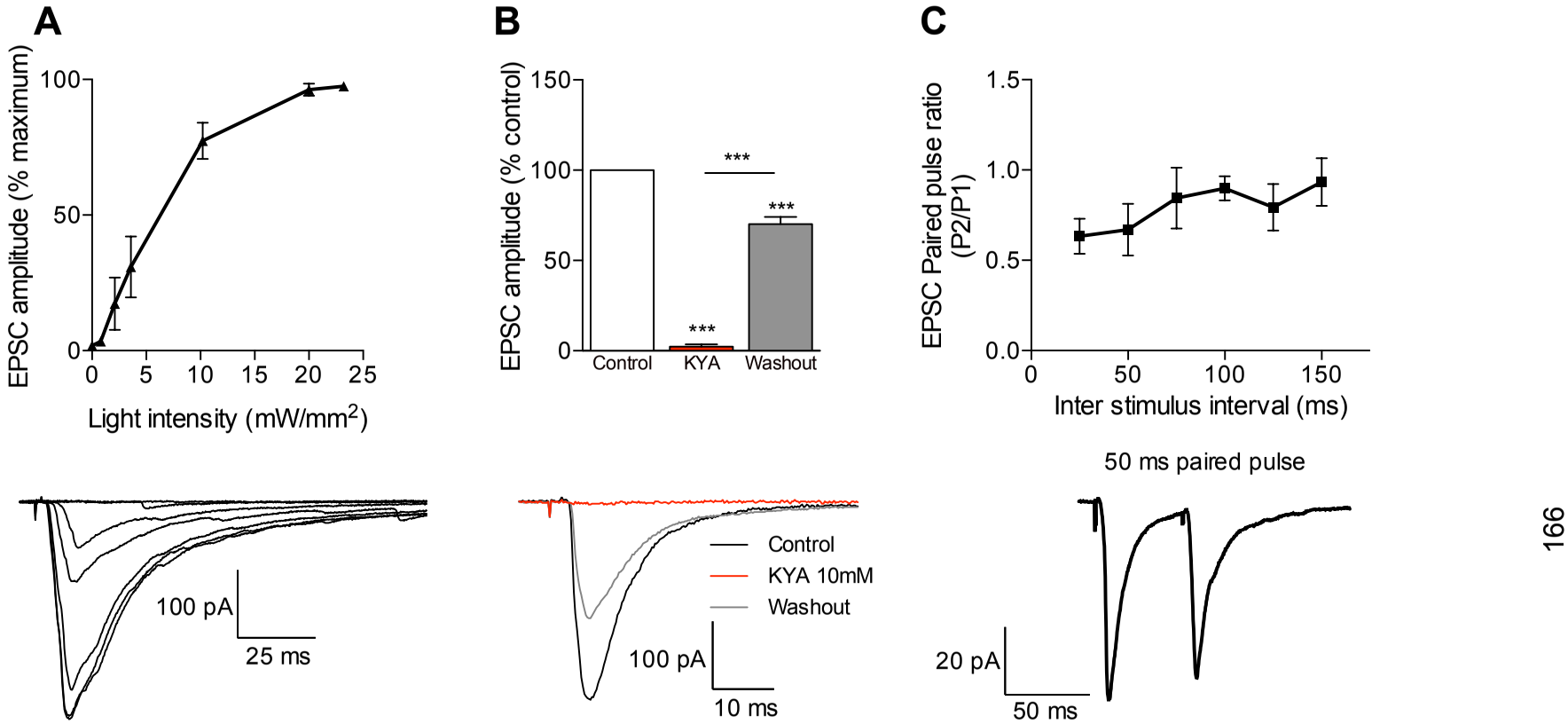

Figure 5.8 Characterisation of light evoked EPSC from contralateral mPFC afferent fibres

*Experiments conducted in mice unilaterally injected in the mPFC with CAG-ChR2-GFP virus. Voltage clamp recordings were made from layer V pyramidal neurons in the contralateral PrL. (**A**) light evoked EPSCs were evoked at varying light intensities and resulting EPSC amplitude measured, normalised to maximum EPSC and plotted against light intensity (n = 6) (top). Example EPSC trace for each light intensity is shown (bottom). (**B**) Light evoked EPSCs were reversibly abolished upon bath application of kynurenic acid (10 mM) in all cells tested (n = 4) (top) example EPSC knockdown traces (bottom) (**C**) Paired light evoked EPSCs were evoked at varying inter-stimulus intervals to measure paired pulse ratios (n = 5) (top) with an example 50 ms paired pulse trace shown (bottom). Data in (B) analysed via one sample t-test (KYA and Washout vs Control) and paired t-test KYA vs Washout *** p ≤ 0.001*

5.2.3.2 Optogenetic release of glutamate from afferent inputs to the mPFC from the thalamus

Brain slices from mice receiving bilateral thalamic injections (Fig. 5.9A), were acquired after 4 weeks of viral expression and whole-cell voltage clamp recordings from layer V pyramidal neurons were made in the PrL. An example fixed injection site for the thalamus is shown in figure 5.9A. Similar to contralateral mPFC experiments 2 ms light pulses reliably produced light evoked EPSCs from layer V pyramidal neurons in all animals tested (Fig. 5.9B). Light evoked EPSCs obtained varied in nature with both monosynaptic and polysynaptic responses observed, although the majority of EPSCs evoked from the thalamus were polysynaptic presumably due to the high level of thalamic innervation and activation of neurons within other layers of the mPFC. The monosynaptic responses obtained were fit to a single exponential decay curve with the averaged properties shown in figure 5.9. The amplitude of light evoked EPSCs at these synapses increased with increasing light intensity (Fig. 5.10A), and EPSCs were mediated by glutamate shown by reversible inhibition with kynurenic acid (10 mM) (Fig. 5.10B). Paired pulse stimulation at different stimulus intervals revealed either paired pulse depression or no facilitation at all, consistent across all intervals (Fig. 5.10C).

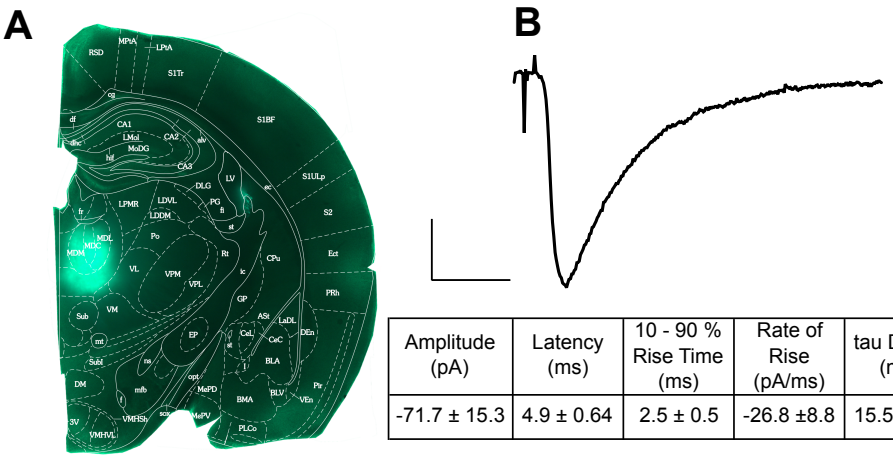

Amplitude (pA)	Latency (ms)	10 - 90 % Rise Time (ms)	Rate of Rise (pA/ms)	tau Decay (ms)
-71.7 ± 15.3	4.9 ± 0.64	2.5 ± 0.5	-26.8 ±8.8	15.5 ± 2.5

Figure 5.9 CAG-ChR2-GFP expression within the thalamus and averaged monosynaptic EPSC from mPFC LV pyramidal neuron

*(**A**) Example fixed brain slice showing the expression of CAG-ChR2-GFP injected into the thalamus after 4 weeks expression. (**B**) Averaged light evoked monosynapic EPSC recorded from layer V pyramidal neuron in the contralateral PrL (top) was fitted with a single exponential decay curve and averaged EPSC parameters calculated and shown in table (bottom) (n = 4). Scale bar; 20 pA, 15 ms.*

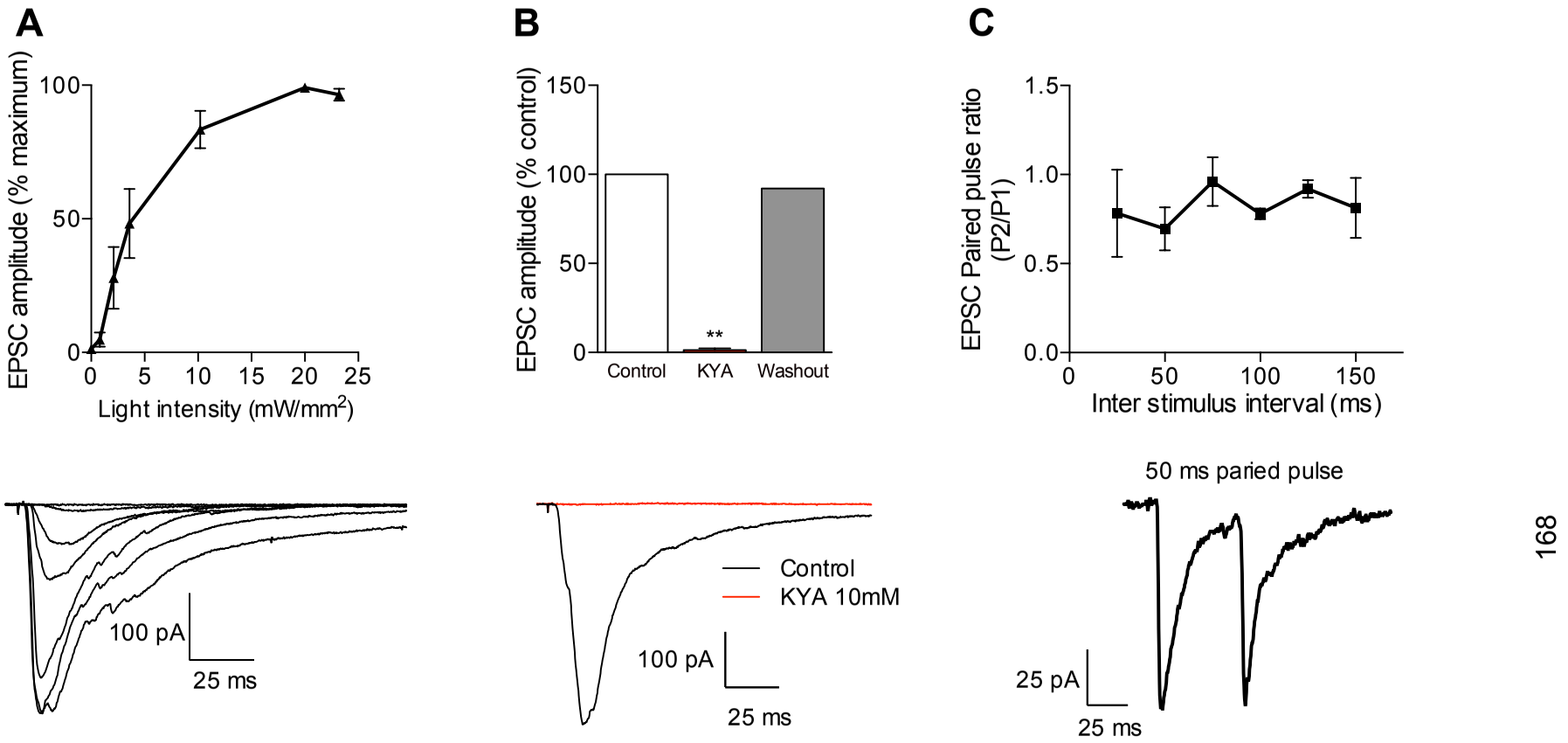

Figure 5.10 Characterisation of light evoked EPSC from thalamic afferent fibres

*Experiments conducted in mice bilaterally injected in the thalamus with CAG-ChR2-GFP virus. Voltage clamp recordings were made from layer V pyramidal neurons in the PrL. (**A**) light evoked EPSCs were evoked at varying light intensities and resulting EPSC amplitude measured, normalised to maximum EPSC and plotted against light intensity (n = 5) (top). Example EPSC trace for each light intensity is shown (bottom).*
*(**B**) Light evoked EPSCs were reversibly abolished upon bath application of kynurenic acid (10 mM) (control + KYA; n = 2, washout; n = 1) (top), example EPSC knockdown traces (bottom) (**C**) Paired light evoked EPSCs were evoked at varying inter-stimulus intervals to measure paired pulse ratios (n = 3) (top) with an example 50 ms paired pulse trace shown (bottom). Data represents mean ± S.E.M. Data in (B) analysed via one sample t-test (KYA vs Control) ** p ≤ 0.01.*

5.2.3.3 Optogenetic release of glutamate from afferent inputs to the mPFC from ventral hippocampus

Brain slices from mice receiving bilateral ventral hippocampal injections (Fig. 5.11A), were initially acquired after 4 weeks of viral expression however as no responses were observed after 4 weeks, the virus was left to express for an additional 2 weeks in all subsequent animals. The injection sites were inspected with an example shown in figure 5.11A. EPSC light responses were obtain in 5 of the 8 animals. Light pulses of 2 ms produced predominantly monosynaptic responses in layer V pyramidal neurons. These monosynaptic EPSCs responses were fitted to a single exponential decay curve, with the average EPSC parameters shown in figure 5.11. Hippocampal-mPFC EPSC amplitudes increased with increasing light intensity (Fig. 5.12A) and were reversibly abolished via kynurenic acid (Fig. 5.12B) Paired pulse ratio experiments at differing inter-stimulus intervals showed a predominant synaptic paired pulse depression (Fig. 5.12C).

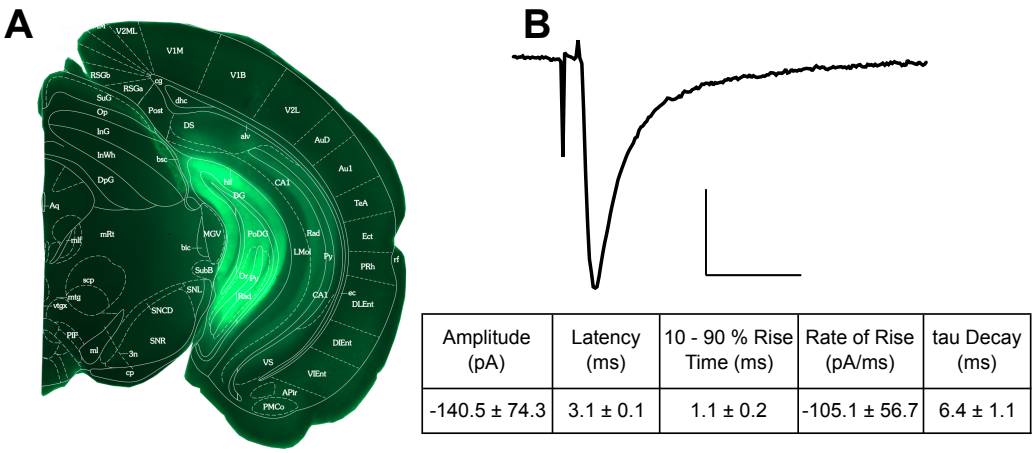

Amplitude (pA)	Latency (ms)	10 - 90 % Rise Time (ms)	Rate of Rise (pA/ms)	tau Decay (ms)
-140.5 ± 74.3	3.1 ± 0.1	1.1 ± 0.2	-105.1 ± 56.7	6.4 ± 1.1

Figure 5.11 CAG-ChR2-GFP expression within the ventral hippocampus and averaged monosynaptic EPSC from mPFC LV pyramidal neuron

*(**A**) Example fixed brain slice showing the expression of CAG-ChR2-GFP injected into the ventral hippocampus after 6 weeks expression. (**B**) Averaged light evoked monosynapic EPSC recorded from layer V pyramidal neuron in the contralateral PrL (top) was fitted with a single exponential decay curve and averaged EPSC parameters calculated and shown in table (bottom) (n = 4). Scale bar; 20 pA, 15 ms.*

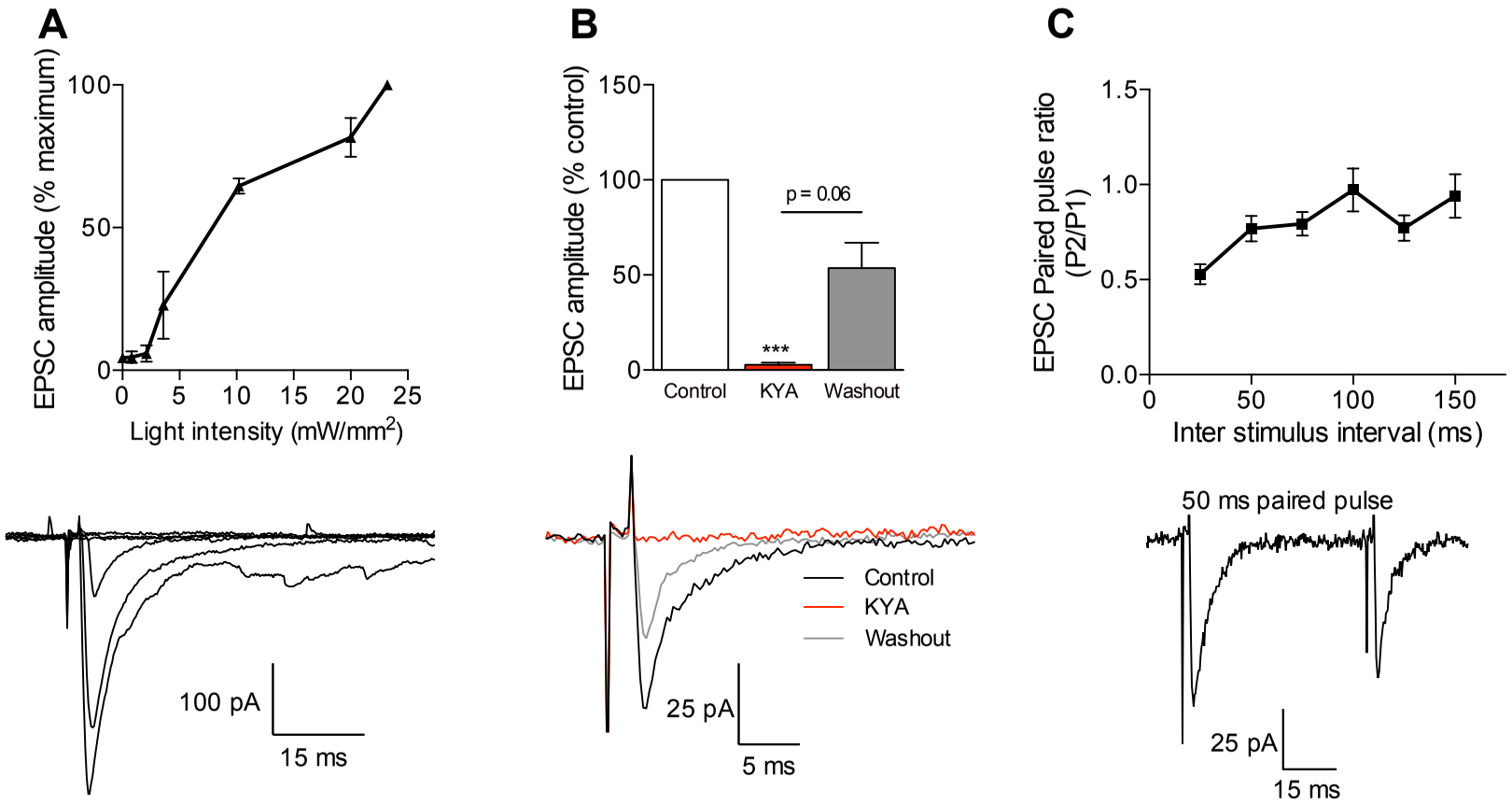

Figure 5.12 Characterisation of light evoked EPSC from ventral hippocampal afferent fibres

*Experiments conducted in mice bilaterally injected in the ventral hippocampus with CAG-ChR2-GFP virus. Voltage clamp recordings were made from layer V pyramidal neurons in the PrL. (**A**) light evoked EPSCs were evoked at varying light intensities and resulting EPSC amplitude measured, normalised to maximum EPSC and plotted against light intensity (n = 4) (top). Example EPSC trace for each light intensity is shown (bottom). (**B**) Light evoked EPSCs were reversibly abolished upon bath application of kynurenic acid (10 mM) in all cells tested (n = 3)(top) example EPSC knockdown traces (bottom) (**C**) Paired light evoked EPSCs were evoked at varying inter-stimulus intervals to measure paired pulse ratios (n = 7) (top) with an example 50 ms paired pulse trace shown (bottom). Data represents mean ± S.E.M. Data in (B) analysed via one sample t-test (KYA and Washout vs Control) and paired t-test KYA vs Washout *** p ≤ 0.001.*

5.2.3.4 Optogenetic release of glutamate from afferent inputs to the mPFC from basolateral amygdala

Brain slices were obtained from animals injected bilaterally into the BLA after 6 weeks expression, similar to ventral hippocampal experiments. The injection sites for all animals were observed with an example shown in figure 5.13A. Of the inspected brain slices the injection sites were notably variable with a large viral spread, this meant clear expression within the BLA was not always obvious. Perhaps reflective of this was that of the 7 mice injected only 2 produced reliable light evoked EPSCs. The EPSC responses obtained upon 2 ms blue light pulses were predominantly monosynaptic with calculated parameters shown in figure 5.13. Light evoked EPSC amplitudes reliably increased with light intensity (Fig. 5.14A), and paired pulse stimulation revealed a combination of paired pulse facilitation and paired pulse depression at shorter intervals but a robust paired pulse depression at longer inter-stimulus intervals (Fig. 5.14B). Due to the limited number of cells recorded from the glutamatergic nature of the EPSC was not tested. Literature suggests that projecting glutamatergic inputs from the BLA may also excite local mPFC interneurons leading to a feed-forward inhibition of pyramidal neurons within the mPFC (Dilgen et al., 2013). To observe if light pulses produced an inhibitory response in the layer V pyramidal neurons, cells were held at 0 mV; under this condition no inhibitory currents were observed in the 3 cells tested.

Light evoked glutamate release was achieved, with varying success, from all of the afferent input pathways targeted for optogenetic stimulation. Comparing the resulting EPSCs may identify differences in the innervation and the synaptic properties of the different afferent inputs to layer V pyramidal neurons of the PrL.

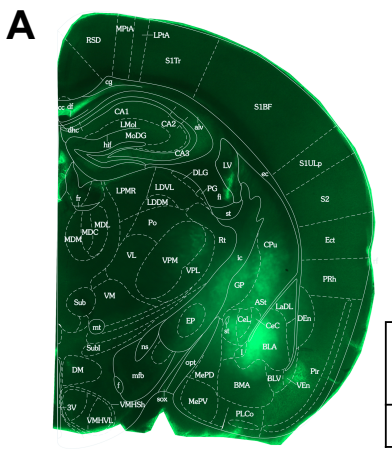

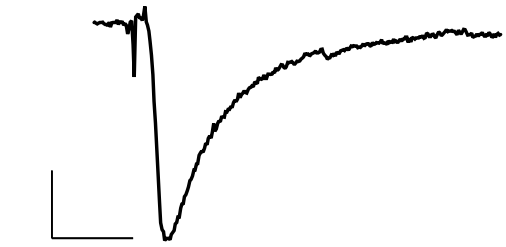

Amplitude (pA)	Latency (ms)	10 - 90 % Rise Time (ms)	Rate of Rise (pA/ms)	tau Decay (ms)
-66.7 ± 18.7	3.4 ± 0.44	2.1 ± 0.4	-27.9 ±8.1	13.4 ± 3.2

Figure 5.13 CAG-ChR2-GFP expression within the BLA and averaged monosynaptic EPSC from mPFC LV pyramidal neuron

*(**A**) Example fixed brain slice showing the expression of CAG-ChR2-GFP injected into the BLA after 6 weeks expression. (**B**) Averaged light evoked monosynapic EPSC recorded from layer V pyramidal neuron in the contralateral PrL (top) was fitted with a single exponential decay curve and averaged EPSC parameters calculated and shown in table (bottom) (n = 4). Scale bar; 20 pA, 15 ms.*

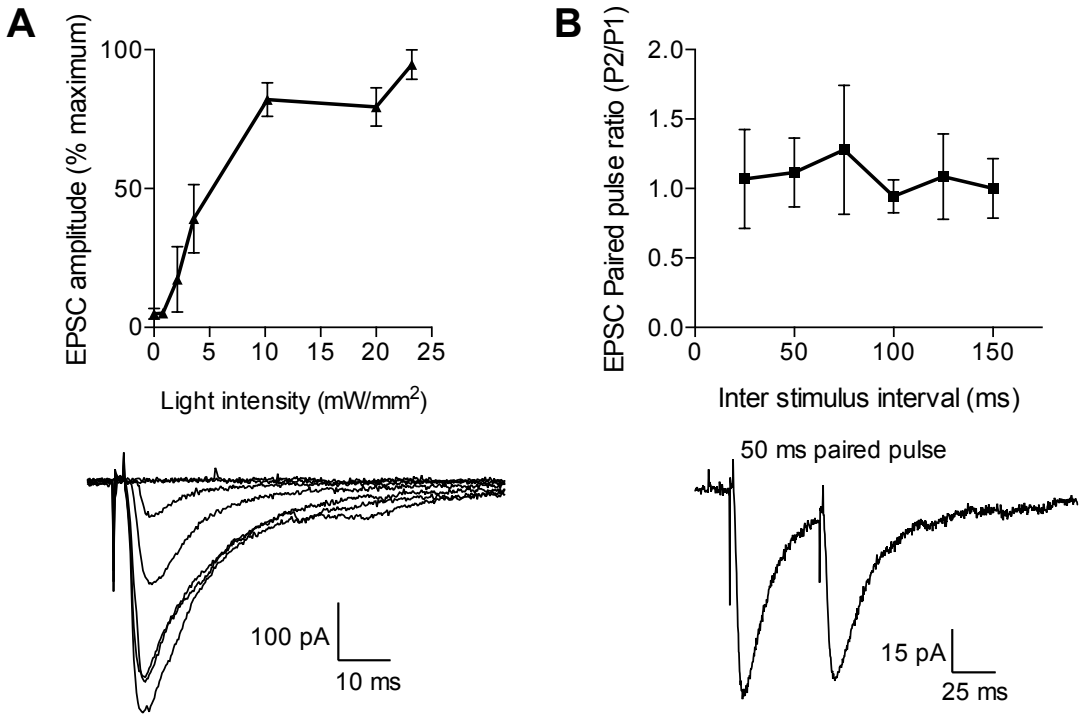

Figure 5.14 Characterisation of light evoked EPSC from the afferent fibres of the basolateral amygdala

*Experiments conducted in mice bilaterally injected in the BLA with CAG-ChR2-GFP virus. Voltage clamp recordings were made from layer V pyramidal neurons in the PrL. (**A**) light evoked EPSCs were evoked at varying light intensities and resulting EPSC amplitude measured, normalised to maximum EPSC and plotted against light intensity (n = 4) (top). Example EPSC trace for each light intensity is shown (bottom). (**B**) Paired light evoked EPSCs were evoked at varying inter-stimulus intervals to measure paired pulse ratios (n = 3) (top) with an example 50 ms paired pulse trace shown (bottom). Data represents mean ± S.E.M.*

Stimulus response curves for each input indicate a similar increase in the EPSC amplitude with increasing light intensity between inputs, with a slight rightward shift in response curve for ventral hippocampal inputs (Fig. 5.15A). Although differences in stimulus response relationships may represent differences in relative synaptic excitability, with optogenetics, input response relationships also depends on levels of ChR2 expression, which will vary between animals and afferent inputs, limiting neurophysiological interpretation. To investigate any differences in the synaptic release probability between afferent fibres paired pulse ratios were compared (Fig. 5.15B). All inputs show a reliable paired pulse depression at all intervals tested, with BLA inputs, producing a more varied paired pulse ratio upon shorter inter-pulse intervals, these data suggesting that most inputs possess a high probability of synaptic release.

Differences in synaptic properties were assessed by comparing the parameters of the monosynaptic EPSCs. EPSCs evoked at approximately 50 % maximum, possessed similar amplitudes across inputs with the exception of hippocampal inputs that produced a more variable response with a larger average amplitude, although differences were not statistically different (Fig. 5.15C). Differences in 10 – 90% rise time and decay times may indicate differences in the proximal location of the synapse to the soma of the neuron. For both rise and decay times, hippocampal inputs displayed the fastest rise and decay times followed by contralateral mPFC, BLA and then thalamic inputs (Fig. 5.15D,E). Although the differences in these parameters were not statistically different, these observations may suggest that hippocampal inputs make more proximal synaptic connections in layer V with thalamic inputs synapsing at more distal locations.

Synaptic latencies represent the time between the start of light stimulation and the commencement of the downward EPSC conductance. This latency to response can be accounted for by conductance across the axon to the pre-terminal and the synaptic delay (Boudkkazi et al., 2007), and so can provide evidence for differences in the synaptic release. Hippocampal and BLA synapses possessed the shortest latencies with thalamic and mPFC synapses possessing longer latencies (Fig. 5.15F). These differences perhaps suggest hippocampal and BLA inputs have a higher release probability, however caution

must be taken when interpreting synaptic latencies whilst using optogenetics, as a delay between light stimulation and ChR2 dependent depolarisation and action potential firing adds an additional time delay, which may vary with levels of ChR2 expression and ChR2 localisation relative to presynaptic boutons.

5.2.4 α7 nAChR modulation of thalamic, contralateral mPFC and ventral hippocampal inputs

Experiments were next conducted to observe if α7 nAChRs could modulate the levels of light evoked glutamate release from these specific afferent inputs. The amplitude, rate of rise and 10 – 90 % rise time were assessed in addition to the measurement of paired pulse ratio at 50 ms. Inputs from the contralateral mPFC ventral hippocampus and thalamus were assessed; due to the limited number of successful transfections of ChR2 into the BLA, α7 nAChR modulation of input from the BLA could not be assessed.

5.2.4.1 α7 nAChR modulation of contralateral mPFC inputs

A minimum 10 min baseline of light evoked EPSCs from the contralateral mPFC was recorded before successive 10 min applications of the α7 nAChR PAM PNU-120596 (10 μM) alone, PNU-120596 in the presence of the α7 nAChR agonist PNU-282987 (300 nM) with the final addition of the α7 nAChR antagonist MLA (100 nM). Due to variable n number upon the final addition of MLA, multiple ANOVAs were performed to analyse significance. Application of the α7 nAChR PAM did not significantly alter the amplitude, rise time or rate of rise of EPSCs while co-application of the α7 nAChR agonist and PAM resulted in a significant reduction in EPSC amplitude but no change in rate of rise or 10 – 90 % rise time (ANOVA; Control, PNU-1, PNU-1 + PNU-2; n = 4) (Fig. 5.16A-C). EPSCs in the presence of the α7 nAChR antagonist MLA had unaltered amplitudes, rise time and rate of rise compared to control (ANOVA; Control, PNU-1, PNU-1 + PNU-2, MLA; n = 3).

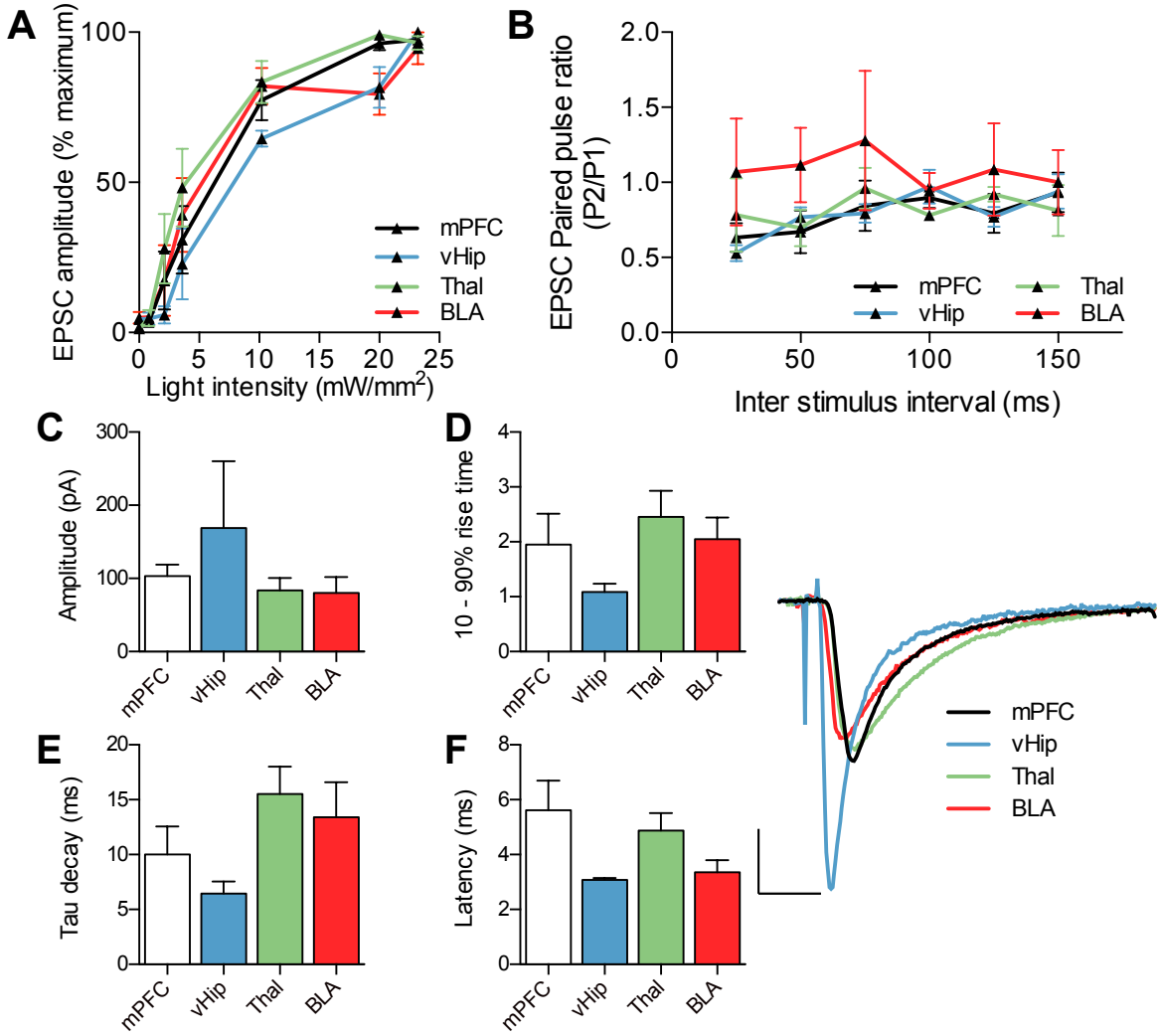

	Amplitude (pA)	Latency (ms)	10 - 90 % Rise Time (ms)	Rate of Rise (pA/ms)	tau Decay (ms)	n
mPFC	-81.6 ± 10.3	5.6 ± 1.1	1.9 ± 0.6	-42.0 ± 9.9	10.0 ± 2.6	5
vHip	-140.5 ± 74.3	3.1 ± 0.1	1.1 ± 0.2	-105.1 ± 56.7	6.4 ± 1.1	4
Thalamus	-71.7 ± 15.3	4.9 ± 0.64	2.5 ± 0.5	-26.8 ±8.8	15.5 ± 2.5	4
BLA	-66.7 ± 18.7	3.4 ± 0.4	2.1 ± 0.4	-28.0 ± 8.1	13.4 ± 3.2	4

Figure 5.15 Comparison of light evoked EPSCs from different afferent fibres

*Experiments conducted in mice injected into the mPFC, vHip, Thalamus or BLA with CAG-ChR2-GFP virus. Voltage clamp recordings were made from layer V pyramidal neurons in the PrL held at -60 mV (**A**) Light evoked EPSCs were evoked at different light intensities and normalised to maximal response (mPFC; n = 6, Thal; n = 5, vHip; n = 4, BLA; n = 4). (**B**) Paired EPSCs were evoked by light pulses with variety of interpulse intervals and paired pulse ratios were analysed by dividing the second response by the first (mPFC; n = 6, Thal; n = 3, vHip; n = 7, BLA; n = 3). Single monosynaptic light evoked EPSCs roughly 50% maximal were analysed for (**C**) amplitude, (**D**) rise time, (**E**) Tau decay, (**F**) latency and plotted in histograms and calculated values shown in table (bottom). Representative traces were created by averaging monosynaptic EPSCs from each cell and superimposed and aligned from onset of light impulse (right). All data shown as mean ± S.E.M. Data in (C-F) analysed via one-way ANOVA with Tukey's post hoc test, no statistical differences were found between inputs for any parameter tested. Scale bar; 30 pA, 10 ms.*

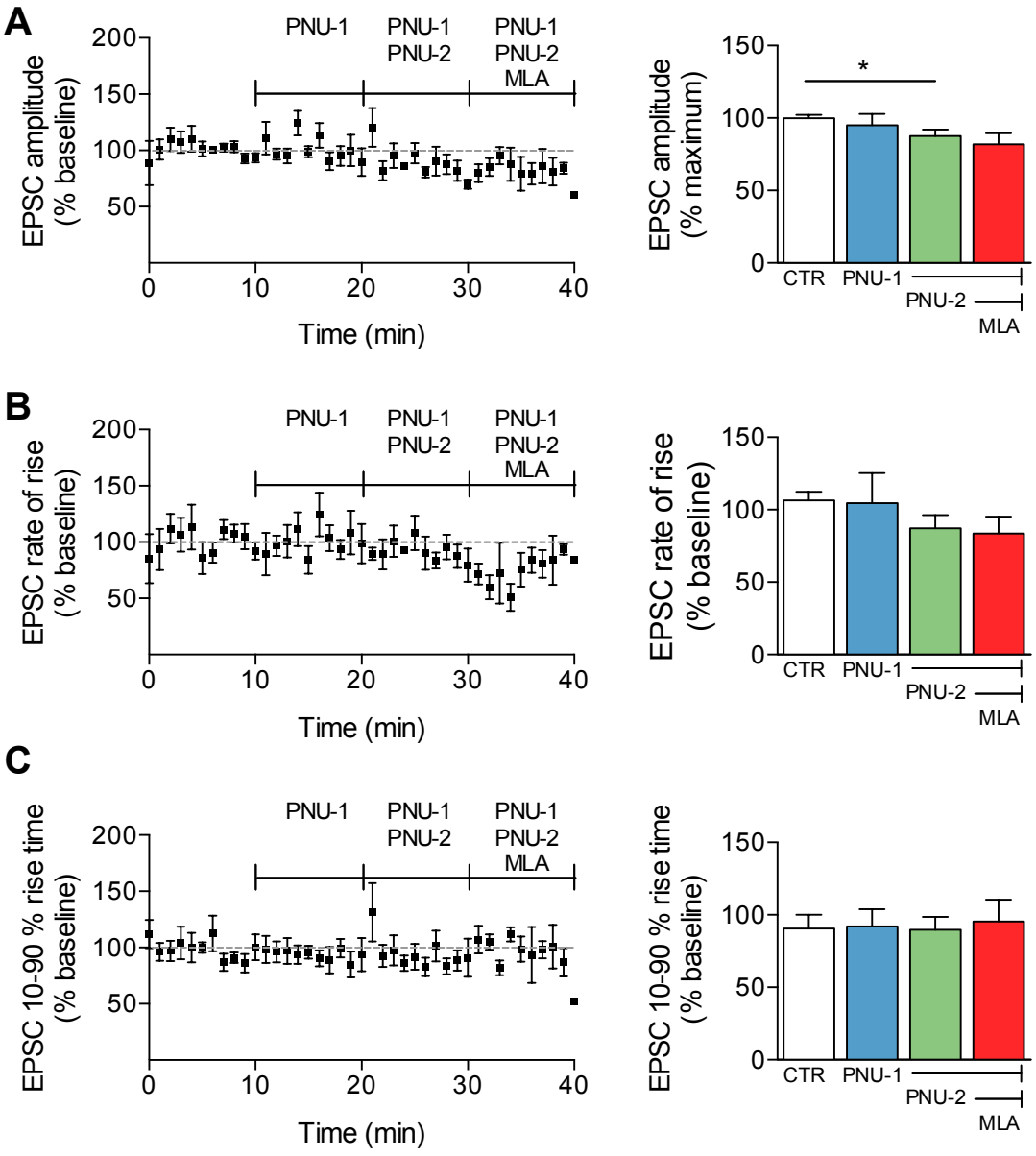

Figure 5.16 Light evoked EPSC from contralateral mPFC afferent fibres in response to α7 nAChR activation and antagonism

*Experiments conducted in mice unilaterally injected in the mPFC with CAG-ChR2-GFP virus. Voltage clamp recordings were made from layer V pyramidal neurons in the contralateral PrL. Neurons were held at -60 mV and light evoked EPSCs were evoked at 0.05 Hz by a single or 50 ms paired pulse 2 ms blue light. A stable EPSC baseline of at least 10 min was obtained in control aCSF before 10 min bath applications of the α7 nAChR PAM PNU-120596 (10 μM) (PNU-1) alone, the α7 nAChR PAM and agonist PNU-282987 (300 nM) (PNU-2), followed by application of the α7 nAChR PAM, agonist and MLA (100 nM). (**A**) Light evoked EPSC amplitudes, (**B**) rate of rise and (**C**) 10 – 90 % rise time were analysed. Time-courses (left) show EPSCs normalised to baseline. Histograms (right) represents averaged data across entire 10 min drug application. All data shown as mean ± S.E.M. Significance assessed via multiple repeated measures ANOVA's with Dunnett's post hoc tests between each treatment and control; * significantly different, p ≤ 0.05; (Control, PNU-1, PNU-2; n = 4, MLA; n = 3).*

To assess if α7 nAChR activation could alter the probability of release of glutamate the paired pulse ratios were also measured upon sequential application of the α7 nAChR drugs. For the contralateral mPFC the α7 PAM alone or in the presence of the α7 nAChR agonist did not alter the paired pulse ratio compared to control, addition of MLA however significantly increased the paired pulse ratio (Fig. 5.17), suggesting antagonism of α7 nAChRs may decrease the probability of release from contralateral mPFC fibres.

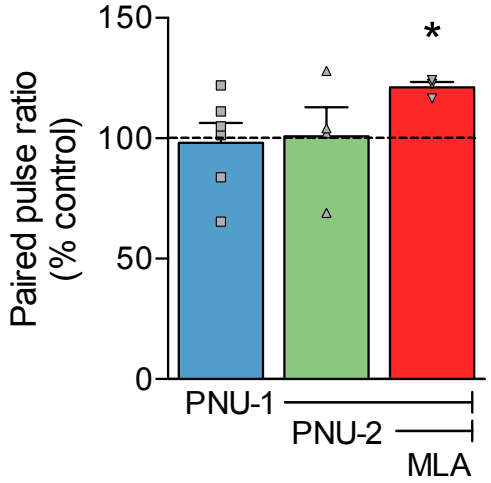

Figure 5.17 Paired pulse ratios EPSC from contralateral mPFC afferent fibres in response to α7 nAChR activation and antagonism

*Experiments conducted in mice unilaterally injected in the mPFC with CAG-ChR2-GFP virus. Voltage clamp recordings were made from layer V pyramidal neurons in the contralateral PrL. Neurons were held at -60 mV and light evoked EPSCs were evoked at 0.05 Hz by a 50 ms paired 2 ms blue light pulse. A stable EPSC baseline of at least 10 min was obtained in control aCSF before 10 min bath applications of the α7 nAChR PAM PNU-120596 (10 μM) (PNU-1) alone, the α7 nAChR PAM and agonist PNU-282987 (300 nM) (PNU-2), followed by application of the α7 nAChR PAM, agonist and MLA (100 nM). Paired pulse ratios were calculated by dividing the second pulse by the first and then normalised to the control paired pulse ratio. All data shown as mean ± S.E.M. Significant differences assessed to via one sample t-tests * significantly different, p ≤ 0.05 (PNU-1; n = 6 PNU-2; n = 4 MLA; n = 3).*

5.2.4.2 α7 nAChR modulation of ventral hippocampal inputs

Electrical stimulation of hippocampal inputs provided no evidence for α7 nAChR modulation of this pathway (Fig. 5.3). To investigate this further, similar experiments were conducted using optogenetics. Ventral hippocampal inputs were evoked continuously until a stable 10 min baseline was obtained after which the EPSCs were evoked continuously in the presence of sequential 10 min bath applications of the α7 nAChR PAM PNU-120596 alone (10 μM), PNU-120596 in the presence of the α7 nAChR agonist PNU-282987 (300 nM) with the final addition of the PNU-120596 + PNU-282987 and the α7 nAChR antagonist MLA (100 nM). The amplitude and rate of rise of light evoked EPSCs were unchanged upon the application of PNU-120596 alone, but application of PNU-120596 and PNU-282987 significantly decreased both the amplitude and rate of rise compared to control (Fig. 5.18A,B). Addition of MLA appeared to not alter either the EPSC amplitude or average rate of rise but increased the variability, rendering the EPSC amplitude and rate of rise to be no longer significant from control (Fig. 5.18B). The EPSC rise time remained unchanged in the presence of all of the drug combinations (Fig. 5.18C).

Paired pulse ratios were also measure for the inputs from the ventral hippocampus, and were unchanged compared to control from any of the drug treatments (Fig. 5.19).

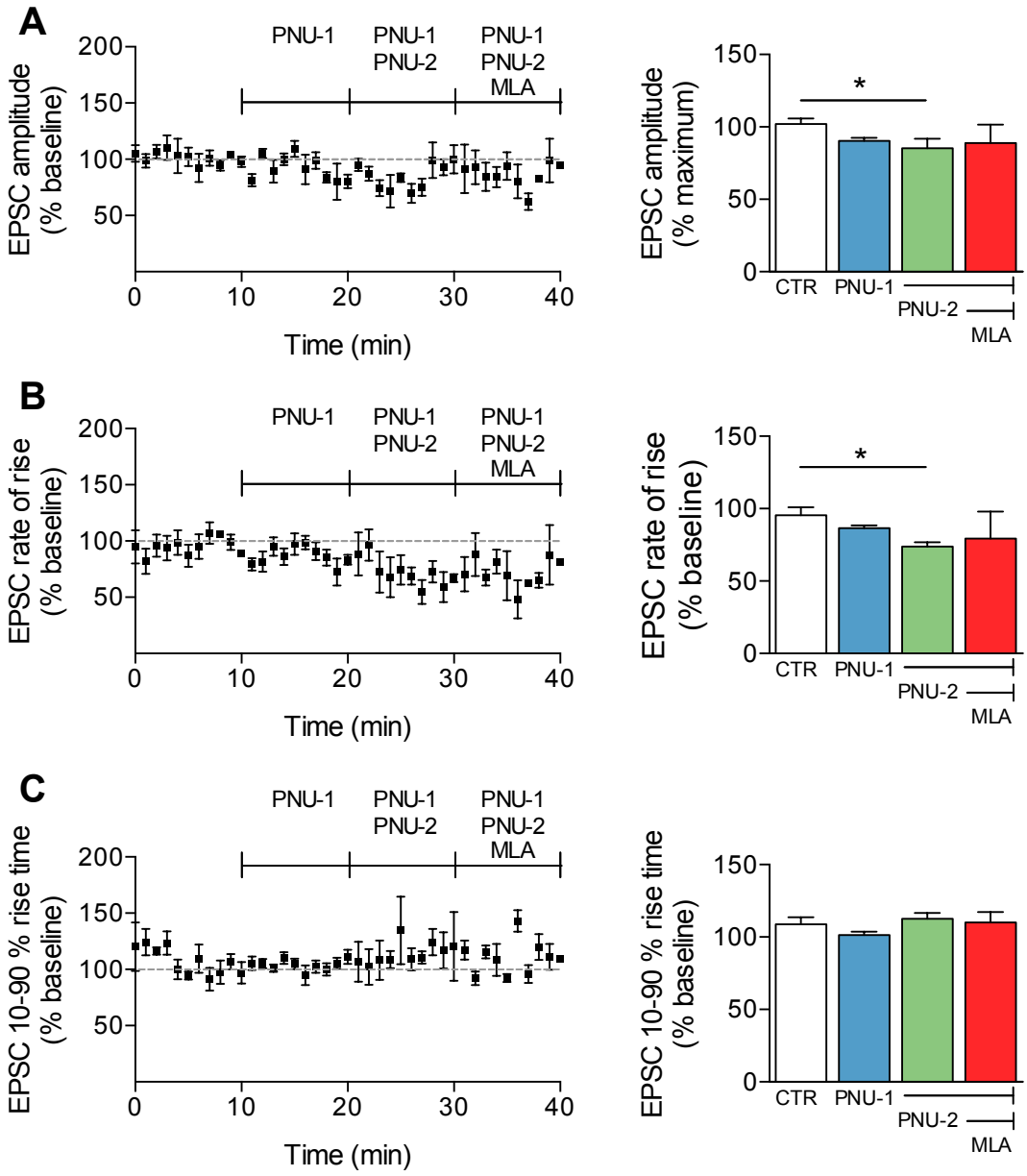

Figure 5.18 Light evoked EPSC from ventral hippocampal afferent fibres in response to α7 nAChR activation and antagonism

*Experiments conducted in mice bilaterally injected in the ventral hippocampus with the CAG-ChR2-GFP virus. Voltage clamp recordings were made from layer V pyramidal neurons in the PrL. Neurons were held at -60 mV and light evoked EPSCs were evoked at 0.05 Hz by a single or 50 ms paired pulse 2 ms blue light pulse. A stable EPSC baseline of at least 10 min was obtained in control aCSF before 10 min bath applications of the α7 nAChR PAM PNU-120596 (10 μM) (PNU-1) alone, the α7 nAChR PAM and agonist PNU-282987 (300 nM) (PNU-2), followed by application of the α7 nAChR PAM, agonist and MLA (100 nM). (**A**) Light evoked EPSC amplitudes, (**B**) rate of rise and (**C**) 10 – 90 % rise time were analysed. Time-courses (left) show EPSCs normalised to baseline. Histograms (right) represents averaged data across entire 10 min drug application. All data shown as mean ± S.E.M. Significance assessed via repeated measures ANOVA with Dunnett's post hoc test between each treatment and control; * significantly different, p ≤ 0.05; n = 3.*

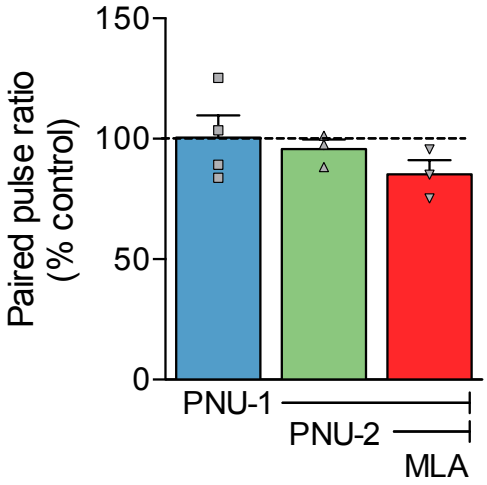

Figure 5.19 Light evoked 50 ms paired pulse ratios EPSC from ventral hippocampal afferent fibres in response to α7 nAChR activation and antagonism

*Experiments conducted in mice bilaterally injected in the ventral hippocampus with the CAG-ChR2-GFP virus. Voltage clamp recordings were made from layer V pyramidal neurons in the PrL. Neurons were held at -60 mV and light evoked EPSCs were evoked at 0.05 Hz by a 50 ms paired 2 ms blue light pulse. A stable EPSC baseline of at least 10 min was obtained in control aCSF before 10 min bath applications of the α7 nAChR PAM PNU-120596 (10 μM) (PNU-1) alone, the α7 nAChR PAM and agonist PNU-282987 (300 nM) (PNU-2), followed by application of the α7 nAChR PAM, agonist and MLA (100 nM). Paired pulse ratios were calculated by dividing the second pulse by the first and then normalised to the control paired pulse ratio. All data shown as mean ± S.E.M. Significant differences assessed to via one sample t-tests * significantly different, p ≤ 0.05 (PNU-1; n =4 PNU-2, MLA; n = 3)*

5.2.4.3 α7 nAChR modulation of thalamic inputs

Optogenetic release of glutamate from thalamic inputs were also measured in response to α7 nAChR modulation and antagonism. It was found that the α7 nAChR PAM alone or in the presence of the α7 nAChR agonist failed to alter the EPSC amplitude, rise time or rate of rise compared to control with no change in EPSC parameters upon addition of MLA (analysed separately with an additional ANOVA) (Fig. 5.20A-C). These results are in contrast to those seen previously using a different optogenetic virus (Fig. 5.6), and are discussed in detail in section 6.4.3.4.

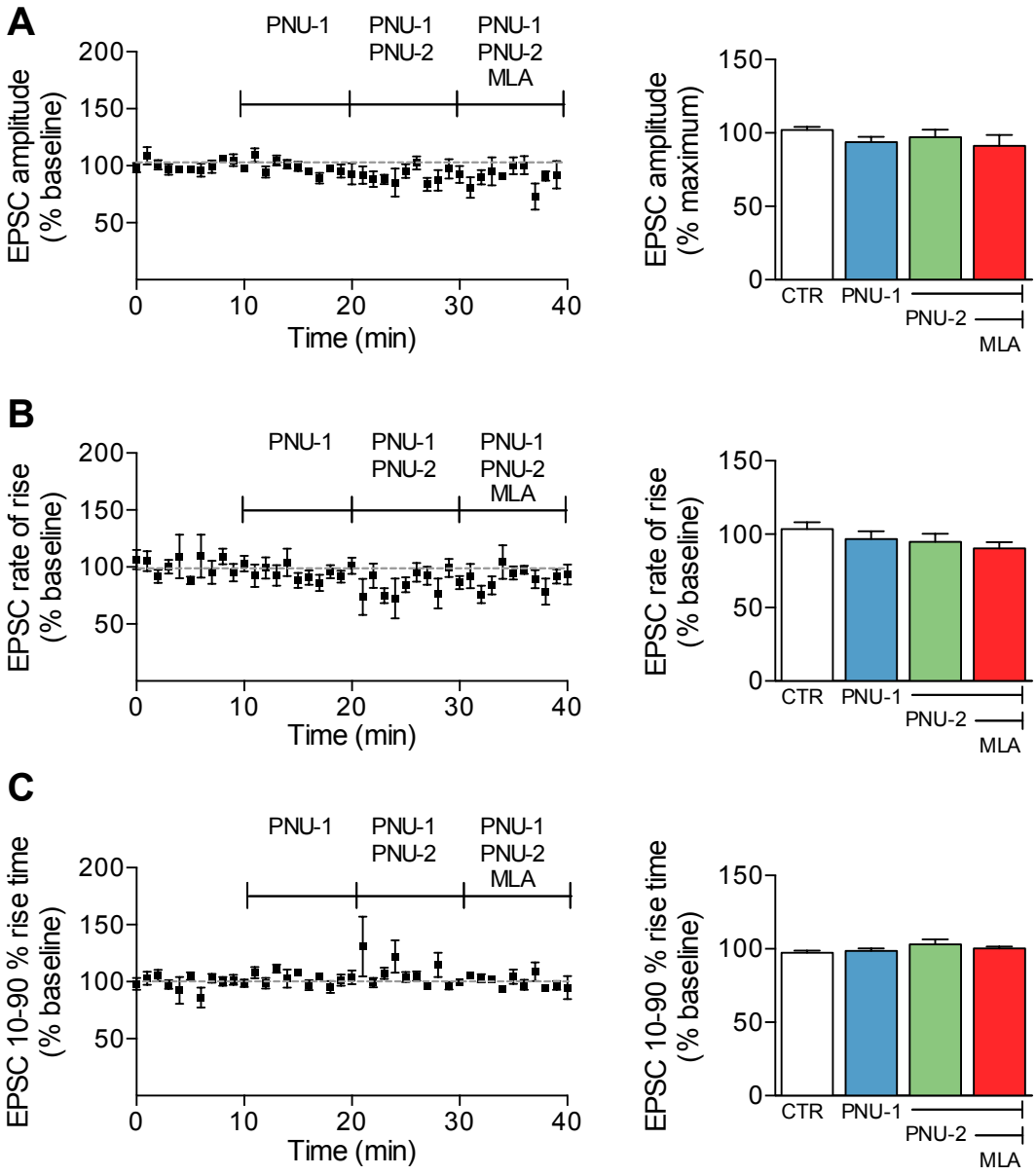

Figure 5.20 Light evoked EPSC from thalamic afferent fibres in response to α7 nAChR activation and antagonism

*Experiments conducted in mice bilaterally injected in the thalamus with the CAG-ChR2-GFP virus. Voltage clamp recordings were made from layer V pyramidal neurons in the PrL. Neurons were held at -60 mV and light evoked EPSCs were evoked at 0.05 Hz by a single or 50 ms paired pulse 2 ms blue light. A stable EPSC baseline of at least 10 min was obtained in control aCSF before 10 min bath applications of the α7 nAChR PAM PNU-120596 (10 μM) (PNU-1) alone, the α7 nAChR PAM and agonist PNU-282987 (300 nM) (PNU-2), followed by application of the α7 nAChR PAM, agonist and MLA (100 nM). (**A**) Light evoked EPSC amplitudes, (**B**) rate of rise and (**C**) 10 – 90 % rise time were analysed. Time-courses (left) show EPSCs normalised to baseline. Histograms (right) represents averaged data across entire 10 min drug application. All data shown as mean ± S.E.M. Significance assessed via multiple repeated measures ANOVA's with Dunnett's post hoc tests between each treatment and control; * significantly different, p ≤ 0.05; (Control, PNU-1, PNU-2; n = 4, MLA; n = 3).*

Paired pulse ratios in response to α7 nAChRs were also measured from thalamic inputs but similar to other EPSC parameters α7 nAChR PAM alone or in the presence of the α7 nAChR agonist or addition of MLA failed to significantly alter the paired pulse ratio (Fig. 5.21). However the ratio on average was slightly lower for α7 nAChR PAM alone and with the agonist and slightly higher than control upon addition of MLA, which would be the predicted change in paired pulse ratio via the activation and antagonism of presynaptic α7 nAChRs.

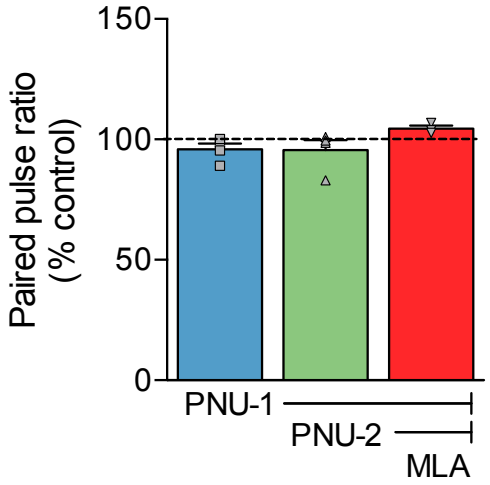

Figure 5.21 Light evoked 50 ms paired pulse ratios EPSC from thalamic afferent fibres in response to α7 nAChR activation and antagonism

*Experiments conducted in mice bilaterally injected in the thalamus with the CAG-ChR2-GFP virus. Voltage clamp recordings were made from layer V pyramidal neurons in the PrL. Neurons were held at -60 mV and light evoked EPSCs were evoked at 0.05 Hz by a 50 ms paired 2 ms blue light pulse. A stable EPSC baseline of at least 10 min was obtained in control aCSF before 10 min bath applications of the α7 nAChR PAM PNU-120596 (10 μM) (PNU-1) alone, the α7 nAChR PAM and agonist PNU-282987 (300 nM) (PNU-2), followed by application of the α7 nAChR PAM, agonist and MLA (100 nM). Paired pulse ratios were calculated by dividing the second pulse by the first and then normalised to the control paired pulse ratio. All data shown as mean ± S.E.M. Significant differences assessed to via one sample t-tests to control * significantly different, p ≤ 0.05 (PNU-1, PNU-2; n = 4, MLA; n = 3)*

5.3 Summary

The aim of this thesis chapter was to investigate in more detail which of the numerous afferent inputs to the PrL might possess presynaptic α7 nAChRs. To achieve this aim a variety of different methodologies were utilised, including the selective pharmacological suppression of thalamic inputs, the selective electrical stimulation of hippocampal afferent fibres, and implementation of optogenetics to selectively express and stimulate excitatory light gated ion-channels within specific afferent inputs to the PrL.

These diverse methodologies had mixed success and a summary of the main findings from this chapter can be found in table 5.1. In general the findings were quite variable and in some cases inconsistent, however some of the findings were interesting. Suppression of thalamic inputs with DAMGO prevented the α7 nAChR PAM mediated increase in sEPSCs that was shown in previous chapters, whilst some data suggest light evoked EPSCs from the thalamus can be enhanced by α7 nAChR activation. This suggests that inputs from the thalamus may be modulated by presynaptic α7 nAChRs. In addition α7 nAChR antagonism increased the paired pulse ratio of contralateral mPFC inputs which may suggest α7 nAChRs also reside on these inputs. For a more detailed discussion of these findings and an evaluation of the experimental limitations in this chapter, see section 6.4.3.

In the next chapter the findings from this chapter and the previous two results chapters will be discussed together in the context of each other and the existing literature.

BLA-mPFC	**Optogenetics** • Very few cells received light evoked responses, which meant contribution of α7 nAChR activation was not assessed.	
mPFC-mPFC	**Optogenetics** • Decrease in EPSC amplitude, but no change in paired pulse ratio upon α7 nAChR activation with α7 nAChR PAM + agonist. • α7 nAChR antagonism significantly increased the paired pulse ratio. *Possible evidence for presynaptic α7 nAChRs on inputs from contralateral mPFC*	
vHip - mPFC	**Electrical stimulation of afferent fibre bundle** • No alteration in EPSC parameters upon α7 nAChR activation or antagonism	**Optogenetics** • EPSC amplitude and rate of rise decreased upon α7 nAChR activation with PAM and agonist • EPSC 10 – 90 % rise time remained unchanged upon α7 nAChR activation or antagonism • Paired pulse ratios remained unchanged upon α7 activation or antagonism.
Thal-mPFC	**μ-opioid receptor suppression of thalamic inputs** • Suppression of thalamic inputs with μ-opioid agonist (DAMGO) reduced sEPSC frequency. • α7 nAChRs PAM in presence of DAMGO failed to increase sEPSC frequency as seen previously. *Evidence for presynaptic α7 nAChRs on thalamic inputs*	**Optogenetics** • No change in EPSC parameters in response to α7 nAChR activation or antagonism • Paired pulse ratios, followed predicted trend but not statistically different. *Preliminary data from Vrije University* • Increase EPSC amplitude upon α7 nAChR activation with PAM + agonist *Evidence for presynaptic α7 nAChRs on thalamic inputs*

Table 5.1 Summary of the major findings within chapter 5

Pharmacologic suppression of thalamic inputs and optogenetic stimulation of afferent inputs suggests that α7 nAChRs may reside on thalamic inputs to the PrL. Alteration in the paired pulse ratio stimulation of afferent inputs from the contralateral mPFC suggest that α7 nAChRs may also reside on afferent inputs from the contralateral mPFC.

Chapter 6:

Discussion

Chapter 6: Discussion

6.1 Introduction

In this chapter the results obtain in chapters 3 - 5 will be discussed and compared to the findings within the literature. Following the discussion of each results chapter the significance and future direction of this research will be discussed ending with an overall conclusion of the research presented in this thesis.

6.2 α7 nAChR regulation of network activity

In the following sections the results obtained in chapter 4 will be discussed. In chapter 4 it was found that α7 nAChRs could modulate increases in both excitatory and inhibitory network activity. Experiments demonstrated that this regulation of network activity is achieved via α7 nAChRs localisation on excitatory glutamatergic nerve terminals and inhibitory interneuron cell bodies. What's more is that endogenous ACh appears to preferentially activate α7 nAChRs that mediate excitatory rather than inhibitory neurotransmission. The next sections will discuss these findings in more detail.

6.2.1 α7 nAChR mediated increases in inhibition

One of the key findings in chapter 4 was that co-application of both the selective α7 nAChR agonist PNU-282987 and the α7 nAChR PAM PNU-120596 led to an increase in frequency of $GABA_A$-mediated synaptic events on layer V pyramidal neurons, suggesting that α7 nAChRs can directly increase the levels of inhibition within the mPFC (Fig. 4.7).

The ability of nAChRs to regulate GABAergic transmission in the prefrontal cortex is reasonably well established in the literature. Studies using nicotine and

ACh to activate all nAChRs within brain slices of the mPFC, have measured increases in sIPSC frequency received by layer V pyramidal neurons attributed to both α7 and α4β2 nAChRs (Couey et al., 2007; Aracri et al., 2010; Poorthuis et al., 2012).

The results in this thesis demonstrate that in the presence of TTX mIPSCs were not enhanced in response to selective α7 nAChR activation suggesting that the increase in GABAergic input to layer V mPFC neurons is not due to α7 nAChRs expressed on the terminals of interneurons (Fig. 4.17). These findings are in agreement with others who demonstrate that TTX abolishes the effects of nicotine or ACh on mPFC inhibition (Couey et al., 2007; Aracri et al., 2010; Poorthuis et al., 2012).

By directly recording from GABAergic interneurons in the PrL, I have also shown that α7 nAChR activation (with co-application of a selective agonist and PAM), leads to direct depolarisation and action potential discharge within the recorded interneurons, providing evidence for α7 nAChRs being postsynaptically expressed likely on the soma (but also potentially on dendrites) of these interneurons (Fig. 4.20). Interestingly I show that, at least in layer V of the PrL, this effect is specific to NFS but not FS interneurons (Fig 4.20, 4.19).

This selective effect on NFS interneurons may come about due to differential expression of α7 nAChRs within certain interneurons. Indeed, Couey et al., (2007) demonstrated, via single cell PCR, that α7 nAChR mRNA was absent in FS interneurons but present in approximately 30% of NFS (RSNP & LTS) interneurons. Further, Gulledge et al., (2007) demonstrated similar findings to this thesis in that FS interneurons do not respond to nAChR activation whilst NFS interneurons do. Other groups have found evidence that FS interneurons may also be regulated by α7 nAChRs (Poorthuis et al., 2012). Here, puff application of ACh to the soma of interneurons within layer V revealed that 53% of FS interneurons and 65% of NFS interneurons possessed fast α7 nAChR mediated currents. The reasons for the discrepancies in findings between Poorthuis et al., and Gulledge et al., are uncertain, both studies directly puff applied ACh to the soma of recorded interneurons however Poorthuis et al.,

applied ACh at 1 mM vs the 100 μM ACh used by Gulledge et al., This may suggest that α7 nAChRs are present on layer V FS interneurons but are only detected upon very high concentrations of agonist, perhaps reflecting a very low level of expression, which might have been below the detectable threshold in this thesis and not picked up by single cell PCR by Couey et al., (2007).

Although data presented in this thesis demonstrates α7 nAChRs located somatodendritically on a subset of GABAergic interneurons, an alternative mechanism by which α7 nAChR activation could increase interneuron activity is via an increase in excitatory (glutamatergic) input onto these interneurons. Indeed, others have shown that nAChR activation can increase sEPSC frequency on GABAergic interneurons in Layer V of mPFC (Alkondon et al., 2000; Couey et al., 2007; Aracri et al., 2010; Arroyo et al., 2012). Couey et al., (2007) demonstrated that nicotine increased the sEPSC frequency onto both FS and LTS interneurons, whilst Aracri et al., (2010) showed that a nicotine mediated increase in sIPSCs in layer V pyramidal neurons could be prevented by removing glutamatergic activity. However, in both of these studies, nicotine was used as a nAChR agonist, rather than selective α7 nAChR ligands. The relative contributions of α7 and α4β2 nAChRs mediating this effect in both studies are unclear, however it may suggest the α7 nAChR mediated increases in inhibition shown in this thesis are glutamate dependent. Experiments in chapter 4 aimed to test this by recording α7 nAChR mediated sIPSCs from layer V pyramidal neurons in the presence of DNQX (Fig. 4.13). Under these conditions the α7 nAChR mediated increase in inhibition was still present, indicating that, in our hands, the α7 nAChR mediated increase GABAergic input was not due to a feedforward mechanism.

Reciprocal inhibition between interneurons has also been reported in response to nAChR activation. In human cortical slices, Alkondon et al., (2000) show that in response to ACh, interneurons receive inhibitory signalling from other interneurons, although this was primarily attributed to effects mediated by α4β2 nAChRs. In addition Arroyo et al., (2012) used optogenetics to evoke endogenous ACh release in mice, and observed that interneurons within the cortex receive direct nAChR mediated currents in the majority of interneuron

subtypes excluding FS interneurons. Interestingly upon ACh release these FS interneurons instead received pronounced disynaptic inhibitory currents via other nAChR expressing interneurons. In this thesis FS interneurons failed to depolarise in response to α7 nAChR activation (Fig. 4.19), potentially due to differences in α7 nAChRs expression. This differential nAChR sensitivity of interneurons might therefore provide a potential mechanism by which α7 nAChR activation could bring about both inhibition and disinhibition of pyramidal neurons.

In my experiments, no direct α7 nAChR-mediated effects was seen in FS interneurons within layer V of the mPFC. As noted above, this could either be because this subtype of interneuron does no express α7 nAChRs or that they are present but in very low levels. Alternatively, it is interesting to speculate that FS interneurons do possess α7 nAChRs and the lack of α7 nAChR–mediated depolarisation shown in these experiments may be due to simultaneous lateral inhibition from other interneurons that do express α7 nAChRs. To test this, experiments could be conducted whereby both sEPSCs and sIPSCs are recorded from different inhibitory interneurons in response to α7 nAChR activation and inhibition, to observe evidence of α7 nAChR mediated reciprocal inhibition or feedforward excitation of interneurons.

6.2.2 α7 nAChR mediated increases in excitation

Increased GABAergic input to layer V pyramidal neurons in the PrL was only seen following combined bath-application of both a selective α7 nAChR agonist and α7 nAChR PAM, application of α7 nAChR PAM alone was without effect (Fig. 4.7). In direct contrast, glutamatergic input to layer V pyramidal neurons in the PrL was enhanced upon application of a selective α7 nAChR PAM alone (Fig. 4.2). This suggests that the PAM acts to potentiate the endogenous actions of ACh on glutamatergic inputs. The effect of the PAM was to increase the frequency of both spontaneous and miniature EPSCs (Fig. 4.2 and 4.22), suggesting that the presynaptic nerve terminal is the locus of this effect.

α7 nAChR currents have the ability to directly depolarise neurons and possess a relatively high permeability to calcium, these attributes enable α7 nAChRs to partake in the cell signalling required to induce presynaptic neurotransmitter release. In numerous brain regions including the hippocampus (Gray et al., 1996; Sharma et al., 2008; Cheng & Yakel, 2014), VTA (I. W. Jones & Wonnacott, 2004; Good & Lupica, 2009; Garzón et al., 2013) and striatum (Kaiser & Wonnacott, 2000; Marchi et al., 2002) α7 nAChRs have been assigned a role for mediating presynaptic glutamate release. However evidence for their involvement in presynaptic release in the mPFC is less clear. Synaptosome studies indicate that α7 nAChR activation with selective agonists, and potentiation with a positive allosteric modulator can increase glutamate release, (B.-W. Wang et al., 2006; Dickinson et al., 2008; Livingstone, Dickinson, et al., 2009), whilst electron microscopy suggest that α7 nAChRs may be expressed at presynaptic terminals in the guinea pig PFC (Lubin et al., 1999). More direct *in vivo* measurements in combination with local infusions of α7 nAChR selective agonists and antagonists reveal that α7 nAChRs can transiently increase the levels of glutamate in the rat mPFC (Konradsson-Geuken et al., 2009; Bortz et al., 2013).

Presynaptic α7 nAChRs have the potential to increase glutamate release via multiple intracellular mechanisms, all of which rely on increases in presynaptic calcium. The direct influx of calcium though the α7 nAChR itself is thought to be needed for the enhancement of transmitter release (Sharma & Vijayaraghavan, 2003; Sharma et al., 2008) but alone is insufficient and requires additional calcium induced calcium release from internal calcium stores (Sharma & Vijayaraghavan, 2003; Dickinson et al., 2008; Cheng & Yakel, 2014). Whereas some studies show that the direct depolarising current upon α7 nAChR activation is also coupled to activation of VGCCs (B.-W. Wang et al., 2006; del Barrio et al., 2011), although this is still unclear (Gray et al., 1996; Dickinson et al., 2008). Regardless of its source, activation of presynaptic α7 nAChRs results in elevations of presynaptic calcium, which is shown to mediate transmitter release. This enhanced calcium is thought to bring about transmitter release via activation of multiple signalling molecules including PKA and CAMKII and the phosphorylation of other key molecules ERK2 and Synapsin

(B.-W. Wang et al., 2006; Dickinson et al., 2008; Sharma et al., 2008; Cheng & Yakel, 2014). In this work we show that the α7 nAChR PAM PNU-120596 enhances the frequency of spontaneous and miniature EPSCs (Fig. 4.2 and 4.22), however, the downstream signalling mechanism of how this was achieved was not investigated.

6.2.3 Why have presynaptic α7 nAChRs in the mPFC not previously been observed using electrophysiology?

Although evidence for α7 nAChRs regulating presynaptic glutamate release in the mPFC exists in the form of synaptosome and *in vivo* studies, previous *in vitro* electrophysiology studies investigating the role of nAChRs in regulating glutamate release have failed to find evidence for presynaptic α7 nAChR (Lambe et al., 2003; Poorthuis et al., 2012; Aracri et al., 2013), reasons for this are unclear. Lambe et al., (2003) demonstrate that nicotine (10 μM) can increase the frequency of sEPSCs to layer V neurons an effect that is sensitive to TTX and absent in β2 KO mice. They found this effect was not seen upon 30 sec rapid bath application of the selective α7 nAChR agonist choline, and the nicotine induced increase in sEPSC frequency was inhibited by the selective α4β2 antagonist, DhβE, suggesting that α4β2 have a role in glutamate release. Couey et al., (2007) replicated these experiments and found a TTX and mecamylamine (non-selective nAChR antagonist) sensitive increase in sEPSC frequency upon bath application of nicotine (10 μM), but did not test if this effect was mediated by α4β2 or α7 nAChRs. Whilst, Poorthius et al., (2012) found similar observations using ACh (1 mM) as an agonist, seeing an increase in glutamate release that was also blocked by TTX and absent in β2 KO mice. Although these studies clearly demonstrate a role for α4β2 nAChRs in regulating glutamate release, the direct contribution of α7 nAChRs to regulating glutamate release has not been directly tested either pharmacologically or with α7 nAChR KO mice. This could suggest an α7 nAChR mediated increase in glutamate release may have been masked by the predominant α4β2 nAChR

mediated effect on glutamate release or that α7 nAChRs have been inadvertently desensitised due to bath application of agonists.

6.2.4 Do α7 nAChRs desensitise upon bath application of agonists?

Other research groups have been unsuccessful in finding electrophysiological evidence for an α7 nAChR dependent enhancement of glutamate release in the mPFC, which might be explained by the pharmacological approach used to probe the receptor. Studies by others, mentioned in the previous section have bath applied non-selective nAChR agonists, ACh and nicotine and have failed to provide evidence for an α7 nAChR mediated glutamate increase. In this thesis the selective α7 nAChR agonist PNU-282987 alone, was also bath applied and failed to increase the frequency of spontaneous EPSCs (Fig. 4.10). A possible explanation for this lack of effect could be due to the desensitisation of the α7 nAChRs in response to agonist application. α7 nAChRs studied *in vitro* characteristically possess fast transient currents, mediated by the fast opening and rapid desensitisation of the receptor in response to high concentrations of agonist (Papke & Thinschmidt, 1998; Papke & Porter Papke, 2002). Whether this rapid desensitisation of nAChRs is prolonged throughout the duration of bath application of agonists in the mPFC is not clear. In hippocampal brain slices a short (4 sec) application of a high concentration of ACh (40 μM) rendered α7 nAChR unresponsive to an additional 'test-pulse' of choline (Mike et al., 2000). Whilst nicotine (1 μM) bath applied to hippocampal brain slices has been shown to desensitise α7 nAChRs involved in synaptic plasticity induction (Yamazaki et al., 2005). In contrast in the VTA, prolonged bath application of nicotine (250 nM) does not desensitise α7 nAChRs on glutamatergic terminals nor does nicotine (300 nM) at α7 nAChRs on dopaminergic neurons (Mansvelder et al., 2002; Wooltorton et al., 2003). In the mPFC α7 nAChR mediated currents induced by puff-application of ACh were also not desensitised to prolonged bath application of nicotine (100 nM), in pyramidal and interneurons across all mPFC layers (Poorthuis et al., 2013). This suggests that α7 nAChRs have the potential to desensitise in response to

bath application of agonists, but this may not be the same in all brain regions. It should be noted that in the studies that have failed to observe α7 nAChR desensitisation have used 'smoking concentrations' of nicotine (100 – 300 nM). These concentrations are lower than the ACh (~ 1 mM) and nicotine (~10 μM) concentrations typically used to studied nAChR mediated network effects (see previous section). It is therefore still unclear if α7 nAChRs desensitise to these higher agonist concentrations in the mPFC. In addition it is still not clear to what degree α7 nAChRs desensitise to the bath applied agonist PNU-282987 (300 nM) used in this thesis. If rapid desensitization of α7 nAChRs did occur with 300 nM PNU-282987, this would provide an explanation for the lack of affect α7 nAChRs exert on sEPSC and sIPSC activity in the absence of the α7 nAChR PAM (Fig. 4.10).

An interesting observation that questions α7 nAChRs desensitisation to agonist application was made whilst recording from NFS interneurons, here upon application of PNU-282987 alone step like depolarisations were observed (Fig. 4.21). These voltage steps, also observed by others in the hippocampus (Kalappa et al., 2010; Uteshev, 2012a), are thought to be direct single α7 nAChR currents, which surprisingly are able to be measured via whole-cell patch clamp (Uteshev, 2012b). Although this may suggest that in the presence of the α7 nAChR agonist that α7 nAChRs are not desensitised, an interesting observation was that upon reversal of desensitisation by the addition of the α7 nAChR PAM, the depolarisation steps seemingly increased in number and amplitude and a pronounced change in membrane potential and action potential firing was observed. This could suggest that the depolarisation steps upon addition of the α7 nAChR agonist alone, represent the agonist binding to the α7 nAChRs and causing them to cycle through a closed-open-desensitised-closed state (see section 1.4.4). Presumably addition of the α7 nAChR PAM by reversing and preventing receptor desensitisation allows the receptors to cycle through a closed-open-closed state, resulting in a higher number of activated (non-desensitised) α7 nAChRs, leading to the pronounced membrane depolarisation and action potential discharge. If this is true this might indicate that the α7 nAChRs agonist PNU-282987 applied alone at 300 nM causes the α7 nAChR to desensitise. It would be interesting to investigate this further by

altering the PNU-282987 concentration to observe if this is a concentration dependent mechanism.

6.2.5 α7 nAChR PAM and agonist co-application has a dual effect on inhibition and excitation

PNU-120596 and PNU-282987 co-application led to an increase in interneuron activity leading to increased inhibition of layer V pyramidal neurons (Fig 4.7). However in the same cells, this increase in inhibition also appeared to reverse the increased in sEPSC frequency achieved via the α7 nAChR PAM alone (Fig. 4.2). One explanation for this may be that excitatory inputs onto layer V pyramidal neurons are sensitive to enhanced interneuron activity, perhaps due to expression of presynaptic $GABA_B$ receptors on glutamatergic terminals. Activation of presynaptic $GABA_B$ receptors can decrease transmitter release via inhibition of calcium channels (Sakaba & Neher, 2003). In the mPFC $GABA_B$ receptors have been shown to regulate transmitter release onto layer II/III pyramidal neurons (Y. Wang et al., 2010). However their contribution to regulating glutamate release onto layer V pyramidal neurons is unclear. An alternative explanation for the decrease in excitation upon co-application of PNU-120596 and PNU-282987 is that the enhanced inhibitory interneuron activity led to a suppression of action potential firing of nearby pyramidal neurons, in turn synapsing onto the recorded layer V neuron and thus causing an overall decrease in synaptic glutamate release.

It should be noted that in these experiments PNU-120596 and PNU-282987 were not co-applied directly to the brain slice but were only applied together after PNU-120596 had been applied alone. It is therefore unclear if PNU-120596 and PNU-282987 co-application is able to cause an independent decrease in basal excitation. These experiments should be conducted and additional experiments in which $GABA_B$ antagonists are utilised could be used to further investigate a possible presynaptic inhibitory mechanism.

Additional experiments were conducted however to investigate if the effect on excitation with the α7 nAChR PAM and the agonist was dependent on the enhanced inhibition. Upon eliminating the effects of postsynaptic α7 nAChRs on inhibitory interneurons by addition of TTX (Fig. 4.23), application of the PAM and agonist led to an increase in the mEPSC frequency compared to control. These findings show that the α7 nAChRs PAM and agonist co-application is capable of increasing the level of presynaptic glutamate release, but under an intact network this effect is balanced out / reduced by the predominant increase in inhibition.

6.2.6 Endogenous tonic ACh favours the activation of excitation rather than inhibition

The ability of the α7 nAChR PAM alone to increase glutamatergic input to layer V PrL pyramidal neurons indicates that tonic endogenous ACh release within the brain slice has the capacity to increase glutamate release within the PrL, an effect potentiated by enhancing endogenous ACh with the acetylcholinesterase inhibitor, donepezil (Fig. 4.24B). Contrastingly, tonic ACh release appears to have little effect on inhibitory signalling. The PAM alone failed to increase the frequency of sIPSCs onto pyramidal neurons even upon enhanced endogenous ACh (using donepezil) (Fig. 4.24C), and during interneuron recording there was no evidence of α7 nAChR mediated changes in membrane potential or depolarisation steps in the presence of the PAM alone (Fig. 4.19B, 4.20B). These differential effects suggest that α7 nAChRs controlling excitation and inhibition may be exposed to distinct types of acetylcholine signalling.

Interestingly, inhibiting the actions of tonic ACh release at α7 nAChRs with the α7 nAChR antagonist MLA revealed only a slight decrease in sEPSC frequency that was not deemed statistically significant (Fig. 4.5A). This suggests that within the acute brain slice, the low level of tonic ACh activates only a small number of α7 nAChRs, which produces only a small effect on excitation. Addition of the α7 nAChR PAM in contrast significantly increased sEPSC frequency. As the PAM increases peak current and mean open time of the

receptor, the addition of the α7 nAChR PAM might lower the threshold for endogenous ACh to elicit α7 nAChR mediated transmitter release.

To overcome the low level of tonic ACh within the slice donepezil was applied, however, donepezil alone failed to increase the sEPSC frequency from control (Fig. 4.24A). These findings might indicate donepezil at the concentration used here (10μM) only resulted in a small increase in endogenous, tonic, ACh. However, studies by others in the hippocampal brain slice showed that donepezil, applied at a lower concentration (100 nM), was sufficient to increase sEPSC activity onto CA1 interneurons with an effect after 5 min application but a peak effect after a 20 min donepezil application (Alkondon et al., 2013). This may suggest, in these mPFC experiments, an effect of donepezil alone may have been revealed by a prolonged application, instead of the 5 min application used here.

6.2.7 Do diverse ACh release mechanisms explain the differential effects on excitation and inhibition?

The bi-directional effect of α7 nAChR signalling on excitation and inhibition suggests that tonic ACh release seemingly favours α7 nAChR mediated excitation (Fig. 6.1), indicating that the spatial and temporal dynamics in which ACh signals within the mPFC is important in network regulation. The major source of acetylcholine within the mPFC is from cholinergic afferents originating from the basal forebrain. These fibres are distributed throughout the cortical layers of the mPFC with prominent innervation in the deepest (layer V and VI) and most superficial (layer I) layers, with less innervation in layer III (Bloem, Schoppink, et al., 2014). These cholinergic fibres rarely form synapses within the cortex, and primarily mediate acetylcholine release through varicosities (Lendvai & Vizi, 2008). This varicose cholinergic innervation, has led to the notion that ACh is primarily released via volume diffuse transmission, however *in vivo* studies have demonstrated that ACh is released via phasic transients of ACh (Parikh et al., 2007), that are critical for attention and cue detection (Gritton et al., 2016). In addition, optogenetically evoked acetylcholine within brain slices

activates cortical inhibitory interneurons via synaptic and non-synaptic signalling (Bennett et al., 2012), suggesting ACh signalling is diverse acting via both volume and synaptic mechanisms in the cortex. This diverse ACh signalling may explain the different effects of endogenous ACh signalling acting on excitation and inhibition in this thesis.

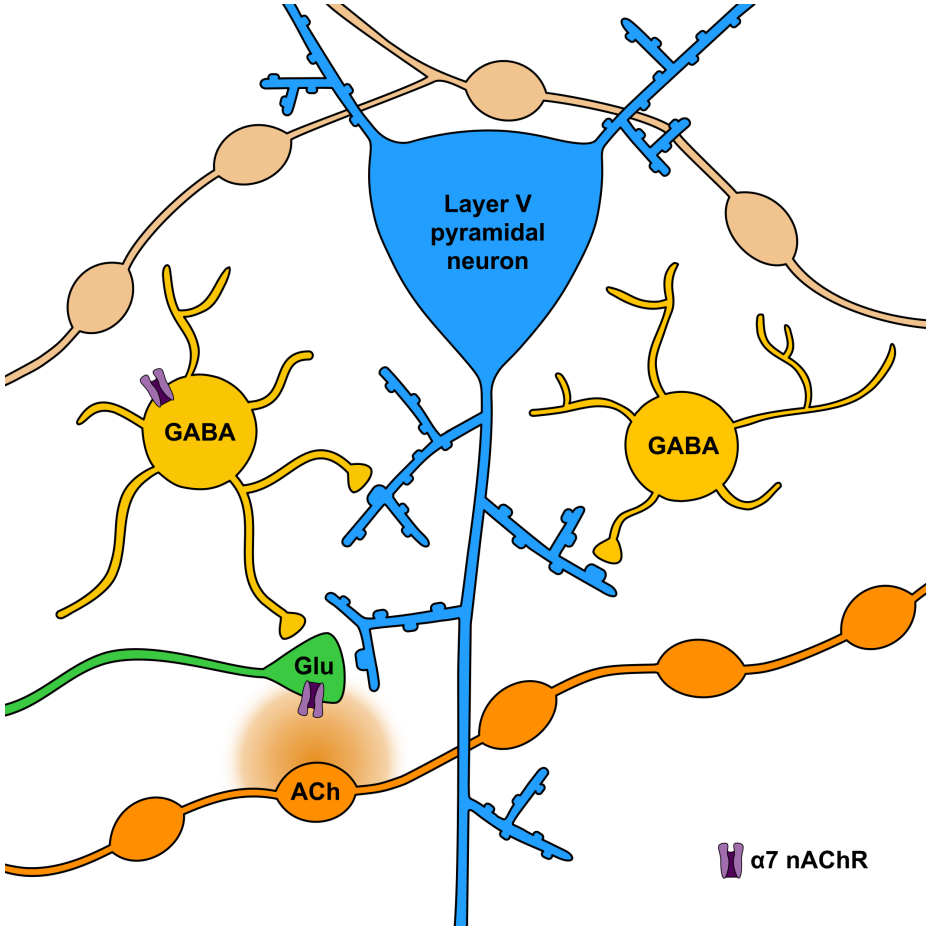

Figure 6.1 Location of α7 nAChRs in relation to tonic ACh release

α7 nAChRs are found somatodendritically on GABAergic inhibitory interneurons and presynaptically on glutamatergic inputs. Endogenous ACh seemingly targets presynaptic α7 nAChRs perhaps due to the proximity of tonically releasing ACh varicosities to presynaptic α7 nAChRs.

Different modes of acetylcholine release

Although direct synaptic contacts between cholinergic inputs and neurons within in the cortex are rare (Aracri et al., 2010; Descarries et al., 1997), evidence suggests that at least some interneurons can receive direct synaptic connections from cholinergic fibres (Henny & B. E. Jones, 2008; Bennett et al.,

2012). In contrast the extra-synaptic location of presynaptic α7 nAChRs suggests that these receptors do not form direct synapses, as axonal-terminal synapses are rare. Perhaps the difference in excitation and inhibition modulation in response the α7 nAChR PAM in the current study represents a difference in distinct signalling modes, in which α7 nAChR mediated activation of inhibitory interneurons is activity dependent, through active synapses, whereas spontaneous tonic acetylcholine has a more neuromodulatory effect at presynaptic α7 nAChRs controlling excitation, via a more diffuse volume transmission.

Differences between the location of ACh release sites and α7 nAChRs

Another factor that may explain why tonic ACh doesn't appear to activate α7 nAChRs on inhibitory interneurons, could be explained by the distance between the tonically releasing ACh varicosity and the α7 nAChRs on the interneurons (Fig. 6.1). If they are spatially separated, tonically released ACh may not be within the vicinity of the α7 nAChRs to activate the inhibitory interneuron. This could suggest that to activate α7 nAChR containing interneurons requires a more substantial ACh release to overcome this spatial difference, perhaps via phasic ACh release. In the rat mPFC, *in vivo* microdialysis shows that phasic ACh release (evoked by K+) results in an ACh concentration up to 5 μM, which is a 5 fold increase compared to the measured 1 μM tonic ACh (Mattinson et al., 2011). This high ACh concentration increase may be sufficient to overcome any spatial separation between the release site and the α7 nAChRs on the interneuron. Indeed optogenetic studies in which phasic acetylcholine is evoked has demonstrated that the large rises in ACh is sufficient to activate inhibitory interneurons (Arroyo et al., 2012), although this might be mediated by direct ACh synapses onto interneurons. Differences in the locations of the α7 nAChRs controlling excitation and inhibition to the ACh release sites, might suggest that inhibitory interneurons are only engaged upon very high levels of ACh signalling, which might be a mechanism by which these interneurons regulate the cortical network.

Cholinergic interneurons as a source of ACh

In addition to ACh innervation from the basal forebrain, the mPFC receives a local source of ACh release from cholinergic interneurons (Engelhardt et al., 2007). These interneurons are typically bipolar and are mainly located in superficial cortical layers (Eckenstein & Thoenen, 1983) and, although quite sparse, they possess axonal processes that innervate multiple cortical layers (Engelhardt et al., 2007). It has been shown that cholinergic interneurons within the neocortex receive direct synaptic connections from both pyramidal neurons and inhibitory interneurons indicating that their activity is regulated by the cortical circuitry. Cholinergic interneurons do not reciprocate this connectivity and do not themselves form synapses onto pyramidal or inhibitory interneurons. Interestingly however, cholinergic interneuron activity does increase the frequency of sEPSCs, but not sIPSCs, onto pyramidal neurons; an effect that is nAChR-dependent and thought to be mediated via presynaptic nAChRs (Engelhardt et al., 2007). These findings provide an interesting theory for the work in this thesis. It could be speculated that presynaptic α7 nAChRs on excitatory glutamatergic terminals receive a unique source of ACh from cholinergic interneurons that regulates transmitter release, whilst α7 nAChRs on inhibitory interneurons are activated by a different source of ACh, perhaps from afferent fibre input from the basal forebrain. If cholinergic interneurons partake in this mode of modulation in the PrL is not clear. A potential experiment to test this would be to use a transgenic mouse line such as ChAT-GFP mice to fluorescently identify local cholinergic interneurons within the PrL, and use dual patch clamp recordings of pyramidal neurons and cholinergic interneurons and record sEPSCs/mEPSCs in pyramidal neurons whilst stimulating the release of ACh from cholinergic interneurons.

Different sensitivities of terminals and interneurons to the activation of α7 nAChRs

The different effects on inhibition and excitation with endogenous ACh signalling might also be explained by the relative differences in sensitivity of the excitatory terminals and interneurons to the activation of α7 nAChRs. α7 nAChRs on presynaptic terminals can directly interact with neurotransmitter

release mechanisms. This can be achieved by directly contributing to presynaptic calcium levels or by providing a depolarising current to indirectly increase presynaptic calcium. In the presence of the α7 nAChR PAM, which increases the peak current and average open time of the channel (Hurst et al., 2005), both of these effects on transmitter release are likely to be pronounced. In contrast, for an increase in sIPSC activity to be observed, interneurons are required to be depolarised sufficiently to induce action potential firing and thus transmitter release. Therefore, the threshold for the level of α7 nAChR activation needed to induce spontaneous transmitter release may be lower for presynaptic terminals than it is for an interneuron. If this were the case, even if the levels of endogenous ACh acting at terminal α7 nAChRs and α7 nAChRs on interneurons were equal, it would be expected that the α7 nAChR PAM would have a more influential effect at altering terminal depolarisation and transmitter release than full depolarisation of an interneuron. Experiments in this thesis aimed to investigate this possibility. When recording from interneurons, the α7 nAChR PAM didn't alter the resting membrane potential or lead to step-like α7 nAChR depolarisations (Fig. 4.19, 4.20). If any tonic endogenous ACh was acting at these receptors we may expect to see at least a small change in the membrane potential or some evidence of α7 nAChR activation in the presence of the α7 nAChR PAM, which suggests the endogenous levels of ACh in the vicinity of the interneurons is below the threshold for α7 nAChR activation. This is a different pattern to that seen in the CA1 region of the hippocampus, where a different (type I) α7 nAChR PAM, 5-HI, administered alone to hippocampal slices was sufficient to cause CA1 inhibitory interneuron action potential firing and GABA release resulting in an increase in sIPSC frequency and amplitude to nearby neurons (Mok & Kew, 2006).

6.2.8 α7 nAChRs modulate evoked excitatory neurotransmission

Experiments in which EPSCs were generated via electrical stimulation of layer II/III afferent fibres provided contrasting findings to experiments observing

spontaneous activity. α7 nAChR antagonism with MLA, resulted in a reduction in the amplitude of evoked EPSCs (Fig. 4.25), coinciding with an increased paired pulse ratio (Fig. 4.26), suggesting that α7 nAChRs exert on going, tonic, regulation of evoked glutamate release, by a presynaptic mode of action. This finding was in contrast with experiments investigating spontaneous EPSCs (discussed above), where MLA alone, caused only a slight decrease in sEPSC frequency, that was not deemed statistically significant (Fig 4.5A). In addition α7 nAChR PAM, which enhanced sEPSC activity, had no effect at modulating evoked EPSCs (Fig 4.25). As the effects of positive allosteric modulation and antagonism rely on endogenous ACh signalling, these findings point to differences in the ability of endogenous ACh to regulate spontaneous vs. evoked transmitter release. Several potential mechanisms for this are discussed below.

Evoked transmission enhances the levels of endogenous ACh

As previously discussed, one potential reason for why MLA had a minimal effect on sEPSC frequency is that low levels of ACh are present within the acute brain slice. During evoked EPSC experiments the levels of endogenous ACh might be higher, and might explain why MLA had a more pronounced effect on evoked transmission. Indeed evoked stimulation of afferent inputs is shown to elevate the levels of choline within the visual cortex brain slice; Lucas-Meunier et al., (2009) found that upon electrical stimulation of layer II fibres (at 0.05 Hz) the choline concentration increased two-fold compared to tonic choline levels measured via chemoluminescence. Choline levels were further enhanced upon a theta burst stimulation, similar to the one used in this thesis in chapter 3. Therefore, it could be speculated that upon electrical stimulation the levels of endogenous ACh are raised to a level sufficient to activate α7 nAChRs and enhance glutamate release, which can be subsequently blocked by MLA. This elevated ACh upon electrical stimulation might also explain why PNU-120596 had no effect at enhancing evoked transmission (Fig. 4.25), as under elevated ACh α7 nAChRs on terminals may be sufficiently activated to induce a maximal effect on transmitter release, where further positive allosteric modulation has little effect.

Presynaptic α7 nAChR activity dependent on the threshold for transmitter release

Evoked glutamate release is dependent on action potentials reaching the presynaptic terminal leading to a large presynaptic depolarisation and subsequent high levels of presynaptic calcium through VGCC. Endogenous ACh, which is also evoked during electrical stimulation, can also open α7 nAChRs to provide additional presynaptic calcium. A potential reason why the α7 nAChR PAM fails to increase the levels of transmitter release could be that the level of presynaptic calcium under the mentioned condition is already above a maximal threshold, and so additional calcium or depolarisation upon addition of the PAM has little added effect. However during electrical stimulation upon removing the added presynaptic calcium provided by endogenously activated α7 nAChRs (with the antagonist MLA), the calcium levels may be reduced enough so they are below a release threshold and thus reduce transmitter release as seen in figure 4.25.

The opposite might be true for spontaneous release in which the levels of presynaptic calcium are likely to be lower and perhaps below a release threshold. Under these conditions antagonising α7 nAChRs will remove calcium from presynaptic terminals that are already below a release threshold and therefore little effect on spontaneous release is observed as seen in figure 4.5. Conversely addition of the α7 nAChR PAM during spontaneous release can increase the presynaptic depolarisation and calcium above the firing threshold and thus get an increase in spontaneous transmitter release (Fig. 4.2).

This might suggest that the α7 nAChRs ability to modulate presynaptic release in the PrL is dependent on the synapses basal level of activation and probability of release. To test this hypothesis the levels of extracellular calcium within the bath aCSF could to increased to give an overall increase in probability of release, under these conditions it may be expected that MLA could reduce spontaneous transmitter release, and perhaps α7 nAChR positive allosteric modulation have a diminished effect.

Could the effects of MLA be mediated via inhibition of interneurons?

Although the likely explanation for the reduction in evoked glutamate release in response to MLA application is by inhibition of α7 nAChRs located at glutamatergic nerve terminals, an alternative hypothesis remains in which MLA may reduce glutamate release via an indirect mechanism dependent on inhibitory interneurons. As seen in figure 4.20, NFS interneurons have been shown to be sensitive to α7 nAChR activation, and, as discussed in section 6.2.1, these interneurons may play a part in inhibiting other interneurons that subsequently inhibit pyramidal neurons or glutamatergic afferent inputs to pyramidal neurons. Under the conditions of electrical stimulation, the elevated ACh levels might enhance this lateral inhibition pathway by activating interneurons. In turn, addition of MLA would reduce the lateral inhibition of interneurons, this disinhibtion of interneurons would then consequently lead to increased inhibitory drive onto glutamatergic afferents, resulting in a reduction in the evoked EPSC amplitude and enhanced EPSC paired pulse ratio observed upon addition of MLA (Fig. 4.25, 4.26). A simple experiment to test this rather complicated scenario would be to inhibit interneuron activity with a GABA receptor antagonist to isolate direct and indirect effects. These experiments were attempted, however, removing inhibition within the PrL network as see in section 4.2.3 leads to recurrent network activity, and upon electrical stimulation this led to macroscopic glutamatergic currents, which made the experiment not possible.

α7 nAChR PAM + agonist reduces evoked glutamate transmission

Whilst MLA reduced evoked excitatory transmission, activating α7 nAChRs with a combination of α7 nAChR PAM and agonist also resulted in a decrease in evoked glutamate release (Fig. 4.25). Previous experiments demonstration that this same drug combination increases the overall level of network inhibition (Fig. 4.7), which might suggest that the decrease in evoked EPSCs upon addition of the α7 nAChR PAM and agonist is caused by increased inhibition. Interestingly the α7 nAChR PAM and agonist also reduced the spontaneous release of glutamate (Fig. 4.2), which is consistent with the reduction in evoked glutamate. As previously suggested, the decrease in sEPSC activity seen upon addition of

the α7 nAChR PAM and agonist may be mediated via presynaptic $GABA_B$ receptors. This mechanism may also explain the decrease in evoked EPSC magnitude. However, in considering this it is surprising that the α7 nAChR PAM and agonist did not affect the paired pulse ratio (Fig. 4.26), which may be expected upon activation of a presynaptic $GABA_B$ receptor. This perhaps indicates an alternative unknown synaptic mechanism.

Evoked EPSC experiments were conducted to help better understand how evoked neurotransmitters is modulated by α7 nAChR modulation to help form a potential mechanism by which stimulus-induced synaptic plasticity is modulated by α7 nAChR activity, these potential mechanism and the findings of chapter 3 are discussed in the next section.

6.3 α7 nAChR mediated modulation of synaptic plasticity

Initial experiments in this thesis aimed to investigate the potential for α7 nAChRs to partake in stimulus-induced plasticity, subsequent experiments that were discussed above have hopefully provided insight into the possible mechanisms by which α7 nAChR activity can mediated PrL synaptic plasticity.

6.3.1 Induction of LTP and LTD within the prelimbic cortex

Before investigating α7 nAChRs contribution to PrL plasticity, initial experiments were conducted to optimise a field recording protocol to induce synaptic plasticity within the PrL. Theta burst stimulation applied to layer II/III fibres within the PrL led to a stable stimulus-induced LTP dependent on the number of theta burst repeats (Fig. 3.2B). The majority of stimulus-induced plasticity mechanisms are attributed to being NMDAR dependent, however other NMDAR independent mechanisms of stimulus-induced plasticity are possible (section 1.3.3). The NMDAR antagonist D-AP5 reduced the stimulus-induced plasticity indicating the resulting LTP was at least partly dependent on NMDAR activation

(Fig. 3.2C). Interestingly, however, a small (no significant) residual potentiation appeared to remain, although this may be due to incomplete NMDAR blockade, it may indicate an additional NMDAR independent plasticity is induced. Similar findings were shown by others where D-AP5 failed to completely block the level of stimulus-induced LTP within the mPFC (Y. Y. Huang et al., 2004). The identity of this possible residual plasticity was not investigated in this thesis but could provide invaluable information about a potential mechanism by which α7 nAChRs may modulate plasticity.

In addition to LTP, LTD was also investigated. A 3 Hz low frequency stimulation did not induce pronounced LTD but did provide a sub threshold stimulation with which modulation of LTD induction by α7 nAChR agents could be studied (Fig. 3.3). Other stimulation protocols were not investigated, so it is not possible to determine if 3 Hz stimulation was “too strong” or “too weak” for inducing stable LTD without additional pharmacological modulation. The induction of LTD is also often dependent on NMDAR activation and activation of CaMKII. The failure of a 3 Hz stimulation may thus be due to inadequate NMDAR activation, however the converse could also be true. Over expression of CaMKII within the mPFC has been shown to reduce the levels of LTD, which may explain the lack of LTD seen in this thesis (Ma et al., 2015). Interestingly Ma et al., (2015) reliably induced LTD with a 1 Hz LFS, perhaps suggesting that a 3 Hz stimulation is “too strong”. Although NMDAR dependent LTD is a common form of synaptic plasticity it is not the only mechanism of LTD induction in the mPFC (as discussed in section 1.3.3). As the pharmacology of LTD was not investigated in this thesis the potential mechanisms by which α7 nAChRs may modulate plasticity are not fully elucidated and should be further investigated.

6.3.2 α7 nAChR modulation of mPFC LTP through direct excitatory mechanisms

Various studies have demonstrated that systemic administration of nicotine in both mice and rats can affect synaptic plasticity in the mPFC (Brunzell et al., 2003; Goriounova & Mansvelder, 2012b; Schochet et al., 2005). However few

studies have investigated the mechanisms by which nicotinic receptor activation within the mPFC can modulate mPFC synaptic plasticity. The results of this thesis add to the literature by demonstrating that α7 nAChRs in the PrL play a role in modulating synaptic plasticity in the mPFC. Experiments shown in chapter 3, reveal that the α7 nAChR antagonist MLA and α-bungarotoxin can reduce stimulus-induced LTP within layer V of the PrL (Fig. 3.4). Modulation of LTP is mostly attributed to alterations in postsynaptic calcium signals within the dendritic spines (Koester & Sakmann, 1998; Sjöström & Nelson, 2002; Magee & Johnston, 1997), with increases in intracellular calcium levels mediated by multiple mechanisms including but not limited to, increases in signalling through NMDARs and GluA2-lacking AMPARs, VGCC, mGluR activation and calcium induced calcium release. Elevations in postsynaptic calcium signalling are also dependent on the amount of neurotransmitter release and subsequent postsynaptic depolarisation, meaning post synaptic plasticity can be limited if the level of glutamate release is reduced (Mansvelder & McGehee, 2000). The experiments in chapter 4 have shown that α7 nAChR antagonism can significantly reduce the magnitude of evoked glutamatergic EPSCs onto layer V pyramidal neurons (Fig. 4.25), furthermore this reduction in EPSC magnitude also co-insides with a decreased probability of glutamate release (Fig. 4.26), suggesting that MLA, acting at presynaptic α7 nAChRs may reduce the levels of glutamate release upon stimulation of layer II/III fibres. It is interesting to speculate that this decrease in transmitter may be the cause of the reduction in LTP upon α7 nAChR antagonism.

Although data presented here are the first to show this role of α7 nAChRs in modulating LTP within the mPFC, similar effects have been seen in other brain regions. In the VTA, nicotine enhances LTP in dopaminergic neurons, an effect attributed to enhanced glutamate release upon nicotine activating presynaptic α7 nAChRs (Mansvelder & McGehee, 2000). Similarly, in the hippocampus presynaptic α7 nAChRs can alter the levels of LTP by enhancing glutamate release at CA1 and CA3 pyramidal neurons (Ji et al., 2001; Gu et al., 2012; Sharma et al., 2008; Kroker et al., 2011; Cheng & Yakel, 2014). Interestingly, postsynaptic α7 nAChRs can also modulate plasticity in the hippocampus (Ji et al., 2001; Gu et al., 2012). These postsynaptic α7 nAChRs contribute to the

dendritic intracellular calcium levels, but require the simultaneous activation of NMDARs to induce LTP. Postsynaptic α7 nAChRs can also modulate an mGluR dependent form of plasticity in the hippocampus (Welsby et al., 2006). A possibility arises of course that the reduction in LTP upon antagonism of α7 nAChRs may be dependent on both pre and post synaptic expression of α7 nAChRs on excitatory neurons. Such a mechanism was shown by (Gu et al., 2012) in an elegant study where they selectively inserted α7 nAChRs into the CA3 and then CA1 regions, of cultured hippocampal slices from α7 nAChR knock out mice. This selective expression of α7 nAChRs enabled the authors to investigate pre and then post synaptic α7 nAChRs independently at the CA3-CA1 synapse, and their modulatory effect on LTP in response to optogenetically released acetylcholine. They found that both pre and post synaptic α7 nAChRs co-ordinated the magnitude and direction of plasticity, which depended on the timing of cholinergic and Schaffer collateral inputs.

However, as discussed previously the location of post synaptic α7 nAChRs on layer V pyramidal neurons is unclear and, in my experiments, there was no evidence for their postsynaptic expression. Therefore, it is unlikely that inhibition of postsynaptic α7 nAChRs is the mechanism underlying modulation of LTP by MLA in these experiments.

6.3.3 α7 nAChR modulation of mPFC LTP through modulation of inhibitory signalling

In this thesis it was shown that that activation of α7 nAChRs with a combination of selective agonist and positive allosteric modulator caused a reduction in stimulus-induced LTP (Fig. 3.7A). On one level it is hard to explain how both blockade (with MLA) and activation (with a combination of PAM and agonist) of α7 nAChRs can both lead to the same effect: inhibition of stimulus-induced LTP. However, as previously discussed, the combination of α7 nAChR PAM and agonist led to activation of layer V inhibitory interneurons and subsequent inhibition of layer V pyramidal neurons (Fig. 4.20 and 4.7). This therefore

suggests that α7 nAChR induced activity of inhibitory interneurons can influence the formation and expression of LTP within layer V of the PrL.

Similar mechanisms have been shown in both the hippocampus and mPFC. Within the hippocampus ACh administered directly to interneurons acts at nAChRs to enhance inhibition to pyramidal neurons, which in turn inhibits the formation of stimulus evoked LTP, although the contribution via α7 nAChRs was not tested (Ji et al., 2001). In the mPFC, Couey et al., (2007) show that nicotine can alter the polarity of spike-timing-dependent plasticity in layer V pyramidal neurons and convert LTP into LTD; an effect dependent on local inhibitory interneurons. Couey et al., demonstrated that this effect is mediated by nAChRs acting on inhibitory interneurons, with a suggestion that this could be partially mediated by α7 nAChRs. AS apposed to the studies by Couey et al., the experiments in this thesis provide definitive evidence that α7 nAChR activation can reduce synaptic plasticity, independently of other nAChRs, in a mechanism likely to involve activation of inhibitory interneurons. What's more the work in this thesis shows that inhibiting the actions of endogenous ACh at α7 nAChRs (with MLA) can also reduce the levels of synaptic plasticity. Highlighting that the findings of Couey et al., might not be reflective of nAChRs physiological role in regulating plasticity in response to endogenous ACh. Couey et al. go onto to show that the nAChR dependent increase in inhibition decreases the calcium signals within the dendrites of the layer V pyramidal neurons, thus altering the threshold for synaptic potentiation. Although not tested in this thesis, a similar mechanism likely explains the reduction in LTP upon α7 nAChR activation with the PAM and agonist. Couey et al., overcame the nAChR dependent block in plasticity by applying a burst of back propagating action potentials to increase intracellular dendritic calcium concentrations. It would be interesting to see in our experiments whether a stronger stimulation protocol, which would presumably increase postsynaptic calcium, could also attenuate the α7 nAChR dependent decrease in plasticity.

A decrease in dendritic calcium levels via activation of inhibitory interneurons directly innervating pyramidal neurons is a likely cause of the reduction in stimulus-induced LTP in response to α7 nAChR activation. However I also

demonstrate that α7 nAChR activation with the agonist and PAM decreases the magnitude of evoked EPSCs (Fig. 4.25), potentially via increased GABAergic input to glutamatergic nerve terminals. This reduction in glutamate release might also explain the reduction in plasticity observed upon α7 nAChR activation.

Couey et al., 2007, observed a similar reduction in evoked EPSCs in response to nAChR activation with nicotine, but failed to consider this as a potential mechanism for reduced plasticity. However they did show that $GABA_B$ receptor antagonism failed to attenuate nAChR induced reduction in plasticity, which suggest an interneuron dependent decrease in glutamate release cannot solely account for the reduction in LTP. Whether a reduction in glutamate signalling contributes to the direct inhibitory driven reduction in plasticity remains uncertain. Similarly, as discussed previously, MLA might bring about a reduction in excitation via lateral inhibition of inhibitory interneurons. This might suggest that antagonism of α7 nAChRs acts to decrease stimulus-induced LTP in an interneuron dependent manner, rather than by directly altering excitatory transmission, as discussed above.

6.3.4 The bi-directional modulation of LTP by α7 nAChRs

The finding with MLA shows that 'endogenous' activation of α7 nAChRs – either by tonically-released ACh or ACh released by electrical stimulation, enhances stimulus-induced LTP. In contrast, more global activation of α7 nAChRs – by bath application of a combination of α7 nAChR PAM and agonist leads to inhibition of LTP (Fig. 3.7A). As discussed above, this is thought to arise via direct effects on excitatory and inhibitory signalling respectively, and suggests that the location, or level, of α7 nAChR activation determines the magnitude of synaptic plasticity. This bi-directional regulation of plasticity is intriguing and correlates with findings in the hippocampus (Ji et al., 2001; Lagostena et al., 2008; Kroker et al., 2011; Gu & Yakel, 2011). In the hippocampus, Lagostena et al., (2008) show that S-24795, a partial agonist of α7 nAChRs, enhances LTP at low concentrations but reduces LTP at higher concentrations. Likewise,

Kroker et al., (2011) showed a similar bell-shaped concentration dependent increase in LTP with another partial α7 nAChR agonist, SSR180711. In this thesis, differences in LTP magnitude were observed between endogenous ACh release and one concentration of a globally applied α7 nAChR agonist and PAM. It would be interesting to investigate with further experiments if LTP levels are modulated in response to a range of α7 nAChR agonist concentration alone and in the presence of the α7 nAChR PAM. These experiments may reveal a similar bell shaped response curve in LTP levels in response to the levels of α7 nAChR activation.

In addition to the level of α7 nAChR activation, the location of the receptors activated within the PrL network upon stimulus-induced LTP might also account for the bi-directional effects on LTP. During stimulus-induced plasticity experiments, electrical stimulation is focussed to layers II/III of the PrL, this would presumably create a local increase in ACh release in the vicinity of the electrical stimulation. This local increase in ACh may activate excitatory inputs possessing α7 nAChRs innervating layer II/III, whilst failing to activate α7 nAChRs within other more distant cortical regions (e.g. Layer V). If this were the case, an enhancement of LTP would be expected (which could in turn be inhibited by bath application of α7 nAChR antagonists). In contrast, bath application of α7 nAChR agonists, would initiate a region wide α7 nAChR activation recruiting inhibitory interneurons across all layers, leading to an inhibition of LTP. This hypothesis is consistent with studies conducted in the hippocampus, showing that selectively enhancing the ACh concentration to inhibitory interneurons possessing α7 nAChRs can inhibit LTP, whilst increasing ACh concentration to the dendrites promotes the formation of LTP (Ji et al., 2001). It would be interesting to conduct similar experiments in the PrL to determine if local increases in α7 nAChR activation can indeed alter the direction and magnitude of PrL plasticity.

6.3.5 The effect of α7 nAChR positive allosteric modulation on LTP

In common with the findings shown here, Nakauchi & Sumikawa, (2012) conducted similar experiments in the hippocampus, and found that antagonising and enhancing the effects of endogenous ACh acting at α7 nAChRs with MLA and PNU-120596 could reduce and enhance the levels of stimulus-induced LTP respectively. This effect was shown to be dependent on endogenous ACh and not replicated via application of nicotine that they demonstrate desensitises α7 nAChRs. Interestingly, they observed the effect of endogenous ACh only upon a weak theta burst stimulation, and PNU-120596 had no effect when a stronger theta burst stimulation was used. In this thesis PNU-120596 also failed to increase LTP using a strong theta burst stimulation (Fig. 3.8A). PNU-120596 was also tested with a reduced theta burst stimulation, but PNU-120596 still failed to enhance LTP (Fig. 3.8B,C). This could indicate that the weak theta burst stimulation used here was still too strong; the weak theta burst used by Nakauchi et al. consisted of 2 bursts at 5 Hz, whilst in this thesis the 'weak'1x theta burst consisted of 7 bursts at 7 Hz, (both burst consisting of 4 pulses at 100 Hz).

Interestingly Nakauchi et al., reason that PNU-120596 enhances endogenous ACh mediated plasticity by directly increasing postsynaptic calcium through α7 nAChRs expressed postsynaptically on CA1 pyramidal neurons. If postsynaptic α7 nAChRs are expressed within the PrL layer V pyramidal neurons it may be expected that PNU-120596 may enhance LTP in a similar mechanism. The lack of effect of PNU-120596 in these experiments might therefore indicate the mechanism of LTP here is not via postsynaptic but rather presynaptic α7 nAChRs. If endogenous ACh acts to modulate plasticity via presynaptic mechanisms the inability of PNU-120596 to modulate plasticity is consistent with other findings, discussed earlier, that demonstrate positive allosteric modulation of α7 nAChRs has little effect in modulating evoked neurotransmission in contrast to α7 nAChR antagonism (Fig. 4.25).

6.3.6 α7 nAChR modulation of mPFC LTD

In addition to showing that α7 nAChRs can modulate levels of LTP in the PrL, experiments in this thesis also show that α7 nAChRs can modulate the levels of LTD. Similar to LTP, LTD can be initiated by a range of cellular mechanisms (section 1.3.3), however in general most forms of LTD involves glutamatergic activation of NMDARs, and is reliant on elevated levels of postsynaptic calcium. I have shown that MLA application in the presence of a low frequency stimulation induces a stable form of LTD (Fig. 3.6), indicating that endogenous ACh seemingly acts at α7 nAChRs to supress the formation of LTD. Within the mPFC only one study has directly demonstrated an effect of nAChRs in modulating LTD; Bueno-Junior et al., (2012) used *in vivo* electrophysiology in rats and demonstrated that activation of all nAChR subtypes with nicotine promotes the formation of thalamocortical LTP while supressing the formation of LTD. Although the contribution of different nAChR subtypes were not investigated, these findings are intriguingly similar to the effects α7 nAChR activation has on LTP and LTD shown here.

In addition to the mPFC, studies in the hippocampus have also observed a similar bi-directional modulation of plasticity with α7 nAChRs. The Sumikawa lab observe strikingly similar findings to those shown here, whereby α7 nAChR antagonism with MLA enhances LTD (Nakauchi & Sumikawa, 2014; Fujii & Sumikawa, 2001). Upon low frequency stimulation a slight synaptic depression (93 ± 3% from control) was observed, similar to experiments in this thesis (95 ± 5% from control), in addition, consistent with my findings in the PrL, administration of 100 nM MLA significantly enhanced the levels of LTD. The group went on to show that the enhanced LTD was NMDAR dependent suggesting that the MLA induced enhancement in LTD is regulated by an increase in excitation and postsynaptic calcium (Nakauchi & Sumikawa, 2014). If this is also assumed to be the case in the PrL, MLA might enhance LTD by increasing excitation of layer V pyramidal neurons. A possible mechanism for this could be that α7 nAChR antagonism with MLA inhibits a cholinergic activation of inhibitory interneurons. This would suggest that under the LFS induction conditions GABAergic interneurons are actively inhibiting pyramidal

neurons to supress LTD formation. Although this was not fully tested in this thesis, Bai et al., (2012) using an identical LFS to the one used in this thesis, demonstrated that the $GABA_A$ receptor antagonist, bicuculline, converted a subthreshold LTD (as seen in this thesis) to a long lasting stable LTD in the rat PrL.

However this theory also assumes that during LFS endogenous ACh acting through α7 nAChRs is contributing to the activation of these interneurons. This, however, is in contradiction to previous evidence in this thesis showing that tonic endogenous ACh has little effect on inhibitory interneurons. However, it may be that the levels of endogenous ACh interneurons are exposed to may differ depending on the stimulation conditions. For example, basal tonic release of ACh within the un-stimulated brain slice is insufficient to activate α7 nAChRs on interneurons. Upon single pulse electrical stimulation or the rapid but short LTP theta burst protocol (112 pulses over 1 min) the relative levels of ACh are likely to be enhanced, but perhaps not enhanced enough to fully activate α7 nAChRs on interneurons across all layers. In comparison, a low frequency stimulation (2700 pulses over 15 min) used to induce LTD, could result in a prolonged elevation of ACh, which may reach a threshold to activate α7 nAChRs on interneurons. As mentioned previously Lucas-Meunier et al., (2009), demonstrated that theta burst stimulation of layer II enhanced the levels of endogenous ACh two-fold compared to single stimulation within the visual cortex brain slice, so it may not be unexpected that ACh may increase even more during the prolonged LFS. Although this theory might be speculative, under these conditions MLA would result in disinhibition of pyramidal neurons during low frequency stimulation explaining the enhancement of LTD, and would explain why administration of the α7 nAChR PAM + agonist has no effect on LTD induction (Fig. 3.7B).

An alternative hypothesis is that the ability of MLA to reduce evoked glutamate release from afferent glutamatergic input (as shown previously in this thesis) leads to the induction of LTD. This theory might suggest that the LFS used for this thesis is ‘too strong’, and by reducing the overall glutamate release may result in a stable form of LTD. Although this theory is plausible, using this theory to explain the effect on LTD with PNU-120596 and PNU-282987 (Fig. 3.7), is

more difficult. PNU-120596 and PNU-282987, whose major effect is to enhance inhibition, would also presumably reduce excitation, however this drug combination had no effect on LTD induction. However PNU-120596 and PNU-282987 would presumably also act at excitatory terminal α7 nAChRs to increase excitation, these dual effects on increasing excitation and increasing inhibition might cancel each other out, which might explain the lack of LTD induction with this drug combination. These theories could be tested in more detail by separating the effects of α7 nAChR activation at interneurons and excitatory terminals with additional fEPSP experiments in the presence of GABA receptor blockade. This would help elucidate the contribution of α7 nAChR in the regulation of PrL LTD.

In summary the level or location of ACh acting on α7 nAChRs appears to be critical for the induction of plasticity within the PrL. With the modulation of plasticity seemingly depending on the relative contributions of α7 nAChRs located on glutamatergic nerve terminals and on GABAergic interneurons. This theory is supported by the mechanisms of α7 nAChR regulation within the hippocampus. However to fully investigate this, future experiments in which endogenous ACh is more tightly regulated (via the use of optogenetics) during LTP / LTD experiments would be critical to understand exactly how the timing, location and level of ACh release acting at α7 nAChRs can regulate plasticity mechanisms.

6.3.7 Other neuromodulatory processes controlling plasticity in the mPFC

6.3.7.1 α7 nAChRs on glia could modulate plasticity

As outlined above, the effects of α7 nAChR modulation of plasticity could be explained by direct effects at interneurons and glutamatergic synapses. However, other α7 nAChR dependent plasticity mechanisms have also been shown in the hippocampus. Work from Prof. Darwin Berg's lab, using cultured hippocampal slices, showed that activation of α7 nAChRs residing on

astrocytes in the hippocampus can drive the increase in AMPAR recruitment at glutamatergic synapses (X. Wang et al., 2013). However, this effects was only seen after 1 day of exposure to α7 nAChR agonists, and so the timescale in which α7 nAChRs mediate glia dependent changes in plasticity may not correlate with the timescale of the induction of LTP in this thesis. There is further evidence that α7 nAChRs are expressed on the glia of the rat neocortex and can regulate glutamate release, Patti et al., (2007) demonstrated rapid α7 nAChR-induced glutamate release from glia using an in vitro gliosome preparation. To date, no studies have directly investigated the role of glutamate release from glia on plasticity in the mPFC.

6.3.7.2 Modulation of plasticity by α7 nAChRs could be mediated by dopamine

An alternative hypothesis is that α7 nAChR modulation of plasticity is not due to the direct effects of α7 nAChRs on interneurons and glutamatergic synapses, but due to modulation of the neurotransmitter dopamine. Dopamine within the mPFC is known to regulate synaptic plasticity with a bell-shaped concentration dependence. Too little and too much dopamine precludes LTP formation whilst intermediate concentrations of dopamine (3 μM) facilitates induction of LTP (Kolomiets et al., 2009). Furthermore, dopamine at low concentrations facilitates the production of LTD (Otani et al., 1998), which has led to the theory that dopamine regulates the threshold for the induction of LTD and LTP in the mPFC, in a concentration-dependent manner (Otani et al., 2015). This biphasic regulation of LTP and LTD correlate with the results found within this thesis, suggesting that the α7 nAChR mediated effects may in some way be intricately linked with dopamine-induced modulation of plasticity.

There is evidence to support a link between α7 nAChRs and dopamine release, from both *in vitro* and *in vivo* studies. Microdialysis and synaptosome studies reveal that application of the selective α7 nAChR agonist choline, in the presence of PNU-120596 leads to a large elevation of dopamine which can be

reduced by both α7 nAChR and glutamatergic selective antagonists (Livingstone, Dickinson, et al., 2009; Livingstone, Srinivasan, et al., 2009). Other studies using the mixed α7 nAChR partial agonist / $5HT_3$ antagonist, RG3487, showed similar results, whereby RG3487 increased the levels of DA within the mPFC, using microdialysis in rats (M. Huang et al., 2014). Interestingly, Huang et al., found that this elevation in dopamine follows a bell shaped dose-response curve, with low and high levels of α7 nAChR activation reducing dopamine, but moderate α7 nAChR agonist doses enhancing DA levels. This tight regulation of dopamine levels by α7 nAChRs could provide an alternative or additional mechanisms by which α7 nAChRs can modulate plasticity. Whether the α7 nAChR mediated enhancement in dopamine levels are sufficiently elevated to modulate plasticity in the experiments in this thesis is unclear, but additional LTP / LTD experiments to investigate the link between the two neuromodulators would be interesting to study.

6.4 Elucidating the presynaptic loci of α7 nAChRs

The results in this thesis demonstrate a presynaptic location of α7 nAChRs on the terminals of glutamatergic inputs to layer V pyramidal neurons of the prelimbic cortex and the presence of these presynaptic receptors may modulate the levels of synaptic plasticity. The physiological significance of these presynaptic receptors would be enhanced by understanding the afferent fibres on which they reside. It was hypothesised that α7 nAChRs are unlikely to be expressed on all excitatory inputs to layer V pyramidal neurons. The final chapter of this thesis therefore aimed to investigate if α7 nAChRs are expressed on a subset of inputs from a discrete brain region. To achieve this, the selective measurements of specific inputs needed to be conducted, which possessed a technical challenge. In an attempt to address these questions several different methodologies were implemented including selective stimulation of discrete fibre inputs, pharmacological suppression of a population of excitatory inputs and selective activation of discrete inputs using

optogenetics. Each of these methodologies had their limitations and were used with varying success which will be discussed below.

6.4.1 Pharmacological suppression of thalamic inputs to the mPFC

Inputs to a brain region can be selectively investigated by activating or supressing a subset of inputs. There are no known pharmacological methods by which a subset of inputs to the PrL can be activated, but there is evidence that this approach can be used to selectively inhibit a subset of inputs to the PrL. Pharmacological suppression of specific fibre inputs requires the population of fibre inputs to selectively express inhibitory machinery that can be pharmacologically targeted, however examples of such targets are rare. One target that has been used by others to selectively supress thalamocortical inputs, is the μ-opioid receptor (Lambe et al., 2003). The μ-opioid receptor is a G_i/G_o coupled GPCR, activation of these receptors at nerve terminals would therefore act to inhibit transmitter release (Chartoff & Connery, 2014; J. T. Williams et al., 2001). Therefore, if μ-opioid receptors are selectively localised on thalamocortical inputs to the PrL, activation of μ-opioid receptors would inhibit glutamate release only from thalamocortical inputs, with no effect on glutamatergic inputs deriving from other brain regions. In this thesis activation of α7 nAChRs did not result in an increase in sEPSC frequency when the μ-opioid receptor agonist, DAMGO was co-applied (Fig. 5.1). This suggests that α7 nAChRs may be expressed on glutamatergic inputs from the thalamus, and not on glutamatergic inputs from other brain regions.

This conclusion can only be reached on the condition that μ-opioid receptors are exclusively expressed on thalamic inputs. Evidence to support this comes from a study showing that μ-opioid receptor activation attenuated the actions of presynaptic $5HT_{2A}$ receptor (Marek & Aghajanian, 1998), which via thalamic lesion and radioligand binding studies were shown to be present on thalamic inputs to the PrL (Marek et al., 2001). In addition, the thalamus contains mRNA for the μ-opioid receptor (Mansour et al., 1994). Although this evidence does point towards μ-opioid receptor expression on thalamic afferents, it does not

prove or disprove that μ-opioid receptors are also expressed on other afferent inputs. Indeed upon thalamic lesion and radioligand binding, Marek et al., (2001) did not observe a full reduction in [^{3}H]DAMGO binding, which might suggest that that μ-opioid receptors are expressed on other fibre inputs to the cortex. Therefore it can be reasoned that based on the findings of this thesis that α7 nAChRs are expressed on thalamic inputs to the cortex, however this single experiment cannot discount the possibility they are expressed on a separate set of afferent inputs.

The signalling mechanism(s) by which G_i/G_o coupled G-protein receptors inhibit transmitter release aren't fully understood, but could derive from inhibition of adenylyl cyclase, inhibition of VGCC, activation of outward rectifying potassium currents or direct inhibition of vesicular release machinery (Betke et al., 2012; Chartoff & Connery, 2014). α7 nAChRs are presumed to regulate transmitter release via altering presynaptic calcium levels either directly, via calcium entry through α7 nAChRs, or indirectly, via depolarisation-induced activation of VGCC. However it has recently been proposed that presynaptic α7 nAChRs can enhance transmitter release by increasing cAMP levels (Cheng & Yakel, 2015). Together, this suggests that α7 nAChRs and μ-opioid receptors may have opposite effects on transmitter release, potentially through effects on intracellular calcium levels or on cAMP levels.

6.4.2 Selective stimulation of hippocampal inputs to the mPFC

In addition to the excitatory inputs to the PrL from the thalamus, there is considerable glutamatergic input in the mPFC deriving from the hippocampus. The hippocampal-mPFC pathway is important for mediating cognitive processes including working memory and attention (Floresco et al., 1997; Godsil et al., 2013) and both regions synchronise their activity during such cognitive processes (O'Neill et al., 2013). The cognitive processes mediated by this pathway are regulated by activation of α7 nAChR *in vivo* animal models (Wallace & Porter, 2011), which could indicate that the hippocampal-mPFC pathway is a potential substrate for presynaptic α7 nAChRs to modulate

excitatory activity in the PrL. To investigate this, methodology described by Parent et al., (2010) was utilised to isolate a discrete fibre input that selectively contained fibres originating from the ventral hippocampus. Upon electrical stimulation of these fibres, monosynaptic glutamatergic EPSCs were recorded from layer V pyramidal neurons (Fig. 5.2). In some instances, evoked IPSCs were also observed, indicating hippocampal afferents also connect to inhibitory interneurons and partake in a feedforward inhibitory pathway, in agreement with the findings of others (Gabbott et al., 2002). The potential ability of α7 nAChR activation to regulate glutamate release from hippocampal afferent fibres connecting to layer V pyramidal neurons was then investigated. α7 nAChR activation had no effect on amplitude, rate of rise or rise time on hippocampal-mPFC evoked EPSCs (Fig. 5.3). This suggests that α7 nAChRs are not present on glutamatergic inputs deriving from the hippocampus. However, it is possible that single monosynaptic EPSCs, as used here, may be relatively insensitive to the presynaptic actions of α7 nAChRs, therefore paired pulse ratio measurements may have been an appropriate additional experiment to fully discount α7 nAChRs regulation of presynaptic activity. In addition it may have been interesting to investigate if the feedforward inhibitory mechanism could be modulated by α7 nAChRs, by recording EPSCs from inhibitory interneurons in response to hippocampal stimulation.

A major assumption for these experiments was that the fibre bundle isolated within these brain slices contained afferent fibres exclusively from hippocampus. Parent et al., (2010) used retrograde tracer studies to show that the fibres activated were from the hippocampus and although the brain slice and stimulation methodology used for the experiments in this thesis followed that of Parent et al., retrograde tracer studies were not conducted under our laboratory conditions. For this reason the exact selective origin of the fibres cannot be confirmed, leaving the possibility that the evoked EPSCs recorded are mediated from inputs other than those of the hippocampus.

6.4.3 Selective stimulation of afferent inputs to the mPFC with optogenetic stimulation

Optogenetic experiments were designed to enable selective release of glutamate from discrete afferent fibres to the PrL to determine if these inputs could be modulated by α7 nAChRs.

6.4.3.1 The effects of α7 nAChRs activation on the network activity of adult mice

To investigate further other afferent inputs that may be responsive to α7 nAChR activation or inhibition, optogenetic methodologies were investigated. These experiments required the use of mice that were nearly twice the age of mice used previously. Obtaining suitable brain slices from aged rodents is inherently challenging as slicing the brain of aged rodents tends to lead to an increase in neuronal death. For these reasons the majority of electrophysiology recordings within the literature are made from brain slices of juvenile or adolescent rodents, but this brings with it limitations in translatability to older more mature neuronal networks. The mPFC is known to undergo network maturation through adolescence into adulthood (Sowell et al., 2003; Gogtay et al., 2004) and α7 nAChR expression and function may also change through these development changes (Zhang et al., 1998). It was therefore important to test if the effects of α7 nAChR activation on spontaneous network activity, shown previously in juvenile mice, were also seen in older animals. This would not only ensure the validity of subsequent optogenetic studies but also investigate any differences between age groups of mice. It was found that upon repeating the original spontaneous EPSC and IPSC experiment in 9-12 weeks old rodents that α7 nAChRs played the same role in controlling both excitation and inhibition within the PrL (Fig. 5.4).

Interestingly in this experiment, co-administration of the α7 nAChR PAM and agonist led to a destabilisation of the holding current when held at -60 mV similar to that observed in the presence of picrotoxin (Fig. 4.14C) and TTX (Fig.

4.23). The cause of this destabilisation of the membrane current is unclear and could be brought about via multiple mechanisms. For example, in the presence of TTX and picrotoxin the effects of activating somatic α7 nAChRs on inhibitory interneurons are attenuated, meaning the current destabilisation is most likely brought about via elevations in α7 nAChR mediated excitation. However, with the experiments conduced with older animals, the PrL network remained pharmacologically intact, enabling α7 nAChRs to enhance both inhibition and excitation. In this particular experiment the destabilisation in membrane current may therefore be caused via enhanced inhibition, perhaps leading to space clamp issues, where distal dendrites were insufficiently voltage clamped. To test this hypothesis, limited studies were performed where a proportion of the chloride in the intracellular recording solution was substituted a with fluoride leading to an intracellular block of $GABA_A$ receptors (Akaike et al., 1989). Under these conditions, initial studies suggested that co-administration of the α7 nAChR PAM and agonist did not lead to holding current fluctuations (data not shown). Therefore, although not fully tested, this indicates that the membrane destabilisation was likely due to α7 nAChR-induced increases in inhibition.

As the GABA receptor mediated membrane destabilisation was only observed in older mice, this suggests that there may be age related differences in the inhibitory network. This could be due to different sensitivities of the inhibitory network to α7 nAChR activation (perhaps due to alter receptor expression levels) or due to age related differences in basal inhibitory tone. Comparing the basal IPSC frequency between different aged mice, there was a significantly higher sIPSC frequency in older mice (Fig. 5.4), compared with younger mice (Fig. 4.7) (Old: 863 ± 75 vs Young: 629 ± 104, events per min; $p < 0.001$, K-S test). However as these results were not obtained from a single controlled experiment, these differences may be due to differences in brain slice quality between experiments. The levels of α7 nAChRs expression are thought to remain constant between the ages of mice used in this thesis, but evidence of $GABA_A$ receptor subunit changes during postnatal development through to adulthood might indicate cortical inhibition is altered during postnatal development (Yu et al., 2006).

Aside from the potential differences α7 nAChRs partake in inhibitory signalling in older animals, it would appear that α7 nAChR still dynamically regulate excitation and inhibition in the adult the PrL network. This conformation also validated the use of older animals in optogenetic experiments to investigate the afferent location of α7 nAChRs.

6.4.3.1 Viral expression of channelrhodopsin from various brain regions

Initial optogenetic experiments were conducted at Vrije University, Amsterdam, where a number of brain regions (VTA, BLA, ventral hippocampus, thalamus and contralateral mPFC) were targeted for selective expression of the excitatory opsins: ChR2 and Chrimson. Viral injections of CAMKII – ChR2 – eYFP into the VTA and BLA were unsuccessful in producing light-evoked EPSCs in either layer V or II/III pyramidal neurons in the PrL (section 5.2.3), suggesting that the level of opsin expression within these afferent fibres was insufficient. Possible explanations include a low number of neurons expressing the viral promoter gene, or, a low number of neurons from these brain regions projecting to the PrL. Although there is some evidence of glutamatergic input to the PrL from the VTA (Gorelova et al., 2012), the literature provides no evidence of optogenetic control of the glutamatergic pathways between the VTA and PrL, which perhaps suggests that this glutamatergic pathway is not dense enough to enable optogenetic experiments. However the glutamatergic pathway between the BLA and PrL has been targeted by others with optogenetics, using a similar virus and similar expression time (Little & Carter, 2013). Another possible cause of limited opsin expression is the insufficient level of virus reaching the targeted brain region due to inaccurate/diffuse injection locations. The small volumes of both the VTA and the BLA and their ventral location within the brain means achieving an accurate injection is technically challenging. The accuracy of the injection sites was inspected for each animal but the precise accuracy of the injection was difficult to assess due to the spread of the virus after weeks of expression. In addition the virus may have needed a longer expression period to reach sufficient levels in the projecting fibres. Additional microscopy

experiments would have aided the determination of opsin expression levels in the VTA and BLA afferents within the PrL, however due to limited time and number of mice this was not possible. In contrast to the VTA and BLA, viral injections of both CAMKII – ChR2 – eYFP and Syn – Chrimson – tdTomato viruses into the thalamus enabled reliable glutamatergic responses from thalamic afferents to be evoked (Fig. 5.5). The successful expression of these viruses within thalamic afferents is not unsurprising due to the prominent afferent pathway between the thalamus and the PrL (Hoover & Vertes, 2007; Vertes, 2006), and others have optogenetically targeted this pathway with similar viruses (Little & Carter, 2012; Cruikshank et al., 2012).

Further experiments were conducted at Bath University. In an attempt to increase the levels of ChR2 expression, viruses containing the ubiquitous CAG promoter (Niwa et al., 1991), were used in these experiments, which had previously been used by others to selectively evoke glutamate from the BLA to the mPFC (Little & Carter, 2013). The CAG – ChR2 – GFP virus was injected into the ventral hippocampus, contralateral mPFC, thalamus and BLA to assess their afferent pathways to the PrL. As the CAG promoter is not specific to a particular cell type the VTA was not targeted due to the prominent dopaminergic pathway to the PrL. In the brain regions tested we found optogenetic control in all brain regions tested but with mixed success. Experiments targeting the contralateral mPFC and thalamus were very successful with light responses in all animals tested. As the ventral hippocampus interconnects strongly with the PrL it was expected that injections into this brain region would have also been reliable, however, light responses were only seen in approximately half of the animals tested. This is likely to be due to the inaccuracy of the viral injections. The viral injections were targeted to the CA1 region, as neurons within this layer interconnect with the mPFC. However inspection of the injection location, (Fig. 5.11), revealed the majority of the viral expression was restricted to the dentate gyrus, with only a limited expression within the CA1. This could be due to the lack of viral spread across the hippocampal fissure, which separates the dentate gyrus and the CA1 region, and suggests that viral injections should have been targeted to more lateral regions of the hippocampus.

In addition to the ventral hippocampus, targeting of the BLA was met with little success with only 2 of the 7 animal produced reliable responses. These findings, similar to initial experiments carried out in Vrije University, are likely due to difficulty in achieving accurate injections to the relatively small BLA. In addition to the accuracy of the viral injection location is the spread of the virus (Fig. 5.13). For both BLA targeted experiments in Vrije University and Bath University, the AAV5 serotype was used. Different AAV serotypes have different characteristic spreading patterns and expression profiles (Aschauer et al., 2013; Watakabe et al., 2015). In general AAV5 is thought to have the largest viral spread volume, which may have led to limited expression within the BLA itself. Other serotypes may have been more appropriate such as AAV2 which has a lower volume of spread, although this is offset with a lower transduction level (Aschauer et al., 2013). Choosing the appropriate serotype is not straight forward with the successful gene delivery and expression dependent on the promoter, the serotype and brain region injected and so achieving optimal expression levels across brain regions is challenging.

In addition to the virus itself the time of expression is another variable to be considered. Experiments conducted at Bath University allowed the CAG – ChR2 – GFP virus to express for 6 weeks and although this was sufficient for the thalamus and contralateral mPFC, a longer expression time for the virus injected into the BLA or hippocampus might have provided a higher success rate. Although, others that have used a similar optogenetic virus targeting the same BLA-PrL pathway found 2-3 weeks expression time was sufficient (Little & Carter, 2012; Little & Carter, 2013).

Finally, the limited success of obtaining light evoked EPSCs in layer V pyramidal neurons might alternatively indicate that afferents from both the BLA and ventral hippocampus might have limited connectivity with layer V neurons, and connect with other pyramidal neurons or interneurons within the PrL. Indeed, glutamatergic afferents from the BLA are known to directly connect with PrL interneurons in a feedforward inhibitory mechanism (Dilgen et al., 2013).

Nonetheless despite limited success, optogenetics did allowed afferent-specific EPSC measurements onto layer V pyramidal neurons from all of the brain

regions targeted. This enabled comparisons of the nature of these inputs, and in most cases investigations into whether these inputs are modulated by α7 nAChRs.

6.4.3.2 Comparing the synaptic inputs to layer V pyramidal neurons

Although the BLA had limited success, the responses that were obtained were mostly monosynaptic, as opposed to other inputs which produced both monosynaptic and polysynaptic responses. The monosynaptic responses obtained from each of the brain regions were compared, to uncover potential differences in synaptic properties and current kinetics. The kinetic properties between brain regions were quite diverse. Notably, light evoked EPSCs from ventral hippocampal afferents possessed fast rise and decay kinetics and larger amplitudes compared to EPSCs produced from release from other afferent inputs (Fig. 5.15) although these were not statistically different (potentially due to small sample sizes). These differences might indicate postsynaptic receptor levels or subtype expression might be different depending on the specific input fibres, a finding that may warrant further investigation. Differences could also represent variations in the location of synaptic contact relative to the neuron soma between different afferent inputs (Han et al., 2013; S. H. Williams & Johnston, 1991). However the levels or location of ChR2 expression may also account for some of these differences rather than physiological differences between synapses so caution should be made on interpreting these differences. In addition to the EPSC kinetics the paired pulse ratio of these inputs were compared and were found to be very similar across all synaptic inputs, indicating the probability of release is similar for all of these afferent inputs.

6.4.3.3 α7 nAChR regulation of afferent inputs from the contralateral mPFC and the ventral hippocampus

To investigate the potential location of α7 nAChRs on a particular subset of afferent inputs, optogenetic experiments aimed to assess if α7 nAChR activation or antagonism would lead to alterations in the release of glutamate from these afferent inputs. Inputs from the thalamus, ventral hippocampus and contralateral mPFC were assessed. BLA inputs were not investigated due to the limited success of optogenetic control of these inputs.

Layer V EPSCs and paired pulse ratios, evoked via light stimulation of the afferent fibres of the contralateral mPFC, thalamus and ventral hippocampus remained unchanged in response to positive allosteric modulation of α7 nAChRs with the PAM applied alone (Fig. 5.16 – 5.21). These findings are consistent with electrically stimulated EPSC experiments where the α7 nAChR PAM had no effect on EPSCs properties, paired pulse ratios or LTP, and are also in agreement with the idea that positive allosteric modulation of the α7 nAChRs is insufficient to alter the levels of evoked glutamate release in this particular assay (discussed above). Application of TTX to the tissue completely abolished the light and electrically evoked EPSCs (data not shown), so the mechanism by which the α7 nAChR PAM alters transmitter release may be action potential independent with the effect occluded in the presence of action potentials. Alternatively, the potentiating effect of the PAM may be too small to have an observable effect on evoked transmitter release, and perhaps a more sensitive assay would unveil an α7 nAChR PAM-mediated effect.

Interestingly, co-administration of the α7 nAChR agonist with the PAM led to mixed effects on glutamate release from the afferent fibres investigated. The amplitude of light evoked EPSCs from contralateral mPFC and ventral hippocampal afferents significantly decreased in response to the α7 nAChR agonist (Fig. 5.16 and 5.18), consistent with the effect seen when recording locally evoked EPSCs (stimulating in Layers II/III ; Fig. 4.25). Elevated inhibitory signalling might explain this decrease in EPSC magnitude and as theorised earlier may be due to presynaptic inhibition via $GABA_B$ receptors in response to

elevated GABA release. However the paired pulse ratios for both electrically and light evoked EPSCs remained unchanged in response to the α7 nAChR agonist and PAM co application (Fig. 5.17 and 5.19), which if the mechanism of reduced transmitter release was via presynaptic $GABA_B$ receptors we might expect to observe an increase in the paired pulse ratio, reflecting an decreased probability of release.

Addition of MLA did not result in an EPSC amplitude that was statistically different from control for ventral hippocampal inputs or contralateral mPFC inputs (Fig. 5.16 and 5.18), which may suggest that MLA was antagonising the effect of the α7 nAChR PAM + agonist, although inspection of the averaged data, suggests this is not obviously the case, and the lack of significance to control is likely to be due to a reduced n number and increased variability.

Due to limited number of available slices, experiments in which MLA was applied alone directly to the slice were not conducted. Consequently it is difficult to ascertain if MLA alone is able to alter the light evoked EPSCs, these experiments might have provided evidence that α7 nAChR antagonism could supress transmitter release, as seen in previous electrically evoked EPSC experiments. Interestingly however when conducting optogenetic paired pulse ratio experiments, inputs from the mPFC (but not from the ventral hippocampus), exhibited a significantly increased paired pulse ratio in response to MLA (Fig. 5.17). This paired pulse ratio change in response to α7 nAChR antagonism could indicate α7 nAChRs reside presynaptically on glutamatergic afferents from the mPFC, which is consistent with the increased paired pulse ratio seen when electrically-evoking inputs from layer II/III inputs (Fig. 4.26).

In summary, both ventral hippocampal and contralateral mPFC inputs to prelimbic layer V pyramidal neurons appear to be largely sensitive to α7 nAChR activation with an agonist and PAM, a mechanism perhaps involving increased inhibition. Added to this is the possibility that contralateral mPFC inputs may also be regulated by presynaptic α7 nAChRs. Further investigations should be conducted to investigate the effects of MLA alone for all inputs but in particular for inputs of the contralateral mPFC to confirm any presynaptic expression on these inputs.

6.4.3.4 α7 nAChR regulation of afferent inputs from the thalamus

Two separate sets of data were obtained assessing the responsiveness of thalamic afferents to α7 nAChR activation. The first set of experiments conducted at Vrije University used a combination of CAMKII – ChR2 – eYFP and Syn – Chrimson – tdTomato viruses to evoke EPSCs from thalamic afferents. α7 nAChR activation with a PAM and agonist led to a significant increase in EPSC amplitude. Subsequent addition of MLA appeared to reduce this increase in EPSC amplitude, although the effect was not statistically significant (Fig 5.6). α7 nAChR PAM + agonist application also resulted in an increased rate of rise but this was not statistically significant, perhaps due to an increased variability in responses. EPSC rise time did not appear to show any change in response to any of the α7 nAChR drug applications with no statistical significance observed, which provides no evidence to suggest that the increased thalamic input is localised to a particular dendritic compartment.

These data indicate that α7 nAChR activation can enhance the function of thalamocortical synapses to layer V pyramidal neurons presumably by increasing glutamate release. However, for these experiments paired pulse ratio measurements were not conducted, and so if this effect is brought about via presynaptic α7 nAChRs on thalamic terminals is still uncertain.

These findings complement the previous spontaneous EPSC experiments in which thalamic afferents supressed with DAMGO attenuated the effect of the α7 nAChR PAM (Fig. 5.1). Together these findings suggest that α7 nAChRs may play a role in regulating the release of glutamate from thalamic afferents in addition to the known role of α4β2 in this process (Lambe et al., 2003). Previous studies have demonstrated that acetylcholine acting at nicotinic receptors can regulate the thalamocortical pathway (Kawai et al., 2007; Bueno-Junior et al., 2012; Lambe et al., 2003) with α4β2 nAChRs being assigned the primary role in this regulation. The findings in this thesis suggest that α7 nAChRs in addition to α4β2 might also regulate glutamate levels via a potential presynaptic mechanism. In agreement with this are *in vivo* electrophysiology studies in the mPFC that have shown that locally applied MLA can block the

increased number of excitatory spikes observed upon local application of nicotine during stimulation of the MD thalamus (Gioanni et al., 1999).

Contrary to the positive findings obtained in the first set of optogenetic experiments carried out in Vrije University, the results of the subsequent repeated experiments at Bath University are more equivocal. In these experiments, an alternative CAG – ChR2 – GFP virus was used and injected into the thalamus under the same stereotaxic co-ordinates. Upon α7 nAChR activation and antagonism the light evoked EPSCs from thalamic afferents were unchanged in amplitude, rate of rise and rise time (Fig. 5.20). Measurements of the paired pulse ratios of these responses were also unaltered in response to α7 nAChR activation or inhibition (Fig. 5.21). However closer inspection of the paired pulse ratios in figure 5.21 shows the values do alter in the predicted pattern that might be expected for presynaptic α7 nAChRs, (a decrease in ratio for the PAM alone and PAM and agonist, with an increase in ratio for the antagonist MLA). These changes were small and not deemed statistically significant, perhaps due to low sample size, and perhaps additional experimental repeats may reveal a significant effect.

The findings in figure 5.20 were surprising and contradictory to the previous experiments carried out in Vrije University, which sheds some doubt over the initial findings that α7 nAChRs can regulate glutamate release from thalamic afferents. These experiments were conducted in different laboratories, and as much as the conditions were controlled between experiments, the differing setups and equipment might explain the differences in the results obtained.

The most obvious difference between the experiments carried out at Vrije University and the University of Bath is the different viruses used. The CAMKIIα and Synapsin promoters used to drive the expression of the ChR2 and Chrimson in the initial experiments were neuronal specific as opposed to the non-specific CAG promoter used in the subsequent experiment. This difference in cell type specificity may have led to different sub-populations of neurons being targeted. Watakabe et al., (2015) compared in mouse and marmoset cortex the transfection success of different AAV5 viruses containing CAMKII, Synapsin and a similar non-specific promoter to the one used in this thesis; the

CMV promoter. They found that the non-specific promoter lead to limited neuronal expression and high levels of expression in glia. Further, use of the virus with the non-specific promoter appeared to have toxic effects on neurons. It was not tested if similar effects were seen in the thalamic injections in this thesis, but if so, the reduced health of thalamic projecting neurons might be a possible cause for the differing effects. An additional hypothesis might be that within the thalamus region injected, only a percentage of the projecting neurons to the PrL functionally express presynaptic α7 nAChRs, if the CAMKIIα and synapsin viruses preferentially activate only these α7 nAChR positive neurons, light stimulation would evoke release from afferents that would be sensitive to α7 nAChR modulation. In contrast the CAG virus might transduce both α7 nAChR expressing and non-expressing neurons that project to the PrL, leading to a lower percentage of α7 nAChR sensitive fibres activated, upon optical stimulation.

Finally another possible explanation could be the differences in the population of synapses that are activated, due to differences in light stimulation methods. Initial experiments conducted in Vrije University, used a fluorescence light source directed through the microscope objective lens to illuminate the top of the slice in the vicinity of layer V around the recorded neuron. In experiments conducted in Bath University light stimulation was provided by an LED bulb manually positioned to illuminate the slice from beneath, which was not restricted to layer V and illuminated multiple layers of the PrL. Both light stimulation methods produced a light evoked EPSC with similar amplitude, (Vrije Uni.: 338 ± 74 pA vs Bath Uni.: 239 ± 111 pA; $p > 0.05$; taken from baseline EPSCs in Fig. 5.6 and Fig. 5.20) however the location of activated fibres relative to the recorded neuron is likely to be different. Electrophysiology recordings are often taken from neurons near the upper surface of the slice, therefore light stimulation using an upright objective lens is likely to stimulate synapses close to the soma of the recorded neuron in layer V. If α7 nAChRs selectively regulate inputs residing in a specific layer or dendritic location, the differences in light stimulation might explain the differences in α7 nAChR effects.

In summary it is difficult to determine the reasons why these two experiments led to differing findings, and highlights the importance of reproducibility of data. As shown here even though data may be deemed statistically significant this does not necessarily mean these findings are reproducible in other laboratory environments. However these initial optogenetic findings along with spontaneous EPSC data where thalamic inputs were supressed via μ-opioid receptor activation do suggest that α7 nAChRs are present on thalamocortical glutamatergic inputs. To further determine whether activation of α7 nAChRs can reproducibly enhance optogenetically-evoked glutamate release from thalamocortical inputs, future experiments should aim to better replicate the conditions of the original experiment by the use of the same CAMKII – ChR2 – eYFP virus and by adapting the method of light stimulation to better match that used in the original experiments. In addition the low sample size throughout the optogenetic experiments means interpretations of these findings should be taken with caution and additional repeats should be conducted to confirm the observed findings.

6.5 Summary of findings

To summarise the main findings within this thesis, it has been shown that α7 nAChRs play a key role in regulating the network activity of the PrL. Presynaptic expression of α7 nAChRs on excitatory nerve terminals can alter the levels of glutamate release onto the principle output layer V pyramidal neurons (Fig. 4.2 and 4.22). This regulation of glutamate release appears to be mediated via endogenous ACh release, with spontaneous glutamate release being enhanced by α7 nAChR positive allosteric modulation and acetylcholinesterase inhibition (Fig. 4.24), and evoked glutamate release being inhibited by α7 nAChR antagonism (Fig. 4.25). This endogenous ACh regulation of excitation is able to alter the levels of synaptic plasticity, with α7 nAChR antagonism both reducing LTP and enhancing LTD (Fig. 3.4 and 3.6).

In contrast α7 nAChRs expressed on inhibitory interneurons are able to alter the network inhibition. This appears not to be mediated via tonic endogenous ACh release but requires more prominent α7 nAChR activation, with for example an exogenous α7 nAChR agonist in the presence of a α7 nAChR positive allosteric modulator. Conditions that may represent more pronounced, phasic or synaptic ACh release (Fig. 4.7 and 4.24). This increase in α7 nAChR mediated inhibition also modulates PrL synaptic plasticity, with pronounced α7 nAChR activation reducing LTP (Fig. 3.7). Whilst evoked endogenous ACh acting at α7 nAChRs on inhibitory interneurons, may also supress the levels of LTD (Fig. 3.6).

In an attempt to identify a defined subset of glutamatergic afferent inputs that may possess presynaptic α7 nAChRs, several methodologies were utilised. Interesting data may suggest that afferent inputs from the thalamus (Fig 5.1 and 5.6), and potentially the contralateral mPFC (Fig. 5.17), might be regulated by presynaptic α7 nAChRs, although more work is needed to confirm this.

6.6 Broader significance of the work

6.6.1 α7 nAChRs potential mechanisms in cognitive function

In section 1.5 of the introduction it was highlighted the importance of α7 nAChRs in mPFC in cognitive behaviour. In attention, α7 nAChRs seemingly play a role in the performance of behavioural attention tasks in rodents (Hahn et al., 2011; Rezvani et al., 2009; Young et al., 2004), however it still remains unclear how ACh acting at these receptors mediates these processes. Studies have demonstrated that during attention tasks there are distinct modes of ACh release (Parikh & Sarter, 2008). Phasic increases in ACh are observed just before accurate cue detection, whilst tonic ACh release is elevated throughout the duration of the task, these different modes of ACh release are proposed to mediate different aspects of attention. Interestingly this thesis shows α7 nAChRs mediate different network processes, seemingly in response to different types of ACh release, this may correlate to different aspects of

attention. Indeed, both phasic and tonic elevations of ACh during attention also co-insides with elevations of glutamate, which suggests that a ACh- glutamate interaction is critical for attention performance. Interestingly it has been suggested that α7 nAChRs play a more prominent role when there is a high attention demand (Bloem, Poorthuis, et al., 2014). Correspondingly the levels of tonic ACh increase with the intensity of the task and the attentional efforts needed to perform the task (Parikh & Sarter, 2008). In this thesis α7 nAChRs have been shown to regulate the levels of glutamate release in response to elevations of tonic ACh, and so by augmenting glutamate release this may provide a mechanism by which α7 nAChRs regulate attention. It could be speculated that in response to the elevated tonic ACh release during high demanding attention task, α7 nAChRs, by increasing glutamate release from afferent inputs, may play a role in sharpening/enhancing certain glutamatergic signals, which might be required for attention performance.

During attention the phasic increases in ACh have been proposed to engage interneurons which has been suggested reduces the noise and 'clear' the network of unimportant inputs to allow better integration of salient inputs which enables accurate performance in the task (Totah et al., 2009; Poorthuis & Mansvelder, 2013). The experiments in this thesis also demonstrate that increasing the level of α7 nAChR activation (which presumably would correlate to elevations in ACh concentration during phasic release) leads to a dominant increase in inhibition. It is therefore interesting to speculate that the phasic high concentration increases in ACh preceding the accurate detection of the cues, may be acting at α7 nAChRs on interneurons. Therefore the differential modulation of the PrL network by α7 nAChRs as demonstrated in this thesis, might enable these receptors to orchestrate the network processes needed during attention, which are brought about via tonic and phasic release of ACh.

In addition to attention, working-memory is also a process thought to be implicated via ACh signalling. Working-memory is mediated by the mPFC and α7 nAChRs play a key role in the performance of working-memory tasks in rodent studies (Briggs et al., 1997; Fernandes et al., 2006), however the direct involvement of α7 nAChRs in working-memory is not clear. Working-memory is

known to be implicated with the PFC microcircuit in which glutamatergic signalling through NMDARs are able to sustain the activity of PFC neurons, required for working-memory (Goldman-Rakic, 1995). Studies in non-human primates have shown that in the dorsomedial PFC (the equivalent of the rodent prelimbic cortex) endogenous ACh acting at α7 nAChRs can enhance working memory performance (Yang Yang et al., 2013). Yang et al. show that α7 nAChRs can enhance the NMDAR mediated persistent firing during working memory in layer III pyramidal neurons. The work in this thesis demonstrates (at least in mice) that α7 nAChRs can enhance glutamate transmission, which might explain the effects shown here. Indeed Yang et al. suggest that presynaptic α7 nAChRs may contribute to this mechanism along with postsynaptic α7 nAChRs. Yang et al, (2013) went onto show that the selective α7 nAChR agonists (PHA) can enhance working-memory performance and interestingly in an inverted-U dose dependent manner with low and high concentrations having little effect. The authors suggest this could be due to non-specific enhancement of excitatory circuits but it's interesting to speculate this could be in part brought about via the recruitment of inhibitory interneurons as suggested in this thesis upon pronounced α7 nAChR activation, which may disrupt the cortical network during working-memory.

The PFC network activity during cognitive tasks is complex and so determining how α7 nAChRs can regulate these processes is difficult. However the work in this thesis at least provides a potential mechanism to explain how α7 nAChRs may bring about some of these changes, which has previously been lacking in the literature.

This thesis aimed to determine the afferent inputs that might be modulated by presynaptic α7 nAChRs. Each of these selective pathways appears to have a role in cognitive functions within the mPFC (section 1.2.2.1). The hippocampal-mPFC pathways is engaged in working-memory processes (Godsil et al., 2013), the BLA-mPFC pathway is implicated with fear conditioning and anxiety (Felix-Ortiz et al., 2016), whilst the significance of the contralateral mPFC pathway is still unclear. In this thesis evidence suggests that the thalamic inputs may possess presynaptic α7 nAChRs but the significance of this is still uncertain. *In*

vivo electrophysiology experiments demonstrate that nicotine acting at nAChRs can enhance plasticity at the thalamus-mPFC synapse in the rat (Bueno-Junior et al., 2012), and so the potential for presynaptic α7 nAChRs on thalamic inputs might provide a mechanism for this alteration in plasticity. The precise role of the thalamic-mPFC pathway has not been defined, but studies indicate it is engaged in different cognitive functions such as working-memory (Parnaudeau et al., 2013). This pathway is believed to allow integration of inputs into the mPFC, which occurs via simultaneously engaging inhibitory interneurons to reduce the noise of the network whilst synapsing onto excitatory pyramidal neurons (Delevich et al., 2015). Presynaptic α7 nAChRs on these thalamic inputs may promote this process by enhancing the glutamatergic signalling in response to acetylcholine. Indeed the phasic cholinergic transients seen during cue detection during attention also co-inside with phasic glutamate transients originating from the thalamus (Parikh et al., 2010), as mentioned above this could provide a mechanism by which presynaptic α7 nAChRs mediate its effects on attention. However the studies in this thesis demonstrating thalamic inputs possess α7 nAChRs are not conclusive, so any contribution of presynaptic α7 nAChRs during processes mediated by thalamic input to the PrL is just speculation.

6.6.2 α7 nAChRs potential influence in disease and clinical implications

The mPFC is also associated with several neurological disorders in which α7 nAChRs have also been implicated such as schizophrenia and Alzheimer's disease (section 1.5.2). Schizophrenia is associated with mutations in the α7 nAChR subunit gene *CHRNA7*, and reductions α7 nAChRs are observed post mortem in schizophrenia brains. Similarly in Alzheimer's disease α7 nAChR function is impaired, potentially via its interaction with amyloid-β. Both Schizophrenia and Alzheimer's diseases involve a dysregulation of synaptic plasticity, which may correlate with the findings of this thesis that show α7 nAChRs can modulate PrL synaptic plasticity. In addition to synaptic plasticity,

mPFC network activity is dysregulated during schizophrenia with a general loss in excitation and inhibition. This dysregulation may be in part mediated via an impaired α7 nAChRs regulation of excitation and inhibition, although it is unlikely that α7 nAChR deficits are the sole cause of these diseases.

Indeed, α7 nAChRs have been touted as a potential therapeutic for both Alzheimer's disease and schizophrenia to try and compensate or enhance the signalling that is impaired with these disease states. Several schizophrenia animal models have been used to highlight the possible therapeutic potential α7 nAChR activation might provide. In one animal model that exhibit the auditory gating deficits observed in a cohort of schizophrenia sufferers, show that upon systemic administration of the α7 nAChR agonist PNU-282987, the auditory gating deficit is restored, mediated by α7 nAChR dependent enhancement in inhibitory signalling in the hippocampus (Hajós et al., 2005). This restoration of sensory gating was also observed for the α7 nAChR PAM PNU-120596 (Hurst et al., 2005). Other animal models have studied the ketamine-induced cognitive deficits, which mimic the NMDAR hypofunction seen within schizophrenia. A host of α7 nAChR ligands can reverse these ketamine induced cognitive deficits, including the α7 nAChRs agonists; nicotine and A-582941, the α7 nAChR PAMs; PNU-120596 and CCMI and the acetylcholine esterase inhibitor galantamine (Nikiforuk et al., 2016; C. Wood et al., 2016).

For Alzheimer's disease in which cholinergic signalling is impaired, targeting α7 nAChRs have also become a promising therapeutic approach. Current treatments to alleviate the cognitive impairments associated with the disease have been to enhance endogenous ACh with acetylcholinesterase inhibitors. The use of the α7 nAChR PAM PNU-120596 used in this thesis, might also be a useful therapeutic tool to use in combination with acetylcholinesterase inhibitors. Callahan et al., (2013) conducted experiments in aged rodents and non-human primates and demonstrated that PNU-120596 in combination with the acetylcholinesterase inhibitor used in this thesis, donepezil, enhanced the performance in learning and memory tasks. The effect of PNU-120596 and donepezil was shown to be α7 nAChR dependent and was bigger than donepezil administration alone. The findings in this thesis demonstrate that this

same drug combination can enhance excitation within the mPFC in response to tonic endogenous ACh release, and may go in some way to explain its effect on learning and memory found by Callahan et al., (2013).

The findings in this study also highlight the importance of considering the net effect of enhancing α7 nAChR activity. The results in this thesis show that PNU-120596 administered with a selective α7 nAChR agonist results in increased inhibition of the cortical network which is shown to impair LTP formation, whilst endogenous tonic release appears to have the opposite effect. This is an important consideration if the aim of therapeutic intervention is to promote learning and memory, and suggests that enhancing α7 nAChR activity with an agonist will not necessarily bring about the desired therapeutic result. Instead it is important to study the complexities of α7 nAChR modulation of the mPFC network in response to endogenous ACh signalling, like this thesis has attempted to do. This will hopefully help guide a more targeted therapeutic approach. The findings of this thesis perhaps suggests that the use of a positive allosteric modulator might be a beneficial approach, as this would selectively enhance the endogenous ACh function that is diminished in Alzheimer's and other diseases.

6.7 Further work and conclusions

6.7.1 Are other cells within the cortex similarly regulated by α7 nAChRs?

The prelimbic cortex contains a diverse range of cell types, across the multiple cortical layers. The cells within these cortical layers comprise the microcircuit within the cortex that enable information integration processing and output. The work of this thesis has focused on layer V pyramidal neurons and to some degree layer V interneurons. This cellular layer is commonly studied as it is thought to be the primary output layer of the cortex. However, other neurons within the cortex also play an important role in mediating information processing and plasticity. Whether α7 nAChRs can also regulate the network activity of

these neurons is unclear. Recent studies have demonstrated that neurons within layer 1 of the prelimbic cortex are also regulated by α7 nAChRs; Tang et al., (2015) showed that activation of postsynaptic α7 nAChRs enhances AMPAR currents and the AMPA/NMDA receptor ratios. In addition they showed that activation of presynaptic α7 nAChRs enhanced the frequency of mEPSCs and decreased the paired pulse ratio of evoked AMPAR currents, suggesting presynaptic α7 nAChRs can also regulate glutamate release in layer I of the PrL. Neurons within layer I of the cortex are primarily GABAergic interneurons (Christophe et al., 2002), it would be interesting to record the spontaneous activity from other pyramidal neurons and inhibitory interneurons within different layers in response to α7 nAChRs activation. In addition to spontaneous activity, Tang et al., (2015) showed that α7 nAChRs expressed postsynaptically can regulate layer 1 inhibitory interneurons. The work in this thesis has shown that postsynaptic α7 nAChRs differentially regulates different subtypes of layer V inhibitory interneurons, and α7 nAChRs have been shown by others to be expressed on different interneuron subtypes in layers II/III (Poorthuis et al., 2012). Whether these α7 nAChR positive interneurons in other layers respond to α7 nAChR PAM and agonist application is unclear. It would be of interest to conduct similar current clamp recordings, as carried out in this thesis, from the interneurons of other cortical layers to investigate this. In addition to interneurons, the postsynaptic location of α7 nAChRs in pyramidal neurons is still uncertain. For superficial pyramidal neurons there is agreement in the literature for a lack of α7 nAChR expression. For layer V pyramidal neurons, Poorthuis et al., (2012) provide evidence for a postsynaptic α7 nAChR expression, whilst others have failed to replicate such findings (Hedrick & Waters, 2015). Data presented here provide no evidence for post synaptic α7 nAChRs on layer V pyramidal neurons. The reasons underlying this discrepancy in the literature is unclear, but might be due to differences in the methodology used, and perhaps warrants further investigation. Understanding how all the neurons within the cortical layers are regulated by α7 nAChR activity, might provide a clearer picture as to how α7 nAChRs can regulate the inhibitory and excitatory circuits within the PrL as a whole. Doing so may provide a model for how these receptors regulate more complex network activity and mediate or contribute to complex whole-animal behaviours.

6.7.2 Do α7 nAChRs differentially regulate other regions of the mPFC?

In addition to the possibility that α7 nAChRs can regulate cells within different layers of the prelimbic cortex (the dorsal medial PFC), there is the possibility that α7 nAChRs may differentially regulate other subregions of the mPFC, particularly the ventral medial PFC (the infralimbic cortex). The dorsal mPFC (prelimbic cortex) and the ventral mPFC (infralimbic cortex) have been shown to mediate opposing functions during certain cognitive processes in particular to reinstatement of drug seeking behaviour (Van den Oever et al., 2010). A process that is thought to be mediated by acute synaptic plasticity mechanisms within distinct regions of the mPFC. In addition to addiction the two regions are shown to mediate behaviour differences for attention and memory and learning (Cassaday et al., 2014). The ventral and dorsal mPFC receive similar levels of cholinergic innervation from the basal forebrain (Bloem, Schoppink, et al., 2014). However, any potential differences in nAChR expression between the two regions have not been studied. It would be interesting to investigate if acetylcholine acting at α7 nAChRs shows a similar pattern of regulation in network activity and plasticity between these two brain regions. Repeating similar brain slice electrophysiology experiments used in this thesis and by others in the infralimbic cortex may unearth differences in α7 nAChR modulation of spontaneous activity and synaptic plasticity. Investigating these differences may elucidate potential mechanisms for the, often contrasting, functions of these two nearby brain regions.

6.7.3 Are differing synapses between distal brain regions diverse and differentially regulated by α7 nAChRs?

Optogenetic experiments enabled the activation of synapses between discrete brain regions and PrL layer V pyramidal neurons. Although studies have intricately mapped the inputs to the layer V of the mPFC (DeNardo et al., 2015), no present studies have directly compared the properties of synaptic connections between the multiple brain regions connecting to the PrL layer V

neurons. It would be interesting to study how different synapses connecting to the PrL may differ in their synaptic properties and ability to undergo synaptic plasticity. The optogenetic experiments in this thesis superficially investigated potential differences in monosynaptic EPSCs generated from stimulation of different afferent fibres, but due to limited time was not the primary focus of the experiments. Additional electrophysiology experiments including, investigating synaptic summation of inputs, paired pulse and AMPA/NMDA receptor ratios, as well as rectification indices would provide detailed comparisons of the synaptic properties of these different synapses. In addition to looking at the synaptic properties investigating the differences in synaptic plasticity of these inputs might also be interesting to study. Studies have demonstrated the ability to combine optogenetics with STDP to investigate the plasticity of different afferent pathways (Kohl et al., 2011). Here Kohl and colleagues were able to look at contralateral and ipsilateral connectivity between the hippocampus. A similar approach could be taken with inputs to the PrL in which pairings of presynaptic light evoked EPSPs could be paired with single or bursts of postsynaptic action potentials to induce STDP. Initial experiments could compare the resulting level of plasticity between inputs and the required spike timing needed to induce LTP between these different synaptic inputs.

It would then be interesting to investigate potential differential modulation of STDP by activation/inhibition of α7 nAChRs. Several studies have combined electrically evoked STDP with cholinergic modulation in the PrL and show that nicotine administered directly to the brain slice and via chronic treatment in rats can alter the levels of STDP (Couey et al., 2007; Goriounova & Mansvelder, 2012a). These studies electrically stimulate layers II/III fibres and so it is still unclear if nAChRs regulate plasticity differently depending on the specific input to pyramidal neurons in the PrL. Understanding how α7 nAChRs modulate brain region specific plasticity mechanisms would provide an insight into how acetylcholine is engaged in the behavioural and cognitive process assigned to these pathways.

6.7.4 What is α7 nAChR's function in the context of other acetylcholine receptors in modulating network activity?

The research in this thesis has exclusively focused on the role of α7 nAChRs in regulating network activity and plasticity. Investing a receptor in isolation is often important to thoroughly define its role in a network. However doing so also has its limitations. Acetylcholine is the endogenous ligand for not just the α7 nAChR but other nicotinic and muscarinic acetylcholine receptors. Although under certain circumstances acetylcholine may be released with a spatial or temporal precision to selectively activate only α7 nAChRs, it is likely that a single endogenous ACh release event will simultaneously activate α7 nAChRs and other acetylcholine receptors. Demonstrations of this is shown using optogenetics in which the selective stimulation of cholinergic fibres in the cortex results in a duel fast and slow component EPSC mediated by α7 and α4β2 nAChRs respectively within L1 interneurons (Arroyo et al., 2012; Bennett et al., 2012). What's more studies such as these investigating nAChRs, often do so in isolation with the effects of muscarinic receptors being removed by pharmacologically blockade.

Muscarinic ACh receptors might also play a role in regulating the excitability of the mPFC along with nAChRs. Within other regions of the cortex mAChRs and nAChRs can work together to promote processing of sensory inputs from the thalamus whilst inhibiting inputs from other cortical regions. For example excitatory M1 mAChRs expressed on layer V pyramidal neurons enhance postsynaptic excitability (Gulledge et al., 2007). In addition inhibitory M2/4 mAChRs on the terminals of fast spiking interneurons reduce the inhibition of the soma of layer V pyramidal neurons (Kruglikov & Rudy, 2008), both effects promoting principle neuron excitation. Added to this inhibitory presynaptic M4 mAChRs supresses glutamate release from cortical-cortical inputs (Kimura & Baughman, 1997), which is also brought about via nAChRs enhancing activity of non-fast spiking interneurons (which also reduce cortical-cortical inputs). Added to this is ACh's ability to simultaneously enhance release from thalamic inputs via nAChRs. It has been proposed this mechanism of reducing cortical interactions but enhancing the sensitivity of principle neurons to inputs from the

thalamus enables ACh to regulate information processing (Higley & Picciotto, 2014).

This highlights that nAChRs and mAChRs, as would be expected, work in harmony to regulate the cortical network, and the fast actions of nAChRs and the relatively slow actions of mAChRs are likely engaged by ACh to modulate the PrL network. This suggests that to better understand how endogenous ACh regulates a PrL network it would be of benefit to study specific ACh receptor subtype activation together rather than independently – although in practice this is difficult to achieve. In addition as experimental technology advances in which acetylcholine release can be precisely controlled both temporally and spatially, a better picture may emerge of how the range of different acetylcholine receptors work together to modulate the PrL network.

6.8 Final conclusion

The prefrontal cortex is a complex system that regulates a range of advanced cognitive processes. This thesis aimed to address some of this complexity by investigating the contribution of α7 nAChRs in regulating excitatory and inhibitory network signalling within the prelimbic region of the mouse medial prefrontal cortex. The findings of this thesis provide clear evidence that α7 nAChRs have the capacity to modulate synaptic plasticity within the prelimbic cortex. These receptors achieve this via regulation of inhibitory interneurons and excitatory inputs, which may be differentially regulated by endogenous acetylcholine release. What's more α7 nAChRs may selectively modulate excitatory transmission from discrete afferent such as those from the thalamus. This scientific investigation has inevitably provided additional unanswered questions that warrant further investigation, but also provides observations that have potential implications for the mechanisms of cognition and aberrant network activity in neurological disorders.

References

Akaike, N., Inomata, N. & Yakushiji, T. 1989. Differential effects of extra- and intracellular anions on GABA-activated currents in bullfrog sensory neurons. *Journal of Neurophysiology*, 62(6): 1388–1399.

Albuquerque, E.X., Pereira, E.F.R., Alkondon, M. & Rogers, S.W. 2009. Mammalian nicotinic acetylcholine receptors: from structure to function. *Physiological reviews*, 89(1): 73–120.

Alkondon, M., Albuquerque, E.X. & Pereira, E.F.R. 2013. Acetylcholinesterase inhibition reveals endogenous nicotinic modulation of glutamate inputs to CA1 stratum radiatum interneurons in hippocampal slices. *Neurotoxicology*, 36: 72–81.

Alkondon, M., Pereira, E.F., Barbosa, C.T. & Albuquerque, E.X. 1997. Neuronal nicotinic acetylcholine receptor activation modulates gamma-aminobutyric acid release from CA1 neurons of rat hippocampal slices. *Journal of Pharmacology and Experimental Therapeutics*, 283(3): 1396–1411.

Alkondon, M., Pereira, E.F., Eisenberg, H.M. & Albuquerque, E.X. 2000. Nicotinic receptor activation in human cerebral cortical interneurons: a mechanism for inhibition and disinhibition of neuronal networks. *Journal of Neuroscience*, 20(1): 66–75.

Aracri, P., Amadeo, A., Pasini, M.E., Fascio, U. & Becchetti, A. 2013. Regulation of glutamate release by heteromeric nicotinic receptors in layer V of the secondary motor region (Fr2) in the dorsomedial shoulder of prefrontal cortex in mouse. *Synapse*, 67(6): 338–357.

Aracri, P., Consonni, S., Morini, R., Perrella, M., Rodighiero, S., Amadeo, A. & Becchetti, A. 2010. Tonic Modulation of GABA Release by Nicotinic Acetylcholine Receptors in Layer V of the Murine Prefrontal Cortex. *Cerebral Cortex*, 20(7): 1539–1555.

Arredondo, J., Chernyavsky, A.I., Jolkovsky, D.L., Pinkerton, K.E. & Grando, S.A. 2006. Receptor-mediated tobacco toxicity: cooperation of the Ras/Raf-1/MEK1/ERK and JAK-2/STAT-3 pathways downstream of alpha7 nicotinic receptor in oral keratinocytes. *FASEB Journal*, 20(12): 2093–2101.

Arroyo, S., Bennett, C., Aziz, D., Brown, S.P. & Hestrin, S. 2012. Prolonged disynaptic inhibition in the cortex mediated by slow, non-α7 nicotinic excitation of a specific subset of cortical interneurons. *Journal of Neuroscience,* 32(11): 3859–3864.

Aschauer, D.F., Kreuz, S. & Rumpel, S. 2013. Analysis of transduction efficiency, tropism and axonal transport of AAV serotypes 1, 2, 5, 6, 8 and 9 in the mouse brain. *PLoS ONE*, 8(9)

Auger, C. & Marty, A. 2000. Quantal currents at single-site central synapses. *Journal of Physiology*, 526(1): 3–11.

Bai, J., Blot, K., Tzavara, E., Nosten-Bertrand, M., Giros, B. & Otani, S. 2012. Inhibition of Dopamine Transporter Activity Impairs Synaptic Depression in Rat Prefrontal Cortex Through Over-Stimulation of D1 Receptors. *Cerebral Cortex*. 24(4): 945-955.

Barker, G.R.I. & Warburton, E.C. 2008. NMDA receptor plasticity in the perirhinal and prefrontal cortices is crucial for the acquisition of long-term object-in-place associative memory. *Journal of Neuroscience* 28(11): 2837–2844.

Barker, G.R.I., Bird, F., Alexander, V. & Warburton, E.C. 2007. Recognition Memory for Objects, Place, and Temporal Order: A Disconnection Analysis of the Role of the Medial Prefrontal Cortex and Perirhinal Cortex. *Journal of Neuroscience*, 27(11): 2948–2957.

Barria, A., Derkach, V. & Soderling, T. 1997. Identification of the Ca2+/calmodulin-dependent protein kinase II regulatory phosphorylation site in the alpha-amino-3-hydroxyl-5-methyl-4-isoxazole-propionate-type glutamate receptor. *Journal of Biological Chemistry*, 272(52): 32727–32730.

Battaglia, F., Wang, H.-Y., Ghilardi, M.F., Gashi, E., Quartarone, A., Friedman, E. & Nixon, R.A. 2007. Cortical plasticity in Alzheimer's disease in humans and rodents. *Biological Psychiatry*, 62(12): 1405–1412.

Beattie, E.C., Carroll, R.C., Yu, X., Morishita, W., Yasuda, H., Zastrow, von, M. & Malenka, R.C. 2000. Regulation of AMPA receptor endocytosis by a signaling mechanism shared with LTD. *Nature Neuroscience*, 3(12): 1291–1300.

Bennett, C., Arroyo, S., Berns, D. & Hestrin, S. 2012. Mechanisms generating dual-component nicotinic EPSCs in cortical interneurons. *Journal of Neuroscience*, 32(48): 17287–17296.

Betke, K.M., Wells, C.A. & Hamm, H.E. 2012. GPCR mediated regulation of synaptic transmission. *Progress in Neurobiology*, 96(3): 304–321.

Bigl, V., Woolf, N.J. & Butcher, L.L. 1982. Cholinergic projections from the basal forebrain to frontal, parietal, temporal, occipital, and cingulate cortices: a combined fluorescent tracer and acetylcholinesterase analysis. *Brain Research Bulletin*, 8(6): 727–749.

Bitner, R.S., Bunnelle, W.H., Decker, M.W., Drescher, K.U., Kohlhaas, K.L., Markosyan, S., Marsh, K.C., Nikkel, A.L., Browman, K., Radek, R., Anderson, D.J., Buccafusco, J. & Gopalakrishnan, M. 2010. In vivo pharmacological characterization of a novel selective alpha7 neuronal nicotinic acetylcholine receptor agonist ABT-107: preclinical considerations in Alzheimer's disease. *Journal of Pharmacology and Experimental Therapeutics*, 334(3): 875–886.

Bliss, T.V. & Collingridge, G.L. 1993. A synaptic model of memory: long-term potentiation in the hippocampus. *Nature*, 361(6407): 31–39.

Bliss, T.V. & Lomo, T. 1973. Long-lasting potentiation of synaptic transmission in the dentate area of the anaesthetized rabbit following stimulation of the perforant path. *Journal of Physiology*, 232(2): 331–356.

Blitzer, R.D. et al., 1998. Gating of CaMKII by cAMP-regulated protein phosphatase activity during LTP. *Science*, 280(5371), pp.1940–1942

Bloem, B., Poorthuis, R.B. & Mansvelder, H.D. 2014. Cholinergic modulation of the medial prefrontal cortex: the role of nicotinic receptors in attention and regulation of neuronal activity. *Frontiers in Neural Circuits*, 8(17).

Bloem, B., Schoppink, L., Rotaru, D.C., Faiz, A., Hendriks, P., Mansvelder, H.D., van de Berg, W.D.J. & Wouterlood, F.G. 2014. Topographic Mapping between Basal Forebrain Cholinergic Neurons and the Medial Prefrontal Cortex in Mice. *Journal of Neuroscience*, 34(49): 16234–16246.

Bortz, D.M., Mikkelsen, J.D. & Bruno, J.P. 2013. Localized infusions of the partial alpha 7 nicotinic receptor agonist SSR180711 evoke rapid and transient increases in prefrontal glutamate release. *Neuroscience*, 255: 55–67.

Boudkkazi, S., Carlier, E., Ankri, N., Caillard, O., Giraud, P., Fronzaroli-Molinieres, L. & Debanne, D. 2007. Release-dependent variations in synaptic latency: a putative code for short- and long-term synaptic dynamics. *Neuron*, 56(6): 1048–1060.

Boyden, E.S., Zhang, F., Bamberg, E., Nagel, G. & Deisseroth, K. 2005. Millisecond-timescale, genetically targeted optical control of neural activity. *Nature Neuroscience*, 8(9): 1263–1268.

Briggs, C.A., Anderson, D.J., Brioni, J.D., Buccafusco, J.J., Buckley, M.J., Campbell, J.E., Decker, M.W., Donnelly-Roberts, D., Elliott, R.L., Gopalakrishnan, M., Holladay, M.W., Hui, Y.H., Jackson, W.J., Kim, D.J., Marsh, K.C., O'Neill, A., Prendergast, M.A., Ryther, K.B., Sullivan, J.P. & Arneric, S.P. 1997. Functional characterization of the novel neuronal nicotinic acetylcholine receptor ligand GTS-21 in vitro and in vivo. *Pharmacology, Biochemistry and Behavior*, 57(1-2): 231–241.

Brodmann, K. 1909. *Vergleichende Lokalisationslehre der Großhirnrinde*. Leipzig : Barth.

Broersen, L.M. & Uylings, H.B. 1999. Visual attention task performance in Wistar and Lister hooded rats: response inhibition deficits after medial prefrontal cortex lesions. *Neuroscience*, 94(1): 47–57.

Brunzell, D.H., Russell, D.S. & Picciotto, M.R. 2003. In vivo nicotine treatment regulates mesocorticolimbic CREB and ERK signaling in C57Bl/6J mice. *Journal of Neurochemistry*, 84(6): 1431–1441.

Bueno-Junior, L.S., Lopes-Aguiar, C., Ruggiero, R.N., Romcy-Pereira, R.N. & Leite, J.P. 2012. Muscarinic and Nicotinic Modulation of Thalamo-Prefrontal Cortex Synaptic Plasticity In Vivo. *PLoS ONE*, 7(10): doi:10.1371/annotation/d2dbf233-db12-431f-b9b6-4bd31cbca23e.

Callahan, P.M., Hutchings, E.J., Kille, N.J., Chapman, J.M. & Terry, A.V. 2013. Positive allosteric modulator of alpha 7 nicotinic-acetylcholine receptors, PNU-120596 augments the effects of donepezil on learning and memory in aged rodents and non-human primates. *Neuropharmacology*, 67: 201–212.

Caruana, D.A., Warburton, E.C. & Bashir, Z.I. 2011. Induction of Activity-Dependent LTD Requires Muscarinic Receptor Activation in Medial Prefrontal Cortex. *Journal of Neuroscience*, 31(50): 18464–18478.

Cassaday, H.J., Nelson, A.J.D. & Pezze, M.A. 2014. From attention to memory along the dorsal-ventral axis of the medial prefrontal cortex: some methodological considerations. *Frontiers in Systems Neuroscience,* 8(160): doi: 10.3389/fnsys.2014.00160

Chartoff, E.H. & Connery, H.S. 2014. It's MORe exciting than mu: crosstalk between mu opioid receptors and glutamatergic transmission in the mesolimbic dopamine system. *Frontiers in Pharmacology*, 5(116): doi: 10.3389/fphar.2014.00116

Chatzidaki, A. & Millar, N.S. 2015. Allosteric modulation of nicotinic acetylcholine receptors. *Biochemical Pharmacology*, 97(4): 408–417.

Cheng, Q. & Yakel, J.L. 2015. Activation of α7 nicotinic acetylcholine receptors increases intracellular cAMP levels via activation of AC1 in hippocampal neurons. *Neuropharmacology*, 95: 405–414.

Cheng, Q. & Yakel, J.L. 2014. Presynaptic α7 nicotinic acetylcholine receptors enhance hippocampal mossy fiber glutamatergic transmission via PKA activation. *Journal of Neuroscience*, 34(1): 124–133.

Christophe, E., Roebuck, A., Staiger, J.F., Lavery, D.J., Charpak, S. & Audinat, E. 2002. Two types of nicotinic receptors mediate an excitation of neocortical layer I interneurons. *Journal of Neurophysiology*, 88(3): 1318–1327.

Chudasama, Y. & Muir, J.L. 2001. Visual attention in the rat: a role for the prelimbic cortex and thalamic nuclei? *Behavioral Neuroscience*, 115(2): 417–428.

Clarke, P.B. & Reuben, M. 1996. Release of [3H]-noradrenaline from rat hippocampal synaptosomes by nicotine: mediation by different nicotinic receptor subtypes from striatal [3H]-dopamine release. *British Journal of Pharmacology*, 117(4): 595–606.

Collingridge, G.L., Kehl, S.J. & McLennan, H. 1983. Excitatory amino acids in synaptic transmission in the Schaffer collateral-commissural pathway of the rat hippocampus. *Journal of Physiology*, 334(1): 33–46.

Collins, T., Young, G.T. & Millar, N.S. 2011. Competitive binding at a nicotinic receptor transmembrane site of two α7-selective positive allosteric modulators with differing effects on agonist-evoked desensitization. *Neuropharmacology*, 61(8): 1306–1313.

Couey, J.J., Meredith, R.M., Spijker, S., Poorthuis, R.B., Smit, A.B., Brussaard, A.B. & Mansvelder, H.D. 2007. Distributed Network Actions by Nicotine Increase the Threshold for Spike-Timing-Dependent Plasticity in Prefrontal Cortex. *Neuron*, 54(1): 73–87.

Croxson, P.L., Kyriazis, D.A. & Baxter, M.G. 2011. Cholinergic modulation of a specific memory function of prefrontal cortex. *Nature Neuroscience*, 14(12): 1510–1512.

Cruikshank, S.J., Ahmed, O.J., Stevens, T.R., Patrick, S.L., Gonzalez, A.N., Elmaleh, M. & Connors, B.W. 2012. Thalamic control of layer 1 circuits in prefrontal cortex. *Journal of Neuroscience*, 32(49): 17813–17823.

Cull-Candy, S.G. & Leszkiewicz, D.N. 2004. Role of distinct NMDA receptor subtypes at central synapses. *Science Signaling*, (2004)255: doi: 10.1126/stke.2552004re16

D'Souza, M.S. & Markou, A. 2012. Schizophrenia and tobacco smoking comorbidity: nAChR agonists in the treatment of schizophrenia-associated cognitive deficits. *Neuropharmacology*, 62(3): 1564–1573.

Dajas-Bailador, F.A., Mogg, A.J. & Wonnacott, S. 2002. Intracellular Ca2+ signals evoked by stimulation of nicotinic acetylcholine receptors in SH-SY5Y cells: contribution of voltage-operated Ca2+ channels and Ca2+ stores. *Journal of Neurochemistry*, 81(3): 606–614.

Debanne, D., Guérineau, N.C., Gähwiler, B.H. & Thompson, S.M. 1996. Paired-pulse facilitation and depression at unitary synapses in rat hippocampus: quantal fluctuation affects subsequent release. *Journal of Physiology*, 491(1): 163–176.

DeFelipe, J., López-Cruz, P.L., Benavides-Piccione, R., Bielza, C., Larrañaga, P., Anderson, S., Burkhalter, A., Cauli, B., Fairén, A., Feldmeyer, D., Fishell, G., Fitzpatrick, D., Freund, T.F., Gonzalez-Burgos, G., Hestrin, S., Hill, S., Hof, P.R., Huang, J., Jones, E.G., Kawaguchi, Y., Kisvárday, Z., Kubota, Y., Lewis, D.A., Marín, O., Markram, H., McBain, C.J., Meyer, H.S., Monyer, H., Nelson, S.B., Rockland, K., Rossier, J., Rubenstein, J.L.R., Rudy, B., Scanziani, M., Shepherd, G.M., Sherwood, C.C., Staiger, J.F., Tamás, G., Thomson, A., Wang, Y., Yuste, R. & Ascoli, G.A. 2013. New insights into the classification and nomenclature of cortical GABAergic interneurons. *Nature Reviews Neuroscience*, 14(3): 202–216.

DeKosky, S.T. & Scheff, S.W. 1990. Synapse loss in frontal cortex biopsies in Alzheimer's disease: correlation with cognitive severity. *Annals of Neurology*, 27(5): 457–464.

Del Barrio, L., Egea, J., León, R., Romero, A., Ruiz, A., Montero, M., Alvarez, J. & López, M.G. 2011. Calcium signalling mediated through α7 and non-α7 nAChR stimulation is differentially regulated in bovine chromaffin cells to induce catecholamine release. *British Journal of Pharmacology*, 162(1): 94–110.

Del Castillo, J. & Katz, B. 1954. Quantal components of the end-plate potential. *Journal of Physiology*, 124(3): 560–573.

Delevich, K., Tucciarone, J., Huang, Z.J. & Li, B. 2015. The mediodorsal thalamus drives feedforward inhibition in the anterior cingulate cortex via parvalbumin interneurons. *Journal of Neuroscience*, 35(14): 5743–5753.

Dembrow, N. & Johnston, D. 2014. Subcircuit-specific neuromodulation in the prefrontal cortex. *Frontiers in Neural Circuits*, 8(54): doi:10.3389/fncir.2014.00054

Dembrow, N.C., Zemelman, B.V. & Johnston, D. 2015. Temporal dynamics of L5 dendrites in medial prefrontal cortex regulate integration versus coincidence detection of afferent inputs. *Journal of Neuroscience*, 35(11): 4501–4514.

DeNardo, L.A., Berns, D.S., DeLoach, K. & Luo, L. 2015. Connectivity of mouse somatosensory and prefrontal cortex examined with trans-synaptic tracing. *Nature Neuroscience*, 18(11): 1687–1697.

Derkach, V., Barria, A. & Soderling, T.R. 1999. Ca2+/calmodulin-kinase II enhances channel conductance of alpha-amino-3-hydroxy-5-methyl-4-isoxazolepropionate type glutamate receptors. PNAS, 96(6): 3269–3274.

Descarries, L., Gisiger, V. & Steriade, M. 1997. Diffuse transmission by acetylcholine in the CNS. *Progress in Neurobiology*, 53(5): 603–625.

Dégenètais, E., Thierry, A.-M., Glowinski, J. & Gioanni, Y. 2003. Synaptic influence of hippocampus on pyramidal cells of the rat prefrontal cortex: an in vivo intracellular recording study. *Cerebral Cortex*, 13(7): 782–792.

Dickinson, J.A., Kew, J.N.C. & Wonnacott, S. 2008. Presynaptic alpha7- and beta2-Containing Nicotinic Acetylcholine Receptors Modulate Excitatory Amino Acid Release from Rat Prefrontal Cortex Nerve Terminals via Distinct Cellular Mechanisms. *Molecular Pharmacology*, 74(2): 348–359.

Dilgen, J., Tejeda, H.A. & O'Donnell, P. 2013. Amygdala inputs drive feedforward inhibition in the medial prefrontal cortex. *Journal of Neurophysiology*, 110(1): 221–229.

Dineley, K.T., Pandya, A.A. & Yakel, J.L. 2015. Nicotinic ACh receptors as therapeutic targets in CNS disorders. *Trends in Pharmacological Sciences*, 36(2): 96–108.

Dittgen, T., Nimmerjahn, A., Komai, S., Licznerski, P., Waters, J., Margrie, T.W., Helmchen, F., Denk, W., Brecht, M. & Osten, P. 2004. Lentivirus-based genetic manipulations of cortical neurons and their optical and electrophysiological monitoring in vivo. *PNAS*, 101(52): 18206–18211.

Douglas, R.J. & Martin, K.A.C. 2004. Neuronal circuits of the neocortex. *Annual Review of Neuroscience*, 27: 419–451.

Eckenstein, F. & Thoenen, H. 1983. Cholinergic neurons in the rat cerebral cortex demonstrated by immunohistochemical localization of choline acetyltransferase. *Neuroscience Letters*, 36(3): 211–215.

Engelhardt, von, J., Eliava, M., Meyer, A.H., Rozov, A. & Monyer, H. 2007. Functional characterization of intrinsic cholinergic interneurons in the cortex. *Journal of Neuroscience*, 27(21): 5633–5642.

English, J.D. & Sweatt, J.D. 1997. A requirement for the mitogen-activated protein kinase cascade in hippocampal long term potentiation. *Journal of Biological Chemistry*, 272(31): 19103–19106.

Felix-Ortiz, A.C., Burgos-Robles, A., Bhagat, N.D., Leppla, C.A. & Tye, K.M. 2016. Bidirectional modulation of anxiety-related and social behaviors by amygdala projections to the medial prefrontal cortex. *Neuroscience*, 321: 197–209.

Feng, B., Xing, J.-H., Jia, D., Liu, S.-B., Guo, H.-J., Li, X.-Q., He, X.-S. & Zhao, M.-G. 2011. Blocking $\alpha_4\beta_2$ and α_7 nicotinic acetylcholine receptors inhibits the reinstatement of morphine-induced CPP by drug priming in mice. *Behavioural Brain Research*, 220(1): 100–105.

Fernandes, C., Hoyle, E., Dempster, E., Schalkwyk, L.C. & Collier, D.A. 2006. Performance deficit of alpha7 nicotinic receptor knockout mice in a delayed matching-to-place task suggests a mild impairment of working/episodic-like memory. *Genes, Brain and Behavior*, 5(6): 433–440.

Floresco, S.B. & Grace, A.A. 2003. Gating of hippocampal-evoked activity in prefrontal cortical neurons by inputs from the mediodorsal thalamus and ventral tegmental area. *Journal of Neuroscience*, 23(9): 3930–3943.

Floresco, S.B., Seamans, J.K. & Phillips, A.G. 1997. Selective roles for hippocampal, prefrontal cortical, and ventral striatal circuits in radial-arm maze tasks with or without a delay. *Journal of Neuroscience*, 17(5): 1880–1890.

Freeman, W. 1948. Transorbital leucotomy. *Lancet*, 252(6523): 371–373.

Fuchs, J.L. 1989. [125I]alpha-bungarotoxin binding marks primary sensory area developing rat neocortex. *Brain Research*, 501(2): 223–234.

Fucile, S. 2004. Ca2+ permeability of nicotinic acetylcholine receptors. *Cell Calcium*, 35(1): 1–8.

Fujii, S. & Sumikawa, K. 2001. Nicotine accelerates reversal of long-term potentiation and enhances long-term depression in the rat hippocampal CA1 region. *Brain Research*, 894(2): 340–346.

Fujii, S., Jia, Y.S., Yan, A.Z. & Sumikawa, K. 2000. Nicotine reverses GABAergic inhibition of long-term potentiation induction in the hippocampal CA1 region. *Brain Research*, 863(1-2): 259–265.

Gabbott, P., Headlam, A. & Busby, S. 2002. Morphological evidence that CA1 hippocampal afferents monosynaptically innervate PV-containing neurons and NADPH-diaphorase reactive cells in the medial prefrontal cortex (Areas 25/32) of the rat. *Brain Research*, 946(2): 314–322.

Gabbott, P.L.A., Warner, T.A. & Busby, S.J. 2006. Amygdala input monosynaptically innervates parvalbumin immunoreactive local circuit neurons in rat medial prefrontal cortex. *Neuroscience*, 139(3): 1039–1048.

Gabbott, P.L.A., Warner, T.A., Jays, P.R.L., Salway, P. & Busby, S.J. 2005. Prefrontal cortex in the rat: projections to subcortical autonomic, motor, and limbic centers. *Journal of Comparative Neurology*, 492(2): 145–177.

Gao, M., Jin, Y., Yang, K., Zhang, D., Lukas, R.J. & Wu, J. 2010. Mechanisms involved in systemic nicotine-induced glutamatergic synaptic plasticity on dopamine neurons in the ventral tegmental area. *Journal of Neuroscience*, 30(41): 13814–13825.

Garzón, M., Duffy, A.M., Chan, J., Lynch, M.-K., Mackie, K. & Pickel, V.M. 2013. Dopamine D_2 and acetylcholine α7 nicotinic receptors have subcellular distributions favoring mediation of convergent signaling in the mouse ventral tegmental area. *Neuroscience*, 252: 126–143.

Ge, S. 2005. Nicotinic Acetylcholine Receptors at Glutamate Synapses Facilitate Long-Term Depression or Potentiation. *Journal of Neuroscience*, 25(26): 6084–6091.

Gemmell, C. & O'Mara, S.M. 2000. Long-term potentiation and paired-pulse facilitation in the prelimbic cortex of the rat following stimulation in the contralateral hemisphere in vivo. *Experimental Brain Research*, 132(2): 223–229.

Germano, C. & Kinsella, G.J. 2005. Working memory and learning in early Alzheimer's disease. *Neuropsychology Review*, 15(1): 1–10.

Ghoshal, A. & Conn, P.J. 2015. The hippocampo-prefrontal pathway: a possible therapeutic target for negative and cognitive symptoms of schizophrenia. *Future Neurology*, 10(2): 115–128.

Giniatullin, R., Nistri, A. & Yakel, J.L. 2005. Desensitization of nicotinic ACh receptors: shaping cholinergic signaling. *Trends in Neurosciences*, 28(7): 371–378.

Gioanni, Y., Rougeot, C., Clarke, P.B., Lepousé, C., Thierry, A.M. & VIDAL, C. 1999. Nicotinic receptors in the rat prefrontal cortex: increase in glutamate release and facilitation of mediodorsal thalamo-cortical transmission. *European Journal of Neuroscience*, 11(1): 18–30.

Godsil, B.P., Kiss, J.P., Spedding, M. & Jay, T.M. 2013. The hippocampal-prefrontal pathway: the weak link in psychiatric disorders? *European Neuropsychopharmacology*, 23(10): 1165–1181.

Gogtay, N., Giedd, J.N., Lusk, L., Hayashi, K.M., Greenstein, D., Vaituzis, A.C., Nugent, T.F., Herman, D.H., Clasen, L.S., Toga, A.W., Rapoport, J.L. & Thompson, P.M. 2004. Dynamic mapping of human cortical development during childhood through early adulthood. *PNAS*, 101(21): 8174–8179.

Goldman-Rakic, P.S. 1995. Cellular basis of working memory. *Neuron*, 14(3): 477–485.

Goldstein, R.Z. & Volkow, N.D. 2002. Drug addiction and its underlying neurobiological basis: Neuroimaging evidence for the involvement of the frontal cortex. *American Journal of Psychiatry*, 159(10): 1642–1652.

Good, C.H. & Lupica, C.R. 2009. Properties of distinct ventral tegmental area synapses activated via pedunculopontine or ventral tegmental area stimulation in vitro. *Journal of Physiology*, 587(6): 1233–1247.

Gorelova, N., Mulholland, P.J., Chandler, L.J. & Seamans, J.K. 2012. The glutamatergic component of the mesocortical pathway emanating from different subregions of the ventral midbrain. *Cerebral Cortex*, 22(2): 327–336.

Goriounova, N.A. & Mansvelder, H.D. 2012a. Nicotine exposure during adolescence alters the rules for prefrontal cortical synaptic plasticity during adulthood. *Frontiers in Synaptic Neuroscience*, 4(3), doi:10.3389/fnsyn.2012.00003.

Goriounova, N.A. & Mansvelder, H.D. 2012b. Nicotine Exposure during Adolescence Leads to Short- and Long-Term Changes in Spike Timing-Dependent Plasticity in Rat Prefrontal Cortex. *Journal of Neuroscience*, 32(31): 10484–10493.

Goto, Y. & Grace, A.A. 2006. Alterations in medial prefrontal cortical activity and plasticity in rats with disruption of cortical development. *Biological Psychiatry*, 60(11): 1259–1267.

Gotti, C., Zoli, M. & Clementi, F. 2006. Brain nicotinic acetylcholine receptors: native subtypes and their relevance. *Trends in Pharmacological Sciences*, 27(9): 482–491.

Gray, R., Rajan, A.S., Radcliffe, K.A., Yakehiro, M. & Dani, J.A. 1996. Hippocampal synaptic transmission enhanced by low concentrations of nicotine. *Nature*, 383(6602): 713–716.

Griffin, A.L. 2015. Role of the thalamic nucleus reuniens in mediating interactions between the hippocampus and medial prefrontal cortex during spatial working memory. *Frontiers in Systems Neuroscience*, 9(29), doi:10.3389/fnsys.2015.00029.

Gritton, H.J., Howe, W.M., Mallory, C.S., Hetrick, V.L., Berke, J.D. & Sarter, M. 2016. Cortical cholinergic signaling controls the detection of cues. *PNAS,* 113(8): 1089-1097

Gu, Z. & Yakel, J.L. 2011. Timing-dependent septal cholinergic induction of dynamic hippocampal synaptic plasticity. *Neuron*, 71(1): 155–165.

Gu, Z., Lamb, P.W. & Yakel, J.L. 2012. Cholinergic coordination of presynaptic and postsynaptic activity induces timing-dependent hippocampal synaptic plasticity. *Journal of Neuroscience*, 32(36): 12337–12348.

Gubbins, E.J., Gopalakrishnan, M. & Li, J. 2010. Alpha7 nAChR-mediated activation of MAP kinase pathways in PC12 cells. *Brain Research*, 1328: 1–11.

Guillem, K., Bloem, B., Poorthuis, R.B., Loos, M., Smit, A.B., Maskos, U., Spijker, S. & Mansvelder, H.D. 2011. Nicotinic Acetylcholine Receptor 2 Subunits in the Medial Prefrontal Cortex Control Attention. *Science*, 333(6044): 888–891.

Gulledge, A.T., Park, S.B., Kawaguchi, Y. & Stuart, G.J. 2007. Heterogeneity of phasic cholinergic signaling in neocortical neurons. *Journal of Neurophysiology*, 97(3): 2215–2229.

Guzman, S.J., Schmidt, H., Franke, H., Krügel, U., Eilers, J., Illes, P. & Gerevich, Z. 2010. P2Y1 receptors inhibit long-term depression in the prefrontal cortex. *Neuropharmacology*, 59(6): 406–415.

Hahn, B., Sharples, C.G.V., Wonnacott, S., Shoaib, M. & Stolerman, I.P. 2003. Attentional effects of nicotinic agonists in rats. *Neuropharmacology*, 44(8): 1054–1067.

Hahn, B., Shoaib, M. & Stolerman, I.P. 2011. Selective nicotinic receptor antagonists: effects on attention and nicotine-induced attentional enhancement. *Psychopharmacology*, 217(1): 75–82.

Hajós, M., Hurst, R.S., Hoffmann, W.E., Krause, M., Wall, T.M., Higdon, N.R. & Groppi, V.E. 2005. The selective alpha7 nicotinic acetylcholine receptor agonist PNU-282987 [N-[(3R)-1-Azabicyclo[2.2.2]oct-3-yl]-4-chlorobenzamide hydrochloride] enhances GABAergic synaptic activity in brain slices and restores auditory gating deficits in anesthetized rats. *Journal of Pharmacology and Experimental Therapeutics*, 312(3): 1213–1222.

Han, K.-S., Woo, J., Park, H., Yoon, B.-J., Choi, S. & Lee, C.J. 2013. Channel-mediated astrocytic glutamate release via Bestrophin-1 targets synaptic NMDARs. *Molecular Brain*, 6(4): doi: 10.1186/1756-6606-6-4.

Hansel, C., Artola, A. & Singer, W. 1997. Relation between dendritic Ca2+ levels and the polarity of synaptic long-term modifications in rat visual cortex neurons. *European Journal of Neuroscience*, 9(11): 2309–2322.

Hansen, H.H., Timmermann, D.B., Peters, D., Walters, C., Damaj, M.I. & Mikkelsen, J.D. 2007. Alpha-7 nicotinic acetylcholine receptor agonists selectively activate limbic regions of the rat forebrain: an effect similar to antipsychotics. *Journal of Neuroscience Research*, 85(8): 1810–1818.

Harrison, P.J. & Weinberger, D.R. 2005. Schizophrenia genes, gene expression, and neuropathology: on the matter of their convergence. *Molecular Psychiatry*, 10(1): 40–68.

Harvey, J. & Collingridge, G.L. 1992. Thapsigargin blocks the induction of long-term potentiation in rat hippocampal slices. *Neuroscience Letters*, 139(2): 197–200.

Hashimoto, T., Volk, D.W., Eggan, S.M., Mirnics, K., Pierri, J.N., Sun, Z., Sampson, A.R. & Lewis, D.A. 2003. Gene expression deficits in a subclass of GABA neurons in the prefrontal cortex of subjects with schizophrenia. *Journal of Neuroscience*, 23(15): 6315–6326.

Hebb, D.O. 1949. *The Organization of Behavior*. Psychology Press.

Hedrick, T. & Waters, J. 2015. Acetylcholine excites neocortical pyramidal neurons via nicotinic receptors. *Journal of Neurophysiology*, 113(7): 2195–2209.

Heidbreder, C.A. & Groenewegen, H.J. 2003. The medial prefrontal cortex in the rat: evidence for a dorso-ventral distinction based upon functional and anatomical characteristics. *Neuroscience and Biobehavioral Reviews*, 27(6): 555–579.

Hempel, C.M., Hartman, K.H., Wang, X.J., Turrigiano, G.G. & Nelson, S.B. 2000. Multiple forms of short-term plasticity at excitatory synapses in rat medial prefrontal cortex. *Journal of Neurophysiology*, 83(5): 3031–3041.

Henny, P. & Jones, B.E. 2008. Projections from basal forebrain to prefrontal cortex comprise cholinergic, GABAergic and glutamatergic inputs to pyramidal cells or interneurons. *European Journal of Neuroscience*, 27(3): 654–670.

Herry, C. & Garcia, R. 2002. Prefrontal cortex long-term potentiation, but not long-term depression, is associated with the maintenance of extinction of learned fear in mice. *Journal of Neuroscience*, 22(2): 577–583.

Herry, C., Ciocchi, S., Senn, V., Demmou, L., Müller, C. & Lüthi, A. 2008. Switching on and off fear by distinct neuronal circuits. *Nature*, 454(7204): 600–606.

Higley, M.J. & Picciotto, M.R. 2014. Neuromodulation by acetylcholine: examples from schizophrenia and depression. *Current Opinion in Neurobiology*, 29: 88–95.

Hirsch, J.C. & Crepel, F. 1991. Blockade of NMDA receptors unmasks a long-term depression in synaptic efficacy in rat prefrontal neurons in vitro. *Experimental Brain Research*, 85(3): 621–624.

Hirsch, J.C. & Crepel, F. 1992. Postsynaptic calcium is necessary for the induction of LTP and LTD of monosynaptic EPSPs in prefrontal neurons: an in vitro study in the rat. *Synapse*, 10(2): 173–175.

Hoover, W.B. & Vertes, R.P. 2007. Anatomical analysis of afferent projections to the medial prefrontal cortex in the rat. *Brain Structure & Function*, 212(2): 149–179.

Huang, C.-C. & Hsu, K.-S. 2008. The role of NMDA receptors in regulating group II metabotropic glutamate receptor-mediated long-term depression in rat medial prefrontal cortex. *Neuropharmacology*, 54(7): 1071–1078.

Huang, M., Felix, A.R., Kwon, S., Lowe, D., Wallace, T., Santarelli, L. & Meltzer, H.Y. 2014. The alpha-7 nicotinic receptor partial agonist/5-HT3 antagonist RG3487 enhances cortical and hippocampal dopamine and acetylcholine release. *Psychopharmacology*, 231(10): 2199–2210.

Huang, Y.Y., Simpson, E., Kellendonk, C. & Kandel, E.R. 2004. Genetic evidence for the bidirectional modulation of synaptic plasticity in the prefrontal cortex by D1 receptors. *PNAS*, 101(9): 3236–3241.

Hugues, S., Chessel, A., Lena, I., Marsault, R. & Garcia, R. 2006. Prefrontal infusion of PD098059 immediately after fear extinction training blocks extinction-associated prefrontal synaptic plasticity and decreases prefrontal ERK2 phosphorylation. *Synapse*, 60(4): 280–287.

Hurst, R.S., Hajós, M., Raggenbass, M., Wall, T.M., Higdon, N.R., Lawson, J.A., Rutherford-Root, K.L., Berkenpas, M.B., Hoffmann, W.E., Piotrowski, D.W., Groppi, V.E., Allaman, G., Ogier, R., Bertrand, S., Bertrand, D. & Arneric, S.P. 2005. A novel positive allosteric modulator of the alpha7 neuronal nicotinic acetylcholine receptor: in vitro and in vivo characterization. *Journal of Neuroscience*, 25(17): 4396–4405.

Jay, T.M. & Witter, M.P. 1991. Distribution of hippocampal CA1 and subicular efferents in the prefrontal cortex of the rat studied by means of anterograde transport of Phaseolus vulgaris-leucoagglutinin. *Journal of Comparative Neurology*, 313(4): 574–586.

Jay, T.M., Burette, F. & Laroche, S. 1995. NMDA receptor-dependent long-term potentiation in the hippocampal afferent fibre system to the prefrontal cortex in the rat. *European journal of neuroscience*, 7(2): 247–250.

Jay, T.M., Burette, F. & Laroche, S. 1996. Plasticity of the hippocampal-prefrontal cortex synapses. *Journal of Physiology*, 90(5-6): 361–366.

Ji, D., Lape, R. & Dani, J.A. 2001. Timing and location of nicotinic activity enhances or depresses hippocampal synaptic plasticity. *Neuron*, 31(1): 131–141.

Jin, Y., Yang, K., Wang, H. & Wu, J. 2011. Exposure of nicotine to ventral tegmental area slices induces glutamatergic synaptic plasticity on dopamine neurons. *Synapse*, 65(4): 332–338.

John, D. & Berg, D.K. 2015. Long-lasting changes in neural networks to compensate for altered nicotinic input. *Biochemical Pharmacology*, 97(4): 418–424.

Johnston, D. & Brown, T.H. 1983. Interpretation of voltage-clamp measurements in hippocampal neurons. *Journal of Neurophysiology*, 50(2): 464–486.

Jones, I.W. & Wonnacott, S. 2004. Precise localization of alpha7 nicotinic acetylcholine receptors on glutamatergic axon terminals in the rat ventral tegmental area. *Journal of Neuroscience*, 24(50): 11244–11252.

Josselyn, S.A. & Nguyen, P.V. 2005. CREB, synapses and memory disorders: past progress and future challenges. *Current Drug Targets. CNS and Neurological Disorders*, 4(5): 481–497.

Jung, M.W., Baeg, E.H., Kim, M.J., Kim, Y.B. & Kim, J.J. 2008. Plasticity and memory in the prefrontal cortex. *Reviews in the Neurosciences*, 19(1): 29–46.

Jurado, M.B. & Rosselli, M. 2007. The elusive nature of executive functions: a review of our current understanding. *Neuropsychology Review*, 17(3): 213–233.

Kaiser, S. & Wonnacott, S. 2000. alpha-bungarotoxin-sensitive nicotinic receptors indirectly modulate [(3)H]dopamine release in rat striatal slices via glutamate release. *Molecular Pharmacology*, 58(2): 312–318.

Kalappa, B.I., Gusev, A.G. & Uteshev, V.V. 2010. Activation of Functional α7-Containing nAChRs in Hippocampal CA1 Pyramidal Neurons by Physiological Levels of Choline in the Presence of PNU-120596. *PLoS ONE*, 5(11): doi: 10.1371/journal.pone.0013964

Katz, B. & Miledi, R. 1968. The role of calcium in neuromuscular facilitation. *Journal of Physiology*, 195(2): 481–492.

Kawai, H., Lazar, R. & Metherate, R. 2007. Nicotinic control of axon excitability regulates thalamocortical transmission. *Nature Neuroscience*, 10(9): 1168–1175.

Kemp, N. & Bashir, Z.I. 2001. Long-term depression: a cascade of induction and expression mechanisms. *Progress in Neurobiology*, 65(4): 339–365.

Kihara, T., Shimohama, S., Sawada, H., Honda, K., Nakamizo, T., Shibasaki, H., Kume, T. & Akaike, A. 2001. alpha 7 nicotinic receptor transduces signals to phosphatidylinositol 3-kinase to block A beta-amyloid-induced neurotoxicity. *Journal of Biological Chemistry*, 276(17): 13541–13546.

Kilkenny, C., Browne, W., Cuthill, I.C., Emerson, M., Altman, D.G.NC3Rs Reporting Guidelines Working Group. 2010. Animal research: reporting in vivo experiments: the ARRIVE guidelines. *British Journal of Pharmacology*, 160(7): 1577–1579.

Kimura, F. & Baughman, R.W. 1997. Distinct muscarinic receptor subtypes suppress excitatory and inhibitory synaptic responses in cortical neurons. *Journal of Neurophysiology*, 77(2): 709–716.

Klapoetke, N.C., Murata, Y., Kim, S.S., Pulver, S.R., Birdsey-Benson, A., Cho, Y.K., Morimoto, T.K., Chuong, A.S., Carpenter, E.J., Tian, Z., Wang, J., Xie, Y., Yan, Z., Zhang, Y., Chow, B.Y., Surek, B., Melkonian, M., Jayaraman, V., Constantine-Paton, M., Wong, G.K.-S. & Edward S Boyden, E.S.B. 2014. Independent optical excitation of distinct neural populations. *Nature Methods*, 11(9): 972.

Knight, R.T. 1984. Decreased response to novel stimuli after prefrontal lesions in man. *Electroencephalography and Clinical Neurophysiology*, 59(1): 9–20.

Koester, H.J. & Sakmann, B. 1998. Calcium dynamics in single spines during coincident pre- and postsynaptic activity depend on relative timing of back-propagating action potentials and subthreshold excitatory postsynaptic potentials. *PNAS*, 95(16): 9596–9601.

Kohl, M.M., Shipton, O.A., Deacon, R.M., Rawlins, J.N.P., Deisseroth, K. & Paulsen, O. 2011. Hemisphere-specific optogenetic stimulation reveals left-right asymmetry of hippocampal plasticity. *Nature Neuroscience*, 14(11): 1413–1415.

Kolb, B., Buhrmann, K., McDonald, R. & Sutherland, R.J. 1994. Dissociation of the medial prefrontal, posterior parietal, and posterior temporal cortex for spatial navigation and recognition memory in the rat. *Cerebral Cortex*, 4(6): 664–680.

Kolomiets, B., Marzo, A., Caboche, J., Vanhoutte, P. & Otani, S. 2009. Background Dopamine Concentration Dependently Facilitates Long-term Potentiation in Rat Prefrontal Cortex through Postsynaptic Activation of Extracellular Signal-Regulated Kinases. *Cerebral Cortex*, 19(11): 2708–2718.

Konradsson-Geuken, A., Gash, C.R., Alexander, K., Pomerleau, F., Huettl, P., Gerhardt, G.A. & Bruno, J.P. 2009. Second-by-second analysis of alpha 7 nicotine receptor regulation of glutamate release in the prefrontal cortex of awake rats. *Synapse*, 63(12): 1069–1082.

Kouhen, El, R., Hu, M., Anderson, D.J., Li, J. & Gopalakrishnan, M. 2009. Pharmacology of alpha7 nicotinic acetylcholine receptor mediated extracellular signal-regulated kinase signalling in PC12 cells. *British Journal of Pharmacology*, 156(4): 638–648.

Kroker, K.S., Rast, G. & Rosenbrock, H. 2011. Differential effects of subtype-specific nicotinic acetylcholine receptor agonists on early and late hippocampal LTP. *European Journal of Pharmacology*, 671(1-3): 26–32.

Kruglikov, I. & Rudy, B. 2008. Perisomatic GABA release and thalamocortical integration onto neocortical excitatory cells are regulated by neuromodulators. *Neuron*, 58(6): 911–924.

Kumar, A., Singh, A. & Ekavali. 2015. A review on Alzheimer's disease pathophysiology and its management: an update. *Pharmacological Reports*, 67(2): 195–203.

Kuperberg, G.R., Broome, M.R., McGuire, P.K., David, A.S., Eddy, M., Ozawa, F., Goff, D., West, W.C., Williams, S.C.R., van der Kouwe, A.J.W., Salat, D.H., Dale, A.M. & Fischl, B. 2003. Regionally localized thinning of the cerebral cortex in schizophrenia. *Archives of General Psychiatry*, 60(9): 878–888.

Kvitsiani, D., Ranade, S., Hangya, B., Taniguchi, H., Huang, J.Z. & Kepecs, A. 2013. Distinct behavioural and network correlates of two interneuron types in prefrontal cortex. *Nature*, 498(7454): 363–366.

Lafourcade, M., Elezgarai, I., Mato, S., Bakiri, Y., Grandes, P. & Manzoni, O.J. 2007. Molecular components and functions of the endocannabinoid system in mouse prefrontal cortex. *PLoS ONE*, 2(8): doi: 10.1371/journal.pone.0000709

Lagostena, L., Trocme-Thibierge, C., Morain, P. & Cherubini, E. 2008. The partial α7 nicotine acetylcholine receptor agonist S 24795 enhances long-term potentiation at CA3-CA1 synapses in the adult mouse hippocampus. *Neuropharmacology*, 54(4): 676–685.

Lambe, E.K., Picciotto, M.R. & Aghajanian, G.K. 2003. Nicotine induces glutamate release from thalamocortical terminals in prefrontal cortex. *Neuropsychopharmacology*, 28(2): 216–225.

Laroche, S., Davis, S. & Jay, T.M. 2000. Plasticity at hippocampal to prefrontal cortex synapses: Dual roles in working memory and consolidation. *Hippocampus*, 10(4): 438–446.

Lee, A.T., Gee, S.M., Vogt, D., Patel, T., Rubenstein, J.L. & Sohal, V.S. 2014. Pyramidal neurons in prefrontal cortex receive subtype-specific forms of excitation and inhibition. *Neuron*, 81(1): 61–68.

Lench, A., Chamberlain S., Wonnacott, S., Jones, R. 2008. α 7 nicotinic acetylcholine receptors facilitate spontaneous glutamate release in the rat prefrontal cortex. *From the BPS Focused Meeting, Brighton, Winter 2008: Proceedings of the British Pharmacological Society at* http://www.pa2online.org/abstracts/Vol6Issue4abst143P.pdf

Lendvai, B. & Vizi, E.S. 2008. Nonsynaptic chemical transmission through nicotinic acetylcholine receptors. *Physiological Reviews*, 88(2): 333–349.

Leonard, S. & Freedman, R. 2006. Genetics of chromosome 15q13-q14 in schizophrenia. *Biological Psychiatry*, 60(2): 115–122.

Levin, E.D., Bettegowda, C., Blosser, J. & Gordon, J. 1999. AR-R17779, and alpha7 nicotinic agonist, improves learning and memory in rats. *Behavioural Pharmacology*, 10(6-7): 675–680.

Lewis, D.A. & Gonzalez-Burgos, G. 2008. Neuroplasticity of neocortical circuits in schizophrenia. *Neuropsychopharmacology*, 33(1): 141–165.

Léna, C. & Changeux, J.P. 1997. Role of Ca2+ ions in nicotinic facilitation of GABA release in mouse thalamus. *Journal of Neuroscience*, 17(2): 576–585.

Li, X., Rainnie, D.G., McCarley, R.W. & Greene, R.W. 1998. Presynaptic nicotinic receptors facilitate monoaminergic transmission. *Journal of Neuroscience*, 18(5): 1904–1912.

Lisman, J. 1989. A mechanism for the Hebb and the anti-Hebb processes underlying learning and memory. *PNAS*, 86(23): 9574–9578.

Little, J.P. & Carter, A.G. 2012. Subcellular Synaptic Connectivity of Layer 2 Pyramidal Neurons in the Medial Prefrontal Cortex. *Journal of Neuroscience*, 32(37): 12808–12819.

Little, J.P. & Carter, A.G. 2013. Synaptic mechanisms underlying strong reciprocal connectivity between the medial prefrontal cortex and basolateral amygdala. *Journal of Neuroscience*, 33(39): 15333–15342.

Livingstone, P.D. & Wonnacott, S. 2009. Nicotinic acetylcholine receptors and the ascending dopamine pathways. *Biochemical Pharmacology*, 78(7): 744–755.

Livingstone, P.D., Dickinson, J.A., Srinivasan, J., Kew, J.N.C. & Wonnacott, S. 2009. Glutamate–Dopamine Crosstalk in the Rat Prefrontal Cortex is Modulated by Alpha7 Nicotinic Receptors and Potentiated by PNU-120596. *Journal of Molecular Neuroscience*, 40(1-2): 172–176.

Livingstone, P.D., Srinivasan, J., Kew, J.N.C., Dawson, L.A., Gotti, C., Moretti, M., Shoaib, M. & Wonnacott, S. 2009. α7 and non-α7 nicotinic acetylcholine receptors modulate dopamine release in vitroand in vivoin the rat prefrontal cortex. *European Journal of Neuroscience*, 29(3): 539–550.

Lo, A.C., Iscru, E., Blum, D., Tesseur, I., Callaerts-Vegh, Z., Buée, L., De Strooper, B., Balschun, D. & D'Hooge, R. 2013. Amyloid and tau neuropathology differentially affect prefrontal synaptic plasticity and cognitive performance in mouse models of Alzheimer's disease. *Journal of Alzheimer's Disease,* 37(1): 109–125.

Lombardo, S. & Maskos, U. 2015. Role of the nicotinic acetylcholine receptor in Alzheimer's disease pathology and treatment. *Neuropharmacology*, 96: 255–262.

Lopes-Aguiar, C., Bueno-Junior, L.S., Ruggiero, R.N., Romcy-Pereira, R.N. & Leite, J.P. 2013. NMDA receptor blockade impairs the muscarinic conversion of sub-threshold transient depression into long-lasting LTD in the hippocampus-prefrontal cortex pathway in vivo: correlation with γ oscillations. *Neuropharmacology*, 65: 143–155.

Lubin, M., Erisir, A. & Aoki, C. 1999. Ultrastructural immunolocalization of the alpha 7 nAChR subunit in guinea pig medial prefrontal cortex. *Annals of the New York Academy of Sciences*, 868: 628–632.

Lucas-Meunier, E., Monier, C., Amar, M., Baux, G., Frégnac, Y. & Fossier, P. 2009. Involvement of nicotinic and muscarinic receptors in the endogenous cholinergic modulation of the balance between excitation and inhibition in the young rat visual cortex. *Cerebral Cortex*, 19(10): 2411–2427.

Luetje, C.W. 2004. Getting past the asterisk: the subunit composition of presynaptic nicotinic receptors that modulate striatal dopamine release. *Molecular Pharmacology*, 65(6): 1333–1335.

Lugon, M.D.M.V., Batsikadze, G., Fresnoza, S., Grundey, J., Kuo, M.-F., Paulus, W., Nakamura-Palacios, E.M. & Nitsche, M.A. 2015. Mechanisms of Nicotinic Modulation of Glutamatergic Neuroplasticity in Humans. *Cerebral Cortex*, Oct(2015): doi: 10.1093/cercor/bhv252

Lynch, G., Larson, J., Kelso, S., Barrionuevo, G. & Schottler, F. 1983. Intracellular injections of EGTA block induction of hippocampal long-term potentiation. *Nature*, 305(5936): 719–721.

Lynch, M.A. 2004. Long-term potentiation and memory. *Physiological reviews*, 84(1): 87–136.

Ma, J., Duan, Y., Qin, Z., Wang, J., Liu, W., Xu, M., Zhou, S. & Cao, X. 2015. Overexpression of αCaMKII impairs behavioral flexibility and NMDAR-dependent long-term depression in the medial prefrontal cortex. *Neuroscience*, 310: 528–540.

Macmillan, M. 2002. *An Odd Kind of Fame*. MIT Press.

Magee, J.C. 2000. Dendritic integration of excitatory synaptic input. *Nature Reviews Neuroscience*, 1(3): 181–190.

Magee, J.C. & Johnston, D. 1997. A synaptically controlled, associative signal for Hebbian plasticity in hippocampal neurons. *Science*, 275(5297): 209–213.

Makino, H. & Malinow, R. 2009. AMPA receptor incorporation into synapses during LTP: the role of lateral movement and exocytosis. *Neuron*, 64(3): 381–390.

Makris, N., Buka, S.L., Biederman, J., Papadimitriou, G.M., Hodge, S.M., Valera, E.M., Brown, A.B., Bush, G., Monuteaux, M.C., Caviness, V.S., Kennedy, D.N. & Seidman, L.J. 2008. Attention and executive systems abnormalities in adults with childhood ADHD: A DT-MRI study of connections. *Cerebral Cortex*, 18(5): 1210–1220.

Malenka, R.C. & Nicoll, R.A. 1993. NMDA-receptor-dependent synaptic plasticity: multiple forms and mechanisms. *Trends in Neurosciences*, 16(12): 521–527.

Malenka, R.C., Kauer, J.A., Zucker, R.S. & Nicoll, R.A. 1988. Postsynaptic calcium is sufficient for potentiation of hippocampal synaptic transmission. *Science*, 242(4875): 81–84.

Malinow, R., Schulman, H. & Tsien, R.W. 1989. Inhibition of postsynaptic PKC or CaMKII blocks induction but not expression of LTP. *Science*, 245(4920): 862–866.

Mansour, A., Fox, C.A., Thompson, R.C., Akil, H. & Watson, S.J. 1994. mu-Opioid receptor mRNA expression in the rat CNS: comparison to mu-receptor binding. *Brain Research*, 643(1-2): 245–265.

Mansvelder, H.D. & McGehee, D.S. 2000. Long-term potentiation of excitatory inputs to brain reward areas by nicotine. *Neuron*, 27(2): 349–357.

Mansvelder, H.D., Keath, J.R. & McGehee, D.S. 2002. Synaptic mechanisms underlie nicotine-induced excitability of brain reward areas. *Neuron*, 33(6): 905–919.

Mao, D., Gallagher, K. & McGehee, D.S. 2011. Nicotine potentiation of excitatory inputs to ventral tegmental area dopamine neurons. *Journal of Neuroscience*, 31(18): 6710–6720.

Marchi, M. & Raiteri, M. 1996. Nicotinic autoreceptors mediating enhancement of acetylcholine release become operative in conditions of "impaired'' cholinergic presynaptic function. *Journal of Neurochemistry*, 67(5): 1974–1981.

Marchi, M., Risso, F., Viola, C., Cavazzani, P. & Raiteri, M. 2002. Direct evidence that release-stimulating alpha7* nicotinic cholinergic receptors are localized on human and rat brain glutamatergic axon terminals. *Journal of Neurochemistry*, 80(6): 1071–1078.

Marek, G.J. & Aghajanian, G.K. 1998. 5-Hydroxytryptamine-induced excitatory postsynaptic currents in neocortical layer V pyramidal cells: suppression by mu-opiate receptor activation. *Neuroscience*, 86(2): 485–497.

Marek, G.J., Wright, R.A., Gewirtz, J.C. & Schoepp, D.D. 2001. A major role for thalamocortical afferents in serotonergic hallucinogen receptor function in the rat neocortex. *Neuroscience*, 105(2): 379–392.

Maroun, M. & Richter-Levin, G. 2003. Exposure to acute stress blocks the induction of long-term potentiation of the amygdala-prefrontal cortex pathway in vivo. *Journal of Neuroscience*, 23(11): 4406–4409.

Martin-Ruiz, C.M., Haroutunian, V.H., Long, P., Young, A.H., Davis, K.L., Perry, E.K. & Court, J.A. 2003. Dementia rating and nicotinic receptor expression in the prefrontal cortex in schizophrenia. *Biological Psychiatry*, 54(11): 1222–1233.

Marzo, A., Bai, J., Caboche, J., Vanhoutte, P. & Otani, S. 2010. Cellular mechanisms of long-term depression induced by noradrenaline in rat prefrontal neurons. *Neuroscience*, 169(1): 74–86.

Mashour, G.A., Walker, E.E. & Martuza, R.L. 2005. Psychosurgery: past, present, and future. *Brain Research Reviews*, 48(3): 409–419.

Mattinson, C.E., Burmeister, J.J., Quintero, J.E., Pomerleau, F., Huettl, P. & Gerhardt, G.A. 2011. Tonic and phasic release of glutamate and acetylcholine neurotransmission in sub-regions of the rat prefrontal cortex using enzyme-based microelectrode arrays. *Journal of Neuroscience Methods*, 202(2): 199–208.

Mayer, M.L., Westbrook, G.L. & Guthrie, P.B. 1984. Voltage-dependent block by Mg2+ of NMDA responses in spinal cord neurones. *Nature*, 309(5965): 261–263.

McKay, B.E., Placzek, A.N. & Dani, J.A. 2007. Regulation of synaptic transmission and plasticity by neuronal nicotinic acetylcholine receptors. *Biochemical Pharmacology*, 74(8): 1120–1133.

McLean, S., Rothman, R.B. & Herkenham, M. 1986. Autoradiographic localization of mu- and delta-opiate receptors in the forebrain of the rat. *Brain Research*, 378(1): 49–60.

Meredith, R.M., Holmgren, C.D., Weidum, M., Burnashev, N. & Mansvelder, H.D. 2007. Increased threshold for spike-timing-dependent plasticity is caused by unreliable calcium signaling in mice lacking fragile X gene FMR1. *Neuron*, 54(4): 627–638.

Mike, A., Castro, N.G. & Albuquerque, E.X. 2000. Choline and acetylcholine have similar kinetic properties of activation and desensitization on the alpha7 nicotinic receptors in rat hippocampal neurons. *Brain Research*, 882(1-2): 155–168.

Mitchell, A.S. & Chakraborty, S. 2013. What does the mediodorsal thalamus do? *Frontiers in Systems Neuroscience,* 7(37): doi: 10.3389/fnsys.2013.00037

Miwa, J.M., Ibanez-Tallon, I., Crabtree, G.W., Sánchez, R., Sali, A., Role, L.W. & Heintz, N. 1999. lynx1, an endogenous toxin-like modulator of nicotinic acetylcholine receptors in the mammalian CNS. *Neuron*, 23(1): 105–114.

Moghaddam, B. 2003. Bringing order to the glutamate chaos in schizophrenia. *Neuron*, 40(5): 881–884.

Mok, M.H.S. & Kew, J.N.C. 2006. Excitation of rat hippocampal interneurons via modulation of endogenous agonist activity at the alpha7 nicotinic ACh receptor. *Journal of Physiology*, 574(Pt 3): 699–710.

Molina, V., Sanz, J., Reig, S., Martínez, R., Sarramea, F., Luque, R., Benito, C., Gispert, J.D., Pascau, J. & Desco, M. 2005. Hypofrontality in men with first-episode psychosis. *British Journal of Psychiatry*, 186: 203–208.

Molnár, Z. & Cheung, A.F.P. 2006. Towards the classification of subpopulations of layer V pyramidal projection neurons. *Neuroscience Research*, 55(2): 105–115.

Morishita, H., Miwa, J.M., Heintz, N. & Hensch, T.K. 2010. Lynx1, a cholinergic brake, limits plasticity in adult visual cortex. *Science*, 330(6008): 1238–1240.

Morris, S.H., Knevett, S., Lerner, E.G. & Bindman, L.J. 1999. Group I mGluR agonist DHPG facilitates the induction of LTP in rat prelimbic cortex in vitro. *Journal of Neurophysiology*, 82(4): 1927–1933.

Muir, J.L., Everitt, B.J. & Robbins, T.W. 1994. AMPA-induced excitotoxic lesions of the basal forebrain: a significant role for the cortical cholinergic system in attentional function. *Journal of Neuroscience*, 14(4): 2313–2326.

Mulkey, R.M., Endo, S., Shenolikar, S. & Malenka, R.C. 1994. Involvement of a calcineurin/inhibitor-1 phosphatase cascade in hippocampal long-term depression. *Nature*, 369(6480): 486–488.

Munton, R.P., Vizi, S. & Mansuy, I.M. 2004. The role of protein phosphatase-1 in the modulation of synaptic and structural plasticity. *FEBS Letters*, 567(1): 121–128.

Müller, N.G., Machado, L. & Knight, R.T. 2002. Contributions of subregions of the prefrontal cortex to working memory: evidence from brain lesions in humans. *Journal of Cognitive Neuroscience*, 14(5): 673–686.

Nagel, G., Szellas, T., Huhn, W., Kateriya, S., Adeishvili, N., Berthold, P., Ollig, D., Hegemann, P. & Bamberg, E. 2003. Channelrhodopsin-2, a directly light-gated cation-selective membrane channel. *PNAS*, 100(24): 13940–13945.

Nakauchi, S. & Sumikawa, K. 2014. Endogenous ACh suppresses LTD induction and nicotine relieves the suppression via different nicotinic ACh receptor subtypes in the mouse hippocampus. *Life Sciences*, 111(1-2): 62–68.

Nakauchi, S. & Sumikawa, K. 2012. Endogenously released ACh and exogenous nicotine differentially facilitate long-term potentiation induction in the hippocampal CA1 region of mice. *European Journal of Neuroscience*, 35(9): 1381–1395.

Nägerl, U.V., Eberhorn, N., Cambridge, S.B. & Bonhoeffer, T. 2004. Bidirectional activity-dependent morphological plasticity in hippocampal neurons. *Neuron*, 44(5): 759–767.

Neher, E. & Sakmann, B. 1976. Single-channel currents recorded from membrane of denervated frog muscle fibres. *Nature*, 260(5554): 799–802.

Neveu, D. & Zucker, R.S. 1996. Postsynaptic levels of [Ca2+]i needed to trigger LTD and LTP. *Neuron*, 16(3): 619–629.

Nikiforuk, A., Kos, T., Hołuj, M., Potasiewicz, A. & Popik, P. 2016. Positive allosteric modulators of alpha 7 nicotinic acetylcholine receptors reverse ketamine-induced schizophrenia-like deficits in rats. *Neuropharmacology*, 101: 389–400.

Niwa, H., Yamamura, K. & Miyazaki, J. 1991. Efficient selection for high-expression transfectants with a novel eukaryotic vector. *Gene*, 108(2): 193–199.

O'Neill, P.-K., Gordon, J.A. & Sigurdsson, T. 2013. Theta oscillations in the medial prefrontal cortex are modulated by spatial working memory and synchronize with the hippocampus through its ventral subregion. *Journal of Neuroscience*, 33(35): 14211–14224.

Olincy, A., Harris, J.G., Johnson, L.L., Pender, V., Kongs, S., Allensworth, D., Ellis, J., Zerbe, G.O., Leonard, S., Stevens, K.E., Stevens, J.O., Martin, L., Adler, L.E., Soti, F., Kem, W.R. & Freedman, R. 2006. Proof-of-concept trial of an alpha7 nicotinic agonist in schizophrenia. *Archives of General Psychiatry*, 63(6): 630–638.

Otani, S., Bai, J. & Blot, K. 2015. Dopaminergic modulation of synaptic plasticity in rat prefrontal neurons. *Neuroscience Bulletin*, 31(2): 183–190.

Otani, S., Blond, O., DESCE, J.M. & Crepel, F. 1998. Dopamine facilitates long-term depression of glutamatergic transmission in rat prefrontal cortex. *Neuroscience*, 85(3): 669–676.

Otani, S., Daniel, H., Takita, M. & Crepel, F. 2002. Long-term depression induced by postsynaptic group II metabotropic glutamate receptors linked to phospholipase C and intracellular calcium rises in rat prefrontal cortex. *Nneuroscience*, 22(9): 3434–3444.

Paoletti, P., Bellone, C. & Zhou, Q. 2013. NMDA receptor subunit diversity: impact on receptor properties, synaptic plasticity and disease. *Nature Reviews Neuroscience*, 14(6): 383–400.

Papke, R.L. & Porter Papke, J.K. 2002. Comparative pharmacology of rat and human alpha7 nAChR conducted with net charge analysis. *British Journal of Pharmacology*, 137(1): 49–61.

Papke, R.L. & Thinschmidt, J.S. 1998. The correction of alpha7 nicotinic acetylcholine receptor concentration-response relationships in Xenopus oocytes. *Neuroscience Letters*, 256(3): 163–166.

Parent, M.A., Wang, L., Su, J., Netoff, T. & Yuan, L.L. 2010. Identification of the Hippocampal Input to Medial Prefrontal Cortex In Vitro. *Cerebral Cortex*, 20(2): 393–403.

Parikh, V. & Sarter, M. 2008. Cholinergic mediation of attention: contributions of phasic and tonic increases in prefrontal cholinergic activity. *Annals of the New York Academy of Sciences*, 1129: 225–235.

Parikh, V., Ji, J., Decker, M.W. & Sarter, M. 2010. Prefrontal 2 Subunit-Containing and 7 Nicotinic Acetylcholine Receptors Differentially Control Glutamatergic and Cholinergic Signaling. *Journal of Neuroscience*, 30(9): 3518–3530.

Parikh, V., Kozak, R., Martinez, V. & Sarter, M. 2007. Prefrontal acetylcholine release controls cue detection on multiple timescales. *Neuron*, 56(1): 141–154.

Parnaudeau, S., O'Neill, P.-K., Bolkan, S.S., Ward, R.D., Abbas, A.I., Roth, B.L., Balsam, P.D., Gordon, J.A. & Kellendonk, C. 2013. Inhibition of mediodorsal thalamus disrupts thalamofrontal connectivity and cognition. *Neuron*, 77(6): 1151–1162.

Parri, H.R., Hernandez, C.M. & Dineley, K.T. 2011. Research update: Alpha7 nicotinic acetylcholine receptor mechanisms in Alzheimer's disease. *Biochemical Pharmacology*, 82(8): 931–942.

Patti, L., Raiteri, L., Grilli, M., Zappettini, S., Bonanno, G. & Marchi, M. 2007. Evidence that alpha7 nicotinic receptor modulates glutamate release from mouse neocortical gliosomes. *Neurochemistry International*, 51(1): 1–7.

Paulsen, O. & Moser, E.I. 1998. A model of hippocampal memory encoding and retrieval: GABAergic control of synaptic plasticity. *Trends in Neurosciences*, 21(7): 273–278.

Paxinos, G. & Franklin, K.B.J. 2004. *The Mouse Brain in Stereotaxic Coordinates*. Gulf Professional Publishing.

Petilla Interneuron Nomenclature Group, Ascoli, G.A., Alonso-Nanclares, L., Anderson, S.A., Barrionuevo, G., Benavides-Piccione, R., Burkhalter, A., Buzsáki, G., Cauli, B., DeFelipe, J., Fairén, A., Feldmeyer, D., Fishell, G., Frégnac, Y., Freund, T.F., Gardner, D., Gardner, E.P., Goldberg, J.H., Helmstaedter, M., Hestrin, S., Karube, F., Kisvárday, Z.F., Lambolez, B., Lewis, D.A., Marín, O., Markram, H., Muñoz, A., Packer, A., Petersen, C.C.H., Rockland, K.S., Rossier, J., Rudy, B., Somogyi, P., Staiger, J.F., Tamás, G., Thomson, A.M., Toledo-Rodriguez, M., Wang, Y., West, D.C. & Yuste, R. 2008. Petilla terminology: nomenclature of features of GABAergic interneurons of the cerebral cortex. *Nature Reviews Neuroscience*, 9(7): 557–568.

Pettit, D.L., Perlman, S. & Malinow, R. 1994. Potentiated transmission and prevention of further LTP by increased CaMKII activity in postsynaptic hippocampal slice neurons. *Science*, 266(5192): 1881–1885.

Pistillo, F., Clementi, F., Zoli, M. & Gotti, C. 2015. Nicotinic, glutamatergic and dopaminergic synaptic transmission and plasticity in the mesocorticolimbic system: Focus on nicotine effects. *Progress in Neurobiology*, 124C: 1–27.

Pliszka, S.R. 2005. The neuropsychopharmacology of attention-deficit/hyperactivity disorder. *Biological Psychiatry*, 57(11): 1385–1390.

Poorthuis, R.B. & Mansvelder, H.D. 2013. Nicotinic acetylcholine receptors controlling attention: Behavior, circuits and sensitivity to disruption by nicotine. *Biochemical Pharmacology*, 86(8): 1089–1098.

Poorthuis, R.B., Bloem, B., Schak, B., Wester, J., de Kock, C.P.J. & Mansvelder, H.D. 2012. Layer-Specific Modulation of the Prefrontal Cortex by Nicotinic Acetylcholine Receptors. *Cerebral Cortex*, 23(1): 148–161.

Poorthuis, R.B., Bloem, B., Verhoog, M.B. & Mansvelder, H.D. 2013. Layer-specific interference with cholinergic signaling in the prefrontal cortex by smoking concentrations of nicotine. *Journal of Neuroscience*, 33(11): 4843–4853.

Preskorn, S.H., Gawryl, M., Dgetluck, N., Palfreyman, M., Bauer, L.O. & Hilt, D.C. 2014. Normalizing effects of EVP-6124, an α-7 nicotinic partial agonist, on event-related potentials and cognition: a proof of concept, randomized trial in patients with schizophrenia. *Journal of Psychiatric Practice*, 20(1): 12–24.

Preuss, T.M. 1995. Do rats have prefrontal cortex? The rose-woolsey-akert program reconsidered. *Journal of Cognitive Neuroscience*, 7(1): 1–24.

Proulx, É., Piva, M., Tian, M.K., Bailey, C.D.C. & Lambe, E.K. 2014. Nicotinic acetylcholine receptors in attention circuitry: the role of layer VI neurons of prefrontal cortex. *Cellular and Molecular Life Sciences*, 71(7): 1225–1244.

Quik, M., Zhang, D., McGregor, M. & Bordia, T. 2015. Alpha7 nicotinic receptors as therapeutic targets for Parkinson's disease. *Biochemical Pharmacology*, 97(4): 399–407.

Rathouz, M.M. & Berg, D.K. 1994. Synaptic-type acetylcholine receptors raise intracellular calcium levels in neurons by two mechanisms. *Journal of Neuroscience*, 14(11 Pt 2): 6935–6945.

Rein, M.L. & Deussing, J.M. 2012. The optogenetic (r)evolution. *Molecular Genetics and Genomics*, 287(2): 95–109.

Rezvani, A.H., Kholdebarin, E., Brucato, F.H., Callahan, P.M., Lowe, D.A. & Levin, E.D. 2009. Effect of R3487/MEM3454, a novel nicotinic alpha7 receptor partial agonist and 5-HT3 antagonist on sustained attention in rats. *Progress in Neuropsychopharmacology & Biological Psychiatry*, 33(2): 269–275.

Role, L.W. & Berg, D.K. 1996. Nicotinic receptors in the development and modulation of CNS synapses. *Neuron*, 16(6): 1077–1085.

Rose, J.E. & Woolsey, C.N. 1948. The Orbitofrontal Cortex and Its Connections with the Mediodorsal Nucleus in Rabbit, Sheep and Cat. *Association for Research in Nervous and Mental Disease*, 27(1): 210–232.

Rostron, C.L., Farquhar, M.J., Latimer, M.P. & Winn, P. 2008. The pedunculopontine tegmental nucleus and the nucleus basalis magnocellularis: do both have a role in sustained attention? *Biomedical Central Neuroscience,* 9(16), doi: 10.1186/1471-2202-9-16.

Rubia, K., Alegría, A.A. & Brinson, H. 2014. Brain abnormalities in attention-deficit hyperactivity disorder: a review. *Revista de Neurologia*, 58(1): 3–16.

Rubia, K., Overmeyer, S., Taylor, E., Brammer, M., Williams, S.C., Simmons, A. & Bullmore, E.T. 1999. Hypofrontality in attention deficit hyperactivity disorder during higher-order motor control: a study with functional MRI. *American Journal of Psychiatry*, 156(6): 891–896.

Rudy, B., Fishell, G., Lee, S. & Hjerling-Leffler, J. 2011. Three groups of interneurons account for nearly 100% of neocortical GABAergic neurons. *Developmental Neurobiology*, 71(1): 45–61.

Sakaba, T. & Neher, E. 2003. Direct modulation of synaptic vesicle priming by GABA(B) receptor activation at a glutamatergic synapse. *Nature*, 424(6950): 775–778.

Sarter, M., Parikh, V. & Howe, W.M. 2009. Phasic acetylcholine release and the volume transmission hypothesis: time to move on. *Nature Reviews Neuroscience*, 10(5): 383–390.

Schochet, T.L., Kelley, A.E. & Landry, C.F. 2005. Differential expression of arc mRNA and other plasticity-related genes induced by nicotine in adolescent rat forebrain. *Neuroscience*, 135(1): 285–297.

Selig, D.K. & Malenka, R.C. 1997. Extracellular Field Potential Recording in Brain Slices. *Axobits 20*: 7–10.

Semyanov, A. & Kullmann, D.M. 2000. Modulation of GABAergic signaling among interneurons by metabotropic glutamate receptors. *Neuron*, 25(3): 663–672.

Sesack, S.R., Deutch, A.Y., Roth, R.H. & Bunney, B.S. 1989. Topographical organization of the efferent projections of the medial prefrontal cortex in the rat: an anterograde tract-tracing study with Phaseolus vulgaris leucoagglutinin. *Journal of Comparative Neurology*, 290(2): 213–242.

Séguéla, P., Wadiche, J., Dineley-Miller, K., Dani, J.A. & Patrick, J.W. 1993. Molecular cloning, functional properties, and distribution of rat brain alpha 7: a nicotinic cation channel highly permeable to calcium. *Journal of Neuroscience*, 13(2): 596–604.

Sharma, G. & Vijayaraghavan, S. 2003. Modulation of presynaptic store calcium induces release of glutamate and postsynaptic firing. *Neuron*, 38(6): 929–939.

Sharma, G., Grybko, M. & Vijayaraghavan, S. 2008. Action potential-independent and nicotinic receptor-mediated concerted release of multiple quanta at hippocampal CA3-mossy fiber synapses. *Journal of Neuroscience*, 28(10): 2563–2575.

Shi, S.H., Hayashi, Y., Petralia, R.S., Zaman, S.H., Wenthold, R.J., Svoboda, K. & Malinow, R. 1999. Rapid spine delivery and redistribution of AMPA receptors after synaptic NMDA receptor activation. *Science*, 284(5421): 1811–1816.

Shonesy, B.C., Jalan-Sakrikar, N., Cavener, V.S. & Colbran, R.J. 2014. CaMKII: a molecular substrate for synaptic plasticity and memory. *Progress in Molecular Biology and Translational Science*, 122: 61–87.

Silva, A.J., Paylor, R., Wehner, J.M. & Tonegawa, S. 1992. Impaired spatial learning in alpha-calcium-calmodulin kinase II mutant mice. *Science*, 257(5067): 206–211.

Silva, A.J., Stevens, C.F., Tonegawa, S. & Wang, Y. 1992. Deficient hippocampal long-term potentiation in alpha-calcium-calmodulin kinase II mutant mice. *Science*, 257(5067): 201–206.

Sjöström, P.J. & Nelson, S.B. 2002. Spike timing, calcium signals and synaptic plasticity. *Current Opinion in Neurobiology*, 12(3): 305–314.

Smith, M.A., Ellis-Davies, G.C.R. & Magee, J.C. 2003. Mechanism of the distance-dependent scaling of Schaffer collateral synapses in rat CA1 pyramidal neurons. *Journal of Physiology*, 548(1): 245–258.

Soares, M.S., Paiva, W.S., Guertzenstein, E.Z., Amorim, R.L., Bernardo, L.S., Pereira, J.F., Fonoff, E.T. & Teixeira, M.J. 2013. Psychosurgery for schizophrenia: history and perspectives. *Neuropsychiatric Disease and Treatment*, 9: 509–515.

Song, S., Miller, K.D. & Abbott, L.F. 2000. Competitive Hebbian learning through spike-timing-dependent synaptic plasticity. *Nature Neuroscience*, 3(9): 919–926.

Sowell, E.R., Peterson, B.S., Thompson, P.M., Welcome, S.E., Henkenius, A.L. & Toga, A.W. 2003. Mapping cortical change across the human life span. *Nature Neuroscience*, 6(3): 309–315.

Söderman, A., Mikkelsen, J.D., West, M.J., Christensen, D.Z. & Jensen, M.S. 2011. Activation of nicotinic alpha$_7$ acetylcholine receptor enhances long term potentation in wild type mice but not in APP$_{swe}$/PS1deltaE9 mice. *Neuroscience Letters*, 487(3): 325–329.

St Peters, M., Demeter, E., Lustig, C., Bruno, J.P. & Sarter, M. 2011. Enhanced control of attention by stimulating mesolimbic-corticopetal cholinergic circuitry. *Journal of Neuroscience*, 31(26): 9760–9771.

Stephan, K.E., Baldeweg, T. & Friston, K.J. 2006. Synaptic plasticity and dysconnection in schizophrenia. *Biological Psychiatry*, 59(10): 929–939.

Summers, K.L. & Giacobini, E. 1995. Effects of local and repeated systemic administration of (-)nicotine on extracellular levels of acetylcholine, norepinephrine, dopamine, and serotonin in rat cortex. *Neurochemical Research*, 20(6): 753–759.

Tamamaki, N., Yanagawa, Y., Tomioka, R., Miyazaki, J.-I., Obata, K. & Kaneko, T. 2003. Green fluorescent protein expression and colocalization with calretinin, parvalbumin, and somatostatin in the GAD67-GFP knock-in mouse. *Journal of Comparative Neurology*, 467(1): 60–79.

Tang, B., Luo, D., Yang, J., Xu, X.-Y., Zhu, B.-L., Wang, X.-F., Yan, Z. & Chen, G.-J. 2015. Modulation of AMPA receptor mediated current by nicotinic acetylcholine receptor in layer I neurons of rat prefrontal cortex. *Scientific Reports*, 5: doi: 10.1038/srep14099

Teffer, K. & Semendeferi, K. 2012. Human prefrontal cortex: evolution, development, and pathology. *Progress in Research*, 195: 191–218.

Tierney, P.L., Dégenètais, E., Thierry, A.-M., Glowinski, J. & Gioanni, Y. 2004. Influence of the hippocampus on interneurons of the rat prefrontal cortex. *European Journal of Neuroscience*, 20(2): 514–524.

Timmermann, D.B., Grønlien, J.H., Kohlhaas, K.L., Nielsen, E.Ø., Dam, E., Jørgensen, T.D., Ahring, P.K., Peters, D., Holst, D., Christensen, J.K., Chrsitensen, J.K., Malysz, J., Briggs, C.A., Gopalakrishnan, M. & Olsen, G.M. 2007. An allosteric modulator of the alpha7 nicotinic acetylcholine receptor possessing cognition-enhancing properties in vivo. *Journal of Pharmacology and Experimental Therapeutics*, 323(1): 294–307.

Ting, J.T., Daigle, T.L., Chen, Q. & Feng, G. 2014. Acute brain slice methods for adult and aging animals: application of targeted patch clamp analysis and optogenetics. *Methods in Molecular Biology*, 1183: 221–242.

Totah, N.K.B., Kim, Y.B., Homayoun, H. & Moghaddam, B. 2009. Anterior cingulate neurons represent errors and preparatory attention within the same behavioral sequence. *Journal of Neuroscience*, 29(20): 6418–6426.

Unwin, N. 2005. Refined structure of the nicotinic acetylcholine receptor at 4A resolution. *Journal of Molecular Biology*, 346(4): 967–989.

Uteshev, V.V. 2012a. Somatic integration of single ion channel responses of α7 nicotinic acetylcholine receptors enhanced by PNU-120596. *PLoS ONE,* 7(3): doi: 10.1371/journal.pone.0032951

Uteshev, V.V. 2012b. α7 nicotinic ACh receptors as a ligand-gated source of Ca(2+) ions: the search for a Ca(2+) optimum. *Advances in Experimental Medicine and Biology*, 740: 603–638.

Uylings, H.B.M., Groenewegen, H.J. & Kolb, B. 2003. Do rats have a prefrontal cortex? *Behavioural Brain Research*, 146(1-2): 3–17.

Vallés, A.S., Borroni, M.V. & Barrantes, F.J. 2014. Targeting brain α7 nicotinic acetylcholine receptors in Alzheimer's disease: rationale and current status. *CNS drugs*, 28(11): 975–987.

Van De Werd, H.J.J.M., Rajkowska, G., Evers, P. & Uylings, H.B.M. 2010. Cytoarchitectonic and chemoarchitectonic characterization of the prefrontal cortical areas in the mouse. *Brain Structure & Function*, 214(4): 339–353.

Van den Heuvel, M.P. & Fornito, A. 2014. Brain networks in schizophrenia. *Neuropsychology Review*, 24(1): 32–48.

Van den Oever, M.C., Goriounova, N.A., Wan Li, K., Van der Schors, R.C., Binnekade, R., Schoffelmeer, A.N.M., Mansvelder, H.D., Smit, A.B., Spijker, S. & De Vries, T.J. 2008. Prefrontal cortex AMPA receptor plasticity is crucial for cue-induced relapse to heroin-seeking. *Nature Neuroscience*, 11(9): 1053–1058.

Van den Oever, M.C., Spijker, S., Smit, A.B. & De Vries, T.J. 2010. Prefrontal cortex plasticity mechanisms in drug seeking and relapse. *Neuroscience and Biobehavioral Reviews*, 35(2): 276–284.

Vertes, R.P. 2006. Interactions among the medial prefrontal cortex, hippocampus and midline thalamus in emotional and cognitive processing in the rat. *Neuroscience,* 142(1): 1–20.

Vickery, R.M., Morris, S.H. & Bindman, L.J. 1997. Metabotropic glutamate receptors are involved in long-term potentiation in isolated slices of rat medial frontal cortex. *Journal of Neurophysiology*, 78(6): 3039–3046.

Wallace, T.L. & Porter, R.H.P. 2011. Targeting the nicotinic alpha7 acetylcholine receptor to enhance cognition in disease. *Biochemical Pharmacology*, 82(8): 891–903.

Wang, B.-W., Liao, W.-N., Chang, C.-T. & Wang, S.-J. 2006. Facilitation of glutamate release by nicotine involves the activation of a Ca2+/calmodulin signaling pathway in rat prefrontal cortex nerve terminals. *Synapse*, 59(8): 491–501.

Wang, H.Y., Lee, D.H., D'Andrea, M.R., Peterson, P.A., Shank, R.P. & Reitz, A.B. 2000. beta-Amyloid(1-42) binds to alpha7 nicotinic acetylcholine receptor with high affinity. Implications for Alzheimer's disease pathology. *Journal of Biological Chemistry*, 275(8): 5626–5632.

Wang, X., Lippi, G., Carlson, D.M. & Berg, D.K. 2013. Activation of α7-containing nicotinic receptors on astrocytes triggers AMPA receptor recruitment to glutamatergic synapses. *Journal of Neurochemistry*, 127(5): 632–643.

Wang, Y., Neubauer, F.B., Lüscher, H.-R. & Thurley, K. 2010. GABAB receptor-dependent modulation of network activity in the rat prefrontal cortex in vitro. *European Journal of Neuroscience*, 31(9): 1582–1594.

Watakabe, A., Ohtsuka, M., Kinoshita, M., Takaji, M., Isa, K., Mizukami, H., Ozawa, K., Isa, T. & Yamamori, T. 2015. Comparative analyses of adeno-associated viral vector serotypes 1, 2, 5, 8 and 9 in marmoset, mouse and macaque cerebral cortex. *Neuroscience Research*, 93: 144–157.

Welsby, P., Rowan, M. & Anwyl, R. 2006. Nicotinic receptor-mediated enhancement of long-term potentiation involves activation of metabotropic glutamate receptors and ryanodine-sensitive calcium stores in the dentate gyrus. *European Journal of Neuroscience*, 24(11): 3109–3118.

Westphalen, R.I., Gomez, R.S. & Hemmings, H.C. 2009. Nicotinic receptor-evoked hippocampal norepinephrine release is highly sensitive to inhibition by isoflurane. *British Journal of Anaesthesia*, 102(3): 355–360.

Williams, D.K., Wang, J. & Papke, R.L. 2011. Investigation of the molecular mechanism of the α7 nicotinic acetylcholine receptor positive allosteric modulator PNU-120596 provides evidence for two distinct desensitized states. *Molecular Pharmacology*, 80(6): 1013–1032.

Williams, J.T., Christie, M.J. & Manzoni, O. 2001. Cellular and synaptic adaptations mediating opioid dependence. *Physiological Reviews*, 81(1): 299–343.

Williams, S.H. & Johnston, D. 1991. Kinetic properties of two anatomically distinct excitatory synapses in hippocampal CA3 pyramidal neurons. *Journal of Neurophysiology*, 66(3): 1010–1020.

Wood, C., Kohli, S., Malcolm, E., Allison, C. & Shoaib, M. 2016. Subtype-selective nicotinic acetylcholine receptor agonists can improve cognitive flexibility in an attentional set shifting task. *Neuropharmacology*, 105: 106–113.

Wood, J.N. & Grafman, J. 2003. Human prefrontal cortex: processing and representational perspectives. *Nature Reviews Neuroscience*, 4(2): 139–147.

Woolf, N.J. & Butcher, L.L. 2011. Cholinergic systems mediate action from movement to higher consciousness. *Behavioural Brain Research*, 221(2): 488–498.

Wooltorton, J.R.A., Pidoplichko, V.I., Broide, R.S. & Dani, J.A. 2003. Differential desensitization and distribution of nicotinic acetylcholine receptor subtypes in midbrain dopamine areas. *Journal of Neuroscience*, 23(8): 3176–3185.

Wu, G.Y., Deisseroth, K. & Tsien, R.W. 2001. Spaced stimuli stabilize MAPK pathway activation and its effects on dendritic morphology. *Nature Neuroscience*, 4(2): 151–158.

Wyllie, D.J., Manabe, T. & Nicoll, R.A. 1994. A rise in postsynaptic Ca2+ potentiates miniature excitatory postsynaptic currents and AMPA responses in hippocampal neurons. *Neuron*, 12(1): 127–138.

Yamazaki, Y., Jia, Y., Hamaue, N. & Sumikawa, K. 2005. Nicotine-induced switch in the nicotinic cholinergic mechanisms of facilitation of long-term potentiation induction. *European Journal of Neuroscience*, 22(4): 845–860.

Yang, Yang, Paspalas, C.D., Jin, L.E., Picciotto, M.R., Arnsten, A.F.T. & Wang, M. 2013. Nicotinic α7 receptors enhance NMDA cognitive circuits in dorsolateral prefrontal cortex. *PNAS*, 110(29): 12078–12083.

Yang, Ying & Calakos, N. 2013. Presynaptic long-term plasticity. *Frontiers in Synaptic Neuroscience,* 5(8) doi: 10.3389/fnsyn.2013.00008.

Yizhar, O., Fenno, L.E., Prigge, M., Schneider, F., Davidson, T.J., O'Shea, D.J., Sohal, V.S., Goshen, I., Finkelstein, J., Paz, J.T., Stehfest, K., Fudim, R., Ramakrishnan, C., Huguenard, J.R., Hegemann, P. & Deisseroth, K. 2011. Neocortical excitation/inhibition balance in information processing and social dysfunction. *Nature*, 477(7363): 171–178.

Young, J.W., Crawford, N., Kelly, J.S., Kerr, L.E., Marston, H.M., Spratt, C., Finlayson, K. & Sharkey, J. 2007. Impaired attention is central to the cognitive deficits observed in alpha 7 deficient mice. *European Neuropsychopharmacology*, 17(2): 145–155.

Young, J.W., Finlayson, K., Spratt, C., Marston, H.M., Crawford, N., Kelly, J.S. & Sharkey, J. 2004. Nicotine improves sustained attention in mice: evidence for involvement of the alpha7 nicotinic acetylcholine receptor. *Neuropsychopharmacology*, 29(5): 891–900.

Yu, Z.-Y., Wang, W., Fritschy, J.-M., Witte, O.W. & Redecker, C. 2006. Changes in neocortical and hippocampal GABAA receptor subunit distribution during brain maturation and aging. *Brain Research*, 1099(1): 73–81.

Zhang, X., Liu, C., Miao, H., Gong, Z.H. & Nordberg, A. 1998. Postnatal changes of nicotinic acetylcholine receptor alpha 2, alpha 3, alpha 4, alpha 7 and beta 2 subunits genes expression in rat brain. *Journal of Developmental Neuroscience*, 16(6): 507–518.

Zhang, Z.-W. 2004. Maturation of layer V pyramidal neurons in the rat prefrontal cortex: intrinsic properties and synaptic function. *Journal of Neurophysiology*, 91(3): 1171–1182.

Zhao, M.-G., Toyoda, H., Lee, Y.-S., Wu, L.-J., Ko, S.W., Zhang, X.-H., Jia, Y., Shum, F., Xu, H., Li, B.-M., Kaang, B.-K. & Zhuo, M. 2005. Roles of NMDA NR2B Subtype Receptor in Prefrontal Long-Term Potentiation and Contextual Fear Memory. *Neuron*, 47(6): 859–872.

Zhou, F.M., Liang, Y. & Dani, J.A. 2001. Endogenous nicotinic cholinergic activity regulates dopamine release in the striatum. *Nature Neuroscience*, 4(12): 1224–1229.

Zhou, Q., Homma, K.J. & Poo, M.-M. 2004. Shrinkage of dendritic spines associated with long-term depression of hippocampal synapses. *Neuron*, 44(5): 749–757.

Zoli, M., Léna, C., Picciotto, M.R. & Changeux, J.P. 1998. Identification of four classes of brain nicotinic receptors using beta2 mutant mice. *Journal of Neuroscience*, 18(12): 4461–4472.

Zoli, M., Pistillo, F. & Gotti, C. 2015. Diversity of native nicotinic receptor subtypes in mammalian brain. *Neuropharmacology*, 96(Pt B): 302–311.